The role of macromolecular stability in desiccation tolerance

Willem Frederik Wolkers

Promotor: dr. L.H.W. van der Plas

hoogleraar in de plantenfysiologie

Co-promotor: dr. ir. F.A. Hoekstra

universitair hoofddocent bij het departement Biomoleculaire wetenschappen

The role of macromolecular stability in desiccation tolerance

Willem Frederik Wolkers

Proefschrift

ter verkrijging van de graad van doctor
op gezag van de rector magnificus,
van de Landbouwuniversiteit Wageningen,
dr. C.M. Karssen,
in het openbaar te verdedigen
op woensdag 27 mei 1998
des namiddags te vier uur in de aula

The work presented in this thesis was performed at the Wageningen Agricultural University, Department of Plant Physiology, Arboretumlaan 4, 6703 BD Wageningen, The Netherlands.

The project was financially supported by the Life Sciences Foundation, which is subsidized by the Netherlands Organization for Scientific Research (NWO).

We acknowledge Perkin-Elmer Nederland for financially supporting the printing of this thesis.

Cover design: Mark Alberda

CIP-data Koninklijke Bibliotheek, Den Haag
The role of macromolecular stability in desiccation tolerance / W.F. Wolkers.
Thesis Landbouwuniversiteit Wageningen.
ISBN 90-5485-880-k

Contents

List of abbreviations

ABA	abscisic acid
CF	5(6)-carboxyfluorescein
CNBr	cyanogen bromide
D_2O	^2H_2O
dOO	distance between O atoms
DTT	dithiothreitol
DW	dry weight
EDTA	ethylenedimaminetetraacetic acid
EGTA	ethyleneglycol-bis-(β-aminoethylether)N,N'-tetraacetic acid
EPR	electron paramagnetic resonance
FTIR	Fourier transform infrared spectroscopy
νOH	band position of the OH-stretch
PC	phosphatidylcholine
RH	relative humidity
TES	N-tris[hydroxymethyl]methyl-2-aminoethane sulfonic acid
T_g	glass transition temperature
T_m	gel-to-liquid crystalline transition temperature
Tris	tris-hydroxymethyl)-amino methane
WTC	wavenumber-temperature coefficient

Ala(A)	alanine	Ile (I)	isoleucine
Arg(R)	arginine	Leu(L)	leucine
Asn(N)	asparagine	Lys(K)	lysine
Asx(B)	asparagine or aspartic acid	Met(M)	methionine
Gln(Q)	glutamine	Phe(P)	phenylalanine
Glu(E)	glutamic acid	Ser(S)	serine
Glx(Z)	glutamic acid or glutamine	Thr(T)	threonine
Gly(G)	glycine	Tyr(Y)	tyrosine
His(H)	histidine	Val(V)	valine

Chapter 1

General introduction

Dehydration of a living cell

The unique physical and chemical properties of water make it the most important biological solvent. It determines the structure of biomolecules, provides a fluid environment that allows for diffusion of substrates, and gives structure to organelles. Therefore, dehydration of a living cell has a drastic effect on cellular and macromolecular structure (Crowe *et al.*, 1997a). Both dehydration-induced physical and chemical changes cause irreparable changes in desiccation-sensitive tissues, which eventually lead to cell death. The physical changes include, apart from a drastic change in cellular volume, an increase of the concentration of cellular solutes and an increased viscosity of the cytoplasm (Vertucci and Farrant, 1995). The removal of water from membrane lipids, proteins and nucleic acids changes the hydrophobic and hydrophilic interactions determining structure and function (Crowe *et al.*, 1997a). The chemical changes involve the production of free radicals. Because scavenging systems are not functional at low moisture contents, free radicals can accumulate. The deleterious effects of free radicals are manifested primarily in cellular membranes, where peroxidative reactions result in lower levels of fatty acid unsaturation and the formation of free fatty acids and lipid hydroperoxides. This leads to malfunction of membranes and, consequently, to an extensive leakage of cytoplasmic components, either during dehydration or rehydration of the tissue (Seneratna and McKersie, 1983; Seneratna *et al.*, 1985; Tetteroo *et al.*, 1996). Membranes are a primary site of injury, but the cascade of unregulated reactions during the free radical attack may also affect protein and nucleic acid function (Wolff *et al.*, 1986; Dizdaroglu, 1991).

Anhydrobiosis

Water is usually thought to be required for the living state, but numerous organisms are nevertheless capable of surviving essentially complete dehydration. Survival of organisms or organs in a state of almost complete dehydration is known as anhydrobiosis. Examples of anhydrobiosis can be found in both the animal and plant kingdom (Crowe *et al.*, 1992). The dry organisms may remain in anhydrobiosis for decades or even centuries under cold and dry conditions, and resume vital metabolism after rehydration. In higher plants, anhydrobiosis is usually restricted to seeds and pollens, although in some plants anhydrobiosis also occurs in vegetative tissues. The leaves and roots of the resurrection plant *Craterostigma plantagineum*, for example, can be dehydrated to water contents of less than 10% on a DW basis, and yet the plant resumes vital metabolism within a few hours after rehydration (Bartels *et al.*, 1990; Bianchi *et al.*, 1991).

Seeds of many plant species are able to withstand severe desiccation. Their longevity is dependent on storage conditions, i.e., storage-moisture content and -temperature (Roberts, 1973; Ellis and Roberts, 1980; Ellis *et al.*, 1990). The longevity of these so-called orthodox seeds is often decades in open storage. In contrast, seeds of some plant species rapidly lose viability if they are dried below approximately 20% MC on a fresh weight basis (Hong *et al.*, 1996). Examples of these so-called recalcitrant seeds are common in plant species adapted to aquatic and wet tropical habitats (Roberts *et al.*, 1984). Desiccation-sensitivity in recalcitrant seeds forms a serious problem to their conservation, because such seeds are unsuited for conventional seed banking procedures, involving rapid desiccation followed by storage at subzero temperatures.

Accumulation of sugars in anhydrobiotes

The ability to withstand desiccation requires several biochemical adaptations. One adaptation that anhydrobiotes seem to have in common is the accumulation of large amounts of carbohydrates (Crowe *et al.*, 1992). In nematodes, large quantities of trehalose (20% of total DW) are accumulated

during slow dehydration (Madin and Crowe, 1975). In *Artemia* cysts, trehalose also increases to 20% of the DW during the adaptation to the desiccated state (Clegg, 1986). Trehalose also occurs in large quantities in yeast and bacterial spores (Crowe *et al.*, 1984). In desiccation-tolerant higher plant organs, usually sucrose instead of trehalose is present as the major disaccharide (Amuti and Pollard, 1977). Pollen grains may contain as much as 25% of their dry weight in the form of this carbohydrate (Hoekstra *et al.*, 1992). In seeds, not only sucrose, but also oligosaccharides and cyclitols are found in large quantities (Amuti and Pollard, 1977; Koster and Leopold, 1988; Horbowicz and Obendorf, 1994). The high concentration of sugars in anhydrobiotes has led to many biochemical and biophysical studies on their possible protective role in desiccation-tolerant cells. Evidence is accumulating that carbohydrates indeed play such a role in the protection of dried proteins and membranes (Crowe *et al.*, 1997a).

Stabilization of membranes upon dehydration

Mixtures of polar lipids and water are polymorphic, i.e. they can assume various organized structures. The form that normally is associated with biological membranes is the lamellar liquid crystalline phase. There is two-dimensional order, but the acyl chains can be in a state of considerable disorder. At low temperatures the lamellar gel phase is formed. The molecules are then packed more tightly together and the acyl chains are highly ordered. A lipid bilayer consisting of one phospholipid species is characterized by its liquid crystalline-to-gel phase transition temperature, T_m. In a cell membrane, the situation is more complex, because the mixture of lipids, sterols and proteins causes a complex phase transition behavior. In water, the phospholipid headgroups are surrounded by a hydration shell. ^{2}H-NMR studies indicate a primary hydration shell of 11-16 water molecules per lipid, in rapid exchange with the bulk water (Borle and Seelig, 1983). Upon dehydration, the hydration sphere of the phospholipid headgroups is removed and, consequently, the intermolecular distance between the headgroups decreases. This results in increased van der Waals interaction between the lipid tails and, thus, an

increase in T_m. The hydration shell also provides a force that must be overcome for fusion to occur between two bilayers.

When phospholipid vesicles are dehydrated, they leak their contents into the medium (Crowe *et al.*, 1983). The reason for this is two-fold: (1) if vesicles pass T_m during dehydration, temporary defects in the bilayer develop when both gel phase and liquid phase lipids coexist in the bilayer and (2) the vesicles fuse.

Dehydration-induced leakage from the vesicles is prevented when they are dried in the presence of sugars, in particular disaccharides (Crowe *et al.*, 1986). Several mechanisms have been suggested for this protective role of sugars on unilamellar liposomes. Dehydration of vesicles leads to a considerable increase in T_m, but when dried in the presence of carbohydrates, the T_m may fall below that of hydrated vesicles (Crowe *et al.*, 1996). Sugars can interact with the phospholipid headgroups of the membrane and replace water during dehydration. This interaction increases the average distance between the headgroups and thus prevents the lipid tails from being stacked as in the gel phase. Two properties of sugars are considered to be important in retaining the structural integrity of dried vesicles: 1) The ability to form hydrogen bonds with the phospholipid headgroup, and 2) the glassy state of sugars under dry conditions at room temperature. Phase transitions are prevented through a direct sugar-lipid interaction, and fusion is prevented by embedding of the vesicles in a highly viscous glassy matrix, respectively (Crowe *et al.*, 1996; Crowe *et al.*, 1997b).

Stabilization of dried proteins

Most enzymic proteins are functional in aqueous environment, water being essential for their functional folding. Water can act as donor or acceptor of hydrogen bonds. Moreover, water forces apolar amino acids to the interior of the protein by hydrophobic interaction, thus greatly influencing the protein tertiary structure. In general, removal of the hydration shell of proteins results in extensive structural changes (Kuntz and Kauzmann, 1974; Prestrelski *et al.*, 1993). These dehydration-induced conformational changes can be irreversible (Prestrelski *et al.*, 1993), but can also be fully reversible (Griebenow and

Klibanov, 1995). For several proteins with enzymic function, dehydration results in severe loss of activity after subsequent rehydration (Hanafusa, 1969).

Dehydration-labile enzyme preparations which contain added sugars as stabilizers are often successfully preserved by means of freeze-drying, yielding shelf-stable products with a good conservation of activity. The protective role of sugars on proteins has been attributed to maintenance of the native structure in the dried state. Two properties of sugars are considered to be responsible for this stabilization. 1) A direct interaction between proteins and sugars through hydrogen bonding in the dried state (Carpenter and Crowe, 1989), replacing the original hydrogen bonds of water. 2) The formation of a highly viscous glassy state of the sugar-protein mixture. Below the characteristic glass transition temperature, T_g, glasses have solid-like properties. Due to the very low molecular mobility in the glassy matrix (viscosity has risen to above 10^{12} Pa s) proteins are immobilized and fit for long-term storage (Franks *et al.*, 1991; Levine and Slade, 1992).

Stabilization of dried proteins and membranes in desiccation-tolerant cells

The protective effect of sugars on membranes and proteins has led to the formulation of the *"water replacement hypothesis"* (Crowe *et al.*, 1992). This hypothesis suggests that the hydroxyl groups of sugars substitute for water and provide the hydrophilic interactions upon removal of water in desiccation-tolerant cells. However, it should be noted that most of the experiments to confirm this hypothesis concern model experiments using isolated proteins and lipids. So far, no convincing evidence has been provided that the water replacement theory also holds *in situ* in desiccation-tolerant cells.

Alternatively, or next to this water replacement hypothesis, the *"glass formation hypothesis"* attributes the protective effect of sugars on proteins and membranes to the generally good glass-forming properties of sugars.

Crystalline materials transform from a solid to a liquid state at a particular temperature, i.e., the melting point. However, for glasses the transition from solid-like behavior to liquid-like behavior occurs over a relatively broad temperature range. The melting of glasses from the vitrified state into the liquid

state is a second order transition. This means that at T_g the enthalpy, entropy and the volume of the two phases are the same. However, the heat capacity changes upon melting of the glass (Roos, 1995). With Differential Scanning Calorimetry (DSC), this change in heat capacity with melting of the glass can be directly measured. Glasses can be considered as "solidified" liquids, and maintain many properties of liquids. Perhaps the most important is that they retain molecular disorder, just like that in solution. The amorphous structure, when maintained in a highly viscous state, contributes to the long term stability of biomolecules by preventing crystallization and chemical reactions (Franks *et al.*, 1991).

In desiccation-tolerant cells, the presumably highly viscous or vitreous state may serve to inhibit disruption of cellular membranes, denaturation of cytoplasmic proteins and deteriorative radical reactions. Evidence that the cytoplasm of dry soybean seeds and *Typha latifolia* pollen indeed exists in a vitrified state comes from DSC experiments (Williams and Leopold, 1989; Buitink *et al.*, 1996). A glassy state is formed in the cytoplasm of these desiccation-tolerant plant organs when the water content falls below 0.1 g H_2O/g DW at room temperature.

Aim of this thesis

The final goal of the study presented in this thesis was to elucidate the molecular mechanisms involved in the acquisition of desiccation tolerance of higher plant tissues. Particular emphasis was placed on the conformation and molecular interactions of biomolecules, such as proteins, lipids and sugars. The three major aims of this work were:

1) Characterization of the overall *in situ* protein secondary structure in anhydrobiotes during development.

2) Relating the protein stability of desiccation-tolerant cells to their lifespan.

3) Elucidating the molecular interactions in the dry cytoplasmic matrix which are involved in desiccation tolerance and longevity.

For this purpose, somatic and zygotic embryos, whole seeds, pollen and leaves of the resurrection plant, *Craterostigma plantagineum*, were utilized. Where appropriate, model systems were used to support the *in situ* studies. FTIR microspectroscopy was the main experimental technique in these studies.

In the following sections the biophysical and biochemical adaptations during the acquisition of desiccation tolerance and the factors that determine longevity are described and a brief description is given concerning the use of FTIR.

Acquisition of desiccation tolerance in seeds

Embryos in seeds acquire desiccation tolerance halfway their development and prior to the onset of desiccation (Sun and Leopold, 1993; Sanhewe and Ellis, 1996). Capacity to germinate after severe dehydration is often used as a criterion for desiccation tolerance.

During seed development, storage proteins, lipids and starch are accumulated. In the maturation stage, the reserve deposition is terminated and the seed desiccates. As much as 90% of the original water may be lost from seeds (Bewley and Black, 1994). The induction of desiccation tolerance has often been correlated with the plant hormone abscisic acid (ABA). ABA plays a major role during seed development, especially during the maturation phase (Black, 1991). The significance of ABA for seed development has been established with ABA-deficient and ABA-insensitive mutants of *Arabidopsis thaliana*. ABA is required for the induction of dormancy and, thus, precocious germination is prevented (Karssen *et al.*, 1982). Furthermore, ABA is thought to trigger the induction of oligosaccharides and late embryogenesis-abundant (LEA) proteins, which are accumulated during the later stages of seed development (Galau *et al.*, 1986). In seeds, generally sucrose, often together with oligosaccharides such as raffinose, stachyose or verbascose is encountered. Oligosaccharides are known for their ability to form stable glasses (Roos, 1995). It has been suggested that the accumulation of oligosaccharides during seed maturation enables formation of a highly viscous state in the dehydrating tissue (Leopold *et al.*, 1994).

The genes encoding for LEA proteins are expressed in the embryos during the late stages of seed development. However, expression can also be induced in immature seeds and vegetative tissues by ABA (Close *et al.*, 1989; Blackman *et al.*, 1995). On the basis of their amino acid sequences, several families of these proteins have been classified, some of which were suggested to exist as random coils and others as amphiphilic α-helical structures (Dure *et al.*, 1989). The highly conserved sequence blocks found within each group, their abundance, physical properties (hydrophilicity and heat stability) and appearance during water stress suggest that LEAs play an important role during desiccation and rehydration (Galau *et al.*, 1986; Dure *et al.*, 1989). A role in sequestering ion combinations that dissolve with difficulty, such as amino acid salts, has been suggested for some LEA proteins. Other classes of LEA proteins might function as chaperones to preserve membrane structures in drying cells (Close, 1996).

Longevity of desiccation-tolerant cells

There is wide-spread variety in the lifespan of seeds and pollens. In seeds, aging under laboratory conditions occurs at a much lower rate than in pollen, years *vs* weeks, respectively (Hoekstra, 1995). The longevity of pollen and seeds often can be predicted as a function of the storage-moisture content and -temperature (Ellis and Roberts, 1980; Ellis *et al.*, 1990; Buitink *et al.*, 1998). However, even in the dry state, large differences in longevity exist among pollens and seeds.

In the dry state, radical reactions cause irreversible cellular injuries that limit the lifespan. Viability loss of seeds and pollens is often attributed to the loss of membrane integrity (Priestley, 1986; Bewley and Black, 1994; van Bilsen *et al.*, 1994a,b). This loss of membrane integrity is due to chemical and physical changes in the membrane. Loss of viability often coincides with an increased leakage of cytosolic components upon rehydration and with increased levels of free fatty acids. It was shown that deesterification of phospholipids results in accumulation of lysophospholipids and free fatty acids (Nakayama *et al.*, 1981; van Bilsen and Hoekstra, 1993). Accumulation of these

products in the membranes may lead to phase separation of membrane components and increased permeability upon rehydration. When free fatty acids and lysophospholipids are incorporated in liposomes, they cause an increased permeability (McKersie *et al.*, 1989; van Bilsen and Hoekstra, 1993). A strong correlation between pollen longevity and content of esterified linolenic acid in lipid was observed (Hoekstra, 1986). Pollens having high linolenic acid content tend to have a short lifespan. It was suggested that lipid peroxidation of the polyunsaturated fatty acids limits the pollen's lifespan.

Although membrane damage may be the primary reason of seed death, the loss of protein and DNA integrity also could be involved in seed aging during long-term storage. The cascade of uncontrolled radical reactions might result in loss of protein and DNA integrity.

Orthodox seeds usually remain viable for decades in open storage. To accelerate aging and possible changes in membrane and protein composition associated with this aging, conditions of high relative humidity and/or high temperature can be applied (Priestley and Leopold, 1979; McKersie *et al.*, 1988; van Bilsen and Hoekstra, 1993). However, care should be taken to directly compare the biochemical changes during accelerated aging with those during natural, dry, aging. Processes occurring during accelerated aging may be different from those during natural aging.

How to study biomolecules in desiccation-tolerant cells?

There are several spectroscopic techniques available that can be applied to study conformation and molecular interactions of biomolecules, i.e. NMR, ESR, CD, FTIR, Raman, Absorption, Neutron diffraction, and X-ray crystallograpy. However, the dry state of desiccation-tolerant cells drastically limits the number of techniques that can be applied. One of the few suitable techniques for dry tissue analysis is FTIR. With this technique, molecular vibrations can be measured irrespective of the hydration state of the tissue. Molecular vibrations are sensitive to intra- and inter-molecular interactions. In this study, *in situ* FTIR microspectroscopy was used to monitor molecular vibrations in dry desiccation-tolerant cells. On account of characteristic

molecular vibrations, information can be derived on the molecular conformation and the inter-molecular interactions of biomolecules in their native environment. The temperature dependence of several characteristic molecular vibrations was used to study heat-induced protein unfolding and the properties of cytoplasmic glasses. In the following section the application of FTIR to study the molecular conformation and intermolecular interactions of biomolecules is described.

FTIR

The infrared region of the electromagnetic spectrum ranges from 400 - 4000 cm^{-1}. The energy of most molecular vibrations corresponds to the infrared region. A vibration is only infrared-active if it is associated with a change in the electric dipole moment. If a diatomic molecule is considered as a simple harmonic oscillator, the vibrational frequency (f) is:

$$(1) \quad f = \frac{1}{2\pi}\sqrt{\frac{k}{\mu}}$$

where μ is the reduced mass of the two atoms ($\mu = m_1.m_2/(m_1+m_2)$ with m_1 and m_2 as the atomic masses, and k is the force constant determined by the strength of the bond. The potential energy (V) of the oscillator is given by;

$$(2) \quad V = \frac{1}{2}k(r - r_e)^2$$

where r is the distance between the two vibrating atoms and r_e, the equilibrium distance. In infrared spectroscopy the frequency is expressed as wavenumbers ($f = c(1/\lambda)$); this transforms equation 1 into:

$$(3) \quad \frac{1}{\lambda} = \frac{1}{2\pi.c}\sqrt{\frac{k}{\mu}}$$

where $1/\lambda$ represents wavenumber (ν) usually expressed in cm^{-1}.

The IR-technique is of great value in the study of intra- and intermolecular hydrogen bonding. Formation of a hydrogen bond will cause any

Table 1. Band positions of characteristic molecular groups commonly found in biological tissues.

Characteristic group vibration	Wavenumber (cm^{-1})
OH stretch	3600-3000
Asymmetric CH_3 stretch	2950
Asymmetric CH_2 stretch	2920
Symmetric CH_3 stretch	2875
Symmetric CH_2 stretch	2850
HOH scissoring	1650
C=O stretch (Amide-I)	1650
NH bend (Amide-II)	1550
Asymmetric PO stretch	1250
OH in plane bending	1050

stretching vibration to broaden and shift to lower wavenumbers (Vinogradov and Linnel, 1971).

For a macromolecule, there are very many vibrational transitions. However, many of the vibrations can be assigned to particular bonds or groupings. This forms the basis of characteristic group frequencies. The main experimental parameter is the position of the maximum of the absorption band, in cm^{-1}. In Table 1 band positions of characteristic molecular groups commonly found in biological tissues are listed.

The band position of a molecular group depends on the intrinsic molecular vibration and on the micro-environment. Information can be obtained about the molecular structure and interaction with other molecules. Some bands which are of particular importance for protein analysis are the amide-I and amide-II vibrations around 1650 and 1550 cm^{-1}, respectively, arising from the amide backbone of peptides and proteins. Phospholipids have characteristic bands around 2900 and 1250 cm^{-1}. Carbohydrates have bands

around 3300 cm^{-1} and several bands between 1100 and 400 cm^{-1} which can be attributed to OH stretching and bending vibrations.

FTIR has several important advantages over conventional IR methods (Perkins, 1987). The most important advantage is the efficient and rapid collection of data with a superior signal to noise ratio. When a microscope is attached to a FTIR spectrometer a specific sample area can be selected for FTIR analysis. Nowadays, FTIR microspectroscopy can be used for analysis of sample areas as small as 100 μm^2. With FTIR microspectroscopy, protein secondary structure and changes in lipid membrane phase behavior in dry biological tissues can be studied *in situ* (Crowe *et al.*, 1984). IR spectra of biological tissues as a function of temperature show shifts of bands, associated with phospholipid conformation (CH-stretching and bending vibrations) in membranes, with protein secondary structure (C=O stretching vibration) and with sugar-sugar interactions (OH-stretching vibration), which can be measured simultaneously. FTIR has the advantage over other methods such as DSC that, besides transition temperatures, information can be derived on molecular conformation and interaction, e.g. protein secondary structure and interaction of proteins with sugars.

IR-bands in spectra of biomacromolecules such as proteins tend to overlap considerably. This complicates the analysis and interpretation of the spectrum. In order to identify the overlapping components within the composite band, a number of mathematical procedures have been developed (Surewicz *et al.*, 1993). Second derivative analysis and Fourier self-deconvolution have been widely used for identification of bands. Derivation as well as Fourier self-deconvolution transform the absorption bands to lineshapes with narrower width, thereby resolving overlapping components. Often, these methods are referred to as resolution enhancement techniques, but one has to keep in mind that actually only the graphical resolution is improved; the optical resolution is still determined by the spectrometer settings (Pistorius, 1995).

Quantitative information on protein secondary structure components can be obtained by curve-fitting of the IR spectrum. The amide-I band is mostly used for this purpose. In the curve-fitting procedure, the measured spectrum is

regenerated mathematically, by adding a pre-defined number of bands with known peak positions, bandwidths and lineshape functions. Subsequently, these parameters are iterated until the theoretically generated spectrum and the measured spectrum coincide to a high degree (Pistorius, 1995). The resulting fractional areas of the bands assigned to different types of secondary structure are assumed to represent percentages of these structures in a given protein.

Outline of the thesis

The major part of this work concerns a study of the overall protein stability with respect to drying in developing desiccation-tolerant plant organs, and the long-term stability of the overall protein secondary structure in the dried state. For this purpose, pollen, somatic and zygotic embryos (desiccation-tolerant and -sensitive), seeds (orthodox and recalcitrant), and resurrection plants (*Craterostigma plantagineum*) were used as the experimental materials. FTIR microspectroscopy was used as the main experimental technique to study conformational and phase behavior of biomolecules within their native environment.

Aging

In the first part of this thesis (Chapters 2, 3 and 4) the effects of natural and accelerated aging on protein stability of a desiccation-tolerant pollen and seeds were characterized. In Chapter 2, the use of FTIR microspectroscopy to study dry plant tissues (*Typha latifolia* pollen) is explained, with emphasis on the assignment of the different types of protein secondary structure. The band assignment of the characteristic IR group frequencies that were observed for pollen was also useful in the band assignment of the other plant tissues that were studied. Furthermore, a qualitative and quantitative assignment of the protein profile in this pollen was made. Apart from protein secondary structure, membrane phase behavior of the pollen was studied during accelerated aging. In Chapter 3, the heat stability of the proteins in this pollen was studied as a function of the water content. In Chapter 4, the protein secondary structures in

embryos from seeds that were stored for several decades in a seed bank are described. From comparison with similar data from freshly harvested seeds, conclusions can be drawn concerning the long-term protein stability.

Seed development

In order to identify specific protein secondary structures that might be associated with the acquisition of desiccation tolerance, maize embryos were studied in the course of their development. In Chapter 5, changes in protein profile of these embryos subjected to different drying protocols are described.

Physical characteristics of desiccation-tolerant cells

In Chapter 6, the use of FTIR to study glass transitions in carbohydrate glasses is described. The method was also applied to characterize cytoplasmic glasses in pollen and dried leaves of *Craterostigma plantagineum*. In an attempt to link the structure of cytoplasmic glasses to the stability of proteins, maturation-defective mutant seeds of *Arabidopsis thaliana* were investigated (Chapter 7). The increased heat stability of proteins and the properties of glasses were linked to the extent to which seed maturation had progressed.

The role of sugars and LEA-like proteins in desiccation tolerance

In the last part of this thesis (Chapter 8, 9 and 10) isolated sugars and LEA proteins from desiccation-tolerant organs were studied, also in model systems. In Chapter 8, the role of umbelliferose in the acquisition of desiccation tolerance of *Daucus* somatic embryos is depicted. Umbelliferose is a trisaccharide that accumulates in these embryos at the expense of sucrose under conditions that promote desiccation tolerance. The glass forming properties of umbelliferose are compared to those of sucrose. In Chapter 9, results of a model study on protein-sugar interactions in the dry state are described. As a model, the dehydration-labile polypeptide, poly-L-lysine, was used. In an attempt to interpret the results of this model study in terms of a possible role of the dehydration-linked LEA proteins, a study was conducted with LEA-like proteins isolated from *Typha latifolia* pollen (Chapter 10). The isolated heat stable protein was sequenced and aligned with the protein

databank to find resemblances with LEA proteins. The protein structure was determined and its effect on the molecular structure of carbohydrate glasses was investigated.

In Chapter 11, the general discussion, the results of this thesis are placed in a broader perspective.

References

Amuti, K.S., Pollard, C.J. (1977) Soluble carbohydrates of dry and developing seeds. *Phytochemistry* **16,** 529-532.

Bartels, D., Schneider, K., Terstappen, G., Piatkowski, D., Salamini, F. (1990) Molecular cloning of abscisic acid-modulated genes which are induced during desiccation of the resurrection plant *Craterostigma plantagineum*. *Planta* **181,** 27-34.

Bewley, J.D., Black. M. (1994) Seeds, Physiology of Development and Germination. New York and London: Plenum Press pp. 445.

Bianchi, G., Gamba, A., Murelli, C., Salamini, F., Bartels, D. (1991) Novel carbohydrate metabolism in the resurrection plant *Craterostigma plantagineum*. *Plant. J.* **1,** 355-359.

Black, M. (1991) Involvement of ABA in the physiology of developing and mature seeds. *In:* Davies, W.J., Jones, H.G. (eds.) Abscisic Acid: Physiology and Biochemistry. BIOS Scientific Publishers, Oxford UK, pp. 90-124.

Blackman, S.A., Obendorf, R.L., Leopold, A.C. (1995) Desiccation tolerance in developing soybean seeds: the role of stress proteins. *Physiol. Plant.* **93,** 630-638.

Borle, F. Seelig, J. (1983) Hydration of *Escherichia coli* lipids: deuterium T_1 relaxation time studies of phosphatidylglycerol, phosphatidylethanolamine and phosphatidylcholine. *Biochim. Biophys. Acta* **735,** 131-136.

Buitink, J., Walters-Vertucci, C., Hoekstra, F.A., Leprince, O. (1996) Calorimetric properties of dehydrating pollen: Analysis of a desiccation tolerant and an intolerant species. *Plant Physiol.* **111,** 235-242.

Buitink, J., Walters, C., Hoekstra, F.A., Crane, J. (1998) Storage behavior of *Typha latifolia* pollen at low water contents: Interpretation on the basis of water activity and glass concepts. *Physiol. Plant. in press.*

Carpenter, J.F., Crowe, J.H. (1989) An infrared spectroscopic study of the interactions of carbohydrates with dried proteins. *Biochemistry* **28,** 3916-3922.

Clegg, J.S. (1986) The physical properties and metabolic status of *Artemia* cysts at low watercontents: The "water replacement hypothesis." *In:* Leopold, A.C. (ed.) Membranes, Metabolism, and Dry organisms. Cornell University Press, Ithaca, NY. pp. 169-187.

Close, T.J. (1996) Dehydrins: Emergence of a biochemical role of a family of plant dehydration proteins. *Physiol. Plant.* **97,** 795-803.

Close, T.J., Kortt, A.A., Chandler, P.M. (1989) A cDNA-based comparison of dehydration-induced proteins (dehydrins) in barley and corn. *Plant Mol. Biol.* **13,** 95-108.

Crowe, J.H., Crowe, L.M., Carpenter, J.F., Prestrelski, S.J., Hoekstra, F.A. (1997a) Anhydrobiosis: cellular adaptations to extreme dehydration. *In:* Dantzler, W.H. (ed.) Handbook of Physiology section 13, Comparative Physiology, Vol II, Oxford University Press, Oxford. pp. 1445-1477

Crowe, J.H., Crowe, L.M., Chapman, D. (1984) Preservation of membranes in anhydrobiotic organisms: the role of trehalose. *Science* **223,** 701-703.

Crowe, J.H., Crowe, L.M., Jackson, S.A. (1983) Preservation of structural and functional activity in lyophilized sarcoplasmic reticulum. *Arch. Biochem. Biophys.* **220,** 477-484.

Crowe, J.H., Hoekstra. F.A., Crowe, L.M. (1992) Anhydrobiosis. *Annu. Rev. Physiol.* **54,** 570-599.

Crowe, J.H., Hoekstra, F.A., Nguyen, K.H.N., Crowe, L.M. (1996) Is vitrification involved in depression of the phase transition temperature in dry phospholipids? *Biochim. Biophys. Acta* **1280,** 187-196.

Crowe, J.H., Oliver, A.E., Hoekstra, F.A., Crowe, L.M. (1997b) Stabilization of dry membranes by mixtures of hydroxyethyl starch and glucose: The role of vitrification. *Cryobiology* **35,** 20-30.

Crowe, L.M., Womersley, C., Crowe, J.H., Reid, D., Appel, L., Rudolph, A. (1986) Prevention of fusion and leakage in freeze-dried liposomes by carbohydrates. *Biochim. Biophys. Acta* **861,** 131-140.

Dizdaroglu, M. (1991) Chemical determination of free radical-induced damage to DNA. *Free Rad. Biol. Med.* **10,** 225-242.

Dure III, L., Crouch, M., Harada, J., Ho, T.H.D., Mundy, J., Quatrano, R., Thomas, T., Sung, Z.R. (1989) Common amino acid sequence domains among the LEA proteins of higher plants. *Plant Mol. Biol.* **12,** 475-486.

Ellis, R.H., Hong, T.D., Roberts, E.H., Tao, K.L. (1990) Low moisture content limits to relations between seed longevity and moisture. *Ann. Bot.* **65,** 493-504.

Ellis, R.H., Roberts, E.H. (1980) Improved equations for the prediction of seed longevity. *Ann. Bot.* **45,** 13-30.

Franks, F. Hatley, R.H.M., Mathias, S.F. (1991) Materials science and production of shelf stable biologicals. *Bio-Pharm* **4,** 38-42.

Galau, G.A., Hughes, D.W., Dure III, L. (1986) Abscisic acid induction of cloned cotton late embryogenesis-abundant (Lea) mRNAs. *Plant Mol. Biol.* **7,** 155-170.

Griebenow, K., Klibanov, A.M. (1995) Lyophilization-induced reversible changes in the secondary structure of proteins. *Proc. Natl. Acad.Sci. U.S.A.* **92,** 10969-10976.

Hanafusa, N. (1969) Denaturation of enzyme protein by freeze-thawing and freeze-drying. *In:* Tokio, N. (ed.) Freezing and freeze-drying of microorganisms. University Park Press, Baltimore. pp. 117-129.

Hoekstra F.A. (1986) Water content in relation to stress in pollen. *In:* Leopold, A.C. (ed.) Membranes Metabolism and dry Organisms, Cornell University Press, Ithaca, NY, pp. 102-122.

Hoekstra, F.A. (1995) Collecting pollen for genetic resources conservation. *In:* Guarino, L., Ramanatha, V., Rao, R. Reid, R. (eds.) Collecting Plant Genetic Diversity, CAB International, Oxon, pp. 527-550.

Hoekstra, F.A., Crowe, J.H., Crowe, L.M., Van Roekel. T., Vermeer, E. (1992) Do phospholipids and sucrose determine membrane phase transitions in dehydrating pollen species? *Plant Cell Environ.* **15,** 601-606.

Hong, T.D., Linington, S., Ellis, R.H. (1996) Compendium of information on seed storage behaviour. International Plant Genetic Resources Institute Rome.

Horbowicz, M., Obendorf, R.L. (1994) Seed desiccation tolerance and storability: dependence on flatulence-producing oligosaccharides and cyclitols: review and survey. *Seed Sci. Res.* **4,** 385-406.

Karssen, C.M., Brinkhorst-van der Swan, D.L.C., Breekland, A.E., Koornneef, M. (1983) Induction of dormancy during seed development by endogenous abscisic acid: studies on abscisic acid deficient genotype of *Arabidopsis thaliana* (L.) Heynh. *Planta* **157,** 158-165.

Koster, K.L., Leopold, A.C. (1988) Sugars and desiccation tolerance in seeds. *Plant Physiol.* **88,** 829-832.

Kuntz, I.D., Kauzmann, W. (1974) Hydration of proteins and polypeptides. Adv. Protein Chem. **28,** 239-345.

Leopold, A.C., Sun, W.Q., Bernal-Lugo, I. (1994) The glassy state in seeds: analysis and function. *Seed Sci. Res.* **4,** 267-274.

Levine, H., Slade, L. (1992) *In:* Schwartzberg, H., Hatel, R.W. (eds.) Physical chemistry of Foods. pp. 83-221. Marcel Dekker, New York.

Madin, K.A.C., Crowe, J.H. (1975) Anhydrobiosis in nematodes: carbohydrate and lipid metabolism during dehydration. *J. Exp. Zool.* **193,** 335-337.

McKersie, B.D., Crowe, J.H., Crowe, L.M. (1989) Free fatty acid effects on leakage, phase properties, and fusion of fully hydrated model membranes. *Biochim. Biophys. Acta* **982,** 156-160.

McKersie, B.D., Senaratna, T., Walker, M.A., Kendall, E.J., Hetherington, R.R. (1988) Deterioration of membranes during aging in plants: evidence for free radical mediation. *In:* Nooden, L.D., Leopold, A.C. (eds.) Senescence and Aging in Plants, Academic Press, New York, pp 412-465.

Nakayama, Y., Sajo, K., Kito, M. (1981) Decomposition of phospholipids in soybeans during storage. *Cereal Chem.* **58,** 260-264.

Perkins, W.D. (1987) Fourier transform infrared spectroscopy: part II. advantages of FT-IR *J. Chem. Educ.* **64,** A269-A271.

Pistorius, A.M.A. (1995) Biochemical Applications of FT-IR Spectroscopy. *Spectrosc. Eur.* **7,** 8-15.

Prestrelski, S.J., Tedeschi, N., Arakawa, T., Carpenter, J.F. (1993) Dehydration-induced conformational transitions in proteins and their inhibition by stabilizers. *Biophys. J.* **65,** 661-671.

Priestley, D.A. (1986) Seed Aging: Implications for Seed Storage and Persistence in Soil, pp. 1-304. Ithaca, Comstock Publ. Assoc.

Priestley, D.A., Leopold, A.C. (1979) Absence of lipid oxidation during accelerated aging of soybean seeds. Plant Physiol **63,** 726-729.

Roberts, E.H. (1973) Predicting the storage life of seeds. *Seed Sci. Technol.* **1,** 499-514.

Roberts, E.H., King, M.W., Ellis, R.H. (1984) Recalcitrant seeds: their recognition and storage. *In:* Holden, J.H.W. and Williams, J.T. (eds.) Crops Genetic Resources: Conservation and Evaluation. Allen and Unwin, London pp. 38-52.

Roos, Y.H. (1995) Phase Transitions in Foods, Academic Press, London, pp. 1-360.

Sanhewe, A.J., Ellis, R.H. (1996) Seed development and maturation in *Phaseolus vulgaris*. I. Ability to germinate and to tolerate desiccation. *J. Exp. Bot.* **47,** 949-958.

Senaratna, T., McKersie, B.D. (1983) Dehydration injury in germinating soybean (*Glycine max* L. Merr.) seeds. *Plant Physiol.* **72,** 620-624.

Senaratna, T., McKersie, B.D., Stinson, R.H. (1985) Simulation of dehydration injury to membranes from soybean axes by free radicals. *Plant Physiol.* **77,** 472-474.

Sun, W.Q., Leopold, A.C. (1993) Acquisition of desiccation tolerance in soybeans. *Physiol. Plant.* **87,** 403-409.

Surewicz, W.K., Mantsch, H.H., Chapman, D. (1993) Determination of protein secondary structure by Fourier transform infrared spectroscopy: a critical assessment. *Biochemistry* **32,** 389-394.

Tetteroo, F.A.A., de Bruijn, A.Y., Henselmans, R.N.M., Wolkers, W.F., van Aelst, A.C., Hoekstra, F.A. (1996) Characterization of membrane properties in desiccation-tolerant and -intolerant carrot somatic embryos. *Plant Physiol.* **111,** 403-412.

van Bilsen, D.G.J.L., Hoekstra, F.A. (1993) Decreased membrane integrity in aging *Typha latifolia* L. pollen: Accumulation of lysolipids and free fatty acids. *Plant Physiol.* **101,** 675-682.

van Bilsen, D.G.J.L., Hoekstra, F.A., Crowe, L.M., Crowe, J.H. (1994a) Altered phase behavior in membranes of aging dry pollen may cause imbibitional leakage. *Plant Physiol.* **104,** 1193-1199.

van Bilsen, D.G.J.L., Van Roekel, T., Hoekstra, F.A. (1994b) Declining viability and lipid degradation during pollen storage. *Sex. Plant Reprod.* **7,** 303-310.

Vertucci, C.W., Farrant J.M. (1995) Acquisition and loss of desiccation tolerance. *In:* Kigel, J., Galili, G. (eds.) Seed development and germination, Marcel Dekker, New York, pp. 237-271.

Vinogradov, S.N., Linnel, R.H. (1971) Hydrogen Bonding, Van Nostrand Reinhold Company, New York, pp. 1-319.

Williams, R.J., Leopold, A.C. (1989) The glassy state in corn embryos. *Plant Physiol.* **89,** 977-981.

Wolff, S.P., Garner, A., Dean, R.T. (1986) Free radicals, lipids and protein degradation. *Trends Biochem. Sci.* **11,** 27-31.

Chapter 2

Aging of dry desiccation-tolerant pollen does not affect protein secondary structure

Willem F. Wolkers and Folkert A. Hoekstra

Abstract

Protein secondary structure and membrane phase behavior in aging *Typha latifolia* pollen were studied by means of Fourier transform infrared microspectroscopy (FTIR). Membranes isolated from fresh pollen occurred mainly in the liquid crystalline phase at room temperature, whereas the membrane fluidity of aged pollen was drastically decreased. This decrease did not result in large scale irreversible protein aggregation, as was concluded from *in situ* FTIR-assessment of the amide-I bands. Curve fitting on the infrared absorbance spectra enabled estimation of the proportion of different classes of protein secondary structure. Membrane proteins had a relatively large amount of α-helical structure (48%; band at 1658 cm^{-1}), and turn-like structures (at 1637 and 1680 cm^{-1}) were also detected. The secondary protein structure of isolated cytoplasmic proteins resembled that of proteins in whole pollen and was conserved upon drying in the absence of sucrose. The isolated cytoplasmic proteins had a large amount of α-helical structure (43%), and also β-sheet (at 1637 and 1692 cm^{-1}) and turn structures were detected. Heat denaturing experiments with intact hydrated pollen showed low (1627 cm^{-1}) and high (1692 cm^{-1}) wave number bands indicating irreversible protein aggregates. The results presented in this paper show that FTIR is an extremely suitable technique to study protein secondary structure in intact plant cells of different hydration levels and developmental stages.

Also published in Plant Physiology **109**, 907-915 (1995)

Introduction

Cattail (*Typha latifolia*) pollen can be dried to water contents of less than 0.05 g $H_2O.g^{-1}$ DW, without losing viability. In an atmosphere of 40% RH the pollen attains about 0.06 g $H_2O.g^{-1}$ DW and has a maximum life span of approximately 120 d at 24°C in the dark (van Bilsen and Hoekstra, 1993). At the higher RH of 75% the water content increases to approximately 0.20 g $H_2O.g^{-1}$ DW, and viability is lost within as short a period as 12 d. Aging of the pollen coincides with massive leakage of endogenous K^+ upon reimbibition (van Bilsen *et al.*, 1994a), indicative of extensive membrane damage. Free fatty acids and lysophospholipids accumulate at the expense of the phospholipids (van Bilsen and Hoekstra, 1993). Free fatty acids have a destabilizing effect on model membranes in both the hydrated (McKersie *et al.*, 1989) and the dry condition (Crowe *et al.*, 1989b). Lysophospholipid, even in small amounts, is sorted out from model membranes upon drying, to form highly ordered complexes (van Bilsen *et al.*, 1994a). These products of de-esterification are responsible for the 30°C increase of T_m of the rehydrated pollen membranes to approximately room temperature (van Bilsen *et al.*, 1994a). Thus, at room temperature, both gel phase domains and liquid crystalline phase domains coexist in the same membrane, which is generally linked with leakage (Crowe *et al.*, 1989a). Although a clear phase separation could not be resolved by *in situ* FTIR on aged pollen because of the relatively small amount of de-esterification products present, it may have contributed to the massive imbibitional leakage of solutes from this pollen (van Bilsen *et al.*, 1994a).

In suspension, the polar headgroup of a phospholipid typically binds H_2O molecules, the number of which depends on the phospholipid molecular species (Finer and Darke, 1974). Removal of this hydration sphere causes the intermolecular distance between the polar headgroups to decrease, which results in an increased interaction between the acyl chains. The resulting domain having densely packed phospholipids is permeable at its edges. In the case of an intact cell this would lead to the loss of membrane integrity and death. Desiccation-tolerant cells seem to have circumvented such problems

because large amounts of sugars are produced by them (Crowe *et al.*, 1984). Sugars can interact with the polar headgroups and somehow replace the water during dehydration. This interaction increases the average distance between the headgroups and thus prevents the acyl chains from being packed at high density. Two properties of sugars are important in inducing desiccation tolerance: (a) the ability to form hydrogen bonds with the phospholipid polar headgroup, and (b) the ability to form a glassy state under dry conditions at room temperature (Crowe *et al.*, 1994, 1996). In intact dry cells, glasses immobilize the cytoplasm and probably prevent intracellular membrane fusion.

Highly ordered lipid domains indirectly cause the formation of protein domains, since membrane proteins will be excluded from these ordered lipid domains and move to the remaining fluid parts of the membrane. In model membrane systems, the gel phase can induce irreversible protein aggregation (Hemminga *et al.*, 1992). This aggregation *per se*, may cause the loss of membrane integrity and, in the case of aged pollen, may have been responsible for the observed leakage. In this respect, it is interesting that as long ago as 1922 it was suggested that aging of pollen leads to protein denaturation (Knowlton, 1922).

FTIR has proven to be a very useful method to study the conformation of membrane proteins (Haris and Chapman, 1992). The application of FTIR to proteins is based on the assessment of the amide-I bands, located between 1600-1700 cm^{-1}, and the amide-II band. The amide-I absorption band is principally due to an in-plane C=O stretching vibration, whereas the amide-II band is due to the NH bending (Susi, 1969). The structure-sensitive amide-I band in the infrared spectrum can be used to detect changes in the protein secondary structure (Byler and Susi, 1986; Surewicz and Mantsch, 1988). The C=O stretching frequency is very sensitive to changes in the nature of the hydrogen bonds arising from the different types of secondary structure. This leads to a characteristic set of infrared absorption bands for each type of secondary structure (Susi *et al.*, 1967). It has been found that in model systems large protein aggregates coincide with a highly characteristic low wavenumber

band in the amide-I absorption band of the protein backbone (Sanders *et al.*, 1993).

With new FTIR-techniques for *in situ* analysis of small biological samples available (Messerschmidt and Reffner, 1988; Reffner, 1989), we thought that it would be feasible to pursue possible effects of storage on protein secondary structure. In this paper we describe the behavior of proteins in dry cattail pollen during aging. We used IR microspectroscopic methods to investigate protein-protein interactions and/or protein aggregation. Protein structure of whole pollen was compared with that of isolated membranes and the cytoplasmic fraction. We present evidence that protein secondary structure is hardly affected during aging and that proteins are resistant to drying and freeze-drying. In contrast, membrane fluidity studies indicate a significant decrease in fluidity during aging.

Materials and methods

Pollen

Collecting and handling of *Typha latifolia* L. pollen were performed as described earlier (Hoekstra *et al.*, 1991). Aging of the pollen was achieved by incubation of the pollen (1 g) at a constant temperature of 24°C in an atmosphere of 75% RH produced by a well-ventilated saturated NaCl solution. Aging of the pollen was studied after 5 and 12 d. Germination was determined as described previously (Hoekstra *et al.*, 1992a). Pollen was prehydrated in water vapor for at least 1 h at room temperature before imbibition.

Membrane isolation

Microsomal membranes were isolated from the pollen as described earlier (Hoekstra *et al.*, 1991), using 10 mM Tes, 1 mM EDTA, 1 mM EGTA, 1 mM diethylenetriamine-pentaacetic acid, 5 mM ascorbic acid and 1 mM DTT as the isolation medium. In the last step, the membrane fraction was resuspended in either H_2O or D_2O and centrifuged for 45 min at 100,000 x g. The isolated membrane fraction was used directly for further experiments.

Isolation of cytoplasmic proteins

Dried pollen was dissolved in 40 ml of ice-cold water. The pollen suspension was passed through a precooled (2°C) French pressure cell at 5000 p.s.i. After the homogenate was filtered through a serum filter, the suspension was centrifuged two times at 10,000g for 10 min to remove organelles. The supernatant was then subjected two times to a high speed centrifugation (30 min, 180,000g) to remove the membrane fraction. The supernatant was dialyzed against 100 mM NaCl in 10 mM Tris-buffer, pH 7.5, for 48 h, changing the buffer every 12 h. Subsequently, the dilute protein solution was concentrated by ultrafiltration, exclusion size 10 kD, or washed with D_2O before ultrafiltration.

IR spectroscopy

IR spectra were recorded on a Perkin-Elmer 1725 Fourier transform IR-spectrometer equipped with a liquid nitrogen-cooled mercury/cadmium/telluride detector and a Perkin-Elmer microscope interfaced to a personal computer. A homogeneous monolayer of pollen was prepared by slightly pressing the pollen grains between two diamond windows. If individual pollen grains were not arranged in a monolayer, clusters showed up as dark spots on the video screen, which impedes the energy throughput of the IR beam. Therefore, we have recorded only spectra of areas where no optical inhomogeneities could be detected with the IR-microscope. An area of approximately 500 × 500 μm was selected for FTIR analysis. Dehydrated protein samples were prepared on CaF_2 windows in a cabin continuously purged with dry air (RH < 3% at 24°C). The IR spectra to study the membrane fluidity were recorded in a temperature-controlled cell. Fifty to 60 spectra were recorded in the range between -60 and 80°C. IR spectra for protein studies were recorded at room temperature unless otherwise noted. The optical bench was purged with dry CO_2-free air (Balston; Maidstone Kent, UK) at a flow rate of 25 l min^{-1}. The acquisition parameters were 4 cm^{-1} resolution, 512 coadded interferograms (32 in the membrane fluidity studies), 2 cm s^{-1} moving mirror speed, 3500-900 cm^{-1} wave number

range, and triangle apodization function. The time needed for acquisition and processing of a spectrum was 4.5 min.

Data analysis

Spectral analysis and display were carried out using the Infrared Data Manager Analytical software, versions 2.5 and 3.5 (Perkin-Elmer). Membrane fluidity was monitored by observing the band position of either the CH_2 symmetric stretch band at approximately 2850 cm^{-1} or the asymmetric CH_2 stretch vibration at approximately 2920 cm^{-1}. The phase transition temperature was estimated from the discrete shifts in these band positions with temperature. The spectral region between 3000 and 2800 cm^{-1} was selected and second-derivative spectra were calculated. The second-derivative spectrum, was normalized, and the band position was calculated as the average of the spectral positions at 80% of the total peak height. For protein studies the spectral region between 1800 and 1500 cm^{-1} was selected. This region contains the amide-I and the amide-II absorption bands of the protein backbones. Second-derivative spectra were generated using the Perkin-Elmer routine for calculating second-derivative spectra. They were smoothed over 13 data points. The parameters for the Fourier self-deconvolution procedure were: smooth factor of 15.0 and a width factor of 30.0 cm^{-1}, using the interactive Perkin-Elmer routine for Fourier self-deconvolution. The linewidth in the deconvolved spectrum was chosen carefully to avoid introduction of erroneous bands (Surewicz *et al.*, 1993). Difference spectra were generated using an interactive routine (Perkin-Elmer), to subtract the spectrum of water from the corresponding spectrum containing the protein. The water spectra to be subtracted were collected under the same conditions as the membrane spectra. Criteria for the correctness of subtraction were (a) removal of the band near 2200 cm^{-1} and (b) flat baseline between 1800 and 2000 cm^{-1} for samples in H_2O and elimination of the strong band at 1209 cm^{-1} for samples in D_2O, avoiding negative sidelobes. Curve fitting of the original absorbance spectra was performed with Peakfit (Jandel software) of the original absorbance spectra between 1800 and 1500 cm^{-1}. Second-derivative and deconvolved spectra

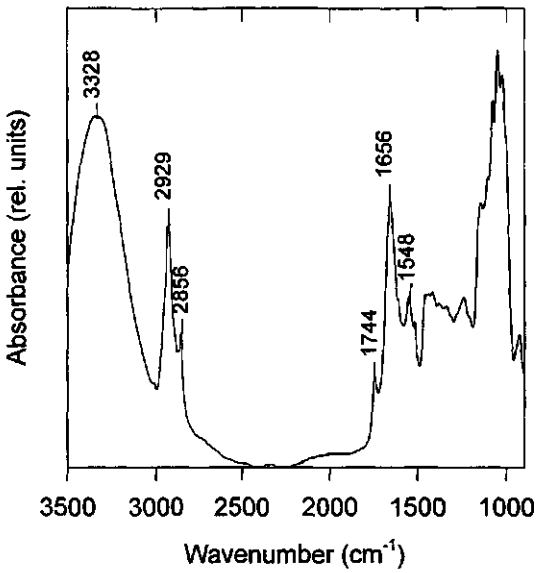

Figure 1. IR absorption spectrum of dry nonaged *T. latifolia* pollen.

were used to determine the number and the positions of the bands as starting parameters for the curve fitting procedure, assuming Pearson or Voigt band shapes.

Results and discussion

Infrared spectra of intact pollen

Figure 1 depicts the IR absorbance spectrum of dry, nonaged pollen. The total spectrum is mainly composed of carbohydrates (sugar and cell wall material), lipids and proteins. The band at 3328 cm^{-1} corresponds to OH-stretch vibrations, mainly arising from sucrose, which is a major component of *T. latifolia* pollen [23 % based on dry weight (Hoekstra *et al.*, 1992b)]. The bands at 2929 and 2856 cm^{-1} represent CH_2 stretch vibrations arising from phospholipids, neutral lipids, and partly from carbohydrates. In the 1800 - 1500 cm^{-1} region, at least 4 bands can be observed. Important bands for protein analysis are the amide-I band at 1656 cm^{-1} and the amide-II band at 1548 cm^{-1}. In the region below 1490 cm^{-1}, the CH_2 wagging (1342 - 1180 cm^{-1}) and scissoring (1455 cm^{-1}) bands occur, which can be very useful to study

membrane conformation (Blume *et al.*, 1988). The phosphate band at 1241 cm^{-1} can be used to study the interaction of phospholipid headgroups with sugars (Crowe *et al.*, 1984).

Membrane fluidity of isolated membranes and aging

Pollen was aged at 75% RH and 24°C for 0, 5 and 12 d. During aging, viability declined from 95% at day 0 to 40% after 5 d, and no pollen tubes were found after 12 d. Membranes isolated from nonaged pollen had an average T_m of about -7°C (Figure 2). In contrast, T_m of membranes isolated from 12-d-aged pollen increased to 25°C, with that from 5-d-aged pollen being intermediate. The shape of the frequency versus temperature curve of the 12-d-aged pollen, in particular, suggests the existence of two lipid populations, one with a T_m of about -12°C, and one of 25°C. This may be explained in several ways. One explanation is that lipid sorting is involved. Thus, due to different phase behavior of the various membrane lipid species, clusters may be formed in the same membrane. Alternatively, as we observe a mixture of various membrane

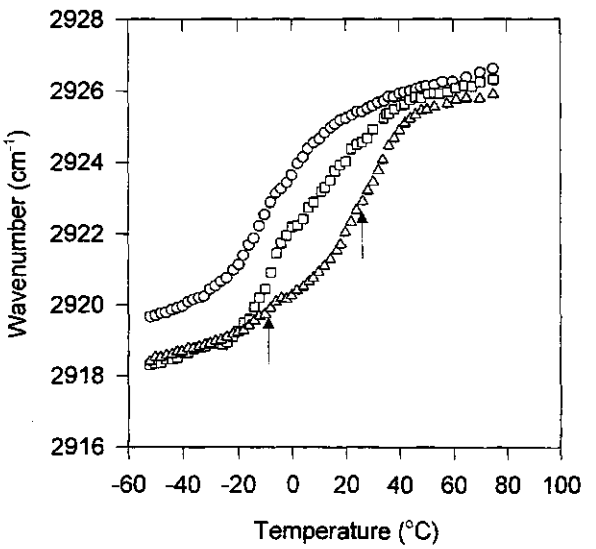

Figure 2. Wavenumber versus temperature plot (FTIR) of microsomal membranes isolated from *T. latifolia* pollen. The data points represent the asymmetric CH_2 stretching vibration of 0-d-aged pollen (circles), 5-d-aged pollen (squares), and 12-d-aged pollen (triangles). The arrows point to two transitions observed in 12-d-aged pollen membranes.

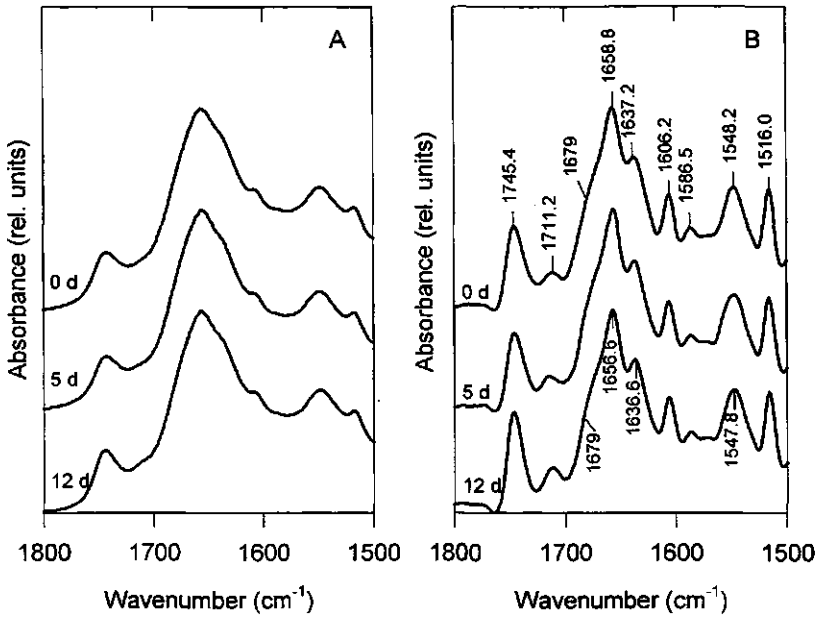

Figure 3. Absorbance (A) and deconvolved absorbance (B) IR spectra of 0-d, 5-d and 12-d-aged dry whole *T. latifolia* pollen. Aging was performed at 24°C in an atmosphere of 75% RH.

systems, one specific stable membrane system may be linked with the transition at -12°C. However, it leaves the observation intact that a considerable shift upwards in the T_m of a part of the isolated membranes occurs with aging. It is important to notice that at room temperature membranes from fresh pollen are mainly in the liquid crystalline phase, whereas in 12-d-aged pollen the membrane fluidity is drastically decreased. On account of the asymmetric stretch vibration data in Figure 2 it can be concluded that a part of the lipids in the rehydrated membranes from the aged pollen will be in gel phase at room temperature. This will cause the pollen to leak during and after rehydration and will considerably reduce viability.

Protein structure of whole grains and aging

For protein structural studies we have mainly focused on the amide-I band, with the absorbance maximum at approximately 1656 cm^{-1}. The amide-II band can give additional information about the protein structure and the solvent

exchange rate of a protein (Haris *et al.*, 1989). Since the original absorbance spectra yield rather broad bands in the amide region, mathematical data treatments such as second derivative analysis and Fourier self deconvolution have to be applied to resolve the fine details of the amide-I and amide-II bands.

Assignment of the several resolved bands to different protein structures is elaborated on later. Figure 3 shows the original and the deconvolved spectra of the 0-, 5- and 12-d-aged whole pollen grains. In order to save space the second derivative spectra are not shown. Both, second derivative and deconvolution analysis show that the amide-I band is composed of three bands, located at approximately 1637, 1657 and 1680 cm^{-1}. These bands do not shift significantly in band position or in relative intensity (see "Assignment and quantification of the protein secondary structure" on page 33), indicating that the proteins are conserved during aging. Even in aged, nonviable, pollen the protein structure was the same as in nonaged pollen, and irreversible protein aggregates (intermolecular β-sheet formation) were not detected as evidenced by the absence of low wavenumber peaks at approximately 1625 cm^{-1} (Prestrelski *et al.*, 1993; Sanders *et al.*, 1993). This was a surprising finding to us, since the membrane fluidity of isolated membranes changed drastically during aging in the sense that gel phase domains are present in the hydrated membranes of 12-d-aged pollen at room temperature (Figure 2). If gel

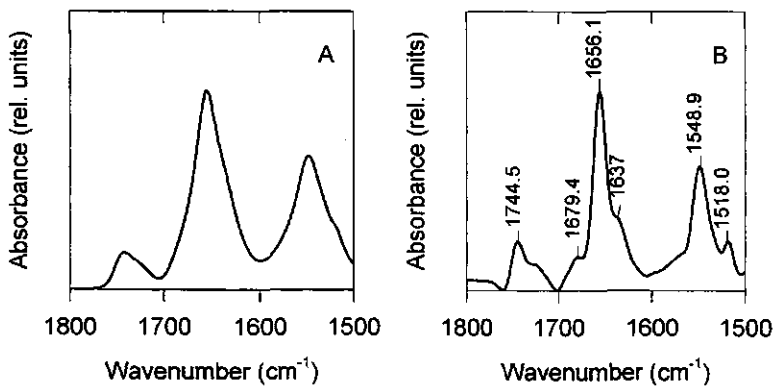

Figure 4. Absorbance (A) and deconvolved absorbance (B) IR spectra of isolated *T. latifolia* pollen membranes (hydrated).

phase domains are present in the membrane, the membrane proteins will favorably move to the remaining liquid crystalline lipid domains of the membrane and form protein domains there. We expected that this would result in irreversible protein aggregation. However, the protein structure was not affected by aging of the pollen.

Protein structure in isolated membranes during aging

To analyze whether particular protein secondary structures are present in specific cellular compartments of the pollen, membrane proteins and cytosolic proteins were characterized. In Figure 4 the original IR absorbance spectrum and the deconvolved spectrum of isolated pollen membranes are shown. The absorbance maximum is located at approximately 1656 cm^{-1}. The 5- and 12-d-aged pollen membranes show similar IR spectra (not shown). In the selected regions at least three broad absorbance bands can be observed: the band at approximately 1744 cm^{-1} can be assigned to ester bonds (lipids), the band at approximately 1656 cm^{-1} represents the amide-I band (proteins), and the band at approximately 1548 cm^{-1} represents the amide-II band (proteins). Deconvolution of the absorbance spectrum shows the presence of at least 7 bands in the 1800 - 1500 cm^{-1} region. Two bands can be distinguished in the ester band, three bands in the amide-I band, and one band in the amide-II band. The band at 1518 cm^{-1} probably represents the tyrosine residues in the protein, and the weak bands in the region from 1610 cm^{-1} to 1565 cm^{-1} may be attributed to the amino acid side chain vibrations (Chirgadze *et al.*, 1975). Three bands can be distinguished in the amide-I band, namely at 1637, 1656 and 1679 cm^{-1}. The IR spectrum of freeze-dried pollen membranes is shown in Figure 5. It can be seen that the IR bands in the hydrated membranes are somewhat sharper than those of the freeze-dried membranes (compare Figures 4 and 5). Furthermore, dehydration shifted the amide-I bands to higher wave numbers (1641, 1658 and 1682 cm^{-1}). Such effects of dehydration on (membrane) protein structure as studied by FTIR have been described earlier (Prestrelski *et al.*, 1993; Sarver and Krueger, 1993), and do not imply a major structural rearrangement of the membrane protein structure.

Our results indicate that aging is not correlated with the formation of irreversible clustered protein aggregates within the membrane. However, formation of reversible protein domains cannot be excluded but is also not very likely , since no line-broadening of the amide-I band has been observed.

Structure of cytoplasmic proteins

Cytoplasmic protein was isolated and purified from the pollen as described in "Materials and methods". Figure 5 shows the spectrum of this protein in the dehydrated state. The 1800 - 1500 cm^{-1} region of dried cytoplasmic proteins is very similar to the same region of the whole pollen grains in Figure 3. As expected, the bands at approximately 1745 cm^{-1} (lipids) and 1606 cm^{-1} (cell wall material) are absent in dried cytoplasmic proteins spectra of Figure 5.

The difference in environments between the *in situ* cytoplasmic protein and the isolated protein is that the latter is not embedded in a sucrose matrix. It is therefore surprising that the proteins retain their structure upon drying in the

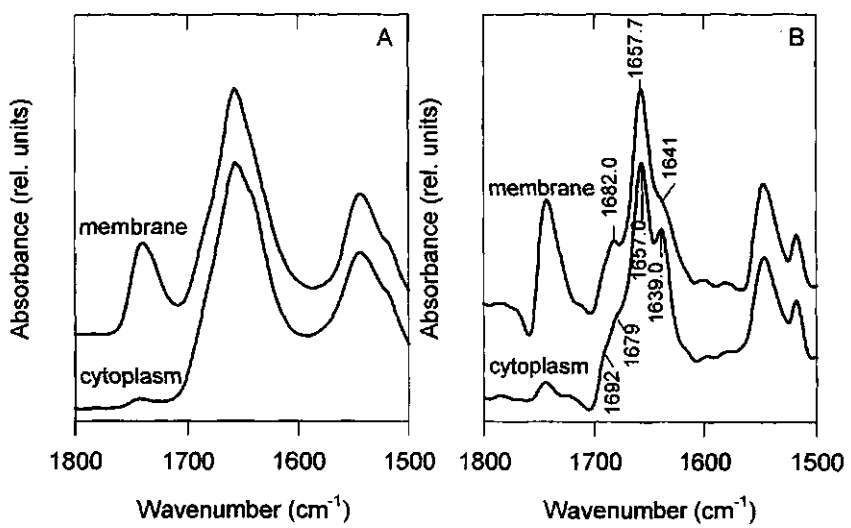

Figure 5. Absorbance (A) and deconvolved absorbance (B) IR spectra of dehydrated cytoplasmic *T. latifolia* pollen proteins and freeze-dried membranes.

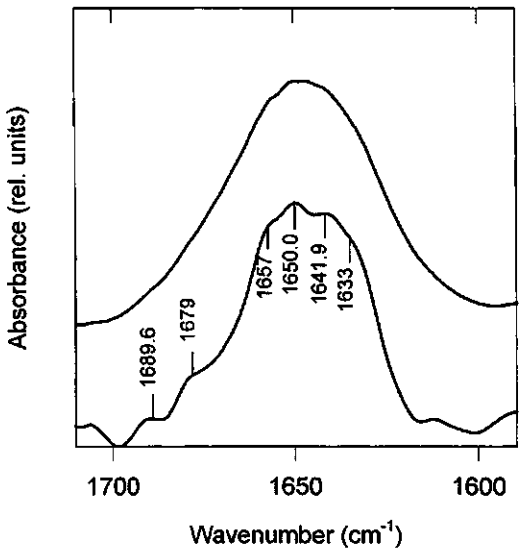

Figure 6. Absorbance (top trace) and deconvolved absorbance (bottom trace) IR spectra of cytoplasmic *T. latifolia* pollen proteins in D_2O.

absence of this sucrose. Water soluble proteins often denature when they are dried, which can be prevented by adding sugar prior to dehydration (Crowe *et al.*, 1987; Carpenter and Crowe, 1989; Prestrelski *et al.*, 1993). The cytoplasmic proteins in *T. latifolia* pollen apparently do not require sugar to maintain their structure upon dehydration. Perhaps the protection of these proteins against dehydration is conserved in the primary amino acid sequence.

As a comparison to the dried cytoplasmic protein, the spectrum of hydrated protein was recorded (Figure 6). Because of the interfering effect of H_2O in the amide-I region, protein structure was studied in D_2O. In D_2O the amide-I band shifts to a lower wave number (1650 cm^{-1}), indicating the presence of solvent-accessible protein regions (Haris *et al.*, 1989). Five amide-I bands can be observed at 1692, 1678, 1657, 1650 and 1641 cm^{-1}. Similar to the membrane proteins the spectral differences between dehydrated and deuterated proteins are not due to a structural rearrangement of the protein structure but represent a solvent effect to the amide-I band. Comparing the amide-I band of cytoplasmic protein in D_2O and in dehydrated state gives

information about the amount of solvent-accessible regions in the protein, which is discussed later.

Protein structure in denatured pollen

The excellent long-term stability of proteins compared to membrane lipids is surprising. This stability may be due to the embedding of proteins in a cytosol, in which sucrose is abundantly present, or may lie in the primary amino acid sequence, which conserves the secondary structure upon dehydration. Infrared spectroscopic studies have shown that sugars effectively prevent aggregation or denaturing of some proteins during dehydration (Prestrelski *et al.*, 1993). To determine whether the present FTIR *in situ* technique of protein structural analysis would indeed reveal denatured proteins, we artificially induced denaturation by heat treatment.

Protein structure in dry *T. latifolia* pollen did not alter upon heating for 1 h at 80°C (spectra not shown). This indicates that these proteins are resistant to heat treatment in the dry state, which has been demonstrated earlier for dry proteins in general by other methods (Ruegg *et al.*,1975; Fujita and Noda,

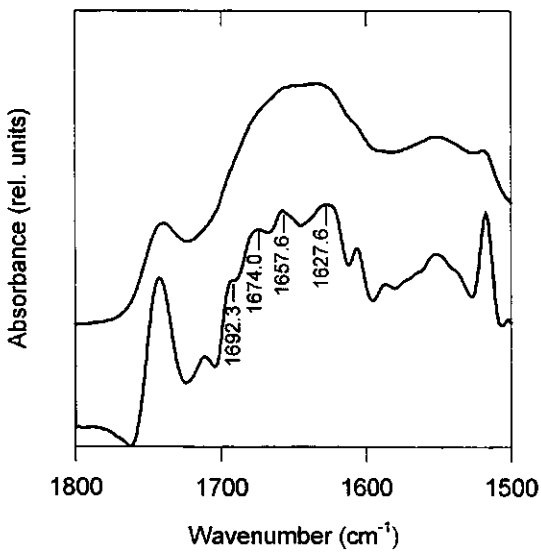

Figure 7. Absorbance (top trace) and deconvolved absorbance (bottom trace) IR spectra of denaturated *T. latifolia* pollen (boiling for 10 min).

1978). However, as expected for hydrated proteins (Ismail *et al.*, 1992; Arrondo *et al.*, 1994), in fully hydrated pollen the proteins are denatured when they are heated at 100°C for 5 or 10 min (Figure 7). The band at approximately 1657 cm^{-1} assigned to intermembrane α-helical structure decreases upon heat treatment in favor of the appearance of a band at approximately 1627 cm^{-1} and 1692 cm^{-1}. The band at approximately 1627 cm^{-1} is in a wavenumber region of the amide-I band, which is not usually observed in native proteins, but is indicative of irreversible protein domains in the membrane. The two bands indicate a special type of tightly packed β-sheet structure (extended β-sheet), characteristic for large protein aggregates in a membrane environment (Prestrelski *et al.*, 1993; Sanders *et al.*, 1993). The proteins in the isolated membranes were also heat denatured, with similar results (spectra not shown).

Assignment and quantification of protein secondary structure

Both theoretical and experimental studies with model polypeptides and proteins have shown that there is a good correlation between the amide-I band frequency and the type of secondary structure (Susi *et al.*, 1967; Surewicz and

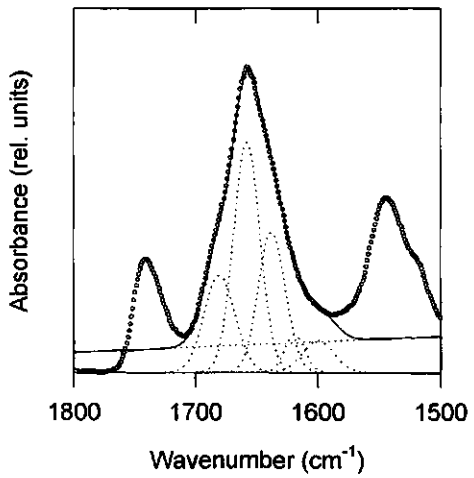

Figure 8. Curve-fitting procedure illustrated for freeze dried *T. latifolia* pollen membranes. Co-adding all the dashed peaks that were mathematically produced, and the absorption maxima of which were selected on account of peak positions in the second-derivative spectrum, results in a fit that resembles the original absorbance spectrum.

Mantsch, 1988; Haris *et al.*, 1989; Bandekar, 1992). Bands in the spectral range 1620 - 1640 cm^{-1} are attributed to β-sheet structure. Polypeptides and proteins in an α-helical conformation give rise to IR absorption in the range 1650 - 1658 cm^{-1}. For samples in water, there is normally overlap of α-helical absorption with that of random coil (Haris and Chapman, 1992). However, these two types of structures can be distinguished by carrying out experiments in D_2O. Because of rapid hydrogen-deuterium exchange of the peptide N-H groups in random coil structure, a large shift of its amide band to lower frequency will be observed (1647 - 1640 cm^{-1}).

The composite amide-I bands as observed in whole pollen, isolated membranes, and isolated cytoplasmic proteins represent different types of protein secondary structure. The band at approximately 1656 cm^{-1} observed in all spectra shown is dominated by α-helical structure, because α-helical vibrations are usually observed between 1650 and 1658 cm^{-1} (Surewicz and Mantsch, 1988; Haris *et al.*, 1989; Bandekar, 1992; Garcia-Quintana *et al.*, 1993). However, contributions from random coil structure to the band at approximately 1656 cm^{-1} cannot be excluded. A distinction between random coil structure and α-helical structure can be made by the different solvent accessibility of both types of secondary protein structure, as is discussed above. In D_2O the random coil absorption band shifts from under the α-helical band to a lower wavenumber range (1647 - 1640 cm^{-1}).

Assignment and quantification of the different secondary structures from IR-spectra can be done by several methods, as discussed by Surewicz *et al.* (1993). We have applied curve-fitting of the original absorbance spectra as described in "Materials and Methods". An example of the curve-fitting procedure [see Surewicz *et al.* (1993) for a critical assessment of the several available mathematical procedures of FTIR protein secondary structure analysis] is shown in Figure 8. Co-adding all the dashed peaks that were mathematically produced, the absorption maxima of which were selected on account of peak positions in the second derivative spectrum, should result in a fit that resembles the original absorbance spectrum. Individual contributions by the various protein secondary structures can thus be estimated (Table I). In the

isolated membranes the α-helical band at approximately 1658 cm^{-1} represents 48 % of the amide-I region. The other two bands at approximately 1637 and 1680 cm^{-1} represent turn structure. There is no major contribution from β-sheet structures in membrane proteins, as indicated by the lack of an absorbance band above 1690 cm^{-1}. A β-sheet structure would have shown two characteristic IR bands: one intense band between 1637 - 1630 cm^{-1} and one low intense band above 1690 cm^{-1} (Susi *et al.*, 1967). Since a band at approximately 1690 cm^{-1} is lacking, the band at approximately 1637 cm^{-1} has to be attributed entirely to turn structures (Mantsch *et al.*, 1993). In general, membrane proteins preferentially attain an α-helical conformation in the apolar membrane environment. Thus, the maximum number of intramolecular hydrogen bonds between C=O and NH groups can be formed per amino acid residue (Engelman *et al.*, 1986). An intermolecular β-sheet conformation in a membrane environment is adopted when large protein aggregates can satisfy the nonintramolecular hydrogen bonded C=O groups by means of intermolecular hydrogen bonding.

In Table 1 the curve-fitting results of the amide-I region of nonaged whole pollen is presented. It can be seen that the contribution of α-helical structure is reduced from 48 % in isolated membranes to 43 % in cytoplasmic

Table 1. Analysis of the amide-I region of various *T. latifolia* proteins.

System	Absorbance Maximum	Relative Area	Assignment
	cm^{-1}	%	
Whole pollen	1636	33	turn/β-sheet
	1658	40	α-helix
	1678	23	turn
	1694	4	β-sheet
Cytoplasmic proteins	1637	33	turn/β-sheet
(dehydrated)	1658	43	α-helix
	1678	18	turn
	1692	6	β-sheet
Membrane proteins	1637	29	turn
(freeze dried)	1658	48	α-helix
	1680	23	turn

proteins and 40 % in whole pollen. The somewhat arbitrary selection of the baseline and the intrinsic linewidth of the composed amide-I bands does not allow for great precision of the percentages of the different secondary structures. The similarity in band pattern and band shape of the whole pollen and that of the cytoplasmic proteins indicates that the protein band of the whole pollen is dominated by the cytoplasmic proteins, which is in accordance with the quantities of proteins in the cytoplasm and the membrane environment (compare Wille *et al.*, 1984; Evans *et al.*, 1991; with van Bilsen *et al.*, 1994b). The dry cytoplasmic protein structure is dominated by a band at approximately 1658 cm^{-1} (Figure 5). In D_2O this band decreases in intensity and bands at approximately 1650 cm^{-1} and 1641 cm^{-1} appear (Figure 6). These bands can be explained by the solvent accessibility of the cytoplasmic proteins. The band at approximately 1641 cm^{-1} is dominated by random coil structure. This band shifts from under the dry 1657 cm^{-1} band and becomes visible only in D_2O. The band at 1650 cm^{-1} is more difficult to explain. The wavenumber of this band is in the range of α-helical absorptions (too high for random coil structure). This band might represent solvent accessible α-helical structure shifting from under the 1657 cm^{-1} band in the dried protein IR spectrum to a lower wavenumber position due to deuteration.

It is rather surprising that the cytoplasmic proteins consist of such a considerable amount of α-helical structure. The presence of these α-helical domains may be the reason that the bulk proteins in pollen are protected against the destructive effects of dehydration. In an α-helical structure intramolecular hydrogen bonds can compensate for the reduced protein-water hydrogen bonds.

Conclusions

The IR-spectra suggest that fresh pollen membranes are mainly in the liquid crystalline phase at room temperature, whereas in aged pollen the membrane fluidity is drastically decreased. Furthermore, gel phase domains may occur in aged pollen membranes at 20°C, which will cause leakage and reduce viability. Formation of gel phase domains may drive the membrane

proteins to the remaining liquid crystalline lipid domains. We expected the resulting protein domains to cause irreversible protein aggregation (denaturation). However, this was not observed on account of *in situ* FTIR-assessment of the amide-I bands. Thus, the massive leakage of solutes from aged pollen as observed previously in our lab (van Bilsen *et al.*, 1994a) is due to changes in membrane viscosity (Figure 2) and not to membrane protein denaturation.

Secondary structure of isolated cytoplasmic proteins resembled that of whole pollen and was conserved upon drying in the absence of sucrose. The major secondary structure component of the cytoplasmic protein fraction is an α-helical structure.

Heat denaturing experiments with intact hydrated pollen show the characteristic low (at approximately 1627 cm^{-1}) and high (at approximately 1692 cm^{-1}) wavenumber bands of irreversible protein aggregates. The results presented in this paper show that *in situ* FTIR microspectroscopy is an extremely suitable technique to study protein secondary structure at different hydration levels and physiological conditions.

Acknowledgements

This project was financially supported by the Life Sciences Foundation, which is subsidized by the Netherlands Organization for Scientific Research.

References

Arrondo, J.L.R., Castresana, J., Valpuesta, J.M., Goni, F.M. (1994) Structure and thermal denaturation of crystalline and noncrystalline cytochrome oxidase as studied by infrared spectroscopy. *Biochemistry* **33,** 11650-11655.

Bandekar, J. (1992) Amide modes and protein conformation. *Biochim. Biophys. Acta* **1120,** 123-143.

Blume, A., Hubner, W., Messner, G. (1988) Fourier transform infrared spectroscopy of ^{13}C=O-labeled phospholipids hydrogen bonding to carbonyl groups. *Biochemistry* **27,** 8239-8249.

Byler, D.M., Susi, H. (1986) Examination of the secondary structure of proteins by deconvolved FTIR spectra. *Biopolymers* **25,** 469-487.

Carpenter, J.F., Crowe, J.H. (1989) An infrared spectroscopic study of the interactions of carbohydrates with dried proteins. *Biochemistry* **28,** 3916-3922.

Chirgadze, Y.N., Fedorov, O.V., Trushina, N.P. (1975) Estimation of amino acid residue side-chain absorption in the infrared spectra of protein solutions in heavy water. *Biopolymers* **14,** 679-695.

Crowe, J.H., Crowe, L.M., Carpenter, J.F., Aurell Wistrom, C. (1987) Stabilization of dry phospholipid bilayers and proteins by sugars. *Biochem. J.* **242,** 1-10.

Crowe, J.H., Crowe, L.M., Chapman, D. (1984) Preservation of membranes in anhydrobiotic organisms: the role of trehalose. *Science* **223,** 701-703.

Crowe, J.H., Crowe, L.M., Hoekstra, F.A. (1989a) Phase transitions and permeability changes in dry membranes during rehydration. *J. Bioenerg. Biomem.* **21,** 77-91.

Crowe, J.H., Hoekstra, F.A., Nguyen, K.H.N., Crowe, L.M. (1996) Is vitrification involved in depression of the phase transition temperature in dry phospholipids? *Biochim. Biophys. Acta* **1280,** 187-196.

Crowe, J.H., Leslie, S.B., Crowe, L.M. (1994) Is vitrification sufficient to preserve liposomes during freeze-drying? *Cryobiol.* **31,** 355-366.

Crowe, J.H., McKersie, B.D., Crowe, L.M. (1989b) Effects of free fatty acids and transition temperature on the stability of dry liposomes. *Biochim. Biophys. Acta* **979,** 7-10.

Engelman, D.M., Steitz, T.A., Goldman, A. (1986) Identifying nonpolar transbilayer helices in amino acid sequences of membrane proteins. *Ann. Rev. Biophys. Chem.* **15,** 321-353.

Evans, D.E., Taylor, P.E., Singh, M.B., Knox, R.B. (1991) Quantitative analysis of lipids and protein from the pollen of *Brassica napus L. Plant Sci.* **73,** 117-126.

Finer, E.G., Darke, A. (1974) Phospholipid hydration studied by deuteron magnetic resonance. *Phys. Lipids* **12,** 1-16.

Fujita, Y., Noda, Y. (1978) Effect of hydration on the thermal denaturation of lysozyme as measured by differential scanning calorimetry. *Bull. Chem. Soc. Japan* **51,** 1567-1568.

Garcia-Quintana, D., Garriga, P., Manyosa, J. (1993) Quantitative characterization of the secondary structure of rhodopsin in disc membrane by means of Fourier transform infrared spectroscopy. *J. Biol. Chem.* **268,** 2403-2409.

Haris, P.I., Coke, M., Chapman, D. (1989) Fourier transform infrared spectroscopic investigation of rhodopsin structure and its comparison with bacteriorhodopsin. *Biochim. Biophys. Acta* **995,** 160-167.

Haris, P.I., Chapman, D. (1992) Does Fourier-transform infrared spectroscopy provide useful information on protein secondary structures. *Trends. Biochem. Sci.* **17,** 328-333.

Hemminga, M.A., Sanders, J.C., Wolfs, C.J.A.M., Spruijt, R.B. (1992) Spectroscopy of lipid-protein interactions: structural aspects of two different forms of the coat protein of bacteriophage M13. *Prog. Lipid Res.* **31,** 301-333.

Hoekstra, F.A., Crowe, J.H., Crowe, L.M. (1991) Effect of sucrose on phase behavior of membranes in intact pollen of *Typha latifolia* L., as measured with Fourier transform infrared spectroscopy. *Plant Physiol.* **97,** 1073-1079.

Hoekstra, F.A., Crowe, J.H., Crowe, L.M. (1992a) Germination and ion leakage are linked with phase transitions of membrane lipids during imbibition of *Typha latifolia* pollen. *Physiol. Plant.* **84,** 29-34.

Hoekstra, F.A., Crowe, J.H., Crowe, L.M., van Roekel, T., Vermeer, E. (1992b) Do phospholipids and sucrose determine membrane phase transitions in dehydrating pollen species? *Plant. Cell. Environ.* **15,** 601-606.

Ismail, A.A., Mantsch, H.H., Wong, P.T.T. (1992) Aggregation of chymotrypsin: portrait by infrared spectroscopy. *Biochim. Biophys. Acta* **1121,** 183-188.

Knowlton, H.E. (1922) Studies in pollen, with special reference to longevity. *Cornell Univ. Agric. Exp. Sta. Memoir.* **52,** 751-793.

Mantsch, H.H., Perczel, A., Hollosi, M., Fasman, G.D. (1993) Characterization of β-turns in cyclic hexapeptides in solution by Fourier transform IR spectroscopy. *Biopolymers* **33,** 201-207.

McKersie, B.D., Crowe, J.H., Crowe, L.M. (1989) Free fatty acid effects on leakage, phase properties, and fusion of fully hydrated model membranes. *Biochim. Biophys. Acta* **982,** 156-160.

Messerschmidt, R.G., Reffner, J.A. (1988) FT-IR microscopy of biological samples: a new technique for probing cells. *In* DE Newsbury ed, Microbeam Analysis. San Francisco Press, Inc, San Francisco, pp 215-217.

Prestrelski, S.J., Tedeschi, N., Arakawa, T., Carpenter, J.F. (1993) Dehydration-induced conformational transitions in proteins and their inhibition by stabilizers. *Biophys. J.* **65,** 661-671.

Reffner, J.A. (1989) Molecular microspectral mapping with the FT-IR microscope. *Inst. Phys. Conf. Ser.* **98,** (chapter 130): 559-569.

Ruegg, M., Moor, U., Blanc, B. (1975) Hydration and thermal denaturation of P-lactoglobulin. A calorimetric study. *Biochim. Biophys. Acta* **400,** 334-342.

Sanders, J.C., Haris, P.I., Chapman, D., Otto. C., Hemminga, M.A. (1993) Secondary structure of M13 coat protein in phospholipids studied by circular dichroism, Raman, and Fourier transform infrared spectroscopy. *Biochemistry* **32,** 12446-12454.

Sarver, R.W., Krueger, W.C. (1993) Infrared investigation on the conformation of proteins deposited on polyethylene films. *Anal. Biochem.* **212,** 519-525.

Surewicz, W.K., Mantsch, H.H. (1988) New insight into protein secondary structure from resolution-enhanced infrared spectra. *Biochim. Biophys. Acta* **952:** 115-130.

Surewicz, W.K., Mantsch, H.H., Chapman, D. (1993) Determination of protein secondary structure by Fourier transform infrared spectroscopy: a critical assessment. *Biochemistry* **32,** 389-394.

Susi, H. (1969) Infrared spectra of biological macromolecules. In: Timasheff, S.N., Fasman, G.D. (eds.) Biological Macromolecules, Vol 2. Marcel Dekker, New York, pp. 575-663.

Susi, H., Timasheff, S.N., Stevens, L. (1967) Infrared spectra and protein conformations in aqueous solutions. I. The amide I band in H_2O and D_2O solutions. *J. Biol. Chem.* **242,** 5460-5466.

van Bilsen, D.G.J.L., Hoekstra, F.A. (1993) Decreased membrane integrity in aging *Typha latifolia* L. pollen: Accumulation of lysolipids and free fatty acids. *Plant Physiol.* **101,** 675-682.

van Bilsen, D.G.J.L., Hoekstra, F.A., Crowe, L.M., Crowe, J.H. (1994a) Altered phase behavior in membranes of aging dry pollen may cause imbibitional leakage. *Plant Physiol* **104,** 1193-1199.

van Bilsen, D.G.J.L., van Roekel, T., Hoekstra, F.A. (1994b) Declining viability and lipid degradation during pollen storage. *Sex Plant Reprod* **7,** 303-310.

Wille, H., Imdorf, A., Wille, M., Kilchenmann, V. (1984) Seasonal course of pollen protein content at some Swiss observation stations. *Schweiz. Bienen Z.* **107,** 407-417.

Chapter 3

Heat stability of proteins in desiccation-tolerant cattail (*Typha latifolia* L.) pollen: a Fourier transform infrared spectroscopic study

Willem F. Wolkers and Folkert A. Hoekstra

Abstract

Secondary structure and aggregation behavior of proteins, as determined *in situ* in *Typha latifolia* pollen, were studied by means of Fourier transform infrared microspectroscopy. The amide-I band, arising from the peptide backbone, was recorded over a temperature range from -50 to 120°C at different hydration levels of the pollen. Dehydration increased the denaturation temperature of the proteins and decreased the extent of protein structural rearrangements due to heating. Below 0.16 g H_2O g^{-1} dry weight (DW), the temperature at which the proteins began to denature increased rapidly. In fully hydrated pollen, denaturation commenced above 60°C, whereas in very dry pollen (0.01 g H_2O g^{-1} DW), it did at approximately 116°C. Temperature-induced aggregation of proteins was accompanied by the appearance of an infrared band in the region between 1625 and 1630 cm^{-1} and a weak band around 1692 cm^{-1}. These bands are characteristic of intermolecular extended β-sheet structures. The α-helical band position (band around 1657 cm^{-1}) did not shift substantially over a temperature range from -40 to 120°C at all the water contents tested, indicating that α-helical structures are particularly heat stable. We show here that the proteins in dry desiccation-tolerant pollen are particularly heat stable.

Also published in Comparative Biochemistry and Physiology **117A,** 349-355 (1997)

Introduction

The adaptation of desiccation-tolerant animals and plants to periods of extreme drought has been the subject of many biophysical and biochemical studies (Crowe *et al.*, 1992; Vertucci and Farrant, 1995; Crowe *et al.*, 1997). Suspended life in desiccated organisms requires protection of biomolecules such as phospholipids in the membranes and proteins and adaptation of the cellular organization. Desiccation-tolerant cells are characterized by the presence of large amounts of sugars, particularly disaccharides (Crowe *et al.*, 1984). An important feature of these sugars in relation to desiccation tolerance is their ability to form a glassy state under dry conditions at room temperature (Williams and Leopold, 1989; Leopold *et al.*, 1994). Also, in model lipid systems the glassy state is crucial for the preservation of vesicles during drying and rehydration (Crowe *et al.*, 1994, 1996). Furthermore, sugars can replace water during dehydration (Crowe *et al.*, 1987) by interacting with the polar headgroups of the membrane phospholipids (Crowe *et al.*, 1996). Labile proteins are protected by sugars from major structural rearrangements during dehydration (Carpenter and Crowe, 1989; Prestrelski *et al.*, 1993).

In previous work using FTIR, we showed the extreme stability of proteins in *Typha latifolia* pollen during accelerated aging (Wolkers and Hoekstra, 1995). Apart from intrinsic properties of these proteins, the excellent stability might stem from the glassy environment in which the proteins are embedded. In this pollen, glasses are formed at room temperature during drying (Buitink *et al.*, 1996), which is expected considering the high sucrose content of 23% on a DW basis (Hoekstra *et al.*, 1992).

FTIR is one of the most suitable techniques for elucidating the structural organization of dehydrated proteins. Information on protein secondary structure can be obtained by a study of the amide-I and amide-II absorption bands arising from the peptide backbone (Susi, 1969; Byler and Susi, 1986; Surewicz and Mantsch, 1988). The amide-I band mainly arises from the C=O stretching vibration and the amide-II band mainly from the N-H bending vibration (Susi *et al.*, 1967).

In the present article, we studied the structural organization of proteins in desiccation-tolerant *T. latifolia* pollen at different water contents, using *in situ* FTIR microspectroscopy. Studies on pollen proteins indicated that the protein fraction consists of many different enzymic proteins and that, different from seed, there is no accumulation of one abundant type of storage protein (Zarsky *et al.*, 1985; Capkova *et al.*, 1994). Insight in the *in situ* stability of these proteins was obtained by studying the temperature-induced protein aggregation. This work entails an exploration of the amide-I and amide-II bands over a broad temperature range to elucidate the events leading to protein reorganization and intermolecular protein aggregation at different hydration levels.

Materials and methods

Pollen

Collecting and handling of *Typha latifolia* L. pollen were performed as described earlier (Hoekstra *et al.*, 1991). The pollen used was harvested in June 1993. To obtain different water contents, pollen was equilibrated for 24 h in air of 20 - 100% RH at 24°C. The RH was regulated by cooling water vapor-saturated air in a distillation column at different temperatures and then heating this air up to 24°C. The RH was measured with a Rotronic hygroscope (±2% RH, Rotronic AG, Zurich, Switzerland).

Membrane isolation

Microsomal membranes were isolated from the pollen as described earlier (Hoekstra *et al.*, 1991), using 10 mM Tes, 1 mM EDTA, 1 mM EGTA, 1 mM diethylenetriamine-pentaacetic acid, 5 mM ascorbic acid and 1 mM dithiothreitol, pH 7.4, as the isolation medium. In the last step, the membrane fraction was resuspended in either H_2O or D_2O and centrifuged for 45 min at 100,000 x g. The isolated membrane fraction was either directly used for FTIR analysis or after lyophilization for 24 h.

IR spectroscopy

IR spectra were recorded on a Perkin-Elmer 1725 Fourier transform IR-spectrometer (Perkin-Elmer, Beaconsfield, Buckinghamshire, UK) equipped with a liquid nitrogen-cooled mercury/cadmium/telluride detector and a Perkin-Elmer microscope interfaced to a personal computer as described elsewhere (Wolkers and Hoekstra, 1995). A homogeneous monolayer of pollen was prepared by slightly pressing the pollen grains between two diamond windows. Fifty to 60 spectra were recorded over a temperature range from -50 to 140°C within a time period of 2 h. The acquisition parameters were 4 cm^{-1} resolution, 32 co-added interferograms, 2 $cm.s^{-1}$ moving mirror speed, 3500-900 cm^{-1} wave number range and triangle apodization function. The time needed for acquisition and processing of a spectrum was 0.5 min.

Data analysis

Spectral analysis and display were carried out using the Infrared Data Manager Analytical Software, versions 2.5 and 3.5 (Perkin-Elmer, Beaconsfield, Buckinghamshire, UK). For protein studies, the spectral region between 1800 and 1500 cm^{-1} was selected. This region contains the amide-I and the amide-II absorption bands of the protein backbones. Second derivative spectra were calculated over this region, and after normalization of these bands, the exact band positions were determined by calculating the average of the spectral positions of the composite amide-I and amide-II bands at 80% of the total peak height. Second derivative spectra were smoothed over 19 data points. Changes in protein secondary structure were monitored from the discrete shifts in position of these bands with temperature. Deconvolved spectra were calculated, using the interactive Perkin-Elmer routine for Fourier self-deconvolution. The parameters for the Fourier self-deconvolution procedure were smooth factor 15.0 and a width factor of 30.0 cm^{-1}. The line width in the deconvolved spectrum was carefully chosen to avoid introduction of erroneous bands (Surewicz *et al.*, 1993).

Results

Assignment of IR bands in dry pollen

The *in situ* aggregation behavior of proteins in *T. latifolia* pollen was studied by FTIR microspectroscopy. Characteristic peaks in the IR spectrum of *T. latifolia* pollen can be attributed to carbohydrates (sugar and cell wall material), lipids and proteins (Wolkers and Hoekstra, 1995). The 1800 - 1500-cm^{-1} region of the IR spectrum contains the protein bands. Figure 1A shows the temperature dependence of the 1800 - 1500-cm^{-1} region of the IR absorbance spectrum of dry pollen (0.02 g H_2O g^{-1} DW). These spectra show the presence of at least four bands in the 1800 - 1500-cm^{-1} region, from which the amide-I band around 1657 cm^{-1} and the amide-II band around 1550 cm^{-1} were selected for protein structural analysis. A broadening of the amide-I and the amide-II band was observed in the higher temperature range.

To resolve the protein secondary structure rearrangement in more detail,

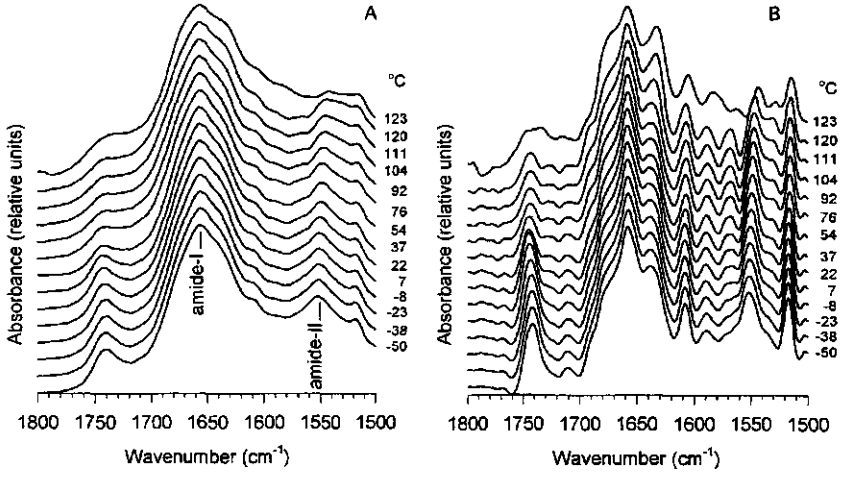

Figure 1. Absorbance (A) and deconvolved (B) IR spectra of the 1800 - 1500-cm^{-1} region of dry (0.02 g H_2O g^{-1} DW) *T. latifolia* pollen as a function of temperature.

deconvolved spectra were calculated (Figure 1B). Deconvolution shows that the amide-I band is composed of at least four bands. These bands have previously been assigned to α-helical structure (1657 cm^{-1}), turn structure (1637 and 1680 cm^{-1}) and β-sheet structure (1637 and 1692 cm^{-1}) (Wolkers and Hoekstra, 1995 and references therein). A band at 1615 cm^{-1} mainly arises from cell wall material, but it also might contain contributions from amino acid side chains such as tyrosine (Chirgadze *et al.*, 1975). The shift of the band around 1637 cm^{-1} to lower wavenumbers with temperature (1630 cm^{-1} in fully denatured pollen) is characteristic for aggregation of pollen proteins (Figure 1B). This can be interpreted as signs of the formation of extended β-sheet structures. In denatured, dry pollen there still was a large amount of remaining α-helical protein structures.

The initial position of the amide-II band at low temperatures is located around 1550 cm^{-1}. This is in agreement with a high α-helical content of the proteins (Bandekar, 1992). This band shifts to lower wavenumbers upon increasing of the temperature, which may be explained by weakening of the

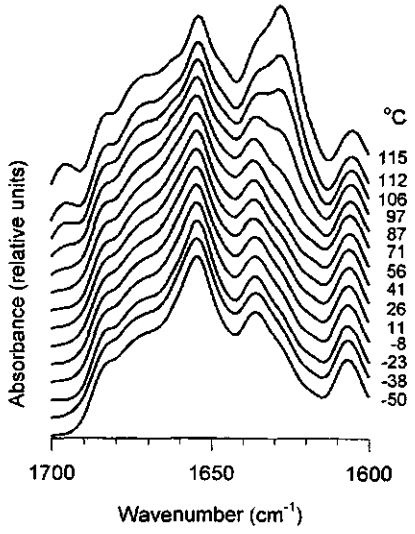

Figure 2. Deconvolved IR spectra of the 1700 - 1600-cm^{-1} region of *T. latifolia* pollen at 0.16 g H_2O g^{-1} DW as a function of temperature.

C=O···H-N internal hydrogen bonds. At higher temperatures, especially above 80°C, the appearance of two other bands around 1568 cm^{-1} and 1535 cm^{-1} can be observed, but the first signs of these bands are already visible at temperatures above 0°C. These bands can be associated with the presence of turn-like structures and β-sheet structures. The relation of these bands with denaturation is not yet clear, but a study of the amide-II bands with temperature can give information about the entropic changes of the N-H bending motions. Because this is beyond the scope of this article we have concentrated on the amide-I region to study protein stability.

Assignment of IR bands in partially hydrated pollen

Figure 2 shows the deconvolved spectra of the amide-I region in pollen with the much higher water content of 0.16 g H_2O g^{-1} DW. Alterations in the protein secondary structure occurred at a much lower temperature (around 70°C) than with the dry pollen (0.02 g H_2O g^{-1} DW), as judged from the appearance of bands at 1627 cm^{-1} and 1697 cm^{-1}. These bands indicate the formation of tightly packed intermolecular β-sheet structures (Prestrelski *et al.*, 1993). In the dry pollen (Figure 1B), these β-sheet structures were much less pronounced.

Proportion of heating-induced protein structural rearrangements at different hydration levels

To resolve possible differences in the proportion of protein denaturation between pollen with either low or elevated water contents, difference spectra are presented (Figures 3A and 3B). These spectra concern the difference between the spectrum recorded at the lowest temperature and all those recorded at higher temperatures. Normalized spectra were used for this purpose. In partially hydrated pollen (0.16 g H_2O g^{-1} DW), a band around 1627 cm^{-1} appeared at temperatures above 70°C, which can be associated with the formation of intermolecular β-sheet structures. Figure 3B shows that also in very dry pollen (0.01 g H_2O g^{-1} DW) denaturation is accompanied by the appearance of a band, in this case, around 1629 cm^{-1}, which began to appear

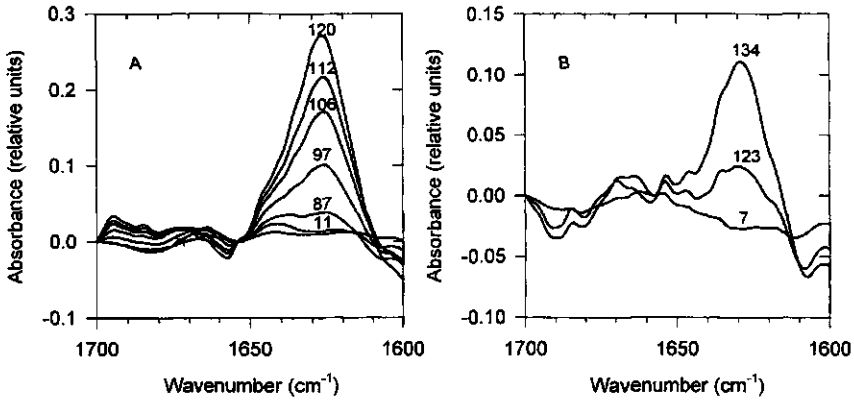

Figure 3. Difference spectra of the 1700 - 1600-cm^{-1} region of *T. latifolia* pollen between the normalized absorbance spectrum at -50°C and the normalized absorbance spectra at the indicated temperatures (°C). The water content of the pollen was 0.16 (A) and 0.01 g H_2O g^{-1} DW (B). The top spectra represent those of fully heat-denatured pollen.

above 110°C. However, in this case, the signal-to-noise ratio of the difference spectra was worse than for the partially hydrated pollen, probably due to scattering of the IR beam. If we assume protein denaturation in pollen to be a two-state model of native and denatured protein (Mücke and Schmidt, 1994), the denaturation temperature can be calculated from the difference spectra by plotting the line heights of the band around 1627 cm^{-1} against the temperature. The midpoint of the discrete shift in such a plot reflects the denaturation temperature (data not shown). The denaturation temperature of protein, calculated in this way, was 126 and 102°C for the very dry pollen (0.01 g H_2O g^{-1} DW) and the partially hydrated pollen (0.16 g H_2O g^{-1} DW), respectively. Fully hydrated pollen (2.0 g H_2O g^{-1} DW) had a denaturation temperature of 72°C.

To estimate the proportion of protein structural rearrangements, the difference spectra of the fully denatured and the native pollen proteins in Figures 3A and 3B were compared according to their surface areas. The calculated area was 8 for the partially hydrated pollen and 4 for dry pollen. This indicates that the amount of protein secondary structure that has undergone a structural rearrangement during heating increased with hydration. The surface area under the difference spectrum of fully hydrated pollen (2.0 g H_2O g^{-1} DW)

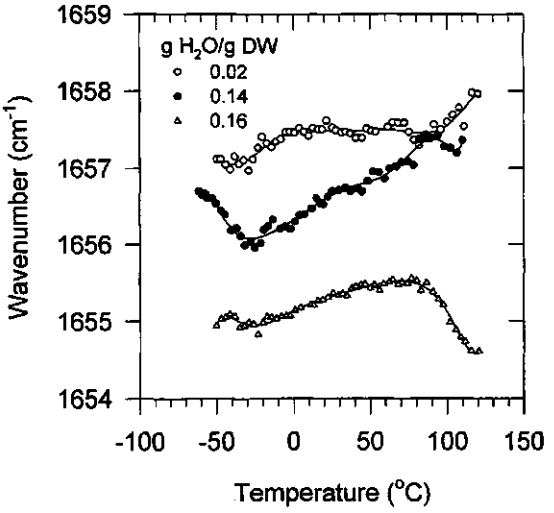

Figure 4. Wavenumber *vs* temperature plot (FTIR) of the amide-I band denoting α-helical protein structure of *T. latifolia* pollen at different water contents. Curve-fitting was performed with the ninth-order polynomial function as an aid to the eye.

was similar (7.8) as in the partially hydrated pollen. This indicates that the extent of protein structural rearrangements is at its maximum at 0.16 g H_2O g^{-1} DW and above.

Temperature stability of α-helical structures

The temperature dependence of the position of the amide-I bands gives information about the flexibility of the C=O vibrations in the different protein secondary structures. Figure 4 shows such a wavenumber versus temperature plot for the α-helical band around 1656 cm^{-1}, which occupies most of the amide-I band of the native proteins. The α-helical band position did not shift substantially over a temperature range from -50 to 120°C (band around 1656 cm^{-1}) for all the water contents shown, indicating that these structures are particularly heat stable. The α-helical band positions tended to decrease with higher hydration levels. This may be due to an alteration of the protein solvent interactions [water causes a downward shift of the band position (Prestrelski *et al.*, 1993 and references therein)].

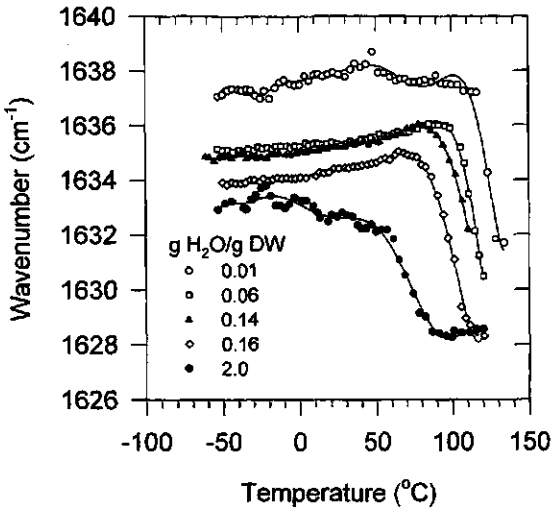

Figure 5. Wavenumber *vs* temperature plot (FTIR) of the amide-I band denoting turn and β-sheet protein structure in *T. latifolia* pollen, at different water contents. Curve-fitting was performed with the ninth-order polynomial function as an aid to the eye.

Temperature stability of turn and β-sheet structures

In Figure 5, the position of the band around 1635 cm^{-1}, assigned to turn structures and β-sheet structures, is plotted as a function of the temperature. As is shown in Figures 2 and 3, protein denaturation is accompanied by the appearance of a band around 1627 cm^{-1} and not by a shift of the band around 1635 cm^{-1} to lower wavenumbers. We could nevertheless obtain a precise determination of the temperature where the position of the band around 1635 cm^{-1} fell to lower wavenumber position. In very dry pollen, this band was observed around 1638 cm^{-1} (dehydration causes upward shifts in band positions, Prestrelski *et al.*, 1993) and initially hardly changed in position with temperature. Above 110°C, the band position sharply fell to lower wavenumbers due to the formation of intermolecular β-sheet structures. The initial band position was lower at higher hydration levels of the proteins. At water contents between 0.06 and 0.16 g H_2O g^{-1} DW, the band initially showed a slight increase with increasing temperature, which is probably due to a weakening of the C=O···H-N internal hydrogen bonds at higher temperatures.

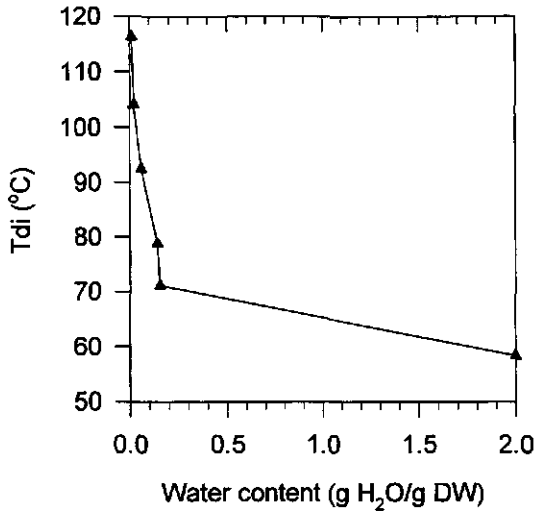

Figure 6. Plot of the temperature at which initial protein denaturation began (Tdi) in *T. latifolia* pollen as a function of the water content.

However, the band position fell upon further increase of the temperature. Figure 6 shows the temperature (derived from Figure 5) where initial denaturation processes started to occur (Tdi) as a function of the water content. The major increase in Tdi occurred below water contents of around 0.16 g H_2O g^{-1} DW.

Temperature stability of membrane proteins

The protein spectrum of whole pollen is mainly composed of cytoplasmic proteins, with a smaller contribution of membrane proteins (Wolkers and Hoekstra, 1995). The heat stability of proteins in microsomal membranes isolated from pollen is shown in Figure 7. The denaturation temperature of hydrated membranes as judged from the amide-I band around 1632 cm^{-1} was around 50°C. During denaturation, membrane proteins exhibited an absorption maximum shifting from 1633 to 1625 cm^{-1}. In the apolar membrane environment, the formation of large clusters of extended β-sheet can be energetically favorable because all the C=O groups are intermolecularly hydrogen bonded (Engelman *et al.*, 1986). After freeze-drying of the membrane pellet, the band around 1632 cm^{-1}, as found in hydrated membranes, did not change much in wavenumber position. This indicates that the amount of solvent

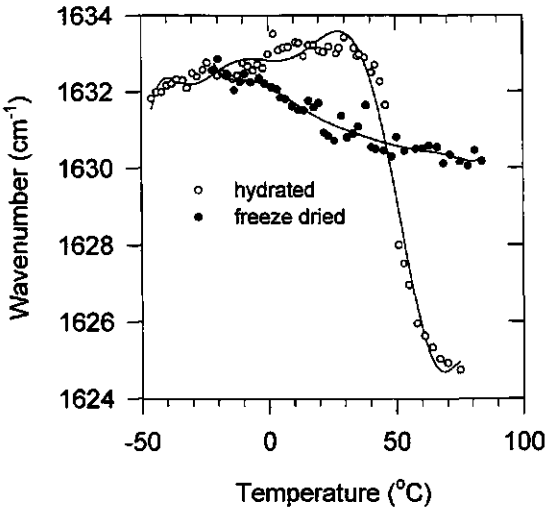

Figure 7. Wavenumber *vs* temperature plot (FTIR) of the amide-I band in membranes (hydrated and freeze-dried) isolated from *T. latifolia* pollen. Curve-fitting was performed with the ninth-order polynomial function as an aid to the eye.

accessible regions in membrane proteins is less than in cytoplasmic proteins. Freeze-dried membrane proteins were protected from denaturation processes up to temperatures of at least 90°C (Figure 7).

Discussion

When pollen is dry, it can be conserved at deep freeze temperatures for decades (Hoekstra, 1995). It also has considerable tolerance to elevated temperatures. For example, survival times of dry apple pollen is 24 h at 50°C, about 6 h at 70°C and about 15 min at 90°C (Marcucci *et al.*, 1982). In other dry anhydrobiotic organisms, such as *Artemia* cysts, a similar tolerance against high temperatures was found (Iwanami, 1973). It has been suggested that desiccation-tolerant pollen is also potentially heat tolerant. In the present study it is shown for the first time that the expected heat stability of proteins in desiccation-tolerant pollen of *T. latifolia* can be measured *in situ* (i.e., in the cytosolic environment).

Previous aging experiments with this pollen in our laboratory have shown the extreme structural stability of the endogenous proteins (Wolkers and

Hoekstra, 1995). The major secondary structure component of the pollen proteins is an α-helical structure, comprising over 40% of the total of all protein secondary structures. The presence of a high α-helical content has also been found in desiccation-tolerant seeds (Golovina *et al.*, 1997). The α-helical band position (band around 1657 cm^{-1}) in both dry and hydrated pollen did not shift substantially over a temperature range from -40 to 120°C, indicating the extreme heat stabilitity of these α-helical structures. The folding of proteins in α-helical structures may be the reason for this heat stability because intramolecular hydrogen bonds can compensate for the reduced protein-water hydrogen bonds.

Protein denaturation is accompanied by the formation of intermolecular extended β-sheet structures. In this study it is demonstrated that dehydration increases the denaturation temperature of the proteins and decreases the extent of protein structural rearrangements during heating. At water contents below 0.16 g H_2O g^{-1} DW, the initial denaturation temperature (Tdi) increases rapidly up to temperatures around 116°C in very dry pollen of 0.01 g H_2O g^{-1} DW. Even at 134°C, the protein secondary structure still resembled that in the nonheated pollen to a large extent. This heat stability of the proteins in dry pollen is in agreement with the ability of pollen to survive heat treatments. Generally, pollen is also cold tolerant (Hoekstra, 1995). In relation to protein secondary structure, this tolerance is corroborated by the spectra in Figures 1 and 2, which, apart from heat tolerance, also indicate cold stability of the proteins down to very low temperatures (-50°C).

The heat and cold stability may be due to the embedding of proteins in a cytosol in which sucrose is abundantly present. Sugars are known for their ability to form glasses at low water contents or low temperatures. The glass transition temperature of *T. latifolia* pollen as studied by differential scanning calorimetry is drastically affected by the hydration level (Buitink *et al.*, 1996). The glass transition temperature falls from 50°C in dry pollen to -50°C in hydrated pollen. At 0.16 g H_2O g^{-1} DW, the glass transition is below 0°C. Thus, the pollen cytoplasm will be in the liquid or in the rubbery state in most of the elevated temperature region that we investigated. The viscosity of a sucrose

matrix in the liquid or rubbery state is much higher than in the glassy state (Slade and Levine, 1994). This may allow for more protein - protein interactions and thus increases the extent of denaturation.

We conclude that *in situ* FTIR microspectroscopy is extremely suitable for analyzing the protein secondary structure components in dry organisms. We show here that the proteins in dry desiccation-tolerant pollen are heat stable, whereas in hydrated pollen the heat stability is considerably less.

Acknowledgements

This project was financially supported by the Life Sciences Foundation, which is subsidized by the Netherlands Organization for Scientific Research.

References

Bandekar, J. (1992) Amide modes and protein conformation. *Biochim. Biophys. Acta.* **1120,** 123-143.

Buitink, J., Walters-Vertucci, C., Hoekstra, F.A., Leprince, O. (1996) Calorimetric properties of dehydrating pollen: Analysis of a desiccation-tolerant and an intolerant species. *Plant Physiol.* **111,** 235-242.

Byler, D.M., Susi, H. (1986) Examination of the secondary structure of proteins by deconvolved FTIR spectra. *Biopolymers* **25,** 469-487.

Capkova, V., Zbrozek, J., Tupy, J. (1994) Protein synthesis in tobacco pollen tubes: preferential synthesis of cell-wall 69-kDa and 66-kDa glycoproteins. *Sex. Plant Reprod.* **7,** 57-66.

Carpenter, J.F., Crowe, J.H. (1989) An infrared spectroscopic study of the interactions of carbohydrates with dried proteins. *Biochemistry* **28,** 3916-3922.

Chirgadze, Y.N., Fedorov, O.V., Trushina, N.P. (1975) Estimation of amino acid residue side-chain absorption in the infrared spectra of protein solutions in heavy water. *Biopolymers* **14,** 679-695.

Crowe, J.H., Crowe, L.M., Carpenter, J.F., Aurell Wistrom, C. (1987) Stabilization of dry phospholipid bilayers and proteins by sugars. *Biochem. J.* **242,** 1-10.

Crowe, J.H., Crowe, L.M., Carpenter, J.F., Prestrelski, S., Hoekstra, F.A. (1997) Anhydrobiosis: cellular adaptations to extreme dehydration. In: WH Dantzler, ed, Handbook of Physiology section 13, Comparative Physiology, Vol II, Oxford University Press, Oxford. pp. 1445-1477

Crowe, J.H., Crowe, L.M., Chapman, D. (1984) Preservation of membranes in anhydrobiotic organisms: the role of trehalose. *Science* **223,** 701-703.

Crowe, J.H., Hoekstra, F.A., Crowe, L.M. (1992) Anhydrobiosis. *Annu. Rev. Physiol.* **54,** 570-599.

Crowe, J.H., Hoekstra, F.A., Nguyen, K.H.N., Crowe, L.M. (1996) Is vitrification involved in depression of the phase transition temperature in dry phospholipids? *Biochim. Biophys. Acta.* **1280,** 187-196.

Crowe, J.H., Leslie, S.B., Crowe, L.M. (1994) Is vitrification sufficient to preserve liposomes during freeze-drying? *Cryobiology* **31,** 355-366.

Engelman, D.M., Steitz, T.A., Goldman, A. (1986) Identifying nonpolar transbilayer helices in amino acid sequences of membrane proteins. *Ann. Rev. Biophys. Chem.* **15,** 321-353.

Golovina, E.A., Wolkers, W.F., Hoekstra, F.A. (1997) Long-term stability of protein secondary structure in dry seeds. *Comp. Biochem. Physiol.* **117A,** 343-348.

Hoekstra, F.A. (1995) Collecting pollen for genetic resources conservation. *In:* Collecting Plant Genetic Diversity (Edited by Guarino, L., Ramanatha Rao, V., Reid, R.), pp. 527-550. Oxon, CAB International.

Hoekstra, F.A., Crowe, J.H., Crowe, L.M. (1991) Effect of sucrose on phase behavior of membranes in intact pollen of *Typha latifolia* L., as measured with Fourier transform infrared spectroscopy. *Plant Physiol.* **97,** 1073-1079.

Hoekstra, F.A., Crowe, J.H., Crowe, L.M., van Roekel, T., Vermeer, E. (1992) Do phospholipids and sucrose determine membrane phase transitions in dehydrating pollen species? *Plant Cell Environ.* **15,** 601-606.

Iwanami, Y. (1973) Heat-resistance of pollen grain and resting egg of brine-shrimp. *Jpn. J. Palynol.* **12,** 25-28.

Leopold, A.C., Sun, W.Q., Bernal-Lugo, I. (1994) The glassy state in seeds: analysis and function. *Seed Sci. Res.* **4,** 267-274.

Marcucci, M.C., Visser, T., Van Tuyl, J.M. (1982) Pollen and pollination experiments. VI. Heat resistance of pollen. *Euphytica* **31,** 287-290.

Mücke, M., Schmidt, F.K. (1994) A kinetic method to evaluate the two-state character of solvent-induced protein denaturation. *Biochemistry* **33,** 12930-12935.

Prestrelski, S.J., Tedeschi, N., Arakawa, T., Carpenter, J.F. (1993) Dehydration-induced conformational transitions in proteins and their inhibition by stabilizers. *Biophys. J.* **65,** 661-671.

Slade, L., Levine, H. (1994) Water and the glass transition: Dependence of the glass transition on composition and chemical structure: Special implications for flour functionality in cookie baking. *J. Food Engin.* **22,** 143-188.

Surewicz, W.K., Mantsch, H.H. (1988) New insight into protein secondary structure from resolution-enhanced infrared spectra. *Biochim. Biophys. Acta* **952,** 115-130.

Surewicz, W.K., Mantsch, H.H., Chapman, D. (1993) Determination of protein secondary structure by Fourier transform infrared spectroscopy: a critical assessment. *Biochemistry* **32,** 389-394.

Susi, H., Timasheff, S.N., Stevens, L. (1967) Infrared spectra and protein conformations in aqueous solutions. I. The amide I band in H_2O and D_2O solutions. *J. Biol. Chem.* **242,** 5460-5466.

Susi, H. (1969) Infrared spectra of biological macromolecules. *In:* Timasheff, S.N., Fasman, G.D. (eds.) Biological Macromolecules, Vol 2. Marcel Dekker, New York, pp. 575-663.

Vertucci, C.W., Farrant, J.M. (1995) Acquisition and loss of desiccation tolerance. *In: Seed Development and Germination* (Edited by Kigel, J., Galili, G.), pp. 237-271. New York, Marcel Dekker.

Williams, R.J., Leopold, A.C. (1989) The glassy state in corn embryos. *Plant Physiol.* **89,** 977-981.

Wolkers, W.F., Hoekstra, F.A. (1995) Aging of dry desiccation-tolerant pollen does not affect protein secondary structure. *Plant Physiol.* **109,** 907-915.

Zarsky, V., Capkova, V., Hrabetova, E., Tupy, J. (1985) Protein changes during pollen development in *Nicotiana tabacum* L. *Biol. Plant.* **27**, 438-444.

Chapter 4

Long-term stability of protein secondary structure in dry seeds

Elena A. Golovina, Willem F. Wolkers and Folkert A. Hoekstra

Abstract

Changes in protein secondary structure during seed aging were studied by *in situ* Fourier transform infrared microspectroscopy. Seeds of onion, white cabbage and radish, harvested in 1969, were stored at 15-20°C and 30% relative humidity. Fresh control seeds were harvested in 1994 and stored under the same conditions. In 1995, the germination capacity of seeds was >90% for the 1994 harvest and zero for the 1969 harvest. Inspection of the amide-I bands in Fourier self-deconvolved IR-spectra of thin slices of embryo axes of the various seeds did not reveal major changes in relative peak height and band position of the different protein secondary structures with aging. No protein aggregration and denaturation were found after long-term storage. Heating of dry viable radish seeds up to 145°C did not cause appreciable protein denaturation. In contrast, boiling hydrated radish seeds for 5 min led to decoiling of the α-helical structure and the appearance of a band at 1627 cm^{-1}. This band is characteristic of intermolecular extended β-sheet structures. We conclude that, despite the loss of viability and the long postmortem storage period, secondary structure of proteins in desiccation-tolerant dry seed is very stable and conserved during several decades of open storage.

Also published in Comparative Biochemistry and Physiology **117A**, 343-348 (1997)

Introduction

Seed of higher plants is reputed to be long-lived either in the desiccated state or in the hydrated state (Priestley, 1986). Although in the hydrated state repair processes can be constantly active, desiccated seed will accumulate small cellular injuries during its storage period until a critical point is reached at which the total of damage becomes irreparable upon imbibition. The lifespan of dry seed often is many years and in some plant families even decades in open storage at 20°C. An extreme example concerns *Nelumbo nucifera* with seeds surviving for at least 400-700 years in bogs in northern China (Priestley and Posthumus, 1982; Shen-Miller *et al.*, 1982). These seeds have a particularly thick-walled pericarp and probably have been dry over the entire storage period.

Stabilization of the structure of proteins and membranes is crucial for desiccation tolerance and long-term survival in the dry state. This stability is provided by sugars that generally accumulate during acquisition of desiccation tolerance (Crowe *et al.*, 1987; Carpenter and Crowe, 1989; Crowe *et al.*, 1992). Sugars also are involved in the formation of glasses (Williams and Leopold, 1989; Koster, 1991). In intact dry cells, glasses immobilize the cytoplasm, slow down the lateral diffusion of molecules and probably prevent intracellular membrane fusion.

Loss of viability with seed aging generally is linked with the loss of membrane integrity (see Priestley, 1986; Bewley and Black, 1994). Although it was suggested by Crocker and Groves, as early as 1915, that protein denaturation might play a role in seed viability loss, this suggestion was not further pursued. Only the extractability of proteins from aged seeds has been shown to decrease, which might be caused by denaturation or disulfide bridge formation (Priestley, 1986 and references therein). Otherwise, proteins in dry seeds are supposed to be packaged with maximum efficiency to be resistant to degradation by adverse climatic conditions, including high temperatures (Brown *et al.*, 1982). The considerable heat tolerance of dry seeds (Niethammer and Tietz, 1961) may stem from the heat stability of their proteins. This tolerance

declines with increasing moisture content (Barton, 1961; Ellis and Roberts, 1980).

FTIR is one of the most suitable techniques for elucidating the secondary structure of dehydrated proteins. Thus, information can be obtained from the amide-I and amide-II bands in the IR-absorption spectrum (Susi, 1969, Byler and Susi, 1986; Surewicz and Mantsch, 1988) and also *in situ* (Wolkers and Hoekstra, 1995, 1997). The amide-I band mainly arises from the C=O stretching vibration and the amide-II band from the N-H bending vibration of the protein backbone (Susi *et al.*, 1967). The C=O stretching frequency is very sensitive to changes in the nature of the hydrogen bonds arising from the different types of secondary structure. This causes a characteristic set of IR-absorption bands for each type of secondary structure (Susi *et al.*, 1967). It has been found in some model systems that a highly characteristic low wave-number band in the amide-I absorption band of the protein backbone is indicative of the formation of large protein aggregates with drying (Prestrelski *et al.*, 1993).

A recent FTIR study on desiccation-tolerant pollen has shown that despite the loss of viability during accelerated aging (12 d at 75% RH, 24°C) protein secondary structure is conserved (Wolkers and Hoekstra, 1995). The viability loss of this pollen has been attributed to the accumulation of free fatty acids and lysophospholipids in the membranes at the expense of the phospholipids, which promotes gel phase domains and leakage of cellular solutes (van Bilsen and Hoekstra, 1993; van Bilsen *et al.*, 1994).

However, the processes occurring during accelerated aging may be different from those during natural aging. Furthermore, natural aging occurs at a much lower rate in seed than in pollen, a matter of years *vs* weeks, respectively (Hoekstra, 1995). It may be that the much longer period of natural aging in seeds (occasionally more than 10-20 years in open storage) has a different effect on protein secondary structure. Although membrane damage may be the primary reason of seed death, changes in protein secondary structure also could be involved in seed aging during long-term storage.

Here, we report on the conservation of protein secondary structure in seed embryos of different plant species after long-term natural aging, using FTIR microspectroscopy.

Materials and methods

Seeds and treatments

Seeds kept in open storage (15-20°C, 30% RH) were from the seed collection of the CPRO-DLO (Wageningen, The Netherlands) and initially had high germinative capacities (>85%). They were harvested in 1969, whereas the fresh controls were harvested in 1994. It concerned onion (*Allium cepa*) cv. Revro and cv. Dinaro, radish (*Raphanus sativus*) cv. Kabouter and cv. Foxyred and white cabbage (*Brassica napus*) cv. R.O.Cross and cv. Bejo seeds, for the harvest years 1969 and 1994, respectively. All fresh controls had a germination index of over 90%, but none of the aged seeds showed a sign of life.

Because H_2O absorbs in the IR in the wavelength region that is used for protein analysis, hydrated radish embryos were analyzed in D_2O. After 6 h of imbibition in H_2O, seeds were surface dried and placed in ample D_2O for 1 h, which was found sufficiently long for full exchange of H_2O for D_2O. Redrying of imbibed radish seed was performed in a cabin continuously purged with dry air (RH < 3% at 24°C). Initially, viable seeds maintained high germinability after 6 h of imbibition in H_2O and subsequent drying.

Slices of dry viable radish embryos were heat-treated by increasing the temperature during 1 h up to 145°C in the sample cell of the IR microscope. Spectra were recorded after cooling to room temperature. Also, hydrated (6 h) viable seeds were boiled for 5 min, and after cooling embryos were isolated and then dried for one d before IR-spectroscopic analysis.

IR spectroscopy

IR spectra were recorded on a Perkin-Elmer 1725 Fourier transform IR-spectrometer (Perkin-Elmer, Buckinghamshire, Beaconsfield, UK) equipped with a liquid nitrogen-cooled mercury/cadmium/telluride detector and a Perkin-

Elmer microscope interfaced to a personal computer as described elsewhere (Wolkers and Hoekstra, 1995). Embryo axes were isolated, and thin slices were cut for use in the FTIR microscope. One slice of appropriate thickness was pressed between two diamond windows and mounted into a temperature-controlled cell. After purging the optical bench for at least 1 h with dry CO_2-free air (Balston; Maidstone, Kent, UK) at a flow rate of 25 l/min, spectra were recorded at room temperature. More than two spectra of different embryo slices were recorded for every treatment, and in the Figures typical spectra are presented. The acquisition parameters were 4 cm^{-1} resolution, 512 co-added interferograms, 2 cm/s moving mirror speed, 3500-900 cm^{-1} wavenumber range and triangle apodization function. The time needed for acquisition and processing of a spectrum was 4.5 min.

Data analysis

Spectral analysis and display were carried out using the Infrared Data Manager Analytical Software, version 3.5 (Perkin-Elmer). The spectral region between 1700 and 1600 cm^{-1} was selected. This region contains the amide-I absorption band of the protein backbones. Deconvolved spectra were calculated, using the interactive Perkin-Elmer routine for Fourier self-deconvolution. The parameters for the Fourier self-deconvolution procedure were smooth factor 15.0 and a width factor of 30.0 cm^{-1}. The line-width in the deconvolved spectrum was carefully chosen to avoid introduction of erroneous bands (Surewicz *et al.*, 1993). Second derivative spectra were calculated, and after normalization of the bands in the region 1700-1600 cm^{-1}, the exact band positions were determined by calculating the average of the spectral positions of the composite amide-I bands at 80% of the total (negative) peak height. Second derivative spectra were smoothed over 13 or 19 datapoints.

Results and discussion

Assignment of bands in IR absorption spectra

Figure 1 depicts the IR-absorption spectrum of a dry nonaged onion seed embryo. Absorption bands can be observed that are associated with carbohydrates (sugar and cell wall material), lipids and proteins. The band around 3300 cm^{-1} corresponds to OH-stretching vibrations, mainly arising from sucrose and cell wall materials. The bands around 2929 and 2854 cm^{-1} represent CH_2 stretching vibrations arising from lipids and partly from carbohydrates. In the 1800-1500 cm^{-1} region, at least three bands can be observed. Important bands for protein analysis are the amide-I band at 1656 cm^{-1} and the amide-II band at 1548 cm^{-1}. In the region below 1490 cm^{-1}, the CH_2 wagging and scissoring bands occur, which can be very useful to study membrane conformation (Blume *et al.*, 1988). The phosphate band around 1240 cm^{-1} can be used to study the interaction of phospholipid headgroups with sugars in model membrane systems (Crowe *et al.*, 1984). However, the interpretation of this band *in situ* is complicated by the presence of phosphate compounds other than phospholipids (Hoekstra *et al.*, 1997).

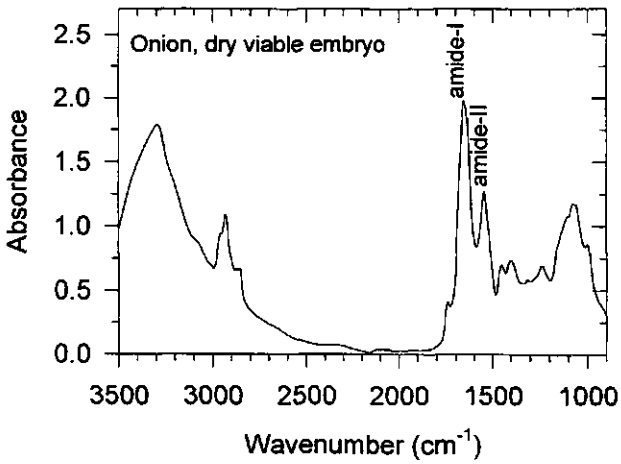

Figure 1. IR absorption spectrum of embryo slice from dry viable onion seed (harvest year 1994). The positions of the protein absorption bands (amide-I and amide-II) are indicated.

Comparison of viable and dead embryos

Onion seed is more short-lived than white cabbage and radish seed (Priestley, 1986). The time it takes for these seeds to lose 50% of the initial viability is approximately 4, 9 and 8 years, respectively. Therefore, these seeds, harvested in 1969 and kept in open storage since then, must have died a considerable number of years ago. With such old seeds, one can excellently analyze protein stability.

To resolve the fine details of the protein secondary structure, deconvolved spectra were calculated over the wavenumber range 1700-1600 cm^{-1}, which comprises the amide-I band (Figure 2). Despite the long storage period, IR-spectra of embryos from nonaged and aged onion seeds were virtually identical, and only slight differences could be observed between such spectra from white cabbage and radish seeds. These slight changes mainly concerned an increase of the band around 1638 cm^{-1} relative to the band around 1658 cm^{-1} in the aged embryos. In an attempt to quantify these slight differences, we calculated correlation coefficients between spectra (both self-deconvolved and second derivative spectra) from aged and nonaged embryos. The correlation coefficients were very high in all the three seed species tested ($r>0.99$), which indicates, also quantitatively, that the changes during storage are minute.

The information about protein secondary structure, obtained by the IR spectra, cannot discriminate between storage and nonstorage proteins in the sample. Different types of proteins might have a different ratio between α-helix and turn structures. The spectra that we obtained are the superposition of absorptions from different protein types. A similar shape of amide-I bands for aged and nonaged embryonic axes would indicate the absence of changes of all components. In the case of very high relative content of storage proteins, changes of minor components (enzymes) may not be visible. That is why we studied embryo axes, which are supposed to contain relatively less storage proteins (Bewley and Black, 1994). We suggest that our statement on the conservation of protein secondary structure applies to every type of protein, including enzymic proteins. In that respect, it is interesting to note that activity of

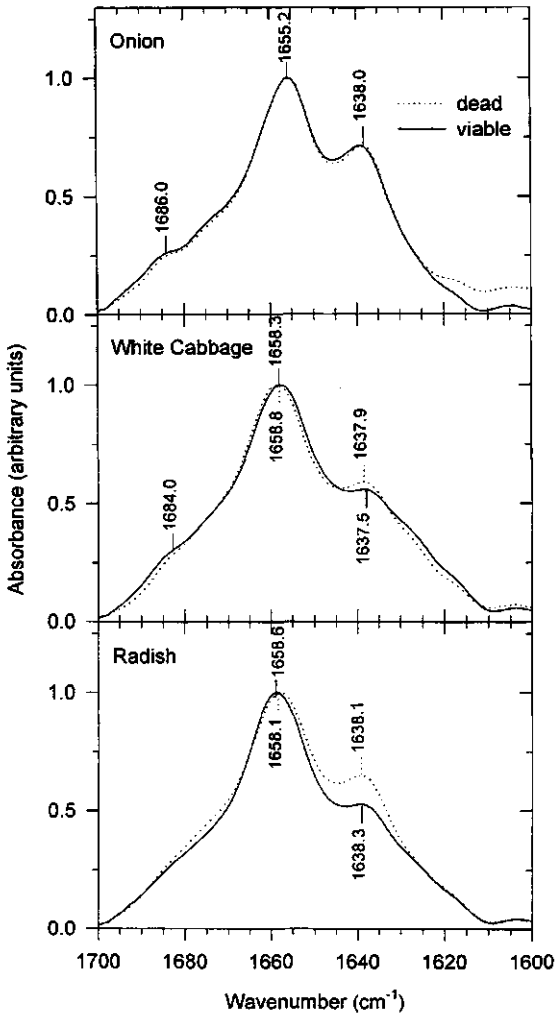

Figure 2. Fourier self-deconvolved IR absorption spectra of the amide-I region of an embryo slice from dry viable (harvest year 1994, >90% germination) and nonviable (harvest year 1969; open storage; 0% germination) seeds of onion, white cabbage and radish.

some seed enzymes was retained for more than 100 years of storage (Priestley, 1986).

Effect of imbibition and redrying

The lack of changes in protein secondary structure in the dry embryos during storage is in contrast to what has been suggested earlier for aged seeds

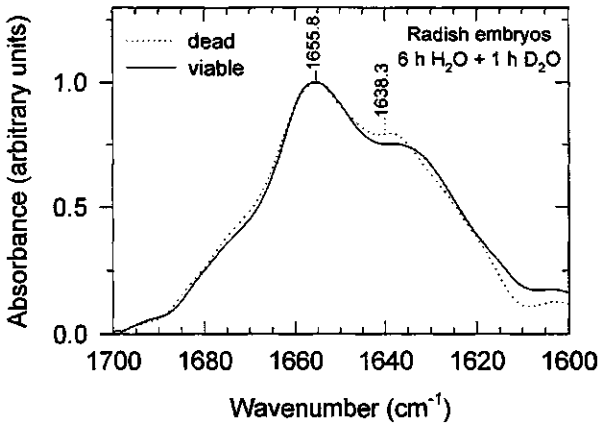

Figure 3. Fourier self-deconvolved IR absorption spectra of slices from nonviable (harvest year 1969) and viable (harvest year 1994) radish embryos after hydration for 6 h in H_2O and subsequent drying for 24 h.

after rehydration (Priestley, 1986). This discrepancy may be due to the fact that the proteins in aged dry seeds are embedded in a very viscous glassy matrix. Possible accumulation of chemical changes in the proteins might not lead to denaturation because of the restricted mobility. To resolve whether this is the case, radish seeds, which had the most pronounced differences between the spectra of aged and viable lots, were imbibed for 6 h to allow the proteins to rearrange according to chemical changes and were then redried (Figure 3). Thus, possible denaturation would be fixed in the dry state. However, this treatment only led to a slightly lower wavenumber position for the peak around 1658 cm^{-1} in the dead seed embryos than in the nonaged ones (Figure 3). The correlation coefficient between these spectra was high ($r > 0.99$) and not essentially different from the dry radish embryos in Figure 2. The peak around 1682 cm^{-1} was somewhat more pronounced in the dead radish embryos than in the viable ones.

Hydration for 6 h and redrying did not reduce the viability of the nonaged seeds. We conclude that there were no chemical changes in proteins during dry storage that could cause denaturation after rehydration.

Assignment of bands in the amide-I region

Both deconvolution and second derivative analysis show that the amide-I band is composed of at least three bands, located around 1638, 1655-1658 and 1684 cm^{-1}, representing different types of protein secondary structure (Figure 2). These bands do not shift much in band position with aging and only slightly in relative intensity, indicating that the proteins are mainly conserved. Bands have previously been assigned to α-helical structure (1657 cm^{-1}), random coil structure (1652 cm^{-1}), turn structure (1637 and 1680 cm^{-1}) and β-sheet structures (1637 and 1690 cm^{-1}) (Wolkers and Hoekstra, 1995 and references therein). In the present dry embryos, we could establish some turn structures and possibly β-sheet structures (Mantsch *et al.*, 1993). Contributions from random coil structure to the main band around 1658 cm^{-1} may be possible, being more likely in embryos of onion (1655 cm^{-1}) than in those of white cabbage and radish (1658 cm^{-1}).

A distinction between random coil structure and α-helical structure in the main band can be made by the different solvent accessibility of both types of protein secondary structure (Holloway and Mantsch, 1989). Thus, in D_2O the absorption band of the more accessible random coil proteins shifts from under

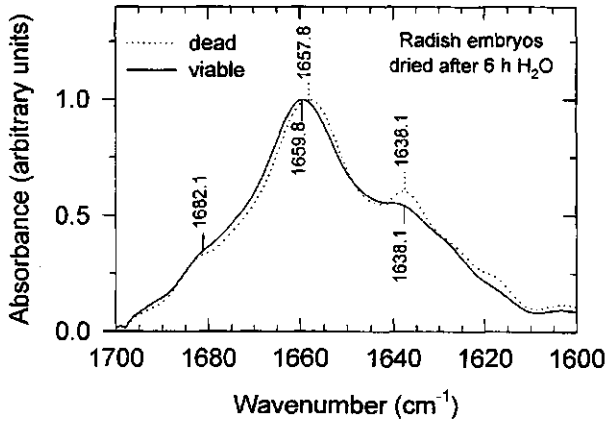

Figure 4. Fourier self-deconvolved IR absorption spectra of slices from nonviable (harvest year 1969) and viable (harvest year 1994) radish embryos after hydration for 6 h in H_2O and subsequent drying for 24 h.1 h.

the α-helical band to a lower wavenumber range (1647-1640 cm^{-1}), leading to a decrease in the peak height of the band at 1658 cm^{-1} *vs* the band at 1638 cm^{-1}. Figure 4 shows that in D_2O the α-helical band of radish embryos decreased in intensity and that, in general, bands shifted to lower wavenumbers (cf. Figures 2 and 4). This shift is not due to a structural rearrangement of the protein structure but represents a solvent effect to the amide-I band. From line-height ratios of the two main peaks in the dry and the hydrated radish sample (in D_2O), it can be concluded that random coil structures do occur but that still a considerable amount of the native proteins is present in the α-helical conformation. The spectra in D_2O of the aged and nonaged radish embryos were very similar ($r > 0.99$), again confirming that there is no protein denaturation in aged seeds.

Moreover, the absence of a low wavenumber peak around 1627 cm^{-1} (Prestrelski *et al.*, 1993; Sanders *et al.*, 1993) confirms that irreversible protein aggregates do not form with aging. However, such a peak at 1627 cm^{-1} was observed in embryos of hydrated radish seed after 5 min of boiling (Figure 5). This band is indicative of tightly packed intermolecular β-sheet structures (Prestrelski *et al.*, 1993).

Appraisal of the extent of denaturation during dry storage

Because the visible changes in the spectra with aging were small (Figure 2; $r > 0.99$), we heat-denatured the proteins in nonaged radish seed in an attempt to appreciate the slight changes observed during aging in terms of denaturation. Figure 5 shows the effect of slow heating to 145°C and subsequent cooling to room temperature on the protein secondary structure of a dry radish embryo slice. The typical signs of denaturation, the band around 1627 cm^{-1} (Wolkers and Hoekstra, 1997), did not develop, which again indicates the extreme stability of the dry embryo proteins *in situ*. This is in agreement with the extreme heat tolerance of dry seeds (Barton, 1961; Niethammer and Tietz, 1961). The correlation coefficient between spectra of the heated embryo and the nonheated control was also high ($r > 0.99$). In contrast, dry pollen proteins began to form the peak at 1627 cm^{-1}, representing

extended intermolecular β-sheet structures above 110°C (Wolkers and Hoekstra, 1995).

More pronounced than in the nonheated viable control are the peaks at 1680.5 and 1692.3 in the heat-treated dry embryo slice (Figure 5). These peaks represent turn structure and antiparallel β-sheet structure, respectively. It is not clear whether they can be associated with protein denaturation. The shift to higher wavenumber position of the α-helix and the turn structure bands after the heating to 145°C and subsequent cooling can be attributed to the removal of the last water from this dry sample during the heating (Prestrelski *et al.*, 1993; Sarver and Krueger, 1993) and does not imply a major structural

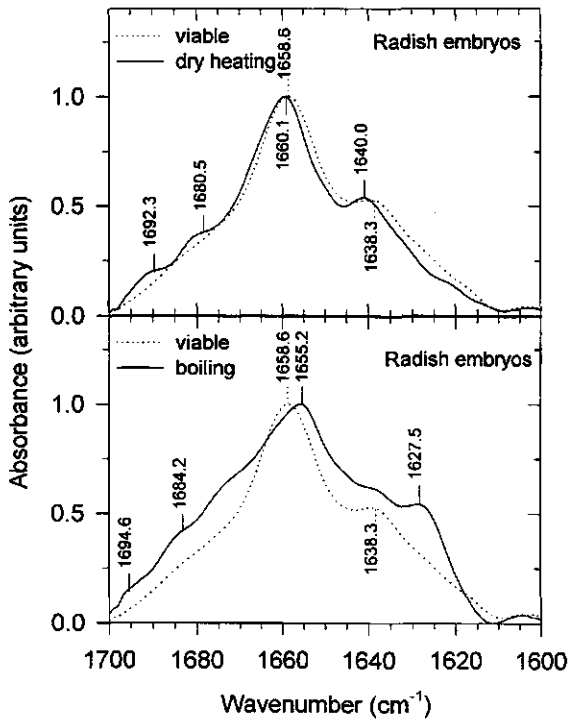

Figure 5. Fourier self-deconvolved IR absorption spectra of slices from viable (harvest year 1994) radish embryos after high temperature treatment. The dry embryo was heated in 1 h to 145°C and then analyzed after cooling. Alternatively, a hydrated (6 h) seed was boiled in water for 5 min and then dried (24 h) before analysis of the embryo.

rearrangement of the protein structure. The heating did not degrade the α-helix band.

In contrast, the α-helix band shifted to a lower wavenumber in redried radish embryos after hydrated seed (6 h) has been boiled for 5 min, which is indicative of decoiling. In none of the spectra of aged embryos were changes observable as in spectra of embryos after boiling.

As to how far the relatively higher turn structure peak (and lower α-helix) in the aged radish embryos (Figure 2) has to be considered as a sign of reduced protein stability is not clear. However, after rehydration for 6 h and redrying peak sizes in the aged and nonaged embryos became more similar (Figure 3), which indicates that it may concern some reversible change. The nonaged seeds are still viable after this treatment.

Our results indicate that long-term natural aging is not correlated with the formation of irreversibly clustered protein aggregates.

Conclusions

Fourier self-deconvolved amide-I bands in IR spectra of thin slices of embryos of *Allium, Brassica*, and *Raphanus* seeds do not reveal major changes in relative peak height and band position of the different protein secondary structures with aging. No apparent protein aggregation or denaturation occur after natural aging. We conclude that despite the loss of viability, the secondary structure of proteins in desiccation-tolerant dry seed embryos is very stable and conserved during several decades of open storage.

Acknowledgements

This project was financially supported by a stipend of the International Agricultural Centre, Wageningen, The Netherlands, to E.A. Golovina. We wish to thank Dr. G. Pet from the Centre of Plant Breeding and Reproduction Research, Wageningen, The Netherlands, for kindly providing the old seed material.

References

Barton, L.V. (1961) *Seed preservation and longevity.* New York, Interscience Publishers.

Bewley, J.D., Black, M. (1994) *Seeds, Physiology of Development and Germination*, pp. 1-445. New York, Plenum Press.

Blume, A., Hubner, W., Messner, G. (1988) Fourier transform infrared spectroscopy of ^{13}C=O-labeled phospholipids hydrogen bonding to carbonyl groups. *Biochemistry* **27**, 8239-8249.

Brown, J.W.S., Ersland, D.R., Hall, T.C. (1982) Molecular aspects of storage protein synthesis during seed development. *In:* The Physiology of Seed Development, Dormancy and Germination, Khan, A.A. (ed.) pp. 3-42. New York, Elsevier Biomedical Press.

Byler, D.M., Susi, H. (1986) Examination of the secondary structure of proteins by deconvolved FTIR spectra. *Biopolymers* **25**, 469-487.

Carpenter, J.F., Crowe, J.H. (1989) An infrared spectroscopic study of the interactions of carbohydrates with dried proteins. *Biochemistry* **28**, 3916-3922.

Crocker, W., Groves, J.F. (1915) A method of prophesying the life duration of seeds. *Proc. Natl. Acad. Sci. USA* **1**, 152-155.

Crowe, J.H., Crowe, L.M., Carpenter, J.F., Aurell Wistrom, C. (1987) Stabilization of dry phospholipid bilayers and proteins by sugars. *Biochem. J.* **242**, 1-10.

Crowe, J.H., Crowe, L.M., Chapman, D. (1984) Preservation of membranes in anhydrobiotic organisms: the role of trehalose. *Science* **223**, 701-703.

Crowe, J.H., Hoekstra, F.A., Crowe, L.M. (1992) Anhydrobiosis. *Annu. Rev. Physiol.* **54**, 570-599.

Ellis, R.H., Roberts, E.H. (1980) The influence of temperature and moisture on seed viability period in barley (*Hordeum distichum* L.). *Ann. Bot.* **45**, 31-37.

Hoekstra, F.A. (1995) Collecting pollen for genetic resources conservation. *In:* Collecting Plant Genetic Diversity. Guarino, L., Ramanatha Rao, V., Reid, R. (eds.) pp. 527-550. CAB International, Oxon, UK.

Hoekstra, F.A., Wolkers, W.F., Buitink, J., Golovina, E.A., Crowe, J.H., Crowe, L.M. (1997) Membrane stabilization in the dry state. *Comp. Biochem. Physiol.* **117A**, 335-341.

Holloway, P.W., Mantsch, H.H. (1989) Structure of Cytochrome b5 in solution by Fourier-transform infrared spectroscopy. *Biochemistry* **28**, 931-935.

Koster, K.L. (1991) Glass formation and desiccation tolerance in seeds. *Plant Physiol.* **96**, 302-304.

Mantsch, H.H., Perczel, A., Hollosi, M., Fasman, G.D. (1993) Characterization of β-turns in cyclic hexapeptides in solution by Fourier transform IR spectroscopy. *Biopolymers* **33**, 201-207.

Niethammer, A., Tietz, N. (1961) *Samen und Frhchte des Handels und der Industrie*, pp. 180-183. 's-Gravenhage, The Netherlands, Dr. W. Junk Uitgeverij.

Prestrelski, S.J., Tedeschi, N., Arakawa, T., Carpenter, J.F. (1993) Dehydration-induced conformational transitions in proteins and their inhibition by stabilizers. *Biophys. J.* **65**, 661-671.

Priestley, D.A. (1986) Seed Aging: Implications for Seed Storage and Persistence in Soil, pp. 1-304. Ithaca, Comstock Publ. Assoc.

Priestley, D.A., Posthumus, M.A. (1982) Extreme longevity of lotus seeds from Pulantien. *Nature* **211**, 148-149.

Sanders, J.C., Haris, P.I., Chapman, D., Otto, C., Hemminga, M.A. (1993) Secondary structure of M13 coat protein in phospholipids studied by circular dichroism, Raman, and Fourier transform infrared spectroscopy. *Biochemistry* **32,** 12446-12454.

Sarver, R.W., Krueger, W.C. (1993) Infrared investigation on the conformation of proteins deposited on polyethylene films. *Anal. Biochem.* **212,** 519-525.

Shen-Miller, J., Schopf, J.W., Beyer, R. (1982) Germination of a ca. 700-year-old lotus seed from China: evidence of exceptional longevity of seed viability. *Am. J. Bot.* **70,** 78.

Surewicz, W.K., Mantsch, H.H. (1988) New insight into protein secondary structure from resolution-enhanced infrared spectra. *Biochim. Biophys. Acta* **952,** 115-130.

Surewicz, W.K., Mantsch, H.H., Chapman, D. (1993) Determination of protein secondary structure by Fourier transform infrared spectroscopy: a critical assessment. *Biochemistry* **32,** 389-394.

Susi, H., Timasheff, S.N., Stevens, L. (1967) Infrared spectra and protein conformations in aqueous solutions. I. The amide-I band in H_2O and D_2O solutions. *J. Biol. Chem.* **242,** 5460-5466.

Susi, H. (1969) Structure and stability of biological macromolecules, *In:* Biological Macromolecules vol. 2, pp. 525-663. Marcel Dekker, New York.

van Bilsen, D.G.J.L., Hoekstra, F.A. (1993) Decreased membrane integrity in aging *Typha latifolia* L. pollen: accumulation of lysolipids and free fatty acids. *Plant Physiol.* **101,** 675-682.

van Bilsen, D.G.J.L., Hoekstra, F.A., Crowe, L.M., Crowe, J.H. (1994) Altered phase behavior in membranes of aging dry pollen may cause imbibitional leakage. *Plant. Physiol.* **104,** 1193-1199.

Williams, R.J., Leopold, A.C. (1989) The glassy state in corn embryos. *Plant Physiol.* **89,** 977-981.

Wolkers, W.F., Hoekstra, F.A. (1995) Aging of dry desiccation-tolerant pollen does not affect protein secondary structure. *Plant Physiol.* **109,** 907-915.

Wolkers, W.F., Hoekstra, F.A. (1997) Heat stability in desiccation-tolerant cattail pollen (*Typha latifolia*). A Fourier transform infrared study. *Comp. Biochem. Physiol.* **117A,** 349-355.

Chapter 5

Fourier transform infrared microspectroscopy detects changes in protein secondary structure associated with desiccation tolerance in developing maize embryos

Willem F. Wolkers, Adriana Bochicchio, Giuseppe Selvaggi and Folkert A. Hoekstra

Abstract

Isolated immature maize (*Zea mays*) embryos have been shown to acquire tolerance to rapid drying between 22 and 25 days after pollination (DAP) and to slow drying from 18-DAP onwards. To investigate adaptations in protein profile in association with the acquisition of desiccation tolerance in isolated immature maize embryos, we applied *in situ* Fourier transform infrared microspectroscopy. In fresh viable 20- and 25-DAP embryo axes, the shapes of the different amide-I bands were identical, and this was maintained after flash drying. On rapid drying, the 20-DAP axes had a reduced relative proportion of α-helical protein structure and lost viability. Rapidly dried 25-DAP embryos germinated (74%) and had a protein profile similar to the fresh control. On slow drying, the α-helical contribution in both the 20- and 25-DAP embryo axes increased when compared with that in the fresh controls, and survival of desiccation was high. The protein profile in dry mature axes resembled that after slow drying of the immature axes. Rapid drying resulted in an almost complete loss of membrane integrity in the 20-DAP embryo axes and much less so in the 25-DAP axes. After slow drying, low plasma membrane permeability ensued in both the 20- and 25-DAP axes. We conclude that slow drying of excised immature embryos leads to an increased proportion of α-helical protein structures in their axes, which coincides with additional tolerance of desiccation stress.

Also published in Plant Physiology, **116**, 1169-1177 (1998)

Introduction

Generally, seeds acquire desiccation tolerance during their development and before physiological maturity (Sun and Leopold, 1993; Sanhewe and Ellis, 1996). This desiccation tolerance is often inferred from the capacity of embryos to germinate after drying. In maize, excised immature embryos acquire the ability to germinate at 14-DAP (Bochicchio *et al.*, 1988). The rate of drying further determines how early in development isolated embryos acquire desiccation tolerance (Bochicchio *et al.*, 1994b). Slow drying over a 6 d period renders them desiccation-tolerant from 18-DAP onwards, whereas rapid dehydration over a 2 d period is tolerated only from 22-DAP onwards. The loss of viability in desiccation-sensitive embryos is often attributed to the loss of plasmalemma integrity after drying, as deduced from the excessive leakage of cytoplasmic solutes (Senaratna *et al.*, 1988; Blackman *et al.*, 1995). Disruption of membrane structures may lead to decompartmentalization of the cellular components, resulting in the release of enzymes that degrade cytoplasmic structures.

The induction and mechanism of desiccation tolerance in higher plant organs have been the subject of many biophysical and biochemical studies (reviewed in Crowe *et al.*, 1992; Vertucci and Farrant, 1995). Survival in the desiccated state requires protection of cytoplasmic proteins and retention of membrane structure upon dehydration and rehydration (Crowe *et al.*, 1987; Hoekstra *et al.*, 1997). Sugars may play a key role in this protection. The function of sugars in desiccation tolerance of anhydrous organisms, including seed embryos, is two-fold. On the one hand di- and oligosaccharides have been suggested to interact with dehydrating membranes and proteins, thus preventing conformational changes (Carpenter *et al.*, 1987; Crowe *et al.*, 1992; Crowe *et al.*, 1997). This has led to the formulation of the so-called "water replacement hypothesis". On the other hand, these carbohydrates could contribute to a glassy state in the dry cytoplasm at ambient temperatures (Burke, 1986; Williams and Leopold, 1989), which is considered important in preventing membrane fusion (Sun *et al.*, 1996) and degradation of cytoplasmic components (Leopold *et al.*, 1994; Hoekstra *et al.*, 1997). In maize embryos, raffinose increases upon slow drying of the embryos (Bochicchio *et al.*, 1994a).

However, no clear correlation has been found between the acquisition of desiccation tolerance in these excised embryos and either the sucrose or raffinose content.

Slow drying of immature seeds also leads to the synthesis of late embryogenesis abundant proteins (LEA proteins), that are suggested to play a role in alleviating dehydration stress (Blackman *et al.*, 1991, 1995; Ceccardi *et al.*, 1994). It is striking that during normal development in the kernel, maize embryos initiate the transcription of a LEA protein RNA just at 22-DAP (Mao *et al.*, 1995), which coincides with the moment that the embryos improve their survival of rapid drying (Bochicchio *et al.*, 1994b). Specific secondary structures (α-helical) for some of these proteins have been predicted (Dure *et al.*, 1989; Dure, 1993). The synthesis of LEA or other proteins during slow drying of excised immature embryos may thus alter the protein profile.

The secondary structure of proteins has been extensively studied using FTIR in the 1800-1500 cm^{-1} spectral region (Susi *et al.*, 1967). Differences in the C=O stretching vibrations of the peptide groups (the amide-I region between 1600-1700 cm^{-1}) provide information on the type of secondary structure, such as α-helix, β-strands, and different kinds of turn structures. *In situ* FTIR has been recently applied to study the overall protein secondary structure in dry pollen (Wolkers and Hoekstra, 1995) and seeds (Golovina *et al.*, 1997b). The advantage of FTIR is that protein secondary structure is measured in the native environment of the proteins and that it is a non-invasive technique. The disadvantage is that FTIR only provides information on the average protein secondary structure.

In the present work, maize embryos were excised at 20- and 25-DAP and exposed to slow drying, rapid drying or flash drying, with embryos matured on the plant as the reference. The overall *in situ* secondary structure of proteins in dry embryo axes was studied using FTIR, in an attempt to link possible changes in structure to the acquisition of desiccation tolerance.

Materials and methods

Plant material and drying treatments

Maize (*Zea mays* L.) plants from the inbred line Lo904 (1994, 1995 and 1996 harvests) were grown in Bergamo and Firenze, Italy. Zygotic embryos were excised from the developing kernels at 20- and 25-DAP and from dry mature kernels (approximately 65-DAP).

Isolated immature embryos were dried to less than 5% water content (on a DW basis) by rapid or slow drying as outlined previously (Bochicchio *et al.*, 1994b). Briefly, rapid drying occurred over a time period of 2 d, and slow drying over a time period of 6 d. Flash drying was performed by placing the excised embryos in a glove box that was continuously purged with dry air (RH < 3%) at ambient temperature for at least 24 h; embryos were dry within a few h.

Desiccation tolerance test

To assess desiccation tolerance of the 20-DAP and 25-DAP excised embryos, we used the germination test according to Bochicchio *et al.* (1988). Briefly, embryos were germinated aseptically in 9-cm Petri dishes (5 embryos per dish) on a solid medium containing 0.8% agar (w/v), 2% sucrose (w/v) and mineral salts at 25°C in a growth chamber, for up to 15 d. Embryos were scored as germinated if their coleoptile and radicle or secondary roots had visibly grown (longer than 0.2 cm).

Membrane integrity measured by EPR spin probe technique

This membrane permeability assay is based on the differential penetration of amphipathic spin probe molecules and the ions of the broadening agent ferricyanide (Miller, 1978; Golovina and Tikhonov, 1994; Golovina *et al.*, 1997a). The ratio (L/W) between the line heights of the lipid (L) and water (W) components of the spectrum was used to quantitatively characterize membrane permeability. The intensity of the lipid signal serves as the reference for the amount of material under investigation, whereas the intensity of the water component is negatively correlated with the amount of ferricyanide molecules that penetrated the cells.

EPR measurements were performed on a Bruker 300E EPR spectrometer. The EPR settings were: modulation amplitude of 0.5 Gauss, field center at 3480 Gauss with a scan range of 100 Gauss and a microwave frequency of 9.8 Ghz. The microwave power was 2.02 mW. The Zeeman field modulation was 100 kHz, and the scan time was 80 seconds. Four scans were accumulated. The nitroxide radical TEMPONE (4-oxo-2,2,6,6-tetramethyl-1-piperidinyloxy, from Sigma, St Louis, MO) and potassium ferricyanide were used as the spin probe and the broadening agent, respectively (Miller, 1978).

A few embryos from each treatment were exposed to moisture-saturated air for 5 h and imbibed on filter paper in a small Petri-dish for another 5 h. Fifteen min before the measurements, the embryos were dipped in a 1 mM TEMPONE/ 100 mM potassium ferricyanide solution. Parts from the embryonic axis were prepared, directly loaded into 2 mm diameter glass capillaries (with sample length of approximately 5 mm) and a small amount of solution was added to keep the material hydrated. The capillaries were accommodated within standard 4 mm diameter quartz tubes.

Sugar determinations - high performance liquid chromatography

Preweighed individual zygotic embryos (3 to 38 mg) were ground in small glass Potter homogenizers in 80% methanol (v/v) in the presence of approximately 0.5 - 1 mg melezitose as the internal standard. The extracts were heated for 10 min at 75°C in a hot water bath. The solvents were then removed by drying in a Speed-Vac (Savant Instruments Inc., Farmingdale, NY) for 2 h, and the final volume was adjusted to 1 mL with water. The debris was removed by centrifugation for 5 min in an Eppendorf centrifuge, after which the extract was ready for analysis.

For the analysis of soluble sugars, we performed high-pH anion exchange HPLC with pulsed electrochemical detection, using a Dionex (Sunnyvale, CA) GP40 gradient pump module and an ED40 pulsed electrochemical detector. Sugars were chromatographed on a CarboPac PA 100 (4x250mm) column (Dionex, Sunnyvale, CA), preceded by a guard column (CarboPac PA100, 4x50mm). The flow rate was 1 mL/min at 4°C.

Fourier Transform Infrared Microspectroscopy

IR spectra were recorded on a Perkin-Elmer 1725 Fourier transform IR-spectrometer (Perkin-Elmer, Buckinghamshire, Beaconsfield, UK) equipped with a liquid nitrogen-cooled Mercury/Cadmium/Telluride (MCT) detector and a Perkin-Elmer Microscope as described previously (Wolkers and Hoekstra, 1995).

The embryos were cross-sectioned, and a slice of the embryo axis was pressed gently between two diamond windows and placed in a temperature-controlled brass cell for IR-spectroscopy. To increase transparency of dry slices, a small amount of fluorolube (Perkin-Elmer) was added. To avoid the interfering effects of water in the IR spectra of slices from fresh embryo axes, the intact embryos were also placed in D_2O for 2 h (2 times refreshing) prior to recording the IR spectra.

For protein studies, the spectral region 1800 - 1500 cm^{-1} was selected. This region contains the amide-I and amide-II absorption bands of the protein backbones. The IR spectra were recorded at room temperature. Deconvolved spectra were calculated using the interactive Perkin-Elmer routine for Fourier

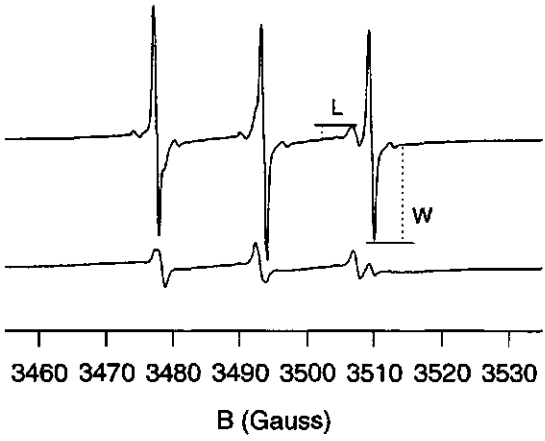

Figure 1. EPR spectra of axes of maize embryos excised at 20-DAP and subjected to slow (upper spectrum) and rapid (lower spectrum) drying. The embryos were prehydrated from the vapor phase for 5 h and subsequently imbibed in H_2O for 5 h. Prior to the measurements, the embryos were labeled in a mixture of TEMPONE (1 mM) and ferricyanide (100 mM) for 15 min. W: line height of the water component; L: line height of the lipid component.

self-deconvolution. The parameters for the Fourier self-deconvolution were a smoothing factor of 15.0 and a width factor of 30.0 cm^{-1}.

Results

Desiccation tolerance and membrane permeability of immature embryos

Embryos were excised at 20- and 25-DAP and subsequently tested for their germination capacity, before and after slow, rapid or flash drying. All fresh embryos were able to germinate. However, none of the rapidly and flash-dried 20-DAP embryos survived, whereas 90% of the slowly dried ones germinated (Table 1). Seventyfour % of the rapidly dried 25-DAP embryos germinated, which could further be improved to 100% after slow drying. This indicates that five more days of development on the ear resulted in acquisition of tolerance to rapid drying and a higher percentage of embryos tolerating slow drying.

Table 1. Effect of slow, rapid or flash drying of maize embryos,excised at different DAP on germination, membrane permeability and sugar content. Germination percentages are means of at least 2 samples, each with more than 20 embryos. The sugar contents are averages of at least 3 extracts from individual embryos. The membrane permeability of embryonic axes of maize embryos was determined from EPR spectra and calculated as the ratio L/W (line height of the lipid peak (L) divided by line height of the water peak (W)) in the high field region of the EPR spectrum (see Figure 1). DAP - days after pollination, SD - slow drying, RD - rapid drying, FD - flash drying. *Determined on five embryos only.

					Sugar (% of DW)		
DAP	Treatment	DW (mg)	Germination (%)	L/W	sucrose	raffinose	stachyose
20	SD	2.5	90.1	0.1032	8.0	1.75	0.00
20	RD	3.1	0	1.9762	7.3	0.00	0.01
20	FD	3.0	0		11.3	0.00	0.00
25	SD	7.7	100	0.1196	9.3	1.86	0.00
25	RD	8.2	73.9	0.5844	8.0	0.03	0.03
25	FD	8.8	100*		7.9	0.03	0.07
65	mature	38	100	0.2343	9.6	1.72	0.00
LSD *(P=0.05)*		1.3			1.6	0.65	0.04

Membrane permeability was measured by an EPR spin probe technique. Figure 1 shows EPR spectra of TEMPONE in 20-DAP embryo axes that were previously subjected to slow or rapid drying. The line height of the aqueous contribution (W) in the rapidly dried 20-DAP embryos was considerably lower than that in the slowly dried 20-DAP embryos, due to broadening effect of ferricyanide ions that had penetrated through the plasma membranes. From such EPR spectra the ratio of the line heights of the lipid peak to the water peak (L/W) was calculated, which is a measure of membrane permeability (Table 1). The inability of the 20-DAP embryos to survive rapid drying coincided with high plasma membrane permeability (Table 1). Low permeability was observed in the slowly dried 20- and 25-DAP embryos, coinciding with a high degree of survival. Fast and rapidly dried 25-DAP embryos had a slightly higher permeability than the slowly dried ones. The mature embryos also had low plasma membrane permeability.

Sugar contents in immature embryos

Sugar analyses of the differently dried immature embryos showed that sucrose was the major component (Table 1). Slow drying was always accompanied by the synthesis of raffinose (close to 2% of the DW). After rapid drying, hardly any raffinose could be detected, even in the 25-DAP embryos.

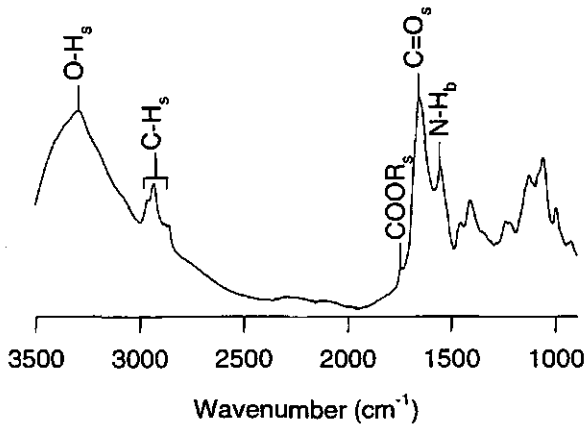

Figure 2. IR absorption spectrum of the axis of a slowly dried maize embryo, 20-DAP. Characteristic group frequencies are indicated in the figure.

The raffinose content of mature dry embryos was similar to that after slow drying of the immature embryos. Although traces of stachyose were detected, there was no clear correlation with the different drying treatments. The sucrose content as a percentage of the DW was stable after the drying treatments, in spite of the fact that the dry matter more than doubled during development from 20- to 25-DAP.

Protein secondary structure in embryo axes

Figure 2 depicts a typical IR absorption spectrum of a dry embryo axis, which is mainly composed of proteins, lipids and carbohydrates (sugar and cell wall material). The broad band around 3287 cm^{-1} corresponds to O-H stretching vibrations, mainly arising from proteins and carbohydrates. The bands at 2928 cm^{-1} and 2856 cm^{-1} represent C-H stretching vibrations, mainly arising from neutral lipids, proteins and carbohydrates. In the 1700 - 1500 cm^{-1} region, the amide-I band around 1650 cm^{-1} and the amide-II band around 1550 cm^{-1} can be observed, which are due to proteins (Wolkers and Hoekstra, 1995). The band around 1740 cm^{-1} in this region is due to ester bonds arising from lipids. We have focussed on the amide-I band to study structural rearrangements in the protein secondary structure during drying of the embryos.

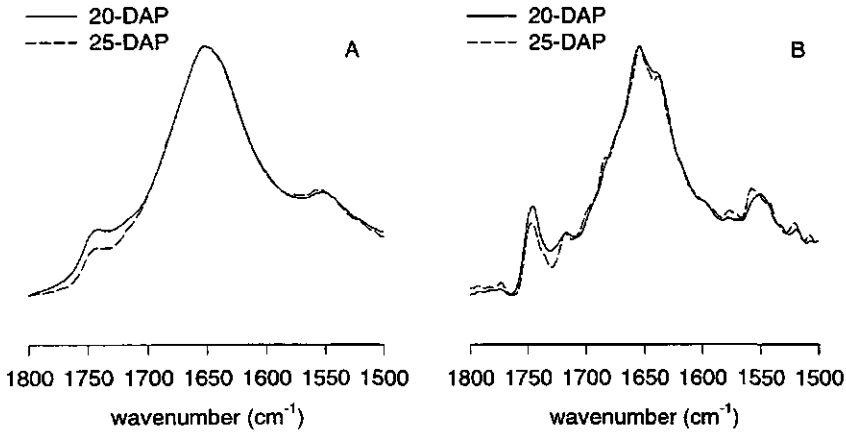

Figure 3. Absorption (A) and deconvolved absorption (B) IR spectra of the axes of fresh maize embryos excised at 20- and 25-DAP.

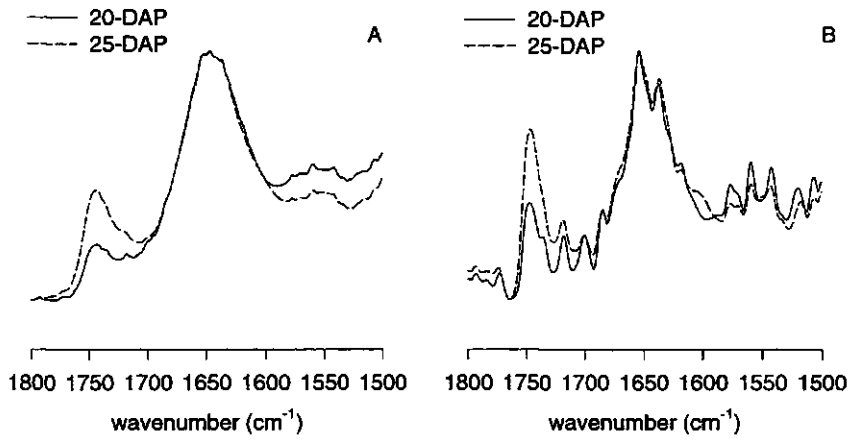

Figure 4. Absorption (A) and deconvolved absorption (B) IR spectra of the axes of fresh maize embryos in D_2O excised at 20- and 25-DAP.

IR-Spectra of fresh 20- and 25-DAP embryo axes

Figure 3A depicts the protein region of IR spectra in axes excised from fresh (hydrated) embryos at 20- and 25-DAP. The spectral features resembled one another. To resolve possible differences in more detail, deconvolved spectra were calculated (Surewicz and Mantsch, 1988). Deconvolution revealed that the amide-I band around 1650 cm^{-1} is composed of several bands, but again, the band features in these deconvolved spectra were very similar (Fig. 3B). This indicates that no changes in type and relative proportion of the overall protein secondary structures were detectable during the 5 d of embryo development from 20- to 25-DAP *in planta*. However, the total amount of protein is expected to have increased because the dry matter increased from approximately 3 to 8 mg during this period (Table 1). The differences in peak height around 1740 cm^{-1} were due to uncontrolled losses of neutral lipid during the sandwiching of the sample between the diamond windows, and were not taken into consideration any further.

The water in the fresh embryos is expected to absorb IR-light around 1650 cm^{-1}. To reduce possible interfering effects of this water, we also studied the protein structure of fresh embryo axes after the H_2O was exchanged for D_2O (Figs. 4A and 4B). In contrast to H_2O, D_2O does not interfere with the amide I band. Spectra in D_2O of the embryo axes at 20- and 25-DAP also were

very similar. However, the maximum band position occurred around 1646 cm^{-1}, whereas in H_2O this band position was around 1652 cm^{-1} (Table 2). This lower band position can be attributed to solvent effect (Haris *et al.*, 1989). Furthermore, the bandwidth at 70% of the maximum band height was less in D_2O than in H_2O. This is an indication that in the fresh embryo axis the amide-I band was indeed broadened by the presence of some H_2O. We did not attempt to subtract this water contribution to the amide I band, because it is difficult to find an appropriate background for water in *in situ* spectra.

Effect of drying rate and developmental age

In figure 5A, the IR spectra of 25-DAP embryo axes after slow and rapid drying are shown. The amide-I band maxima were located at 1653.5 cm^{-1} and 1652.2, respectively. Also with respect to the fresh control these maxima were almost identical. Deconvolution (Fig. 5B) shows that the major component of the amide-I region is a band around 1655 cm^{-1}, which can be assigned to α-helical structures. The other bands around 1637 cm^{-1} and 1680 cm^{-1} reflect β-sheet structures and turn structures (Surewicz *et al.*, 1993). The slight difference in band position and band width between the 25-DAP rapidly and slowly dried embryos as shown in figure 5A and Table 2 stem from the difference in relative proportion of the assigned secondary structures (Fig. 5B).

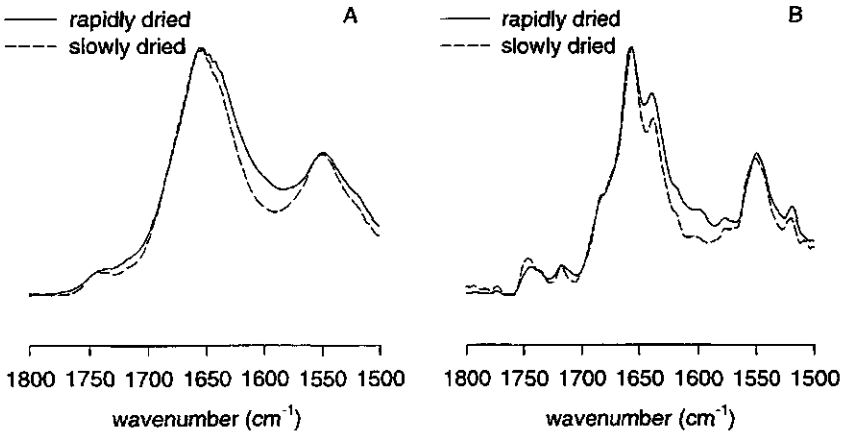

Figure 5. Absorption (A) and deconvolved absorption (B) IR spectra of the axes of maize embryos excised at 25-DAP and subjected to rapid and slow drying.

These differences are addressed later in figure 8.

However, when embryos excised at 20-DAP were subjected to slow, rapid or flash drying, major differences in the overall protein secondary structure between them were observed (Fig. 6A). When compared with slow drying, rapid drying resulted in a shift of the amide-I band to lower wavenumber position and an increased line width (see also Table 2). Flash drying of these 20-DAP embryos gave an intermediate amide-I band pattern. The deconvolved spectra in figure 6B show that this shift to lower wavenumber in the amide-I band was due to a decrease of the α-helical band around 1656 cm^{-1} relative to the β-sheet (and turn structures) band around 1639 cm^{-1}. The decrease of the α-helical contribution to the amide-I region of the spectrum was also reflected in a decrease of the amide-II line height. On slow drying, the protein profiles of the 20- and 25-DAP embryo axes were fairly similar (compare Figs. 5 and 6). For comparison, the spectrum (original and deconvolved) of an axis from a mature, dry 65-DAP embryo is presented in figure 7. The spectrum resembles the spectra of the slowly dried, immature embryo axes (both 20- and 25-DAP).

Table 2. Characteristics of the amide-I band in original IR-absorption spectra from transversal slices of maize embryo axes. The excised embryos were subjected to slow, rapid or flash drying, or analyzed fresh in the presence of H_2O or D_2O. The absorption maximum, ν, and the linewidth, Δν, were determined at 70% of the total band height (means of at least 2 samples).

days after pollination	treatment	ν (cm^{-1})	Δν (cm^{-1})
20	fresh	1651.9	55
25	fresh	1652.1	54
20	fresh in D_2O	1646.3	51
25	fresh in D_2O	1646.7	47
20	slowly dried	1653.5	52
25	slowly dried	1653.5	46
20	rapidly dried	1646.3	68
25	rapidly dried	1652.2	57
20	flash-dried	1652.4	58
25	flash-dried	1652.3	58
65	mature	1653.9	48
LSD (*P = 0.05*)		1.7	12

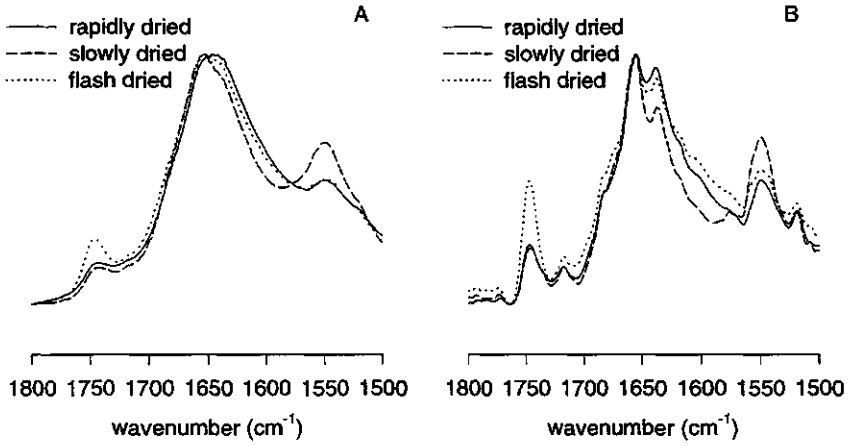

Figure 6. Absorption (A) and deconvolved absorption (B) IR spectra of the axes of maize embryos excised at 20-DAP and subjected to slow, rapid and flash drying.

Statistical verification of the differences in position and width of the amide I band for the differently treated embryos is given in Table 2. The low wavenumber position of the amide I band in D_2O-treated fresh embryos stems from solvent effects (Haris *et al.*, 1989). Considerable differences were observed only between slowly and rapidly dried 20-DAP embryos. This indicates a major difference in the overall protein secondary structure between them. Deconvolved spectra were used to further resolve the changes in specific protein secondary structures.

Figure 8 shows histograms of the line height ratios between α-helical structure and β-sheet/turn structure as derived from the deconvolved absorption spectra. The ratios were significantly higher in the axes of the slowly dried embryos (20- and 25-DAP) and in the mature embryos when compared with those in axes of all the other embryos. This indicates an elevated proportion of α-helical structures in the axes of slowly dried and mature embryos. In the rapidly dried embryos excised at 20-DAP, the line height ratio was significantly lower than those in all the other embryos, indicating a declined contribution of α-helical structures. The rapidly dried embryos excised at 25-DAP and the 20- and 25-DAP flash-dried embryos had line height ratios that were not significantly different from those in the fresh controls (in H_2O and D_2O).

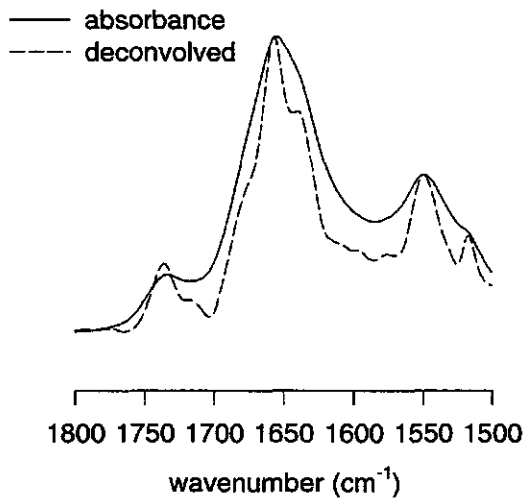

Figure 7. Absorption and deconvolved absorption IR spectra of axes of dry mature maize embryos (65-DAP).

To get insight into the extent that the relative amounts of α-helical structures increase after slow drying of the immature embryos, a curve fitting procedure was applied on the amide-I band (see Wolkers and Hoekstra, 1995 for details). It was calculated on the basis of the relative absorbance, that the α-helical structures increased from an average of 35% of the total of protein secondary structures in the flash-dried axes to 51% in the slowly dried axes (both 20- and 25-DAP).

Discussion

Slow drying of excised immature maize embryos confers tolerance to desiccation at a stage of development in which rapid drying leads to debilitation (Bochicchio *et al.*, 1994b). Thus, it was shown in Table 1, that viable 20-DAP excised embryos survive slow drying but do not tolerate rapid drying. This acquired tolerance to desiccation is accompanied by a considerably reduced leakage of endogenous solutes during rehydration and an increased level of raffinose, apart from the sucrose that is already present in the fresh material. Apparently, accumulation of raffinose is typically the result of slow drying,

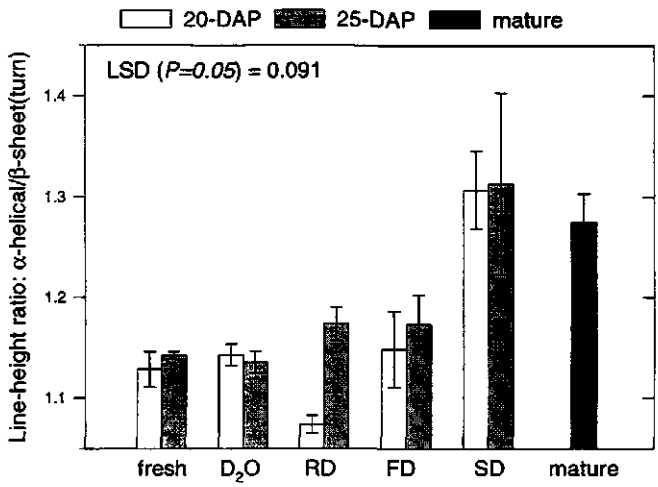

Figure 8. Line-height ratios of the bands denoting α-helical structure and β-sheet/turn structure. The line heights were determined from deconvolved IR absorption spectra of fresh, deuterated (D_2O), rapidly dried (RD), slowly dried (SD) and flash-dried (FD) axes of maize embryos excised at 20- and 25-DAP. Data points are means of at least two samples ± SE.

because it was also observed in the 25-DAP slowly dried embryos and in the mature embryos after maturation drying on the ear.

Acquisition of desiccation tolerance often is associated with the synthesis of oligosaccharides like raffinose and stachyose (Horbowicz and Obendorf, 1994). Nevertheless, a considerable percentage (74%) of the 25-DAP embryos survived rapid drying, in spite of the fact that raffinose was almost absent. Therefore, raffinose is not a prerequisite for desiccation tolerance, as was stipulated earlier for immature maize embryos (Bochicchio *et al.*, 1994b) and primed cauliflower seeds (Hoekstra *et al.*, 1994). As expected, membrane permeability of the rehydrated 25-DAP rapidly dried embryos was much lower than that of the rapidly dried 20-DAP embryos. However, it was higher than after slow drying of the 25-DAP embryos, which also is reflected in the lower germination percentage (74% compared to 100%).

Coinciding with the acquisition of desiccation tolerance in seeds, new proteins are generally synthesized such as LEA proteins. In higher plants, LEA proteins are ubiquitous and may be induced to higher levels of expression also

in other tissues by ABA and/or desiccation stress (Close *et al.*, 1989). They are considered to play a role in the protection against desiccation stress (Blackman *et al.*, 1995), but the exact protective mechanism is unknown. In fresh immature maize embryos, transcripts of a LEA protein appear from 22-DAP onwards, and ABA can stimulate the level of transcription (Mao *et al.*, 1995). In our experiments, the detachment of the embryos from the plant and/or the slow drying might have induced the synthesis of such proteins. Although some of the LEA proteins were predicted to exist as amphipathic helical structures (Dure *et al.*, 1989; Dure, 1993), the direct surroundings such as ionic strenght of the solution have a considerable influence on their secondary structure (Russouw *et al.*, 1995).

Using FTIR we characterized changes in the overall protein secondary structure in developing maize embryo axes that were exposed to different drying regimes. In fresh, immature 20- and 25-DAP maize embryo axes the protein profiles were very similar (see Figs. 3 and 4). Because moisture contents are still high in these fresh axes, the amide-I band might be distorted due to the interfering effect of water in the amide-I region. This problem was circumvented by using D_2O instead of H_2O, because D_2O absorbs at a much lower wavenumber (Haris *et al.*, 1989). Also in D_2O, the results indicate that the proportion of the different protein secondary structures did not change between 20- and 25-DAP, irrespective of the considerable dry matter gain during these five days of development on the plant.

Changes in the protein profile of the embryos can be observed, both in line width and proportion of α-helical structures, depending on the drying treatment. The relative proportion of ordered α-helical structures increased upon slow drying, which was also observed after normal maturation on the plant. We infer this from the reduced line width of the original amide-I band (Table 2) and the increased line height of the band around 1655 cm^{-1} in the deconvolved spectra (Fig. 8).

Rapid drying of the immature embryos resulted in a proportionally lower α-helical content and higher contribution of β-sheet/turn structures. This was particularly prominent in the 20-DAP embryo axes. Such high contribution of β-sheet structures was not observed after flash drying (see Figs. 6 and 8).

Apparently, flash drying fixes the protein profile as is present in fresh embryos. If breakdown of α-helix is responsible for the decreased ratio of α-helix to β-sheet/turn structures in the rapidly dried 20-DAP embryos, then such a fixation after the flash drying would seem logical, simply because there would be less time available for protein breakdown. This idea of breakdown is supported by the high membrane permeability of the 20-DAP rapidly dried axes. Proteases may have been released already during the rapid drying process, to cleave the α-helical structure, increasing the proportion of β-sheet/turn structures. Although our permeability measurements were performed after rehydration, high permeability might have occurred before the embryos were dry. In desiccation-sensitive somatic embryos, phospholipid breakdown already occurred before drying was completed (Tetteroo *et al.*, 1996), which may be linked with high membrane permeability.

Our *in situ* FTIR data show an increased proportion in α-helical structures after slow and maturation drying. This may be due to the effect of drying *per se* on the overall protein secondary structure. However, because flash drying cannot evoke the elevated α-helical content, there must be other reasons for this phenomenon. *De novo* synthesis of proteins associated with the defence against desiccation stress may have caused this increase. Synthesis of storage proteins is unlikely here, since it was reported earlier that it ceases upon slow drying (Jiang *et al.*, 1996). Proteins other than LEAs also may be involved in the increase in α-helical structures. It should be stressed that our FTIR analysis was performed *in situ* and that no other technique can provide information about structure of proteins in their native state. However, the averaging character of FTIR makes it difficult to directly link changes in the overall protein secondary structure to the synthesis of specific proteins.

We conclude that slow drying of immature maize embryos (20- and 25-DAP) causes adaptations in the cytoplasmic protein profile, membranes and sugar composition, which also can be found in embryos of dry mature seeds. These adaptations cannot be completed during rapid drying. The fact that the 25-DAP embryos germinate to a certain extent after rapid drying without increased proportion of α-helical structures in their protein profile, suggests that the increased proportion of α-helices as observed in slowly dried embryos may

not be a prerequisite for desiccation tolerance. However, the total amount of protein is expected to have increased considerably during the five more days of development from 20- to 25-DAP, including α-helical structures. Furthermore, in comparison with the slowly dried 25-DAP embryos, the rapidly dried 25-DAP embryos are more sensitive to desiccation stress, as evidenced by the higher membrane permeability. These considerations contribute to the paradigm that the acquisition of full desiccation tolerance is a gradual process during maturation (Hong and Ellis, 1992; Sun and Leopold, 1993), involving the above mentioned adaptations. Germination is nevertheless possible even if not all of these adaptations have been completed. The full benefit of all these adaptations may become apparent in an increased storage longevity.

Acknowledgements

We would like to thank Mark Alberda for excellent technical assistance and acknowledge the Istituto Sperimentale di Cerealicoltura, Sez. Maiscoltura at Bergamo, Italy, where part of the plants were grown and hand-pollination was carried out.

References

Blackman, S.A., Obendorf, R.L., Leopold, A.C. (1995) Desiccation tolerance in developing soybean seeds: the role of stress proteins. *Physiol. Plant.* **93,** 630-638.

Blackman, S.A., Wettlaufer, S.H., Obendorf, R.L., Leopold, A.C. (1991) Maturation proteins associated with desiccation tolerance in soybean. *Plant Physiol.* **96,** 868-874.

Bochicchio, A., Rizzi, E., Balconi, C., Vernieri, P., Vazzana, C. (1994a) Sucrose and raffinose contents and acquisition of desiccation tolerance in immature maize embryos. *Seed Sci. Res.* **4,** 123-126.

Bochicchio, A., Vernieri, P., Puliga, S., Balducci, F., Vazzana, C. (1994b) Acquisition of desiccation tolerance by isolated maize embryos exposed to different conditions: the questionable role of endogenous abscisic acid. *Physiol. Plant.* **91,** 615-622.

Bochicchio, A., Vazzana, C., Raschi, A., Bartels, D., Salamini, F. (1988) Effect of desiccation on isolated embryos of maize. Onset of desiccation tolerance during development. *Agronomie* **8,** 29-36.

Burke, M.J. (1986) The glassy state and survival of anhydrous biological systems. In AC Leopold, ed, Membranes, Metabolism and Dry Organisms, Cornell University Press, Ithaca, New York, pp 358-363.

Carpenter, J.F., Martin, B., Crowe, L.M., Crowe, J.H. (1987) Stabilization of phosphofructokinase during air drying with sugars and sugar/transition metal mixtures. *Cryobiology* **24,** 455-464.

Ceccardi, T.L., Meyer, N.C., Close, T.J. (1994) Purification of a maize dehydrin. *Protein Expression and Purification* **5**, 266-269.

Close, T.J., Kortt, A.A., Chandler, P.M. (1989) A cDNA-based comparison of dehydration-induced proteins (dehydrins) in barley and corn. *Plant Mol. Biol.* **13**, 95-108.

Crowe, J.H., Crowe, L.M., Carpenter, J.F., Aurell Wistrom, C. (1987) Stabilization of dry phospholipid bilayers and proteins by sugars. *Biochem. J.* **242**, 1-10.

Crowe, J.H., Crowe, L.M., Carpenter, J.F., Prestrelski, S.J., Hoekstra, F.A. (1997) Anhydrobiosis: cellular adaptations to extreme dehydration. In WH Dantzler, ed, Handbook of Physiology section 13, Comparative Physiology, Vol II, Oxford University Press, Oxford. pp. 1445-1477.

Crowe, J.H., Hoekstra. F.A., Crowe, L.M. (1992) Anhydrobiosis. *Annu. Rev. Physiol.* **54**, 570-599.

Dure, L. III (1993) A repeating 11-mer amino acid motif and plant desiccation. *Plant J.* **3**, 363-369.

Dure, L. III, Crouch, M., Harada, J., Ho, T.H.D., Mundy, J., Quatrano, R., Thomas, T., Sung, Z.R. (1989) Common amino acid sequence domains among the Lea proteins of higher plants. *Plant Mol. Biol.* **12**, 475-486.

Golovina, E.A., Tikhonov, A.N. (1994) The structural differences between the embryos of viable and nonviable wheat seeds as studied with the EPR spectroscopy of lipid-soluble spin labels. *Biochim. Biophys. Acta* **1190**, 385-392.

Golovina, E.A., Tikhonov, A.N., Hoekstra, F.A. (1997a) An electron paramagnetic resonance spin probe study of membrane permeability with seed aging. *Plant Physiol.* **114**, 383-389.

Golovina, E.A., Wolkers, W.F., Hoekstra, F.A. (1997b) Long-term stability of protein secondary structure in dry seeds. *Comp. Biochem. Physiol.* **117A**, 343-348.

Haris, P.I., Coke, M., Chapman, D. (1989) Fourier transform infrared spectroscopic investigation of rhodopsin structure and its comparison with bacteriorhodopsin. *Biochim. Biophys. Acta* **995**, 160-167.

Hoekstra F.A., Wolkers, W.F., Buitink, J., Golovina, E.A., Crowe, J.H., Crowe, L.M. (1997) Membrane stabilization in the dry state. *Comp. Biochem. Physiol.* **117A**, 335-341.

Hoekstra, F.A., Haigh, A.M., Tetteroo, F.A.A., Van Roekel, T. (1994) Changes in soluble sugars in relation to desiccation tolerance in cauliflower seeds. *Seed Sci. Res.* **4**, 143-147.

Hong, T.D., Ellis, R.H. (1992) Development of desiccation tolerance in Norway maple (*Acer platanoides* L.) seeds during maturation drying. *Seed Sci. Res.* **2**, 169-172.

Horbowicz, M., Obendorf, R.L. (1994) Seed desiccation tolerance and storability: dependence on flatulence-producing oligosaccharides and cyclitols: review and survey. *Seed Sci. Res.* **4**, 385-406.

Jiang, L., Abrams, S.R., Kermode, A.R. (1996) Vicilin and napin storage-protein gene promoters are responsive to abscisic acid in developing transgenic tobacco seed but lose sensitivity following premature desiccation. *Plant Physiol.* **110**, 1135-1144.

Leopold, A.C., Sun, W.Q., Bernal-Lugo, I. (1994) The glassy state in seeds: analysis and function. *Seed Sci. Res.* **4**, 267-274.

Mao, Z., Paiva, R., Kriz, A.L., Juvik, J.A. (1995) Dehydrin gene expression in normal and *viviparous* embryos of *Zea mays* during seed development and germination. *Plant Physiol. Biochem.* **33**, 649-653.

Miller, R.W. (1978) Osmotically induced removal of water from fungal cells as determined by a spin probe technique. *Plant Physiol.* **62**, 741-745.

Russouw, P.S., Farrant, J., Brandt, W., Maeder, D., Lindsey, G.G. (1995) Isolation and characterization of a heat-soluble protein from pea (Pisum sativum) embryos. *Seed Sci. Res.* **5,** 137-144.

Sanhewe, A.J., Ellis, R.H. (1996) Seed development and maturation in *Phaseolus vulgaris*. I. Ability to germinate and to tolerate desiccation. *J. Exp. Bot.* **47,** 949-958.

Senaratna, T., Gusse, J.F., McKersie, B.D. (1988) Age-induced changes in cellular membranes of imbibed soybean seed axes. *Physiol. Plant.* **73,** 85-91.

Sun, W.Q., Leopold, A.C. (1993) Acquisition of desiccation tolerance in soybeans. *Physiol. Plant.* **87,** 403-409.

Sun, W.Q., Leopold, A.C., Crowe, L.M., Crowe, J.H. (1996) Stability of dry liposomes in sugar glasses. *Biophys. J.* **70,** 1769-1776.

Surewicz, W.K., Mantsch, H.H. (1988) New insight into protein secondary structure from resolution-enhanced infrared spectra. *Biochim. Biophys. Acta* **952,** 115-130.

Surewicz, W.K., Mantsch, H.H., Chapman, D. (1993) Determination of protein secondary structure by fourier transform infrared spectroscopy: a critical assessment. *Biochemistry* **32,** 389-394.

Susi, H., Timasheff, S.N., Stevens, L. (1967) Infrared spectra and protein conformations in aqueous solutions. I. The amide I band in H_2O and D_2O solutions. *J. Biol. Chem.* **242,** 5460-5466.

Tetteroo, F.A.A., de Bruijn, A.Y., Henselmans, R.N.M., Wolkers, W.F., van Aelst, A.C., Hoekstra, F.A. (1996) Characterization of membrane properties in desiccation-tolerant and -intolerant carrot somatic embryos. *Plant Physiol.* **111,** 403-412.

Vertucci, C.W., Farrant, J.M. (1995) Acquisition and loss of desiccation tolerance. In J Kigel, G Galili, eds, Seed development and germination, Marcel Dekker, New York, pp 237-271.

Williams, R.J., Leopold, A.C. (1989) The glassy state in corn embryos. *Plant Physiol.* **89,** 977-981.

Wolkers, W.F., Hoekstra, F.A. (1995) Aging of dry desiccation-tolerant pollen does not affect protein secondary structure. *Plant Physiol.* **109,** 907-915.

Chapter 6

A Fourier transform infrared microspectroscopy study of sugar glasses: application to anhydrobiotic higher plant cells

Willem F. Wolkers, Harriëtte Oldenhof, Mark Alberda and Folkert A. Hoekstra

Abstract

Fourier transform infrared microspectroscopy (FTIR) was used to study glasses of pure carbohydrates and in the cytoplasm of desiccation-tolerant plant organs. The position of the OH-stretching vibration band (νOH) shifted with temperature. Two linear regression lines were observed in νOH against temperature plots. The temperature at the point of intersection between these two lines coincided with the glass transition temperature (T_g), as determined by other methods. The temperature at the intersection point decreased with increasing water content, which further validates that, indeed, T_g was observed. T_g values that were determined for dry glucose, sucrose, maltose, trehalose and raffinose glasses were 27, 57, 91, 108 and 108°C, respectively. The shift of νOH with temperature - the wavenumber-temperature coefficient (WTC) - was higher in sugar glasses having higher T_g. This suggests that glasses are more loosely packed when they have higher T_g. For *Typha latifolia* pollen and dried *Craterostigma plantagineum* leaves we obtained similar νOH *vs* temperature plots as for carbohydrate glasses, indicating that a glass transition was observed. The T_g in dry pollen was ca. 45°C and in dry plant leaves ca. 65°C, with WTC values comparable to those observed in the carbohydrates. The T_g values in these tissues decreased with increasing water contents. Our data suggest that the carbohydrates that are present in the cytoplasm are primary factors contributing to the glassy state. We conclude that FTIR provides new insights in the structure of glasses in carbohydrates and in biological tissues.

Also published in Biochimica et Biophysica Acta **1379,** 83-96 (1998)

Introduction

The physical and chemical mechanisms utilised by seeds, pollens and even entire plants (higher plants) to survive extreme desiccation have been extensively studied (reviewed in Crowe *et al.*, 1992, 1997; Leprince *et al.*, 1993; Leopold *et al.*, 1994; Vertucci and Farrant, 1995; Hoekstra *et al.*, 1997). One of the most important adaptations involved is the formation of a glassy state when the water content falls below 0.2 g H_20 /g DW (Williams and Leopold, 1989; Koster, 1991; Leprince and Vertucci, 1995; Buitink *et al.*, 1996). Soluble carbohydrates are thought to make up the structure of this vitreous or highly viscous state, which may serve to inhibit disruption of cellular membranes (Sun *et al.*, 1996; Crowe *et al.*, 1997; Hoekstra *et al.*, 1997), denaturation of cytoplasmic proteins (Prestrelski *et al.*, 1993; Wolkers and Hoekstra, 1995) and deteriorative radical reactions (Shimada *et al.*, 1991; Leopold *et al.*, 1994). Sugars often occur in large quantities in anhydrobiotes. In seeds, generally sucrose, often together with oligosaccharides such as raffinose, stachyose or verbascose is encountered (Amuti and Pollard, 1977; Horbowicz and Obendorf, 1994). In desiccation-tolerant pollen, sucrose is abundantly present (Hoekstra *et al.*, 1992). The African resurrection plant, *Craterostigma plantagineum* Hochst. is a desiccation-tolerant higher plant that can be dehydrated to water contents as low as 5% and resume normal activity upon rehydration. In its fresh leaves the unusual monosaccharide D-glycero-D-ido-2-octulose is found in large amounts (Bianchi *et al.*, 1991). On dehydration, the octulose is converted into sucrose. The formation of a glassy state by soluble carbohydrates in desiccation-tolerant higher plant organs is one in a cascade of adaptations upon desiccation, although a direct correlation between tolerance and carbohydrate composition and content is rather loose (Bochicchio *et al.*, 1994; Steadman *et al.*, 1996). The contribution of the glassy state to the stability of seeds in storage seems more evident (Sun and Leopold, 1994; Leopold *et al.*, 1994). Particularly seeds in which oligosaccharides with a high T_g accumulate, have been suggested to have extended life spans in storage (Horbowicz and Obendorf, 1994). Beside carbohydrates, also proteins can be easily organised

in a glassy matrix at room temperature when they are dried (Kakivaya and Hoeve, 1975; Noel *et al.*, 1995). Thus, soluble proteins present in the cytoplasm might influence the characteristics of the glassy state.

In contrast to a phase transition of a crystalline compound, the melting of glasses from the vitrified state into the liquid state is a second order transition. At the T_g, the enthalpy, entropy and the volume of the two phases are the same. However, the heat capacity changes upon melting of the glass (Roos, 1995).

The most widely used methods for measuring glass transitions are Dynamic Mechanical Analysis (DMA), Differential Scanning Calorimetry (DSC), Thermally Stimulated Depolarization Currents (TSDC) and Electron Spin Resonance Spectroscopy (ESR). DMA is a method in which the elastic modulus and loss modulus of a sample are measured as the sample is bent, twisted or compressed. Its application to biological tissues is limited (Maki *et al.*, 1994). The application of DSC to measure glass transitions is based on the change in heat capacity with melting of the glass, from which T_g and the enthalpy of relaxation can be derived. However, the abrupt change in heat capacity associated with T_g in dry biological tissues can be very small, which complicates the analysis (Williams, 1994; Leprince and Vertucci, 1995). Nevertheless, DSC has been successfully applied to measure glass transitions in seeds and pollen (Leopold *et al.*, 1994; Buitink *et al.*, 1996). TSDC was used to investigate properties of distinct water pools in biological systems (Bruni and Leopold, 1992; Konsta *et al.*, 1996). Although more sensitive than DSC, application of TSDC to very dry systems is difficult because the success of the technique depends on the presence of water. Using ESR spectroscopy, the rotational diffusion coefficient of a hydrophilic spin probe inserted in the cytoplasm can be determined and used to detect cytoplasmic glasses (Bruni *et al.* 1991; Dzuba *et al.*, 1993). A major drawback of this method is that a spin probe has to be inserted in the biological system and that the location of the spin probe within the cell may change upon dehydration (Golovina *et al.*, submitted).

In the present work, we have used FTIR microspectroscopy to characterise glasses in different sugars and dehydrating biological tissues. From the temperature dependence of the IR-bands arising from the OH-stretching and bending vibrations of the carbohydrates information can be obtained on the hydrogen bonding of a glass. A similar type of study has been carried out on crystalline sugars by Lutz and Van der Maas (1994), who correlated the frequency of the OH-stretching vibration with the geometric parameters of H-bridge formation, e.g. the O-H bond length and the O..O distance. From the temperature-dependent change in the frequency of the OH-band, information can be derived on the strength of the hydrogen bonds. The OH-stretching vibration band is located between 3600 and 3000 cm^{-1} (Vinogradov and Linnel, 1971). OH-bending vibration bands can be found between 1700-1000 cm^{-1} (in plane) or between 1000-400 cm^{-1} (out plane).

This paper reports on the glassy behavior of several mono-, di-, and tri-saccharides as studied by monitoring temperature dependent changes in their IR spectra. We found that the OH-stretching vibration of carbohydrates was most suited to study their glassy behavior. The T_gs that were obtained here, using IR methods, were compared with literature data obtained by DSC, to verify our method. Characteristics of the hydrogen bonding network in the glassy state were studied using the Wavenumber-Temperature Coefficients (WTC) as a parameter for the strength of the hydrogen bonding network. The IR method was also applied to study glasses in biological tissues, of which the cytoplasm was expected to be in a glassy state at ambient temperature. For this purpose *Typha latifolia* pollen and dehydrating leaves of the resurrection plant *Craterostigma plantagineum* were used as the experimental materials. Both tissues are characterised by a high sucrose content (Bianchi *et al.*, 1991; Hoekstra *et al.*, 1992).

Materials and methods

Sugars

Sucrose, glucose, raffinose and trehalose were purchased from Pfahnstiel, (Waukegan, IL). Raffinose was from Sigma (St Louis, MO). Glasses were formed by rapid drying of 10 µl of a sugar solution (20 mg ml^{-1}) on circular CaF_2 (13x2 mm diameter) windows in a cabin continuously purged with dry air (RH < 3% at 24°C). Residual water in the sugar glass was removed by heating the sample up to 70°C for several minutes (100°C in the case of raffinose and trehalose). The absence of water in the sugar glass was verified by the absence of the water band around 1650 cm^{-1}. Rehydration of sugar glasses was achieved by placing the windows containing the glasses for 2 days in closed boxes at different RHs, established by various saturated salt solutions (Vertucci and Roos, 1993).

Pollen

Collecting, handling and storage of *T. latifolia* L. pollen were performed as described earlier (Hoekstra *et al.*, 1991). The pollen used was harvested in June 1994. To obtain different water contents, pollen was equilibrated for 24 h in air of 20 - 100% RH at 24°C. The RH was regulated by cooling water vapour-saturated air in a cooling tower at different temperatures, and then heating this air up to 24°C. The RH was measured with a Rotronic hygroscope (±2% RH, Rotronic AG, Zurich, Switzerland). Water contents, expressed as g H_2O/g DW, were determined by comparing the fresh and dry weight of a sample. Dry weights were measured after heating the pollen for 4 h at 105°C.

Leaves

C. plantagineum Hochst. (Scrophulariaceae) plants, originating from Namibia, were a kind gift of Dr D. Bartels from the Max Planck Institut für Pflanzenzüchtung, Köln, Germany. The plants were grown in a greenhouse. Propagation of the plants was achieved by in vitro culture of leaf explants on a medium according to Bartels *et al.* (1990). Hydrated control plants were directly

agree with the intersection points derived from the plots of the FTIR data.

The above observations led us to the conviction that, indeed, the T_g of dry sugar glasses was observed. The slight differences between the present T_g values obtained by FTIR and those reported in the literature may be due to differences in the preparation method of the glasses. We have therefore defined the temperature at which the intersection occurs as the T_g. At temperatures below the intersection, the sugar is in a glassy state and above, in a liquid state.

OH-bending vibration

We also studied several bands in the fingerprint region of the IR spectrum (1500-900 cm^{-1}). Because the spectrum is rather complex in this region due to overlap of characteristic group frequencies, we have applied second derivative analysis. For each of the measured sugar spectra, only one band in the fingerprint region showed a similar intersection point as the OH-stretching vibration band, indicating a glass transition. In contrast to the frequency *vs* temperature plot of the OH-stretching band, that of the vibration band around 1050 cm^{-1} showed negative WTC (Figure 3D-F). The intersection points were at slightly higher temperature for glucose (31°C), sucrose (62°C)

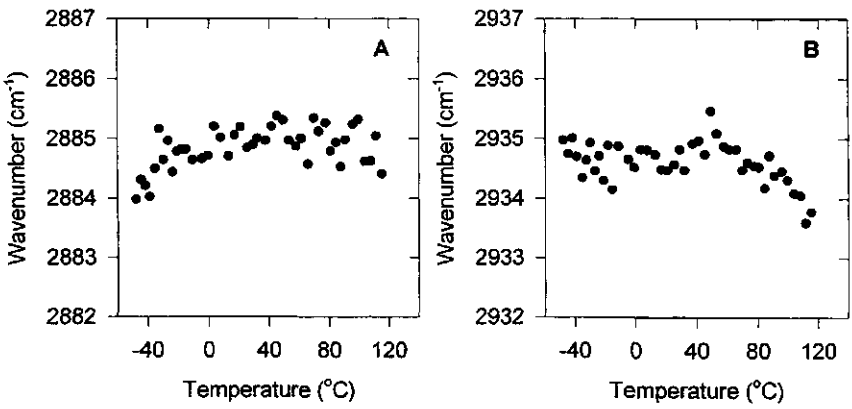

Figure 4. Wavenumber versus temperature plot (FTIR) of the bands around 2935 (A) and 2885 cm^{-1} (B) that can be assigned to CH-stretching vibrations of dried sucrose glasses. The bandpositions were resolved by second derivative analysis of the original absorption spectra.

and raffinose (122°C) than those obtained when analysing the OH-stretching vibration (see also Table 1). As discussed previously, a clear assignment of these bands is difficult. However, it is likely that the OH-bending vibration also responds to a glass transition as does the OH-stretching vibration. The breaks shown in Figure 3 (D-F) are evidence that these band positions can be assigned, at least partly, to OH-deformation vibration. Because more than one band contributes in this region, each with a different temperature dependence, it is dangerous to draw conclusions from the WTC values obtained from Figure 3D-F.

CH-stretching vibration

We also studied the temperature dependence of two bands around 2935 and 2885 cm^{-1}, as determined by second derivative analyses of the region between 3000 and 2800 cm^{-1} for dry sucrose. These bands can be assigned to CH-stretching vibrations (Casal and Mantsch, 1984). Figure 4 shows that the position of these bands hardly changed over the measured temperature range. No abrupt changes around T_g (57°C) were observed. Also the line-width in the original absorption spectra hardly changed over this broad temperature range.

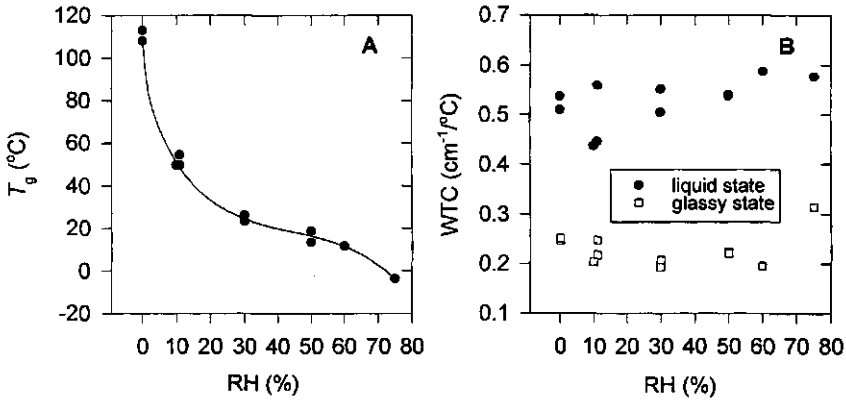

Figure 5. Effect of equilibration at different RHs on characteristics of raffinose glasses. The glass transition temperature, T_g (A), and the Wavenumber Temperature Coefficients (WTC) values (B) in the glassy state and the liquid state were determined from νOH against temperature plots (FTIR).

Similar results were obtained for the other sugars (data not shown). These results indicate that Van der Waals' interactions between CH-groups in the glassy matrix are less important in the structure of the glassy state and that the glassy state is formed by the OH-network.

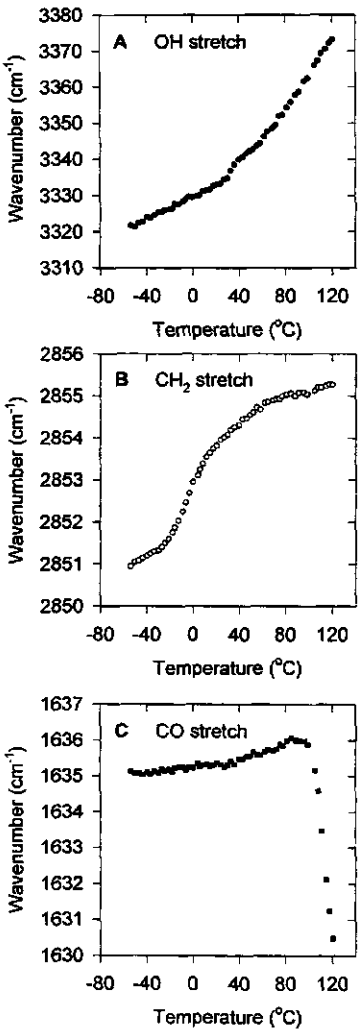

Figure 6. Wavenumber versus temperature plots (FTIR) of *T. latifolia* pollen. The data points represent the OH-stretching vibration, CH_2-stretching vibration and the amide I band around 1635 cm^{-1}. The CH_2 and the amide-I band positions were resolved after second derivative analysis of the original absorption spectra.

WTC

For all the dried sugars the WTC ($cm^{-1}/°C$) for the OH-stretching vibration band was calculated in both the glassy and the liquid state (Table 1). In the liquid state the WTC was almost the same for all the sugars measured. In the glassy state, however, differences in the WTC were observed between mono-, di- and tri-saccharides. For glucose and octulose the WTC was lower than for di- and tri-saccharides. We interpret this to mean that monosaccharide glasses have a more dense structure with stronger interactions. The WTC of the disaccharide, trehalose, was comparable to that of the trisaccharide, raffinose. The glass structure of the trisaccharide, umbelliferose, resembled that of the disaccharide, sucrose, with respect to its T_g and WTC. The anomaly of trehalose was also reflected in its high T_g when compared with sucrose. From Table 1 it can be derived that a higher T_g correlates with an elevated WTC value in the glassy state, but not in the liquid state.

Effect of water on raffinose glasses

To obtain more evidence that indeed glass transitions are observed by the present IR method, the plasticising effect of water on raffinose glass was studied (Figure 5a). The raffinose glass was formed by air-drying of a raffinose solution. Glasses of different water contents were obtained by placing dried glasses at different RHs. Figure 5a indicates that the highest T_g occurred in the sample with the lowest water content (obtained after heating of the dried glass), to level off at higher equilibrium RHs. At RHs above 60%, T_g further decreased. The shape of the curve mirrors a sorption curve, what is expected on account of the RH/water content relationship (see Roos, 1995).

The WTC values that were obtained in the glassy state of these raffinose glasses was approximately 0.23 $cm^{-1}/°C$ in the region RH = 0% to RH = 60% (Figure 5b). At RH = 75%, WTC increased sharply. However, the glass appeared to be rather unstable at this high RH, because it crystallised in some cases. If crystallization was observed, the data were not used. The WTC in the liquid state was considerably higher with an average value of ca. 0.51 $cm^{-1}/°C$. There was no drastic change in WTC values coinciding with the considerable

increase in T_g upon removal of the last residual water from the raffinose glass (cf. Figure 5a).

Glass transitions in anhydrobiotic plants

The success of characterising glasses of pure sugars with FTIR encouraged us to apply the method to dry desiccation-tolerant plant tissues that are known to contain large amounts of soluble sugars.

T. latifolia pollen

Spectra of *T. latifolia* pollen, sandwiched as a monolayer between two diamond windows, show a broad band around 3330 cm^{-1} (see Wolkers and Hoekstra, 1995). Because this pollen has a high sucrose content (23%, Hoekstra *et al.*, 1992), it can be assumed that sucrose is at least partly responsible for the IR-band at 3330 cm^{-1}. A study of the temperature dependence of characteristic group frequencies in the IR spectrum of this pollen (equilibrated to 30% RH = 0.06 g H_2O/g DW) disclosed details on distinct conformational changes occurring during heating (Figure 6). The asymmetric (CH_2) stretching vibration shows that melting of lipids (neutral and polar lipids (Hoekstra *et al.*, 1991)) in this pollen mainly occurs between -20 and 20°C. The proteins (CO stretch) start to denature at temperatures above 100°C (see also Wolkers and Hoekstra, 1997). The temperature dependence of the OH-stretch

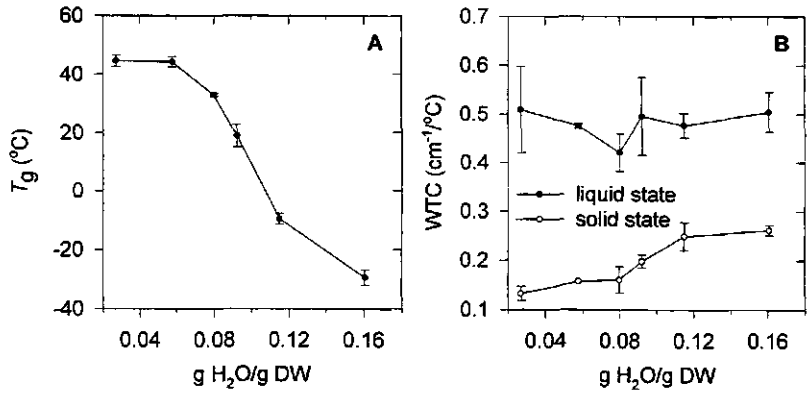

Figure 7. State diagram (A) and WTC values (± SE) in the glassy and liquid state (B) for *T. latifolia* pollen kept at different RHs.

reveals an intersection point around 40°C, which is indicative of a glass transition. Lipid melting and protein denaturation as they occur *in situ*, apparently can be distinguished separately from the melting of glasses.

Figure 7A shows T_gs obtained with pollen of different water contents (after a 2 day equilibration under different RHs). From a high T_g of 45°C at water contents < 0.06 g H_2O/g DW, the T_g curve decreased to -28°C at a water content of 0.16 g H_2O/g DW. At higher water contents (0.35 g H_2O/g DW) the νOH *vs* temperature plot was indicative of a first order transition (data not shown) due to the presence of freezable water (Buitink *et al.*, 1996). The melting of the ice in this sample occurred at around -22°C, and the onset of melting was at -30°C, which might correspond to T_g'.

There was a decrease of WTC in the glassy state with the loss of water (Figure 7B). The WTC values in the liquid state remained rather constant with the different water contents.

C. plantagineum leaves

Leaves of *C. plantagineum* can survive water contents of less than 0.05 g H_2O/g DW (Bianchi *et al.*, 1991). During the drying process, large amounts of sucrose are formed from the monosaccharide, octulose, and the reverse occurs during rehydration. To follow possible formation of a cytoplasmic glass during

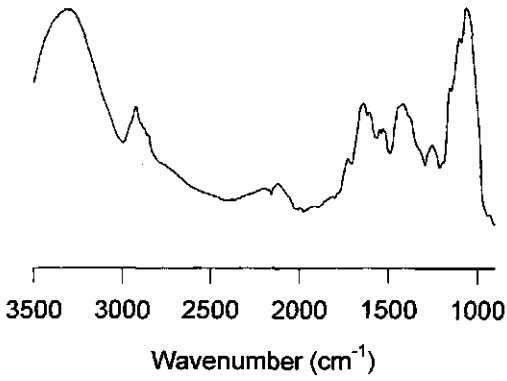

Figure 8. *In situ* IR absorbance spectrum of dried *C. plantagineum* leaves

dehydration, thin leaf sections were cut and sandwiched between two diamond windows. The IR-microscope was used to select a suitable tissue area for FTIR analysis. In Figure 8, the absorption spectrum of a leaf dried on the plant is shown.

In Figure 9, the plots representing the frequency of the OH-stretching vibration band as a function of the temperature for fresh and dehydrated leaves are shown. In the plot of the dried leaf one very sharp discontinuity can be seen, with a calculated T_g of 65°C (0.15 g H_2O/g DW). In the plot of the hydrated leaf (6 g H_2O/g DW) two discontinuities are apparent. The complexity of this curve is due to excess amount of water and the relatively slow rate of cooling of the sample in the sample holder, allowing partial freeze-concentration of cellular solutes. Moreover, the type of sugars differs in the dry and the fresh leaves, i.e., sucrose and octulose, respectively.

It would have been interesting to estimate T_g in an intact leaf that was dried without conversion of octulose into sucrose. Because it is impossible to dry an intact leaf without at least some conversion, cytoplasmic extracts of the

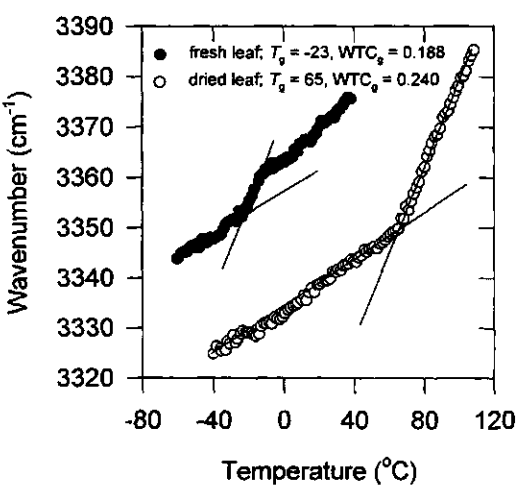

Figure 9. Wavenumber versus temperature plot (FTIR) of dried and hydrated *C. plantagineum* leaves. The data points represent the OH-stretching vibration of dried leaves and hydrated leaves. The determined T_g (°C) and the WTC_g values (cm^{-1}/°C) in the glassy state are also indicated.

fresh and dried leaves were made and droplets were dried on the CaF_2 windows. This allows for inspection of T_g in dry cytoplasmic environment where octulose is still the major soluble sugar (Figure 10).

The T_g determined on dried isolated cytoplasm was 19°C for fresh leaves and 73°C for dried leaves. The T_g of dried cytoplasm from fresh leaves was almost similar to that of purified octulose (21°C, Table 1). The T_g of 73°C of dried cytoplasm from dried leaves (65°C in situ, Figure 9) was higher than that of pure sucrose (57°C), indicating that components other than sucrose also contribute.

In order to get information on the cytoplasmic glass formation during drying of *C. plantagineum* leaves, frequency *vs* temperature plots were made at distinct time intervals, and the intersection points were determined (Figure 11). For this purpose, excised leaves were dried in open Petri dishes exposed to an atmosphere of 30-40% RH. The leaves dehydrated from 8.5 g H_2O/g DW to 1 g H_2O/g DW in about 30 h under these conditions. At leaf water contents above 1 g H_2O/g DW two intersection points were observed (similar as in Figure 9). The intersection points at the low temperature side (left) located around -23°C were

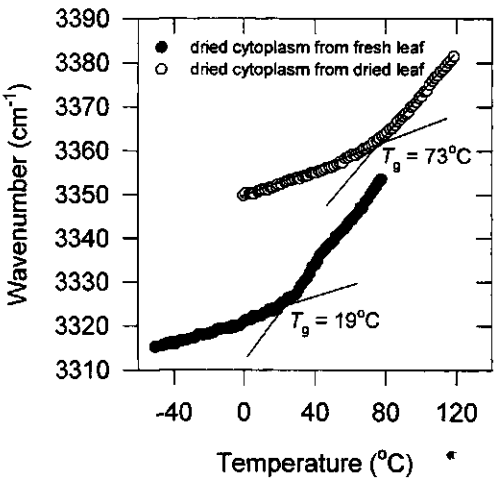

Figure 10. Wavenumber versus temperature plot (FTIR) of dried extracted cytoplasm of fresh and dried *C. plantagineum* leaves. The T_g values are also indicated.

defined here as T_g' (Figure 11A). When the water content dropped below 0.5 g H_2O/g DW only one intersection point was observed, which we assigned to T_g.

Further decrease of the water content led to a rapid increase of T_g. A T_g of 30°C was reached at a leaf water content of approximately 0.12 g H_2O/g DW, which did not change further after 72 h of drying. The initial amounts of octulose and sucrose in the fresh leaves were 0.35 g/g DW and 0.01 g/g DW, respectively. When the leaf water content dropped below 1 g H_2O/g DW, the amounts of octulose (0.04 g/g DW) and sucrose (0.18 g/g DW) remained stable. From this it can be concluded that the rapid increase of T_g below 0.5 g H_2O/g DW occurs after the sugar conversion was completed. The WTC values in the glassy state below a water content of 0.4 g H_2O/g DW scattered around 0.21 cm^{-1}/°C (Figure 11B), which falls in the range of those determined for the sucrose glass. In the leaves dehydrated on the plant, the WTC was somewhat higher, also corresponding with a higher T_g (Figure 9). This higher T_g and WTC suggests an involvement of additional compounds (oligo- or poly-saccharides) in the glassy state in leaves dried on the plant.

Discussion

In the present work FTIR microspectroscopy was used to characterise

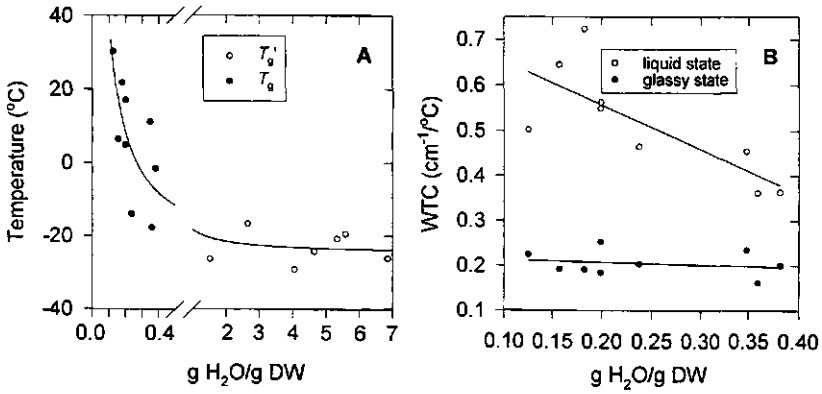

Figure 11. State diagram of dehydrating *C. plantagineum* leaves that were excised from the plant (A). The filled circles represent T_g and the open circles T_g'. WTC values in the glassy and liquid state are shown in (B).

glasses of several soluble carbohydrates and of the cytoplasm in two desiccation-tolerant plant organs. The method is based on a temperature study of IR band positions that were expected to shift with the glass transition.

Sugar glasses, several of which have been extensively characterised by other methods (Slade and Levine, 1991) were prepared for FTIR analysis by air-drying of dilute solutions. This air-drying prevents crystallization (compare Figures 1 and 2). The temperature dependence of characteristic band frequencies in IR spectra of these glasses was investigated around the expected T_g, with special emphasis on the OH vibration bands. In carbohydrate glasses the OH-stretch around 3300 cm^{-1} is well resolved (Vinogradov and Linnel, 1971). The broadness and position of this band indicate that the dry sugar glasses have a wide variety of hydrogen bonds. We found a linear correlation of νOHs with temperature when the sugars were in a glassy state. Upon melting of the glass again a linear correlation, but with higher regression coefficient, was observed. The temperature at intersection of these regression lines coincides well with T_g values obtained by DSC (Orford *et al.*, 1990; Slade and Levine, 1991; Saleki-Gerhardt *et al.*, 1994; Roos 1995). We therefore define the temperature at this intersection as the T_g. The change in WTC can be attributed to an abrupt loosening in the hydrogen bonding network associated with the melting of the glass. Changes in WTC may also occur with respect to the OH-deformation band (in plane). This band could be assigned on account of an abrupt change in the WTC in a similar temperature range as found for the OH-stretch (see Figure 3). Because of the presence of many superpositioned bands in the fingerprint region (1700-1000 cm^{-1}), conclusions with regard to wavenumber positions and WTC have to be drawn with caution. In biological tissues the spectra in this region are even more complex, which is the reason why we have not analysed them further.

Hydrogen bonding leads to a lower wavenumber position of the OH-stretching vibration band (Vinogradov and Linnel, 1971). This effect is due to a weakening of the force constant for the OH-stretching mode, caused by the formation of the H bond. H-bonding also causes a broadening and an increase in band intensity of the OH-stretch. In contrast, the OH-deformation mode is

shifted to a higher wavenumber position. Formation of H bonds constrains the deformation vibration and therefore increases the force constants for these modes. The shifts in wavenumber position of the deformation modes upon H-bonding are substantially smaller than those for the OH-stretching modes (Vinogradov and Linnel, 1971, Figure 3). The temperature dependence of the stretching vibration always yielded positive WTCs (see Figure 3), which denotes a decrease in hydrogen bonding with increasing temperature. In agreement with this, the OH-deformation always yielded negative WTCs.

The lower WTC in the glassy state of mono-saccharide glasses compared with di- and oligo-saccharide glasses is the result of a stronger hydrogen bonding network, associated with a more densely packed glassy structure. Higher T_g values coincided with higher WTCs in the glassy state, but not in the liquid state (Table 1). Apparently, the smaller monosaccharide units can be packed more tightly in the vitrified state. At elevated water contents the OH-stretch of water overrules the OH-stretch of the carbohydrates, which limits the applicability of the method in terms of maximum permissible water content.

The frequency of the OH-stretch has been shown to correlate with the geometric parameters of the H-bridges, e.g. the O-H bond length and the O..O distance (Plaggio *et al.*, 1983; Gould and Hillier, 1994). However, these data have been obtained with crystallised materials and linked to distances as observed in crystals. In our glasses this band position is in the range of 3320-3360 cm^{-1} at room temperature, depending on the sugar analysed (Figure 3). Applying the correlation between νOH and dOO, as given by Lutz and Van der Maas (1994), would indicate that dOO in the glasses is in the range of 2.8 to 2.9 Å. From this work on crystallised sugars a linear relationship between the OH-stretching band position and temperature was obtained that could be linked with atomic distances and the strength of hydrogen bonding. Because not much is known for sugar glasses in that respect, it would be interesting to link the observed wavenumber positions to atomic distances. Only recently, neutron diffraction has been used to measure atomic distances in glucose glasses (Tromp, personal communication). The positive correlation of WTC in the glassy state and T_g suggests that atomic distances increase more rapidly with

heating in sugars having high T_g than in those having low T_g. The more loose structure of high T_g glasses has also been suggested on the basis of ESR experiments (Dzuba *et al.*, 1993). Van der Waals' interactions between CH-groups seem less important for stabilizing the glassy state. We conclude this from a lack of change in the CH-stretch with the glass transition (Figure 4).

We also applied FTIR to study glasses in the cytoplasm of biological tissues. Desiccation-tolerant specimens having high sugar contents, such as pollen and leaves of resurrection plants, were expected to be particularly suitable for that purpose. The dry matter may comprise up to 50% of disaccharides (Bianchi *et al.*, 1991). Various absorption bands, characterising specific molecular groupings in the IR-spectrum of dry desiccation-tolerant *T. latifolia* pollen were analysed in a heating study to discriminate between first and second order transition phenomena (Figure 6). The OH-stretch clearly showed one break, indicative of a second order transition, whereas the CH-stretch displayed two breaks, typical of a first order transition. For the resurrection plant *C. plantagineum*, also a second order behavior of the OH-stretch was observed in spectra of leaves below 0.5 g H_2O/g dry matter. This already strongly suggests that the OH-stretch reflects the glassy behavior in these organs. Other temperature dependent shifts such as the melting of lipids (CH) and the denaturation of proteins (amide region) occurred at different temperature regions (Figure 6).

Further evidence that indeed glasses are observed comes from the effect of water on the position of the breaks in the νOH *vs* temperature plots (see Figures 9 and 11). The temperature at the breaks (T_g) rapidly increased below water contents of 0.5 g H_2O/g DW. Plots of the presumed T_gs against water content have shapes comparable with state diagrams produced for seeds and pollen by other methods (Williams and Leopold, 1989; Bruni and Leopold, 1992; Buitink *et al.*, 1996). Particularly striking is the constant T_g in dry pollen at and below 0.06 g H_2O/g DW (Figure 7A). This phenomenon has been observed earlier in bean seeds by Leprince and Vertucci (1995). We interpret this to result from competition of the glass with other cellular compounds for the

remaining water. Apparently at 0.06 g H_2O/g DW the glass is already dry and further water loss may be from the other compounds.

In contrast to only one sharp intersection point in dry *C. plantagineum* leaves, fresh and partly dehydrated leaves displayed two intersection points, that are apparently associated with the ample water present in these samples. We explain these phenomena as follows. The FTIR instrumentation only permitted slow freezing rates of approximately 5°C/min before the heating (1°C/min) was started. This cooling rate is slow as compared to what is normally used in DSC experiments. Slow cooling may have led to freeze-concentration of the hydrated cytoplasm and, thus, T_g' may have been measured. The melting of ice is then seen at about -10°C (the higher value in Figure 9). Therefore, it is difficult to interpret the slopes of the different states when freezable water is present. Moreover, the OH-stretch vibration bands of water and sugar are superimposed, which limits the applicability of IR spectroscopic methods for the analysis of T_g and WTC. However, below 0.3 g H_2O/g DW no problems are expected, because this water represents the nonfrozen fraction (Crowe *et al.*, 1990; Roos and Karel, 1991a,b). The advantage of FTIR is that it can be applied in any phase (solid or hydrated), although the method is limited to water contents of, say, below 0.5 g/g DW. IR is more sensitive in this region where other techniques such as DSC (Leprince and Vertucci, 1995) are becoming less sensitive.

Dried leaves of *C. plantagineum* are in a glassy state at ambient temperature, whereas fresh leaves are not (Figures 9 and 11). The benefits of a glassy state for desiccation tolerance (Sun *et al.*, 1996; Hoekstra *et al.*, 1997) and life span in storage (Leopold et al., 1994) have been discussed earlier. In fresh leaves the monosaccharide octulose is abundantly present. On dehydration, it is converted into sucrose (Bianchi *et al.*, 1991), and this conversion is completed at 0.5 g H_2O/g dry matter (data not shown). This change in composition strongly influences T_g as demonstrated in Figure 10 showing νOH *vs* temperature plots of dried cell extracts from fresh and dried leaves. The T_g of dried cytoplasm isolated from hydrated leaves (19°C) is comparable with that of the dry octulose glass (21°C), but the T_g of dried

cytoplasm isolated from leaves dried on the plant (73°C) is considerably higher than the T_g of the dry sucrose glass (57°C). This suggests that sucrose is not the sole component involved in the glassy state of dried leaves. The change in sugar composition upon dehydration may serve a purpose in the protection of leaves against desiccation stress. Octulose would not be able to form a glass in the dried leaves at ambient temperature, whereas sucrose does. In the fresh leaf octulose may accumulate without interference with cellular metabolism.

The highest T_g determined in excised leaves dried in Petri-dishes was 30°C (Figure 11), which is lower than the T_g of 65°C as determined for leaves dehydrated on the plant (Figure 9). This discrepancy may stem from differences in drying rate or simply from the influence of the excision. Leaves from both experiments recuperated upon rehydration.

The WTC values of the pollen in the glassy state tended to decrease with the loss of water to assume a stable level below 0.08 g H_2O/g DW. The observed T_g value of dry pollen (around 45°C, Figure 7) together with the average WTC values indicate that the glassy state in this pollen is primarily formed by sucrose, that is abundantly present in this pollen. The WTC of *C. plantagineum* leaves in the glassy state did not show a trend with the water content but scattered around 0.21 cm^{-1}/°C (below 0.5 g H_2O/ g DW).

Conclusions

FTIR is a very promising technique to study glasses in dry soluble carbohydrates and in biological materials in situ. The major advantages of FTIR are the high sensitivity in dry materials as compared to other techniques. The glass transition can be determined by FTIR from a νOHs *vs* temperature plot at the intersection point of two linear regressions in the liquid and in the glassy state. The Wavenumber Temperature Coefficient (WTC) gives information on the packing density of the glassy state. The glass transition is associated with an abrupt change in hydrogen bonding interactions between the sugar OH-groups. Van der Waals' interactions between CH-groups are of less importance in stabilizing the glassy state.

Acknowledgements

This project was financially supported by the Life Sciences Foundation, which is subsidised by the Netherlands Organization for Scientific Research.

References

Amuti, K.S., Pollard, C.J. (1977) Soluble carbohydrates of dry and developing seeds. Phytochemistry **16,** 529-532.

Bartels, D., Schneider, K., Terstappen, G., Piatkowski, D., Salamini, F. (1990) Molecular cloning of abscisic acid-modulated genes which are induced during desiccation of the resurrection plant Craterostigma plantagineum. Planta **181,** 27-34.

Bianchi, G., Gamba, A., Murelli, C., Salamini, F., Bartels, D. (1991) Novel carbohydrate metabolism in the resurrection plant Craterostigma plantagineum. Plant. J. **1,** 355-359.

Bochicchio, A., Rizzi, E., Balconi, C., Vernieri, P., Vazzana, C. (1994) Sucrose and raffinose contents and acquisition of desiccation tolerance in immature maize embryos. Seed Sci. Res. **4,** 123-126.

Bruni, F., Leopold, A.C. (1991) Glass transitions in soybean seed. Relevance to anhydrous biology. *Plant Physiol.* **96,** 660-663.

Bruni, F., Leopold, A.C. (1992) Pools of water in anhydrobiotic organisms: A thermally stimulated depolarization current study. *Biophys J.* **63,** 663-672.

Buitink, J., Walters-Vertucci, C.W., Hoekstra, F.A., Leprince, O. (1996) Calorimetric properties of dehydrating pollen: Analysis of a desiccation-tolerant and an intolerant species. *Plant Physiol.* **111,** 235-242.

Casal, H.L., Mantsch, H.H. (1984) Polymorphic phase behaviour of phospholipid membranes studied by infrared spectroscopy. *Biochim. Biophys. Acta* **779,** 381-401.

Crowe, J.H., Carpenter, J.F., Crowe, L.M., Anchordoguy, T.J. (1990) Are freezing and dehydration similar stress vectors? A comparison of modes of interaction of stabilizing solutes with biomolecules. Cryobiology **27,** 219-231.

Crowe, J.H., Hoekstra, F.A., Crowe, L.M. (1992) Anhydrobiosis. *Annu. Rev. Physiol.* **54,** 570-599.

Crowe, J.H., Crowe, L.M., Carpenter, J.F., Prestrelski, S.J., Hoekstra, F.A. (1997) Anhydrobiosis: cellular adaptations to extreme dehydration. *In:* Dantzler, W.H. (ed.) Handbook of Physiology section 13, Comparative Physiology, Vol II, Oxford University Press, Oxford. Pp. 1445-1477.

Dzuba, S.A., Golovina, E.A., Tsvetkov, Yu D. (1993) Echo-induced EPR spectra of spin probes as a method for identification of glassy state in biological objects. *J. Magn. Reson.* **101,** 134-138.

Golovina, E.A., Hoekstra, F.A., Hemminga, M.A. Drying increases intracellular partitioning of amphiphilic substances into lipid phase: impact on membrane permeability and significance for desiccation tolerance. *Biochemistry* submitted for publication.

Gould, I.R., Hillier, I.H. (1994) The relation between hydrogen-bond strengths and vibrational frequency shifts: a theoretical study of complexes of oxygen and nitrogen proton acceptors and water. *J. Mol. Struct.* **314,** 1-8.

Hoekstra, F.A., Crowe, J.H., Crowe, L.M. (1991) Effect of sucrose on phase behaviour of membranes in intact pollen of Typha latifolia L., as measured with Fourier transform infrared spectroscopy. *Plant Physiol.* **97,** 1073-1079.

Hoekstra, F.A., Crowe, J.H., Crowe, L.M., Van Roekel, T., Vermeer, E. (1992) Do phospholipids and sucrose determine membrane phase transitions in dehydrating pollen species? *Plant Cell Environ.* **15,** 601-606.

Hoekstra, F.A., Wolkers, W.F., Buitink, J., Golovina, E.A., Crowe, J.H., Crowe, L.M. (1997) Membrane stabilization in the dry state. *Comp. Biochem. Physiol.* **117A,** 335-341.

Horbowicz, M., Obendorf, R.L. (1994) Seed desiccation tolerance and storability: dependence on flatulence-producing oligosaccharides and cyclitols: review and survey. *Seed Sci. Res.* **4,** 385-406.

Kakivaya, S.R., Hoeve, C.A.J. (1975) The glass point of elastin. *Proc. Natl. Acad. Sci. USA* **72,** 3505-3507.

Konsta, A.A., Pissis, P., Kanapitsas, A., Ratkovic, S. (1996) Dielectric and conductivity studies of the hydration mechanisms in plant seeds. *Biophys. J.* **70,** 1485-1493.

Koster, K.L. (1991) Glass formation and desiccation tolerance in seeds. *Plant Physiol.* **96,** 302-304.

Leopold, A.C., Sun, W.Q., Bernal-Lugo, I. (1994) The glassy state in seeds: analysis and function. *Seed Sci. Res.* **4,** 267-274.

Leprince, O., Hendry, G.A.F., McKersie, B.D. (1993) The mechanisms of desiccation tolerance in developing seeds. Seed Sci. Res. **3,** 231-246.

Leprince, O., Walters-Vertucci, C. (1995) A calorimetric study of the glass transition behaviours in axes of bean seeds with relevance to storage stability. *Plant Physiol.* **109,** 1471-1481.

Lutz, E.T.G., Van der Maas, J.H. (1994) Hydrogen bonds in crystalline carbohydrates. A variable-temperature FT-IR study. *J. Mol. Struct.* **324,** 123-132.

Maki, K.S., Bartsch, J.A., Pitt, R.E., Leopold, A.C. (1994) Viscoelastic properties and the glassy state in soybeans. *Seed Sci. Res.* **4,** 27-31.

Noel, T.R., Parker, R., Ring, S.G., Tatham, A.S. (1995) The glass-transition behaviour of wheat gluten proteins. *Int. J. Biol. Macromol.* **17,** 81-85.

Orford, P.D., Parker, R., Ring, S.G. (1990) Aspects of the glass transition behaviour of mixtures of carbohydrates of low molecular weight. *Carbohydrate Res.* **196,** 11-18.

Plaggio, P., Tubino, R., Dellepiane, G. (1983) A note on the correlation between infrared frequencies and hydrogen-bond lengths in hydroxyl chains. *J. Mol. Struct.* **96,** 277-281.

Prestrelski, S.J., Tedeschi, N., Arakawa, T., Carpenter, J.F. (1993) Dehydration-induced conformational transitions in protein and their inhibition by stabilizers. *Biophys. J.* **65,** 661-671.

Redgwell, R.J. (1980) Fractionation of plant extracts using ion-exchange Sephadex. Anal. *Biochem.* **107,** 44-50.

Roos, Y.H. (1995) Phase Transitions in Foods, Academic Press, London, pp. 1-360.

Roos, Y., Karel, M. (1991a) Amorphous state and delayed ice formation in sucrose solutions. *Int. J. Food Sci. Technol.* **26,** 553-566.

Roos, Y., Karel, M. (1991b) Nonequilibrium ice formation in carbohydrate solutions. *Cryo Lett.* **12,** 367-376.

Saleki-Gerhardt, A., Zografi. G. (1994) Nonisothermal and isothermal crystallization of sucrose from the amorphous state. *Pharm. Res.* **11,** 1166-1173.

turn/β-sheet band of dried seeds was found at 1634 cm^{-1} (data not shown). The spectra of these LAB-treated double mutant seeds resembled those of *abi3-5* seeds, indicating that LAB treatment can prevent the formation of intermolecular extended β-sheet structures upon drying. Seeds of this LAB-treated double mutant are desiccation-tolerant (Ooms *et al.*, 1994).

Heat stability of proteins in *abi3* seeds

Turn/β-sheet structures

To analyze whether the order of maturation defectiveness of the *abi3* allelic series (*abi3-5* > *abi3-7* > *abi3-1* > wild-type) is also manifested in protein stability, heat denaturation studies were performed. In Figure 3, the position of the IR-band around 1633 cm^{-1} in these ABA-insensitive mutant seeds (derived from spectra as shown in Fig. 2), is plotted as a function of the temperature. Upon heating, this band representing turn and β-sheet structures, shifted to 1627 cm^{-1}. The temperature at which the band around 1633 cm^{-1} falls to lower wavenumber position (and increases in relative proportion), marks the onset of protein denaturation (Wolkers and Hoekstra, 1997).

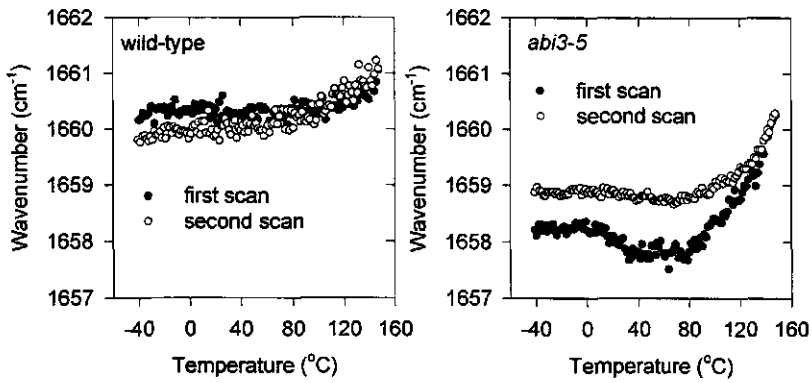

Figure 4. Wavenumber *vs* temperature plots (FTIR) of the amide-I band denoting α-helical protein structure in dried wild-type seeds, and *abi3-5* mutant seeds of *A. thaliana*. Data of 3 seeds were averaged.

In *abi3-5* seeds, the turn/β-sheet band was observed at approximately 1633 cm^{-1} and initially hardly changed in position with temperature (Fig. 3). Above 70°C, this band position sharply fell to level off at 100°C (see Figs. 2 and 3). After cooling, the second heating scan shows that this shift to lower wavenumbers is irreversible. The denaturation temperature of proteins in *abi3-5* seeds was estimated at approximately 87°C, at the midpoint of the denaturation curve. In similar plots of *abi3-7* and *abi3-1* seeds, signs of irreversible protein clustering were observed at much higher temperatures. Also, the heat-induced protein structural rearrangements were less extensive when compared with those in the *abi3-5* seeds, as deduced from the relative proportion of the two major bands in the deconvolved absorbance spectra (data not shown). The *aba1-1 abi3-1* double mutant seeds had band positions at 1627 cm^{-1} already at ambient temperature, which hardly changed on heating. In contrast to the *abi3* mutant seeds, the band position of the turn/β-sheet band in wild-type seeds irreversibly shifted to higher wavenumbers with temperature (from 1630 cm^{-1} to 1635 cm^{-1}) and no signs of intermolecular β-sheet structures were visible.

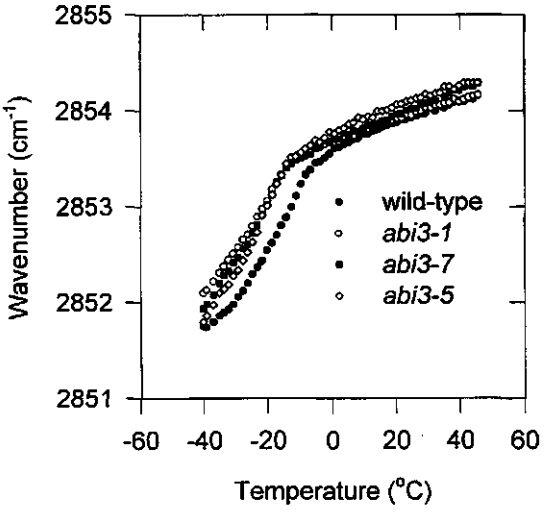

Figure 5. Wavenumber *vs* temperature plots (FTIR) of the symmetric CH_2 stretching vibration band in dried *abi3 A. thaliana* mutant seeds. The data points represent wild-type, *abi3-1*, *abi3-7* and *abi3-5* seeds. Data of 3 seeds were averaged.

Furthermore, hardly any changes in relative proportion of the two major bands were observed, indicating that only very small protein structural rearrangements occur with heating to 150°C (see Fig. 2). A possible explanation for the shift to higher wavenumbers could be the loss of bound water during the heating, which generally is observed in proteins during dehydration (Prestrelski *et al.*, 1993). Hydrated wild-type seeds had a considerably lower denaturation temperature of 67°C and a T_{onset} of 56°C (data not shown).

α-helical structures

Figure 4 shows wavenumber *vs* temperature plots for the α-helical band at approximately 1659 cm^{-1}, which occupies most of the amide-I band of the

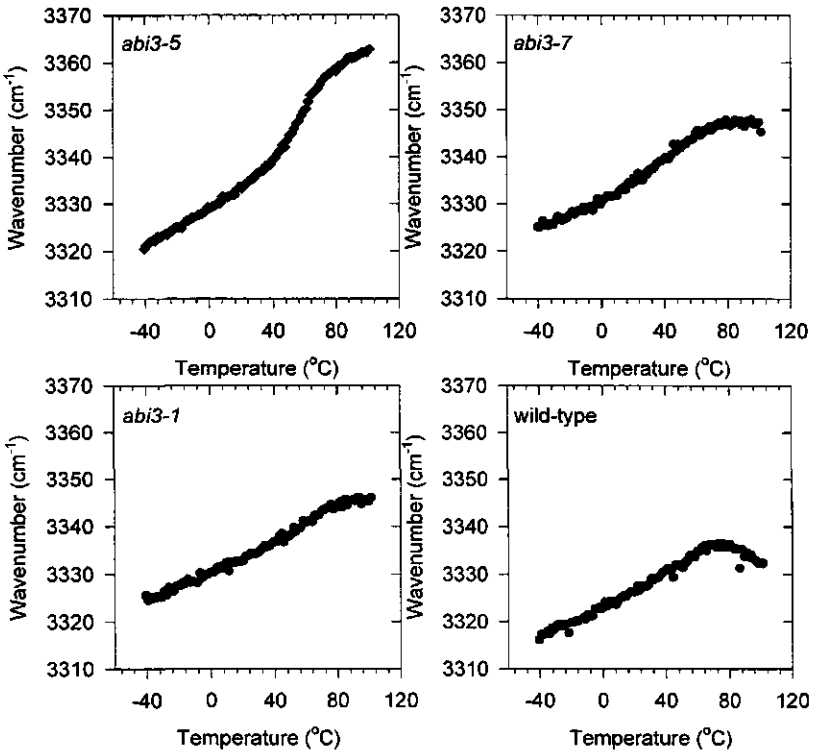

Figure 6. Wavenumber *vs* temperature plot (FTIR) of the OH-stretching vibration band in dried *abi3 A. thaliana* mutant seeds. The data points represent wild-type, *abi3-1*, *abi3-7* and *abi3-5* seeds. Data of 3 seeds were averaged.

native proteins. The α-helical band position in the wild-type seeds did not shift over a temperature range from -40 to 150°C, indicating that these structures are particularly heat stable. A small, but irreversible shift to higher wavenumber position with heating was visible in the *abi3-5* seeds. In *abi3-1* and *abi3-7* seeds, this shift to higher wavenumber position was also observed (data not shown). Such a small upward shift of the α-helical band may be due to an alteration of the protein-solvent interaction (i.e. the amount of bound water) and/or denaturation.

Melting of lipids in *abi3* seeds

Figure 5 depicts the wavenumber *vs* temperature plots of the symmetric CH_2 stretching vibration of seeds of wild-type and several *abi3* alleles. The shape of the plots reflects the melting of oil in these seeds (Wolkers and Hoekstra, 1995). In wild-type seeds, lipids have an average T_m of about -17°C. All of the *abi3* mutant seeds had a lower average T_m of approximately -25°C.

Table 1. Initial WTC (WTC_{in}) and maximal WTC (WTC_{max}) as determined from νOH *vs* temperature plots (Figs. 6 and 8) of *A. thaliana* mutant seeds. Where possible, T_g was determined. For comparison T_g and WTC of dry glucose, sucrose and raffinose glasses are included. LSD for WTC_{in} is 0.065 (at $P = 0.05$); LSD for WTC_{max} is 0.167 (at $P = 0.05$)

Sample	WTC_{in} ($cm^{-1}/°C$)	WTC_{max} ($cm^{-1}/°C$)	T_g (°C)
wild-type	0.14	0.19	nd*
abi3-1	0.14	0.22	*nd*
abi3-7	0.16	0.27	20
abi3-5	0.21	0.58	37
aba1-1 abi3-1	0.18	0.32	21
lec2-1	0.21	0.33	nd
lec1-1	0.24	0.61	20
lec1-3	0.26	0.54	20
glucose	0.15	0.56	27
sucrose	0.20	0.59	57
raffinose	0.25	0.53	108

*nd = not detectable

This may be due to the reduced proportion of eicosenoic acid being the major fatty acid in storage lipids in *A. thaliana* seeds and the increased proportion of linoleic acid (Finkelstein and Sommerville, 1990; De Bruijn *et al.*, 1997).

Properties of the viscous solid matrix in dry *abi3* seeds

The glassy matrix that is formed in dehydrating seeds and pollen depends on hydrogen bonding, likely involving sugars and proteins (Chapters 6, 9, 10). The OH-stretching vibration band around 3330 cm^{-1} (see Fig. 1) is sensitive to hydrogen bonding. The shift of this band with temperature, the Wavenumber Temperature Coefficient (WTC, $cm^{-1}/°C$), gives information on the average strength of hydrogen bonding (Wolkers *et al.*, 1998b). Figure 6 depicts the νOH *vs* temperature plots of seeds of wild-type and various *abi3* alleles. In the plots of the dry *abi3-7* and *abi3-5* seeds, breaks were calculated to occur at

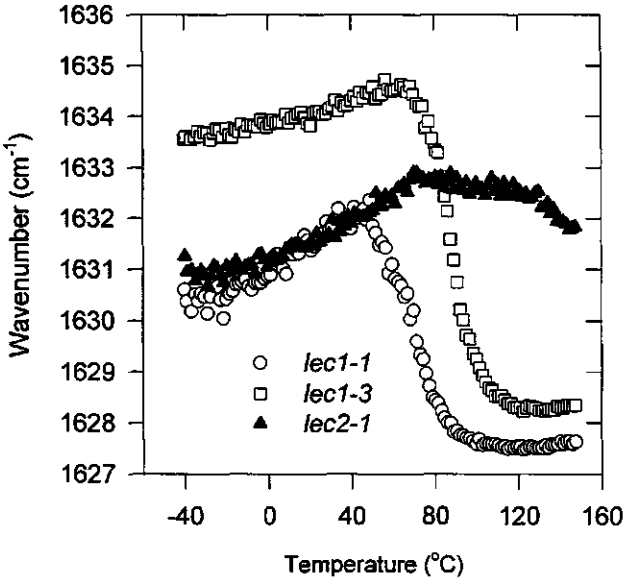

Figure 7. Wavenumber *vs* temperature plot (FTIR) of the amide-I band denoting turn and β-sheet protein structures in dried *lec A. thaliana* mutant seeds. The data points represent *lec1-1*, *lec1-3*, and *lec2-1* mutant seeds. Data of 2 seeds were averaged.

20 and 37°C, respectively. In the plots of wild-type and *abi3-1* seeds, no clear breaks are apparent. Previously, we have attributed such breaks in wavenumber *vs* temperature plots of soluble carbohydrates to glass transitions (Wolkers *et al.*, 1998b). Where possible, the T_g values that could be calculated for the different mutant seeds are given in Table I, with those of glucose, sucrose and raffinose as a comparison.

In wild-type seeds, the position of the OH-stretch increased at a rate of 0.14 cm^{-1}/°C in the temperature region from -40 to 40°C (WTC_{in} in Table 1). A local maximum in this νOH *vs* temperature plot was observed at 62°C. In seeds of *abi3-5*, the WTC was 0.21 cm^{-1}/°C in the region from -40 to 40°C. The other *abi3* mutant seeds have intermediate WTC-values between the wild-type and *abi3-5*. It is striking to note that in *abi3-7* and *abi3-5* seeds, WTC values, reached higher values, particularly above the temperature at which the break occurred (WTC_{max} in Table I). These high WTC values correspond with the generally low heat stability of the endogenous proteins in these more extreme *abi3* mutant seeds.

Leafy cotyledon (*lec*) mutants

Leafy cotyledon (*lec1*) mutants of *A. thaliana* exhibit even more defects in seed maturation than the *abi3* mutants (Meinke *et al.*, 1994; Parcy *et al.*, 1994, 1997). Seeds of *lec1-1* and *lec1-3* do not survive drying. The *lec2-1* mutant seeds are desiccation-tolerant in their axis but not in their cotyledons, and do survive drying. Figure 7 shows the wavenumber *vs* temperature plots of the turn/β-sheet band at approximately 1633 cm^{-1} of the *lec1-1*, *lec1-3* and *lec2-1* seeds. Protein denaturation temperatures in the *lec1-1* and *lec1-3* seeds were determined to be 68 and 89°C, respectively. In the *lec2-1* seeds, only very small signs of protein denaturation were observed at elevated temperatures. The second scans after heating showed that the shifts to lower wavenumber were irreversible (data not shown).

In Figure 8 the νOH *vs* temperature plots of the *lec1* and *lec2* mutants are shown. Data that can be determined from these plots such as WTC_{in}, WTC_{max} and T_g are given in Table I. While the T_g values that were determined

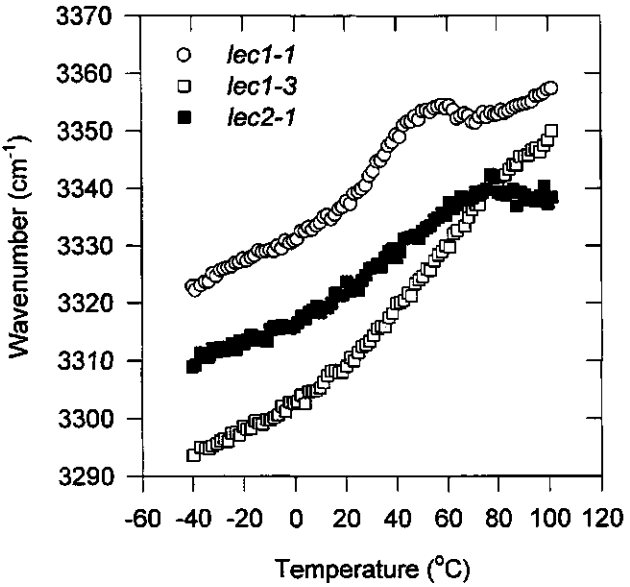

Figure 8. Wavenumber versus temperature plot (FTIR) of the OH-stretching vibration band in dried *lec A. thaliana* mutant seeds. The data points represent *lec1-1*, *lec1-3*, and *lec2-1* mutant seeds. Data of 2 seeds were averaged.

from the clear breaks all were around 20°C, WTC_{max} values were much higher for the *lec-1* mutant seeds than for the *lec2-1* seeds. The νOH *vs* temperature plot of the *lec2-1* seeds resembles that of *abi3-7* seeds most. It is striking to note that similarly as in the *abi3* mutant seeds, also in the *lec1* mutant seeds high WTC_{max} values correspond with low heat stability of the endogenous proteins.

Discussion

Mutations in the *ABI3*, *LEC1* and *LEC2* genes of *Arabidopsis* result in maturation defective mutant seeds (Koornneef *et al.*, 1989; Nambara *et al.*, 1992; Ooms *et al.*, 1993, 1994; Meinke *et al.*, 1994; Parcy *et al.*, 1994, 1997; De Bruijn *et al.*, 1997; Léon-Kloosterziel, 1997).

The *lec1* mutant seeds exhibit drastic alterations in their developmental pattern. They lack oil and protein bodies which are characteristic for wild-type seeds, and their cotyledons have a leaf-like morphology. Mutations in the *ABI3* locus specifically affect the ABA response and associated gene expression during seed development. Mutant seeds can have reduced levels of storage products, i.e. lipids and storage proteins, particularly the *abi3-5*. Several *abi3* mutant seeds that differ in severity of mutation have been physiologically and biochemically characterized (Léon-Kloosterziel, 1997). The first striking physiological difference with wild-type seeds is the inhibiting effect of exogenous ABA on germination (see Table 2). While wild-type seeds need 1 μM ABA to have their germination percentage reduced to half of the original (D_{50}), the *abi3-1* seeds need 10 μM and the *abi3-5* seeds more than 1 mM, the *abi3-7* being intermediate (D_{50} = 100 μM). The sensitivity to ABA suggests the following order of maturation defectiveness: *abi3-5* > *abi3-7* > *abi3-1* > wild-type. In addition, *abi3-5* mutant seeds are lowest in storage proteins, are almost devoid of *LEA* proteins, but contain surprisingly high amounts of soluble sugars (see Table 2). In all these aspects, *abi3-7* seeds are intermediate between *abi3-5* and *abi3-1* seeds.

In the present work we used *in situ* FTIR microspectroscopy to characterize molecular interactions in the cytoplasm of the dried maturation defective mutant seeds. Heat stability of proteins and strength of hydrogen bonding may characterize the viscous solid properties of the cytoplasm, which are involved in stabilization of (macro)molecular and cellular structures.

Table 2. Half maximal ABA responsiveness to germination, D_{50}; total sugar contents as % of dry weight (DW); accumulation of LEA proteins; onset temperature of protein denaturation, T_{onset}, and WTC_{max} in dry mature seeds of the *abi3* mutants and the wild-type. [(1)]Data derived from Léon-Kloosterziel, 1997 and references therein.

Genotype	ABA responsiveness[(1)] (D_{50})	Sugar content[(1)]	LEA[(1)]	T_{onset}	WTC_{max}
	μM	% of DW		°C	cm^{-1}/°C
wild-type	< 1	1.8	++	> 150	0.19
abi3-1	10	4.1	+	135	0.22
abi3-7	100	4.8	+/-	120	0.27
abi3-5	> 1000	6.5	-	70	0.58

Desiccation tolerance and long-term survival are considered to depend on the extent of immobilization of these (macro)molecular and cellular structures (Leopold *et al.*, 1994; Crowe *et al.*, 1997a,b).

Characteristic molecular groupings in IR-spectra of dried *Arabidopsis* seeds were analyzed during heating to monitor melting of lipids (symmetric CH_2-stretch) and cytoplasmic glasses (OH-stretch), and denaturation of proteins (amide-I region). In Table 2 we summarize the onset temperatures of protein denaturation for the wild-type seeds and the *abi3* mutant seeds. The onset temperatures decreased from over 150°C in the wild-type to 70°C in the *abi3-5* seeds. A T_{onset} of 70°C is close to the T_{onset} of 56°C for the hydrated wild-type seed. The order in T_{onset} for the seeds of the *abi3* allelic series is remarkably similar to that of the physiological and biochemical characteristics reported in Table 2. The highest protein stability was found in wild-type seeds and the lowest in the *abi3-5* mutant seeds, in the order wild-type > *abi3-1* > *abi3-7* > *abi3-5*. This indicates that the severity of mutation in the *ABI3* locus is also manifested in protein stability. Low heat stability may be indicative of a reduced longevity of the mutant seeds rather than an immediate reflection of desiccation tolerance. This may be particularly true in the case of *abi3-1* mutant seeds for which FTIR detected slight differences from the wild-type seeds, but for which physiological studies have not provided differences as yet.

In seeds of the *aba1-1 abi3-1* double mutant, intermolecular β-sheet structures already occurred upon drying at room temperature. This may be indicative of protein breakdown due to decompartmentalization-induced protease activity during drying of these seeds. A similarly increased level of denatured proteins was observed in prematurely dried maize embryos (Wolkers *et al.*, 1998a). LAB treatment of the *aba1-1 abi3-1* double mutant plants prevented this drying-induced protein breakdown in the seeds, which coincides with acquisition of desiccation tolerance (Ooms *et al.*, 1994). This supports the hypothesis that stabilization of the protein structure is of crucial importance to desiccation tolerance and long-term survival in the dry state. The packing of proteins in dry seeds is supposed to be such that a maximum efficiency is obtained, in order for seeds to be optimally resistant to degradation by adverse

climatic conditions, including high temperatures (Brown *et al.*, 1982). In the desiccation-sensitive genotypes, the packing of proteins in the cytoplasmic matrix may not be completed, which could explain the reduced heat stability of the endogenous proteins. However, heat-induced protein unfolding also may be facilitated by elevated fluidity of the direct surrounding of the proteins.

The OH-stretching vibration band, reflecting the properties of the glassy matrix in dry seeds, may give information on the extent of molecular interactions through hydrogen bonding and, thus, the molecular packing of the matrix components (Wolkers *et al.*, 1998b). The molecules involved are predominantly soluble carbohydrates, proteins and bound water. By observing the shift in the position of the OH-stretching vibration band with temperature, we assessed the molecular packing in the seeds (Table 2). Strikingly, the WTC_{max} data indicate the same order of severity of the *abi3* mutations as suggested by the physiological and biochemical data in Table 2. The highest WTC_{max} value was found in the *abi3-5* seeds and the lowest in *abi3-1* and wild-type seeds, *abi3-7* seeds being intermediate. We interpret this to mean that the molecular packing density is higher in dry desiccation-tolerant than in desiccation-sensitive seeds, which is associated with a higher, respectively lower protein denaturation temperature.

The suggested relation between protein stability and seed characteristics is also illustrated with the *lec1* and *lec2* mutation. The dried desiccation-sensitive, *lec1-1* and *lec1-3* seeds also have a low heat stability of proteins, which coincides with high WTC_{max} values. The *lec2-1* mutant seeds displayed a complex denaturation behaviour, which may be explained by the fact that they consist of a desiccation-tolerant axis and intolerant cotyledons, but compared with the *lec1* seeds, their proteins were considerably more heat stable.

One could take it for granted that the lower amounts of storage proteins and the higher amounts of sugars in the *abi3* mutant seeds change the IR spectra. Although the averaging character of FTIR analysis makes an unambiguous assignment of a specific molecular group frequency to the contributing compounds difficult, monitoring the temperature dependence of a

band gives important additional information on possible molecular interactions, i.e. the extent of hydrogen bonding. Thus, it was found that the changed carbohydrate content and composition, and possibly also the lack of synthesis of some essential maturation-related proteins in the *abi3* seeds, lead to a reduced physical stability of the viscous solid matrix.

In the case of equal amounts of sugars and proteins, it can be expected that the OH-groups in the sugars are dominating the OH-band, considering the relatively large number of OH-groups in sugars. In dried pollen and leaves of a resurrection plant, for example, the profuse sucrose is the main contributory molecule to the OH-stretch. However, in *Arabidopsis* seeds (and also many other seeds, Wolkers, unpublished data), the contribution of sugar OH-groups will be less prominent than in the aforementioned organisms, due to the generally lower sugar and higher protein content in seeds. In *abi3* seeds the total sugar content decreased in the order of *abi3-5* > *abi3-7* > *abi3-1* > wild-type, whereas the protein content shows the reverse (Table 2). Only the νOH *vs* temperature plot of the *abi3-5* mutant seeds showed a clear break at 37°C (Fig. 6), which is characteristic for a sugar-like glass transition. Together with the WTC values before and after the break, these data resemble those of pure sucrose (Table 1), suggesting that sugar plays a major role in the packing of the cytoplasmic matrix of the *abi3-5* seeds and, to a lesser extent, in the *abi3-7* seeds. In wild-type and *abi3-1* seeds, no such clear breaks in the νOH *vs* temperature plots were found, and WTC values were lower (Table 2).

In *abi3-1* and wild-type seeds, trace amounts of raffinose and stachyose can be found, apart from sucrose (Ooms *et al.*, 1993; Léon-Kloosterziel, 1997). As shown in Table 1, a raffinose glass has a higher WTC-value than a sucrose or glucose glass. The nevertheless low WTC values in these desiccation-tolerant seeds containing raffinose, suggest a dominating presence of other compounds in the hydrogen bonding network. That proteins can fulfil this role has been demonstrated in model systems of sugars and proteins (Chapter 9). Increasing amounts of protein embedded in a sugar matrix considerably decrease the WTC, indicative of increased molecular packing. Ooms *et al.* (1994) suggested that a low ratio of mono- to oligo-saccharides rather than the

total sugar content is involved in the acquisition of desiccation tolerance. This was based on sugar analyses in the *abi3* mutant and *aba1-1 abi3-1* double mutant seeds, and the wild-type seeds. However, we find it hard to believe that a small amount of oligosaccharides (less than 1% of the dry weight) could drastically influence the physical properties of the cytoplasmic matrix. We suggest that in *Arabidopsis* seeds, raffinose might be just a sign of late embryogenic development rather than an important component in the molecular packing of the dry cytoplasm. Other compounds that are synthesized during late embryogenesis, such as (LEA) proteins, may be of much more importance in the formation of a molecularly dense glassy matrix in which (macro)molecules are immobilized.

Acknowledgements

This project was financially supported by the Life Sciences Foundation (SLW), which is subsidized by the Netherlands Organization for Scientific Research (NWO).

References

Bell, L.N., Hageman, M.J. (1996) Glass transition explanation for the effect of polyhydroxy compounds on protein denaturation in dehydrated solids. *J. Food. Sci.* **61,** 372-378.

Carpenter, J.F., Crowe, J.H. (1989) An infrared spectroscopic study of the interactions of carbohydrates with dried proteins. *Biochemistry* **28,** 3916-3922.

Crowe, J.H., Crowe, L.M., Carpenter, J.F., Prestrelski, S.J., Hoekstra, F.A. (1997a) Anhydrobiosis: cellular adaptations to extreme dehydration. *In:* Dantzler, W.H. (ed.) Handbook of Physiology section 13, Comparative Physiology, Vol II, Oxford University Press, Oxford, pp. 1445-1477.

Crowe, J.H., Crowe, L.M., Chapman, D. (1984) Preservation of membranes in anhydrobiotic organisms: the role of trehalose. Science **223,** 701-703.

Crowe, J.H., Oliver, A.E., Hoekstra, F.A., Crowe, L.M. (1997b) Stabilization of dry membranes by mixtures of hydroxyethyl starch and glucose: The role of vitrification. *Cryobiology* **35,** 20-30.

De Bruijn, S.M., Ooms, J.J.J., Karssen, C.M., Vreugdenhil, D. (1997) Effects of abscisic acid on reserve deposition in developing *Arabidopsis* seeds. *Acta Bot. Neerl.* **46,** 263-277.

Finkelstein, R.R., Somerville, C.R. (1990) Three classes of abscisic acid (ABA)-insensitive mutations of *Arabidopsis* define genes that control overlapping subsets of ABA responses. *Plant Physiol.* **94,** 1172-1179.

Golovina, E.A., Wolkers, W.F., Hoekstra, F.A. (1997) Long-term stability of protein secondary structure in dry seeds. *Comp. Biochem. Physiol.* **117A,** 343-348.

Horbowicz, M., Obendorf, R.L. (1994) Seed desiccation tolerance and storability: dependence on flatulence-producing oligosaccharides and cyclitols - review and survey. *Seed Sci. Res.* **4,** 385-405.

Kalichevsky, M.T., Blanshard, J.M.V. (1993) The effect of fructose and water on the glass transition of amylopectin. *Carbohydrate Polymers* **20,** 107-113.

Karssen, C.M., Brinkhorst-van der Swan, D.L.C., Breekland, A.E., Koornneef, M. (1983) Induction of dormancy during seed development by endogenous abscisic acid: studies on abscisic acid deficient genotypes of *Arabidopsis thaliana* (L.) Heynh. *Planta* **157,** 158-165.

Koornneef, M., Hanhart, C.J., Hilhorst, H.W.M., Karssen, C.M. (1989) In vivo inhibition of seed development and reserve protein accumulation in recombinants of abscisic acid biosynthesis nd responsiveness mutants in *Arabidopsis thaliana*. *Plant Physiol.* **90,** 463-469.

Koornneef, M., Jorna, M.L., Brinkhorst-van der Swan, D.L.C., Karssen, C.M. (1982) The isolation of abscisic acid (ABA) deficient mutants by selection of induced revertants in non-germinating gibberellin sensitive lines of *Arabidopsis thaliana* (L.) Heynh. *Theor. Appl. Genet.* **61,** 385-393.

Koornneef, M., Reuling, G., Karssen, C.M. (1984) The isolation and characterization of abscisic acid-insensitive mutants of *Arabidopsis thaliana*. *Physiol. Plant.* **61,** 377-383.

Koster, K.L., Leopold, A.C. (1988) Sugars and desiccation tolerance in seeds. *Plant Physiol.* **88,** 829-832.

Leopold, A.C., Sun, W.Q., Bernal-Lugo, I. (1994) The glassy state in seeds: analysis and function. *Seed Sci. Res.* **4,** 267-274.

Levine, H., Slade, L. (1992) An alternative view of trehalose functionality in drying and stabilization of biological materials. *BioPharm.* **5,** 36-40.

Léon-Kloosterziel, K.M. (1997) Genetic analysis of seed development in *Arabidopsis thaliana*. PhD thesis Wageningen Agricultural University, Wageningen, The Netherlands, ISBN 90-5485-770-6, Wageningen, pp. 1-119.

Meinke, D.W., Franzmann, L.H., Nickle, T.C., Yeung, E.C. (1994) Leafy cotyledon mutants of *Arabidopsis*. *Plant Cell* **6,** 1049-1064.

Meurs, C., Basra, A.S., Karssen, C.M., Van Loon, L.C. (1992) Role of abscisic acid in the induction of desiccation tolerance in developing seeds of *Arabidopsis thaliana*. *Plant Physiol.* **98,** 1484-1493.

Nambara, E., Keith, K., McCourt, P., Naito, S. (1995) A regulatory role for the *ABI3* gene in the establishment of embryo maturation in *Arabidopsis thaliana*. *Development* **121,** 629-636.

Nambara, E., Naito, S., McCourt, P. (1992) A mutant of *Arabidopsis* which is defective in seed development and storage protein accumulation is a new *abi3* allele. *Plant J.* **2,** 435-441.

Ooms, J.J.J., Léon-Kloosterziel, K.M., Bartels, D., Koornneef, M., Karssen, C.M. (1993) Acquisition of desiccation tolerance and longevity in seeds of *Arabidopsis thaliana*. A comparative study using abscisic acid-insensitive *abi3* mutants. *Plant Physiol.* **102,** 1185-1191.

Ooms, J.J.J., Wilmer, J.A., Karssen, C.M. (1994) Carbohydrates are not the sole factor determining desiccation tolerance in seeds of *Arabidopsis thaliana*. *Physiol. Plant.* **90,** 431-436.

Parcy, F., Valon, C., Kohara, A., Miséra, S., Giraudat, J. (1997) The *ABSCISIC ACID-INSENSITIVE3*, *FUSCA3*, and *LEAFY COTYLEDON1* loci act in concert to control multiple aspects of *Arabidopsis* seed development. *Plant Cell* **9,** 1265-1277.

Parcy, F., Valon, C., Raynal, M., Gaubier-Comella, P., Delseny, M., Giraudat, J. (1994) Regulation of gene expression programs during *Arabidopsis* seed development: roles of the *ABI3* locus and of endogenous abscisic acid. *Plant Cell* **6,** 1567-1582.

Prestrelski, S.J., Tedeschi, N., Arakawa, T., Carpenter, J.F. (1993) Dehydration-induced conformational transitions in protein and their inhibition by stabilizers. *Biophys. J.* **65,** 661-671.

Roos, Y.H. (1995) Phase Transitions in Foods, Academic Press, London, pp. 1-360.

Steadman, K.J., Pritchard, H.W., Dey, P.M. (1996) Tissue-specific soluble sugars in seeds as indicators of storage category. *Ann. Bot.* **77,** 667-674.

Vinogradov, S.N., Linnel, R.H. (1971) Hydrogen Bonding, Van Nostrand Reinhold Company, New York.

Williams, R.J., Leopold, A.C. (1989) The glassy state in corn embryos. *Plant Physiol.* **89,** 977-981.

Wolkers, W.F., Bochicchio, A., Selvaggi, G., Hoekstra, F.A. (1998a) Fourier transform infrared microspectroscopy detects changes in protein secondary structure associated with desiccation tolerance in developing maize embryos. *Plant Physiol.* **116,** 1169-1177.

Wolkers, W.F., Hoekstra, F.A. (1995) Aging of dry desiccation-tolerant pollen does not affect protein secondary structure. *Plant Physiol.* **109,** 907-915.

Wolkers, W.F., Hoekstra, F.A. (1997) Heat stability of proteins in desiccation-tolerant cattail pollen (*Typha latifolia*): A Fourier transform infrared spectroscopic study. *Comp. Biochem. Physiol.* **117A,** 349-355.

Wolkers, W.F., Oldenhof, H., Alberda, M., Hoekstra, F.A. (1998b) A Fourier transform infrared microspectroscopy study of sugar glasses: Application to anhydrobiotic higher plant cells. *Biochim. Biophys. Acta* **1379,** 83-96.

Chapter 8

Changed properties of the cytoplasmic matrix associated with desiccation tolerance of dried carrot somatic embryos: an *in situ* FTIR study

Willem F. Wolkers, Frans Tetteroo, Mark Alberda and Folkert A. Hoekstra

Abstract

Abscisic acid-pretreated carrot (*Daucus carota*) somatic embryos survive dehydration when they are slowly dried, whereas rapid drying leads to low survival. In order to determine whether the acquisition of desiccation tolerance changes the physical stability of the cytoplasm, *in situ* Fourier transform infrared microspectroscopy was used. Although protein denaturation temperatures were similar in the embryos after slow or rapid drying, the extent of protein denaturation was higher in the rapidly dried embryos. Slowly dried, desiccation-tolerant, embryos are in a glassy state at room temperature. No clearly defined glassy matrix was observed in the rapidly dried, desiccation-sensitive, embryos. At room temperature, the average strength of hydrogen bonding was much lower in the rapidly dried embryos than in the slowly dried embryos. We interpret this to mean that the molecular packing in the rapidly dried embryos is more loose.

While sucrose is the major soluble carbohydrate after rapid drying, on slow drying, the trisaccharide umbelliferose accumulates at the expense of sucrose. The possibly protective role of umbelliferose was tested on protein and phospholipid model systems, using sucrose as the comparison. Both umbelliferose and sucrose form a stable glass with drying (glass transition temperature of 66 and 60°C, respectively); they depress the transition temperature of dry liposomal membranes equally well; they both prevent leakage from dry liposomes after rehydration, and protect a polypeptide that is

Submitted for publication in Plant Physiology

desiccation-sensitive. The similar protecting properties in model systems and the apparent interchangeability of both sugars in viable dry somatic embryos suggest no special role of umbelliferose in the improved physical stability of the slowly dried embryos. During slow drying also LEA transcripts are expressed. We suggest that LEA proteins embedded in the glassy matrix confer stability to these slowly dried embryos.

Introduction

Desiccation tolerance is the capacity of an organism or tissue to regain vital metabolism after almost complete dehydration. This capacity can be encountered in seeds, pollens, resurrection plants, mosses and ferns, in nematodes, tardigrades, yeasts, fungi spores and in bacteria (reviewed in Crowe *et al.*, 1992; Vertucci and Farrant, 1995; Crowe *et al.*, 1997a).

Carrot (*Daucus carota*) somatic embryos can be rendered tolerant of severe desiccation by a proper combination of treatments (Tetteroo *et al.*, 1994, 1995, 1996, 1998). Addition of ABA at the proper stage of development, a sufficiently slow drying time (at least 4 days), and a subtle rehydration are the main requirements for the acquisition of desiccation tolerance. Rapid drying within a few hours leads to an almost complete loss of viability. These rapidly dried somatic embryos have a considerably higher leakage of potassium and soluble carbohydrates than slowly dried embryos. The excessive leakage of cytoplasmic components on rehydration is associated with irreversible changes in the plasma membranes. Formation of irreversible protein aggregates and an increased T_m have been detected in plasma membranes isolated after rehydration of the rapidly dried embryos, which did not occur in rehydrated plasma membranes of the slowly dried embryos (Tetteroo *et al.*, 1996). This coincided with a decreased phospholipid content and concomitant accumulation of free fatty acids in the rapidly dried embryos. Although no differences in surface morphology were detected between the slowly dried, desiccation-tolerant, and the rapidly dried, desiccation-sensitive embryos, freeze fracture studies indicated clear morphological differences (Tetteroo *et al.*, 1998). Two hours after rehydration, cells of the rapidly dried embryos had a

disorganized appearance with low amounts of organelles visible, whereas those of the slowly dried embryos had many organelles visible and appeared structurally intact. Taken together, the carrot somatic embryogenesis system is very suitable to study the mechanisms that are involved in the acquisition of desiccation tolerance.

High contents of soluble carbohydrates have been suggested to be involved in the acquisition of desiccation tolerance (Crowe *et al.*, 1984). In fresh carrot somatic embryos, soluble sugars, mainly sucrose, may comprise more than 20% of the DW just before drying. On rapid drying, the sugar composition is more or less maintained. However, on slow drying, the trisaccharide umbelliferose increases at the expense of sucrose, and the monosaccharides disappear almost completely (Tetteroo *et al.*, 1994). Umbelliferose is a characteristic sugar in the Apiaceae family (Hopf and Kandler, 1976). Until now, the role of this trisaccharide in seeds has not been investigated, particularly with respect to desiccation tolerance.

Sugars may act in dehydrating seeds as protectants of proteins and membranes (Crowe *et al.*, 1987; 1992). They may form a glassy state, which immobilizes cytoplasmic components and slow down all chemical reactions, including damaging free radical reactions (Leopold *et al.*, 1994). In general, trisaccharides are better glass formers than disaccharides or monosaccharides (Levine and Slade, 1992; Roos, 1995). This might explain why umbelliferose is synthesized at the expense of sucrose upon slow drying of the embryos. Besides sugars, also proteins might influence the glassy properties of the cytoplasmic matrix. Model experiments have shown that proteins interact with sugars to form a glass of higher T_g than sugars alone (Kalichevsky *et al.*, 1993; Bell and Hageman, 1996, Chapter 9). Slight drying usually is perceived by seeds as a signal to synthesize specific proteins such as dehydrins (Blackman *et al.*, 1991, 1992; Hsing *et al.*, 1995) that are, just like sugars, thought to play a role in stabilization of dehydrating cells. It is possible, therefore, that during drying of the carrot somatic embryos a dense solid-like glassy network is formed, consisting of carbohydrates and proteins.

Recently, we have applied *in situ* FTIR to assess the heat-stability of proteins and the glassy cytoplasmic matrix in anhydrobiotic organisms such as pollen (Wolkers and Hoekstra, 1997), seeds (Golovina *et al.*, 1997; Chapter 7) and dried leaves of the resurrection plant *Craterostigma plantagineum* (Wolkers *et al.*, 1998b). This can give information about the stability of the protein *per se* and the properties of the matrix in which the proteins are embedded. Denaturation of endogenous proteins in dry tissues can be studied on account of the changes in the amide-I band profile between 1700 and 1600 cm^{-1}. Thus, we found that proteins in maturation defective mutant seeds of *Arabidopsis thaliana* that are desiccation-sensitive, have much lower heat stability than those in wild-type seeds (Chapter 7). The melting of cytoplasmic glasses can be derived from *in situ* IR spectra, using the shifts with temperature of the OH-stretching vibration. Additional information on the intermolecular interactions through hydrogen bonding in the dry state can be derived from the rate of change of νOH with temperature, the wavenumber-temperature coefficient (WTC). The WTC is a measure of the average strength of hydrogen bonding and can be used to study the molecular packing density of cytoplasmic glasses in dry cells. Using this parameter it was previously found in model systems that proteins have a stabilizing effect on carbohydrate glasses by increasing the average strength of hydrogen bonding in the dry state (Chapter 9). In maturation defective *Arabidopsis* seeds the reduced strength of hydrogen bonding as compared to wild-type seeds has been attributed to the reduced synthesis of maturation-specific proteins (Chapter7).

In this work we used *in situ* FTIR to study the heat stability of proteins and properties of the glassy matrix in slowly dried, desiccation-tolerant, and rapidly dried, desiccation-sensitive carrot somatic embryos. We made an attempt to explain the desiccation tolerance of the slowly dried somatic embryos by the considerably increased umbelliferose content. To that end we analyzed the protecting properties of purified umbelliferose in model systems. These properties were compared with those of sucrose. The role of umbelliferose and *de novo* synthesized proteins in the acquisition of desiccation tolerance is discussed.

Materials and methods

Production, drying and germination of somatic embryos

Seeds of carrot (*Daucus carota* L.), genotypes "RS 1" and "Trophy", were provided by Royal Sluis, Enkhuizen, The Netherlands, and by Dr S. de Vries of the Department of Molecular Biology of the Agricultural University, Wageningen, The Netherlands, respectively.

Somatic embryos were produced, dried and germinated as described earlier (Tetteroo *et al.*, 1995). Rapid and slow drying were carried out as follows. Approximately 1 g of the freshly harvested somatic embryos was transferred to a sterile plastic Petri dish (9 cm) by forceps. The embryos were equally spread out over the surface of the Petri dish. The Petri dishes were closed and placed in hygrostats (Weges and Karssen, 1987). Slow drying was achieved by exposure for 3 days each to different RHs generated by different saturated salt solutions inside the hygrostats at 25°C, in the following order, NaCl (75% RH), $Ca(NO_3)_2$ (51% RH), and $CaCl_2$ (30% RH). Rapid drying was obtained by placing the Petri dishes without cover in an air flow cabinet. Dry weights of the somatic embryos were determined after freeze-drying for 24 h.

Desiccation tolerance of the dry somatic embryos was evaluated by counting the number of germinated specimens. Approximately 100 dry embryos were placed on filter paper in a sterile plastic Petri dish (6 cm). Before imbibition, the embryos inside the closed Petri dish were prehumidified in moisture-saturated air for 4 hours to prevent possible imbibitional damage (Hoekstra *et al.*, 1989). Following this treatment, 1 ml $0B_5$ medium was provided to the embryos (Tetteroo *et al.*, 1995). The Petri dish was sealed with Parafilm and placed in an incubator with a 16 $h.d^{-1}$ photoperiod at 25°C. Somatic embryos were recorded as desiccation-tolerant when they showed clear root growth within 10 days.

Extraction and purification of umbelliferose

Dry somatic embryos (10 g) were boiled in 200 mL of 80% methanol for one h. The embryos were then filtered and washed with 50 mL of 80% methanol, and the filtrates were combined. The methanol was removed from the filtrate by vacuum evaporation, and the remaining aqueous suspension was defatted by passing it through a C18 reversed phase column (Waters Assoc. Milford MA). The suspension was then purified by passing it through a column of Polyclar AT (insoluble polyvinyl-pyrrolidone). After reduction of the volume, the suspension was layered on a Sephadex QAE-A-25-formate column and a Sephadex SP-C-25-H^+ column (Pharmacia, Sweden) and eluted with milli-Q water according to Redgwell (1980). The eluate containing the sugar fraction was freeze-dried to reduce volume. If required, the Sephadex column purification procedure was repeated. Umbelliferose was separated from the other sugars by preparative HPLC on a Shodex OH pak Q-2002 column (20 x 500 mm; Waters, Milford, MA), using milli-Q water of 55°C as the eluent at 3 mL min^{-1} and a refractive index detector (Spectra Physics model SP 8430, San Jose, CA). Using Dionex HPLC (analytical PA-1 column, 9 x 250 mm; see also under "carbohydrate analysis"; Dionex Corporation, Sunnyvale, CA) we further purified the umbelliferose. The NaOH in the eluent recovered from the column was removed using a Dionex anion self-generating suppressor (4mm) and 50 mN H_2SO_4 as the regenerant, flow rate 5 mL min^{-1}. The purified umbelliferose solution was then lyophilised to be used for the FTIR measurements, and also to determine the response factor for the quantitative analysis of umbelliferose by Dionex HPLC. The umbelliferose preparation purified according to the above procedure was characterized by one single peak in the Dionex HPLC chromatogram. Alternatively, extractions were made starting from 50 g of seed that was grinded in 80% methanol in a mortar with a little sand.

Carbohydrate analysis

Per lot of lyophilized somatic embryos approximately 10 mg were mixed with 1 mL 80% methanol containing 1 mg raffinose as the internal standard. The samples were kept at 76°C in a water bath for 15 min to extract the soluble

carbohydrates and to inactivate enzymes. Subsequently, the methanol was evaporated in a Speedvac (Savant Instruments Inc. Farmingdale, NY). The samples were then suspended in 1 mL milli-Q water. After centrifugation in an Eppendorf centrifuge the supernatants were diluted 50 times for HPLC analysis.

Carbohydrates were separated isocratically with a Dionex HPLC system (Dionex Corporation, Sunnyvale, CA) equipped with a pulsed amperometric detector and a 4 x 250 mm Carbopac PA-1 column with guard column. Identification of carbohydrate peaks was by comparing with retention times of standard solutions at two different elution programs. Hundred mM NaOH was used as the eluent, and 1.1 M sodium acetate in 100 mM NaOH was used to clean the column after each run. The data were analyzed using a Spectra Physics integrator model SP 4400 and Spectra Physics software (Labnet, Chromdat; San Jose, CA).

IR spectroscopy

IR spectra were recorded on a Perkin-Elmer 1725 IR-spectrometer (Perkin-Elmer, Beaconsfield, Buckinghamshire, UK), equipped with a liquid nitrogen-cooled mercury/cadmium/telluride detector and a Perkin-Elmer microscope as described previously (Wolkers and Hoekstra, 1995).

The embryos were cross-sectioned, and slices of the embryo axes were pressed gently between two diamond windows and placed in a temperature-controlled brass cell for IR-spectroscopy. Temperature control of the sample in the instrument was with a liquid nitrogen-cooled brass cell with a resistance heater under computer control. The instrument was purged of water vapor with a Balston dry air generator (Balston, Maidstone, Kent, England).

For protein studies, the spectral region 1800 - 1500 cm^{-1} was selected. This region contains the amide-I and amide-II absorption bands of the protein backbones. Deconvolved and second derivative spectra were calculated using the interactive Perkin-Elmer routine for Fourier self-deconvolution. The parameters for the Fourier self-deconvolution were a smoothing factor of 15.0 and a width factor of 30.0 cm^{-1}. Second derivative spectra were smoothed over

19 datapoints. For glass studies, the broad band between 3500 - 3000 cm^{-1}, arising from OH-stretching vibrations, was selected. A wavenumber *vs* temperature plot of this band was used to calculate the T_g of cytoplasmic glasses or sugars (Wolkers et al., 1998b). We previously defined the point of intersection of the two lines regressed to the linear parts of the plot as T_g. The position of the symmetric CH_2 stretching vibration band around 2853 cm^{-1} (lipids) and the C=O stretching vibration band (proteins) around 1635 cm^{-1} were determined from second derivative spectra (19 points smoothing factor). The bands were selected, normalized to unity and the band position was calculated as the average of the spectral positions at 80% of the total peak height.

Preparation of liposomes for FTIR analysis and leakage studies

Egg-PC in $CHCl_3$ (Fluka, Buchs, Switzerland) was used without further purification. After removal of the $CHCl_3$ in vacuum overnight, the dry egg-PC was rehydrated in water at a concentration of 10 mg mL^{-1}. When required, carbohydrates were added externally to the egg-PC suspension to give a mass ratio of 5:1 (sugar:egg-PC). Subsequently, unilamellar vesicles were produced by passing the suspension 35 times through one 100-nm pore size polycarbonate filter (Nuclepore Corp., Pleasanton, CA) as described previously (Van Bilsen *et al.*, 1994). For IR-spectroscopy, 5 μL samples were dried directly on CaF_2 windows for at least three h in a stream of dry air at 23°C (RH < 3%). Before the samples were removed from the dry air box, another window was placed on top of the sample window, with a rubber ring in between, to prevent rehydration of the samples during transfer to the spectrometer and during FTIR analysis. Hydrated liposome samples were concentrated by ultracentrifugation and the pellet was used for FTIR analysis.

For leakage studies, the vesicles were produced at 10 mg mL^{-1} in 1 mM Tes, pH 7.5, containing 0.25 M sucrose and 100 mM CF [Serva, Heidelberg, Germany, purified according to Klausner et al. (1981)]. After the 35 times passage through a polycarbonate filter, the external sucrose and CF were removed from the liposomes by gel filtration (Sephadex G50). Typical concentration of egg-PC after filtration was 3 mg mL^{-1}. Samples of

approximately 30 µg egg-PC containing different concentrations of the various sugars in a total volume of 30 µL, were dried in the caps of Eppendorf tubes for 3 h in dry air (RH < 3%). After rehydration of the sample in 1 mL Tes buffer (1 mM), pH 7.5, in the closed Eppendorf tubes, the fluorescence of CF was measured and the percentage CF retention was calculated according to Crowe and Crowe (1988). The excitation wavelength was 490 nm and the emission wavelength was 515 nm.

RNA extraction and northern hybridization

For the isolation of RNA, 30 - 50 mg embryo material were taken at time intervals of 24 h during slow drying, starting at 0 h and then rapidly dried for 4 h in a flow cabinet. Subsequently the embryos were ground with a mortar and pestle in the presence of liquid nitrogen. Lysis of the material was done in 50 mM Tris-HCl buffer, containing 0.5 M NaCl, 50 mM EDTA, 10 mM β-mercaptoethanol, pH 8.5. Subsequently, the mixture was homogenized in a mixture of 6% 2-butanol, 1% tri-isopropylnaphtalene disulphonate, 2% para-aminosalicylate, 4% sodium-dodecyl sulphate and extracted with phenol/chloroform (1:1, v/v). RNA was precipitated overnight with 2 M LiCl and poly(A)-RNA was obtained by affinity chromatography on oligo(dT)-cellulose. Poly(A)-RNA was electrophoresed on a glyoxal/DMSO gel and blotted onto a nylon membrane (Gene Screen Plus, Dupont USA) as described by Sambrook

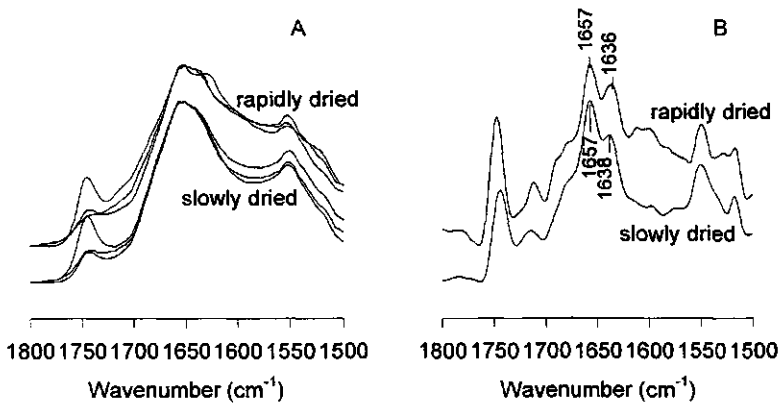

Figure 1. *IR absorption spectra* (A) *of the 1800 - 1500 cm^{-1} region of* slowly and rapidly dried carrot somatic embryos; (B) after deconvolution.

et al. (1989). Hybridization was done using a random-primed DNA labeling kit (Boehringer, Mannheim, Germany). A dehydrin clone, B18 (Close *et al.*, 1989) was used as the probe.

Results

In situ protein secondary structures as influenced by drying rate

Somatic embryos grown in a sucrose- and ABA-containing medium were subjected to slow and rapid drying. Slowly dried embryos usually germinated for more than 90%, whereas the germination of the rapidly dried embryos varied between 0 and 30%. Figure 1A depicts the *in situ* IR spectra of slowly and rapidly dried somatic embryos in the 1800 - 1500 cm^{-1} region. The amide-I band around 1650 cm^{-1} and the amide-II band around 1550 cm^{-1} arise from the protein backbone (Wolkers and Hoekstra, 1995). For protein structural studies we have focussed on the amide-I band. Slight but consistent differences can be observed between the amide-I band profiles of slowly and rapidly dried somatic embryos. The slowly dried embryos had a relatively stronger absorption around

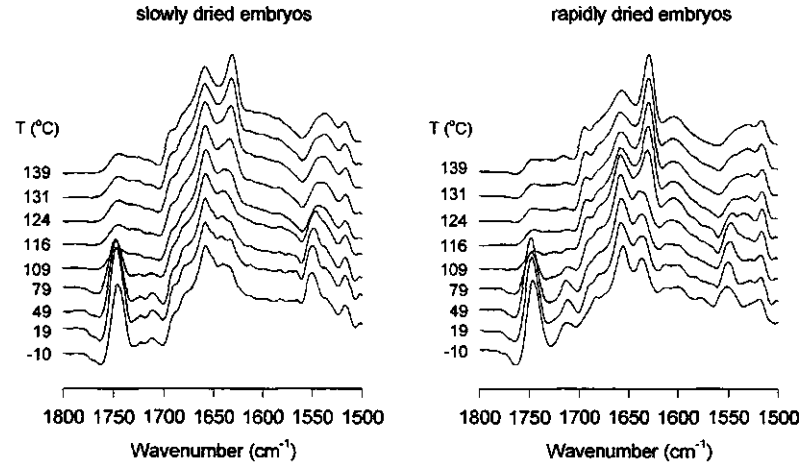

Figure 2. Deconvolved IR absorption spectra of the 1800 - 1500 cm^{-1} region of slowly and rapidly dried carrot somatic embryos as a function of temperature.

1654 cm^{-1} than the rapidly dried embryos. Sometimes, a clear band around 1632 cm^{-1} was observed in spectra of rapidly dried somatic embryos, which may indicate formation of intermolecular protein clusters.

Because the original absorption spectra yielded rather broad bands in the amide-I region, second derivative and deconvolution analysis were used to resolve details. Deconvolution analysis shows that the amide-I band of both the slowly and the rapidly dried somatic embryos is composed of two major bands, located at approximately 1657 and 1637 cm^{-1} (Fig. 1B). The band around 1657 cm^{-1} can be assigned, at least partly, to α-helical structures and the band around 1637 cm^{-1} to turn and β-sheet structures (Wolkers *et al.*, 1998a, and references therein). After deconvolution (Fig 1B), the slight differences in relative bands heights between spectra of the slowly and rapidly dried embryos which are already visible in Figure 1A, are more pronounced.

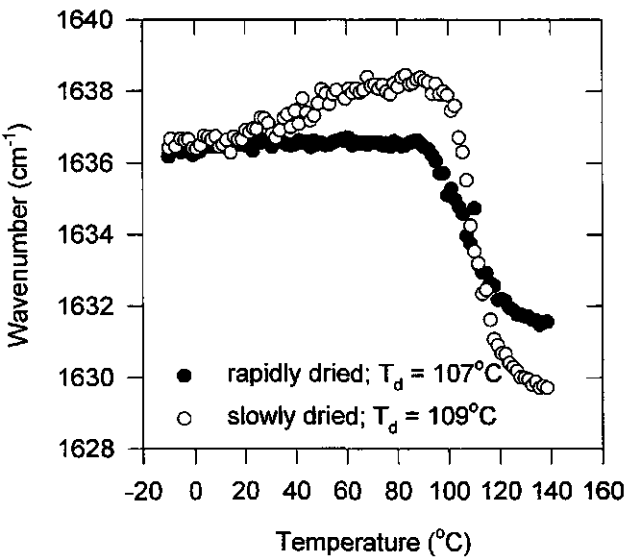

Figure 3. Wavenumber *vs* temperature plots (FTIR) of the amide-I band denoting turn and β-sheet protein structure of slowly and rapidly dried carrot somatic embryos. Data of four individual samples were averaged. T_d - average denaturation temperature.

Heat stability of endogenous proteins

When dry intact tissues are heated and monitored with respect to protein secondary structure, information can be obtained concerning the intrinsic heat stability of the proteins in their native environment (Wolkers and Hoekstra, 1997; Chapter 7). In both the slowly and the rapidly dried somatic embryos, the band at approximately 1637 cm^{-1} shifted with temperature to approximately 1630 cm^{-1}, which is characteristic of intermolecular extended β-sheet structures (Fig. 2). This can be interpreted as protein denaturation and is irreversible, i.e. after cooling, the bands do not return to their original positions. From Figure 2 it also can be seen that the peak height at 1630 cm^{-1} in spectra of the heat-denatured rapidly dried embryos was more pronounced than in those of the slowly dried embryos. This indicates that the extent of protein denaturation is higher in the rapidly dried somatic embryos. The α-helical band at approximately 1657 cm^{-1} hardly shifted in position with temperature for both drying treatments. The heat-induced protein denaturation temperature, T_d, was

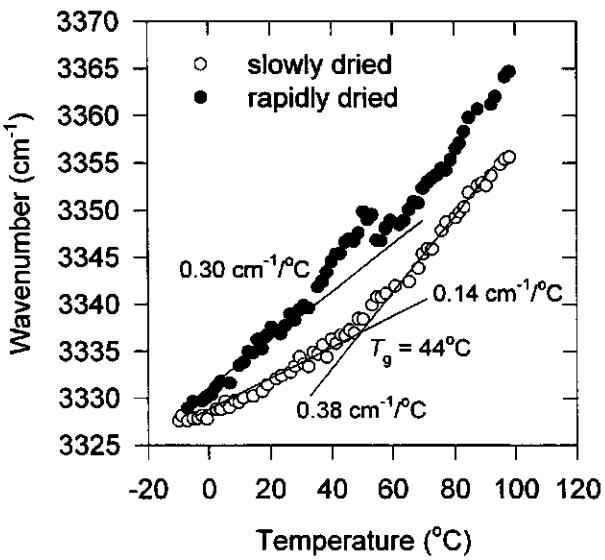

Figure 4. Wavenumber *vs* temperature plot (FTIR) of the OH-stretching vibration band of slowly and rapidly dried carrot somatic embryos (both 0.05 g H_2O/g DW).

derived from a plot of the position of the turn/ß-sheet band (1637 cm^{-1}) *vs* the temperature (Fig. 3). In both the slowly and rapidly dried embryos, the band position sharply fell to lower wavenumbers above 90°C. T_d values that were derived from Figure 3 were 109 and 107°C for slowly and rapidly dried embryos, respectively.

Properties of the dry cytoplasmic glassy matrix

FTIR also was used to study the glassy matrix in the slowly and rapidly dried somatic embryos. For this purpose, the band position of the OH-stretching vibration, arising mainly from the sugar OH groups, was monitored as a function of temperature (Wolkers et al., 1998b). Two linear regression lines can be drawn in the νOH *vs* temperature plot of the slowly dried embryos with an

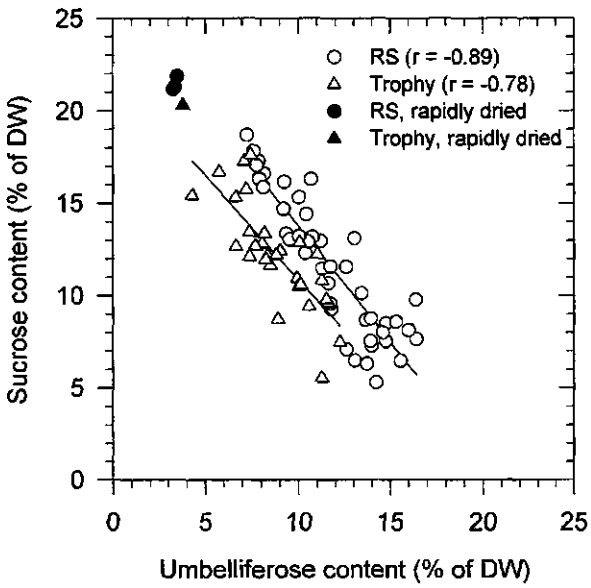

Figure 5. Correlation between the sucrose and umbelliferose contents in each lot of viable (germination percentage ≥ 95%), slowly dried carrot somatic embryos of the CV "RS" and "Trophy". The treatment variables were sucrose and ABA concentration in the maturation medium. The filled symbols represent the sucrose and umbelliferose content after rapid drying.

intersection point at 44°C (Fig. 4). The temperature at the intersection point can be considered as T_g (Wolkers et al., 1998b). This indicates that the slowly dried embryos are in a glassy state at room temperature. The slopes of the regression lines, the WTC values, were 0.14 and 0.38 $cm^{-1}/°C$ below and above T_g, respectively, and are indicative of the average strength of the hydrogen bonding interactions. In the rapidly dried embryos, no clear break in the νOH *vs* temperature plot could be observed, which indicates that there is not one defined T_g. Moreover, the WTC of 0.30 $cm^{-1}/°C$ in the rapidly dried embryos below 40°C was much higher than that of the slowly dried ones. The higher WTC of the rapidly dried embryos suggests a less tight hydrogen bonding network, associated with a more loosely packed glassy structure in these embryos.

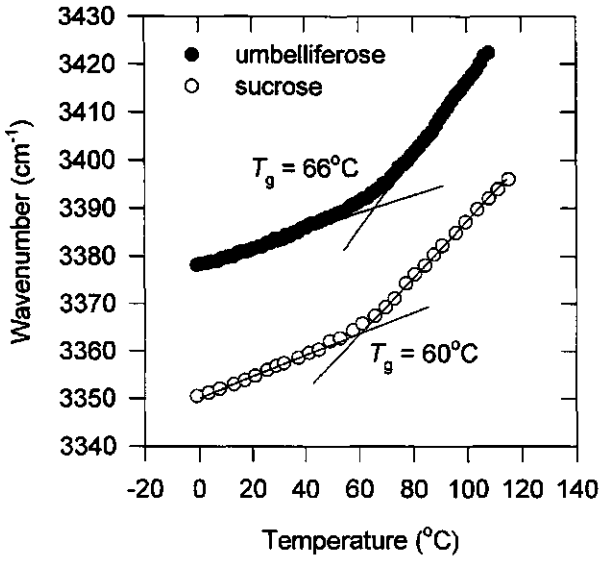

Figure 6. Wavenumber *vs* temperature plots (FTIR) of the OH-stretching vibration band of dry umbelliferose and sucrose glasses. The glass transition temperatures (T_g) were determined from the intersection between the regression lines in the liquid and glassy state.

Effect of drying rate on the major soluble carbohydrates

It has been reported previously that slow drying leads to the accumulation of the trisaccharide, umbelliferose, in carrot somatic embryos (Tetteroo *et al.*, 1994, 1995). This accumulation does not occur when the embryos are subjected to fast drying. Because umbelliferose, apart from sucrose, may comprise a considerable portion of the total dry weight, an important role was attributed to this trisaccharide in the stabilization of the dry cytoplasm. During protocol development for optimizing desiccation tolerance of the somatic embryos, a large number of different treatments were given. The variables in these experiments were genotype (cv RS and Trophy) and concentration of added ABA and sucrose in the maturation medium. While omission of ABA from the maturation medium and fast drying led to reduced viability, the ABA and sucrose concentrations used resulted in optimal survival of the somatic embryos. Figure 5 shows a plot of the umbelliferose against the sucrose contents in each individual lot of slowly dried embryos that had

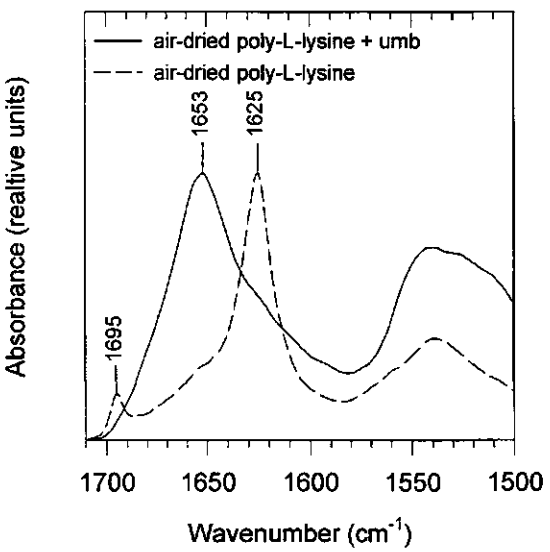

Figure 7. Representative IR absorption spectra of the amide I region of poly-L-lysine (MW=57.4 kDa), dried (30% RH) in the presence or absence of umbelliferose.

germination percentages of 95% or more. The contents of sucrose and umbelliferose in a few rapidly dried embryo lots of low viability (10-28%) are also shown. It is clear that slow drying leads to increased contents of umbelliferose. However, the amounts observed were variable, without apparent effect on desiccation tolerance. The linear regression coefficients of the lines that can be drawn through the data points for both cultivars (r=-0.89 and -0.78 for cv 'RS' and 'Trophy', respectively) suggest that umbelliferose is produced at the expense of sucrose. The apparent interchangeability between these sugars and the generally very high survival of drying further suggest that sucrose and umbelliferose may be both important in relation to desiccation tolerance.

Stabilizing properties of umbelliferose

In an attempt to ascribe the changes in physical stability as observed by *in situ* FTIR to the elevated amounts of umbelliferose in the slowly dried embryos, several properties of umbelliferose were tested in model systems and

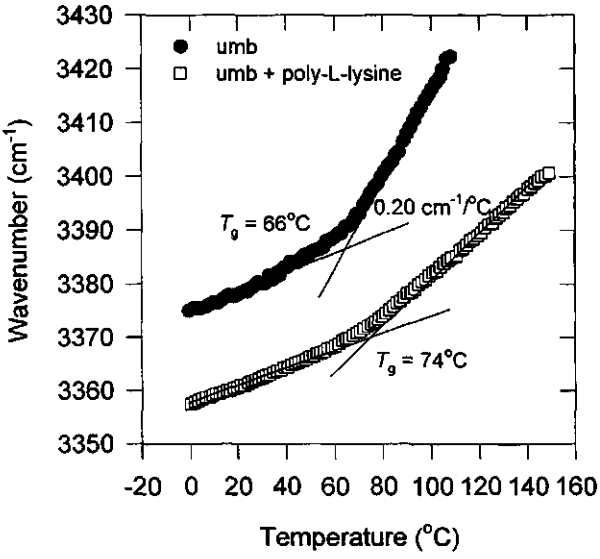

Figure 8. Wavenumber *vs* temperature plot (FTIR) of the OH-stretching vibration band of dry umbelliferose and of a umbelliferose/poly-L-lysine glass (0.25 mg poly-L-lysine/mg umbelliferose). T_g values are determined from the intersection points of the regression lines in the liquid and glassy state.

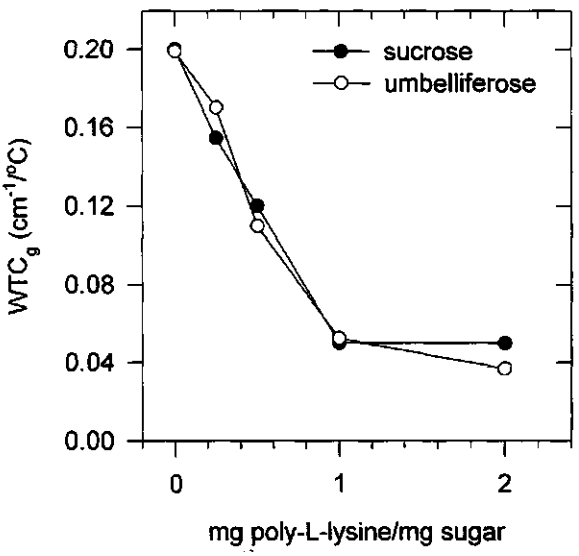

Figure 9. Effect of increasing amounts of poly-L-lysine on the WTC values in dry umbelliferose and sucrose glasses (WTC_g). The values were obtained from wavenumber *vs* temperature plots as in Fig. 8.

compared with those of sucrose.

Glass forming properties

The glass forming properties of pure umbelliferose and sucrose were monitored using FTIR, similarly as for the intact somatic embryos. Figure 6 shows the νOH *vs* temperature plots of umbelliferose and sucrose, from which the T_g values for dry umbelliferose and sucrose glasses were determined at 66°C and 60°C, respectively. Before the measurements, the samples were heated to 80°C for several min, in which all water detectable in the IR spectra was removed. The WTC values in the glassy state were 0.20 cm^{-1}/°C for both umbelliferose and sucrose.

Protein protection

One hypothesized role of sugars in desiccation tolerance is interaction during drying with proteins, which would prevent dehydration-induced conformational changes (Carpenter and Crowe, 1989; Chapter 9). To study

whether umbelliferose is effective in this respect, we selected poly-L-lysine, a synthetic polypeptide that undergoes structural changes with freeze-drying (Prestrelski *et al.*, 1993) and air-drying (Chapter 9). When poly-L-lysine was dried in the presence of umbelliferose, a broad band at 1653 cm^{-1} dominated, representing random coil structure (Fig. 7). A similar spectrum can be observed when poly-L-lysine is dried in the presence of sucrose (Chapter 9). Without carbohydrate, drying led to absorption bands at 1625 and 1695 cm^{-1}, which are indicative of extended β-sheet structure. In the hydrated state, poly-L-lysine exists entirely in the random coil conformation (Jackson *et al.*, 1989; Tiffany and Krimm, 1969; Chapter 9). The above results show that umbelliferose, similarly as sucrose, can prevent dehydration-induced conformational transitions of poly-L-lysine.

Interactive effect with protein on glassy behavior

Sugars and proteins may form a tight hydrogen bonding network when dried together, which leads to increased molecular stability and elevated T_gs.

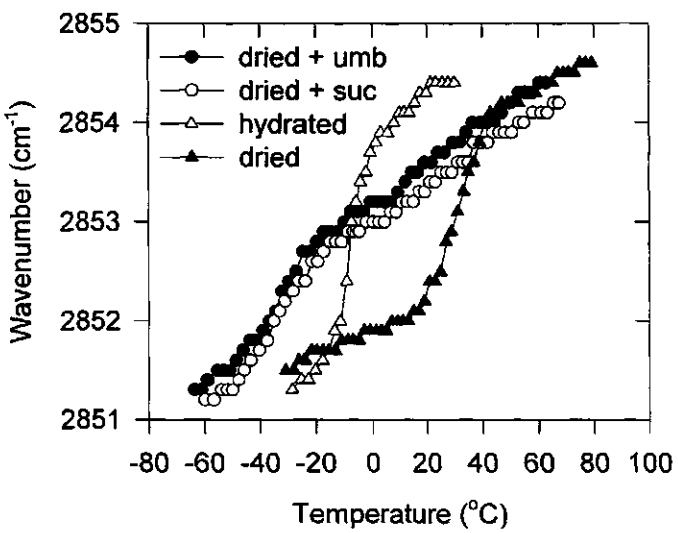

Figure 10. Representative wavenumber *vs* temperature plots (FTIR) of the CH_2 symmetric stretch of egg-phosphatidylcholine (egg-PC) liposomes. The different conditions were: hydrated, air-dried (3% RH), and air-dried (3% RH) in the presence of either sucrose or umbelliferose.

We studied the glassy behavior of dried umbelliferose/poly-L-lysine mixtures on account of the temperature-dependent shifts in the positions of the OH-stretching band (Fig. 8). Poly-L-lysine is particularly suitable in this respect, because it lack OH-groups. Thus, only sugar OH-groups are being studied. With increasing amounts of the poly-peptide in the sugar polypeptide mixture, T_g increased. The WTC_g decreased from 0.20 to 0.05 $cm^{-1}/°C$ in the range from 0 to 1 mg poly-L-lysine/mg umbelliferose, respectively (Fig. 9). The decrease in WTC_g on addition of the polypeptide is interpreted to mean that poly-L-lysine directly interacts through hydrogen bonding with umbelliferose to form a tightly packed molecular network. Sucrose acts very similar in this respect.

Protection of liposomes

Sugars in anhydrobiotic organisms may also play a role in the protection of membranes. By interacting with the polar headgroups of phosholipids, they were found to depress T_m of model membranes (Crowe *et al.*, 1992, 1996).

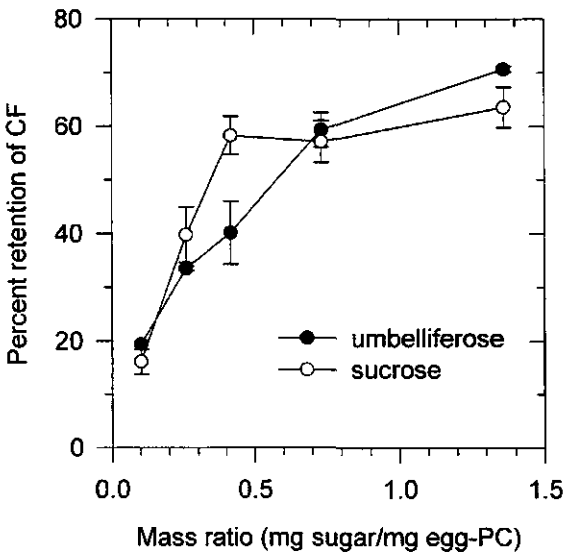

Figure 11. Retention of trapped CF in rehydrated egg-PC liposomes that were air-dried (3% RH) at room temperature for three h in the presence of varying amounts of umbelliferose or sucrose. Data are means of triplicate leakage experiments. Error bars (±SD) are indicated when they exceed symbol size.

Using FTIR we measured the position of the absorption band attributed to the CH_2 symmetric stretching vibration of the acyl chains in egg-PC liposomes. During the transition from the gel-phase to the liquid-crystalline-phase, there is a wavenumber shift from 2851 to 2854 cm^{-1} (Hoekstra *et al.*, 1989). Figure 10 shows that umbelliferose can prevent the dehydration-induced increase of T_m in egg-PC liposomes. While hydrated liposomes have a T_m at approximately -8°C and the air-dried liposomes at 32°C, the T_m of liposomes dried in the presence of umbelliferose was -35°C, far below that of the hydrated control. Sucrose had an identical effect on the dry liposomes. Thus, the lipid bilayer remains in the liquid-crystalline phase during dehydration at 20°C, which is one of the prerequisites for the protection of liposomes in the dry state (Crowe *et al.*, 1994; Crowe *et al.*, 1996, 1997b). Also a slight shift between 10 and 50°C could be observed for both sugars, which points to a slightly inhomogeneous interaction with the headgroups.

Figure 11 shows the effect of air-drying on the retention of the fluorescent label, CF, in egg-PC liposomes that were mixed with increasing amounts of umbelliferose in a total volume of 30 µL. Umbelliferose provided retention of entrapped CF to a similar extent as sucrose did.

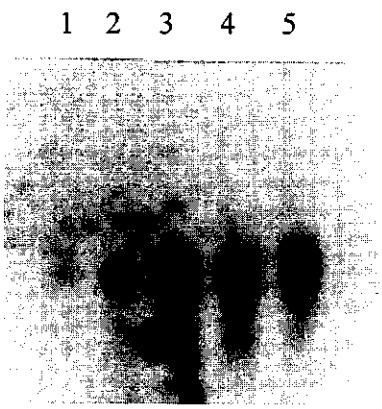

Figure 12. Northern hybridization of RNA isolated from carrot somatic embryos with the dehydrin probe B18 Close *et al.*, 1989). Time course of changes in mRNA levels of B18 mRNA during slow drying of the embryos (lane 1 = 0 h; lane 2 = 24 h; lane 3 = 48 h; lane 4 = 72 h; lane 5= 96 h).

Expression of a dehydrin transcript (B18) during drying

Apart from the type of sugar, proteins can also have an effect on the glassy properties of the cytoplasm (Chapter 9, and references therein). Therefore, mRNAs were extracted regularly during slow drying to study whether there is transcription of mRNA coding for dehydration-specific proteins. The slow drying treatments were always followed by the 4 h rapid drying so that the mRNA extraction was performed on completely dehydrated embryos at all sample points. Figure 12 shows the mRNA expression of a dehydrin transcript (B18) during slow drying of the somatic embryos. From this blot it can be seen that at zero time, which represents rapidly dried embryos, there is no expression of dehydrins. The expression increases during the slow drying, reaching a maximum level of expression after 48 h.

Discussion

Carrot somatic embryos acquire the capacity to become desiccation-tolerant by the addition of ABA to the maturation medium, but the actual tolerance requires slow drying of several days (Tetteroo *et al.*, 1995). Rapid drying within a few hours results in low survival. We therefore used the carrot somatic embryo system to study the mechanisms of desiccation tolerance. In particular, we compared the macromolecular stability of slowly and rapidly dried embryos in relation to the differences in molecular composition between them.

Protein secondary structure

Rapidly dried somatic embryos have leaky plasma membranes, decreased phospholipid contents, elevated free fatty acid contents, and irreversible protein aggregates in their plasma membranes (Tetteroo *et al.*, 1996). However, all these signs of cellular breakdown were observed after rehydration of the dried embryos. Thus, *post mortem* phenomena might have been observed rather than primary damage due to drying *per se*. In order to study the primary effects of drying, it is necessary to assess the embryos in the dry state. The development of FTIR has made it possible to do just that (Crowe *et al.*, 1984; Wolkers and Hoekstra, 1995, 1997; Wolkers *et al.*, 1998a,b).

Our first objective was to study changes in overall protein secondary structure associated with the acquisition of desiccation tolerance. We found that slow drying led to a slightly higher relative proportion of α-helical structures in the dry state. Despite this slight difference, the overall protein secondary structures of the slowly and rapidly dried somatic embryos resembled one another to a large extent. However, in some of the rapidly dried embryos signs of protein breakdown were observed (Fig. 1). A more severe breakdown was observed after rapid drying of immature maize zygotic embryos (Wolkers *et al.*, 1998a).

The slightly higher relative proportion of α-helical structure to the overall protein secondary structure also could indicate that additional proteins are synthesized during the slow drying treatment. In general, drying can induce the synthesis of LEA or LEA-like proteins, for which a role in cellular protection is assumed. We show that, indeed, transcripts of a gene coding for a LEA-like protein are expressed during slow drying of the somatic embryos (Fig. 12). During the rapid drying, time is simply lacking for the synthesis of new proteins. Previously, we reported on an increased proportion of α-helical structures in maize embryos that acquire desiccation tolerance (Wolkers *et al.*, 1998a). A possible explanation for such a higher α-helical content could be that newly synthesized proteins adopt an α-helical conformation in the dry state. Strikingly, a purified group III LEA-like protein from pollen adopts an α-helical structure in the dried state, whereas it has an unordered structure in solution (Chapter 9). In the light of the expression of LEA-like transcripts during slow drying (Fig. 12), we suggest that the observed increase in proportion of α-helical structures in desiccation-tolerant carrot somatic embryos and maize zygotic embryos can be attributed, at least partly, to newly synthesized LEA proteins.

Heat stability of endogenous proteins

During drying, the cytoplasm of the embryos transforms into a glassy matrix, which is thought to immobilize macromolecular and cellular structures, thus providing stability (Williams and Leopold, 1989; Leopold *et al.*, 1994). Using FTIR we were able to assess *in situ* the stability of endogenous proteins

embedded in this dry glassy matrix. No differences in protein denaturation temperatures between rapidly and slowly dried embryos were found. However, the extent of protein denaturation was higher in the rapidly dried embryos as was deduced from the higher relative proportion of irreversible protein aggregates. Apparently, proteins are less well immobilized in the rapidly dried embryos, which permits more heat-induced protein-protein interactions in the dry cytoplasmic matrix of these embryos.

Properties of the viscous-solid matrix

In an attempt to link the differences in heat denaturation behavior between the slowly and rapidly dried embryos to possible differences in glassy behavior, heat induced shifts in the OH-stretch were investigated. We found that slowly dried somatic embryos were in a glassy state at room temperature (T_g = 44°C) and that no clearly defined T_g could be observed for the rapidly dried embryos. Furthermore, the WTC values below 40°C were considerably higher for the rapidly dried specimens that for the slowly dried ones. This means that the average strength of intermolecular hydrogen bonding, or in other words, the molecular packing density, is higher in the slowly dried embryos than in the rapidly dried embryos. The reduced molecular packing density may account for the reduced protein stability in the rapidly dried somatic embryos. High WTC values and low protein stability were also found in desiccation-sensitive, maturation-defective mutant seeds of *Arabidopsis thaliana* (Chapter 7).

Role of umbelliferose in slowly dried carrot somatic embryos

We made an attempt to explain the differences in physical stability between slowly and rapidly dried somatic embryos on account of differences in sugar contents and composition. While sucrose is the major soluble carbohydrate after rapid drying (up to 20% of the DW), on slow drying the trisaccharide, umbelliferose, accumulates at the expense of sucrose, up to 15% of the DW. Because of the quantitative importance of this shift in sugar composition with the acquisition of desiccation tolerance, we compared some

protective properties of umbelliferose with those of sucrose in an attempt to explain the better physical stability of the slowly dried embryos.

Stabilizing properties of umbelliferose compared with sucrose

Both umbelliferose and sucrose form a glassy state upon air-drying. The T_g of umbelliferose was slightly higher than that of sucrose, 66°C compared to 60°C, respectively. Both sugars are equally effective in depressing the T_m of dry egg-PC liposomes. Thus, the liposomes remain in the liquid-crystalline phase during dehydration at ambient temperatures. For protection of liposomes in the dry state, this is one of the prerequisites (Crowe *et al.*, 1994, 1996). Another prerequisite is prevention of liposome fusion, which depends on the presence of good glass forming compounds (Crowe *et al.*, 1997b). As discussed above, both umbelliferose and sucrose are such good glass formers. It is therefore no surprise that both sugars are able to retain CF inside liposomes after dehydration in their presence. Likewise, raffinose and stachyose have this ability, but monosaccharides do not (Crowe *et al.*, 1997b).

It has been suggested that some disaccharides have a role in the protection of proteins during drying (Carpenter *et al.*, 1987). We tested the effect of umbelliferose and sucrose on the retention of the aqueous structure of poly-L-lysine and found that both sugars are equally effective in preventing dehydration-induced conformational transitions of this polypeptide. Umbelliferose also interacts with poly-L-lysine to form a more stable glassy structure than does umbelliferose alone. In this respect, umbelliferose is equally effective as sucrose (Fig. 9).

Taken together, umbelliferose does not have superior stabilizing properties when compared with sucrose. This might explain the apparent interchangeability between these sugars in slowly dried embryos having high survival of desiccation (Fig. 5). Apparently, umbelliferose and sucrose are equally important in relation to desiccation tolerance. However, this does not rule out the possibility that umbelliferose adds to stability that becomes manifest during dry storage.

Possible role of LEA proteins *vs* umbelliferose

The rapidly dried somatic embryos are different from the slowly dried embryos in that they lack dehydration-induced protein synthesis. Such proteins may have an important impact on the glassy matrix of the dry embryos. We have previously shown that LEA proteins purified from pollen increased the T_g and the molecular packing density of a sucrose glass (Chapter 10). Based on the similar physical properties of sucrose and umbelliferose, we suggest that the lower physical stability of the rapidly dried embryos is most likely due to a lack of dehydration-induced proteins, rather than to a lack of accumulated umbelliferose.

Acknowledgements

This project was financially supported by the Life Sciences Foundation, which is subsidized by the Netherlands Organization for Scientific Research. We acknowledge the help of Dr. Henk A. Schols of the Food Science Dept. of the Wageningen Agricultural University and Dr. Steef M. De Bruijn for their help with the Dionex experiments.

References

Bell, L.N., Hageman, M.J. (1996) Glass transition explanation for the effect of polyhydroxy compounds on protein denaturation in dehydrated solids. *J. Food Sci.* **61,** 372-378.

Blackman, S.A., Obendorf, R.L., Leopold, A.C. (1992) Maturation proteins and sugars in desiccation tolerance of developing soybean seeds. *Plant Physiol.* **100,** 225-230.

Blackman, S.A., Wettlaufer, S.H., Obendorf, R.L., Leopold, A.C. (1991) Maturation proteins associated with desiccation tolerance in soybean. *Plant Physiol.* **96,** 868-874.

Carpenter, J.F., Crowe, J.H. (1989) An infrared spectroscopic study of the interactions of carbohydrates with dried proteins. *Biochemistry* **28,** 3916-3922.

Carpenter, J.F., Martin, B., Crowe, L.M., Crowe, J.H. (1987) Stabilization of phosphofructokinase during air drying with sugars and sugar/transition metal mixtures. *Cryobiol.* **24,** 455-464.

Close, T.J., Kortt, A.A., Chandler, P.M. (1989) A cDNA-based comparison of dehydration-induced proteins (dehydrins) in barley and corn. *Plant Mol. Biol.* **13,** 95-108.

Crowe, J.H., Crowe, L.M. (1988) Factors affecting the stability of dry liposomes. *Biochim. Biophys. Acta* **939,** 327-334.

Crowe, J.H., Crowe, L.M., Carpenter, J.F., Aurell, Wistrom. C. (1987) Stabilization of dry phospholipid bilayers and proteins by sugars. *Biochem. J.* **242,** 1-10

Crowe, J.H., Crowe, L.M., Carpenter, J.F., Prestrelski, S.J., Hoekstra, F.A. (1997a) Anhydrobiosis: cellular adaptations to extreme dehydration. In: Dantzler, W.H. (ed.) Handbook of Physiology section 13, Comparative Physiology, Vol II, Oxford University Press, Oxford, UK, pp. 1445-1477.

Crowe, J.H., Crowe, L.M., Chapman, D. (1984) Preservation of membranes in anhydrobiotic organisms: the role of trehalose. *Science* **223,** 701-703.

Crowe. J.H., Hoekstra, F.A., Crowe, L.M. (1992) Anhydrobiosis. *Annu. Rev. Physiol.* **54,** 570-599.

Crowe, J.H., Hoekstra, F.A., Nguyen, K.H.N., Crowe, L.M. (1996) Is vitrification involved in depression of the phase transition temperature in dry phospholipids? *Biochim. Biophys, Acta* **1280,** 187-196.

Crowe, J.H., Leslie, S.B., Crowe, L.M. (1994) Is vitrification sufficient to preserve liposomes during freeze-drying? *Cryobiol.* **31,** 355-366.

Crowe, J.H., Oliver, A.E., Hoekstra, F.A., Crowe, L.M. (1997b) Stabilization of dry membranes by mixtures of hydroxyethyl starch and glucose: The role of vitrification. *Cryobiology* **35,** 20-30.

Golovina, E.A., Wolkers, W.F., Hoekstra, F.A. (1997a) Long term stability of protein secondary structure in dry seeds. *Comp. Biochem. Physiol.* **117A,** 343-348

Hoekstra, F.A., Crowe, J.H., Crowe, L.M, (1989) Membrane behavior in drought and its physiological significance. *In:* Taylorson RB (ed.) Recent Advances in the Development and Germination of Seeds. Plenum Press, New York and London, pp. 71-88.

Hopf, H., Kandler, O. (1976) Physiologie der Umbelliferose. *Biochem. Physiol. Pflanzen* **169,** 5-36.

Hsing, Y.I.C., Chen, Z.Y., Shih, M.D., Hsieh, J.S., Chow, T.Y. (1995) Unusual sequence of group 3 LEA mRNA inducible by maturation or drying soybean seeds. *Plant Mol. Biol.* **29,** 863-868.

Jackson, M., Haris, P.I., Chapman, D. (1989) Conformational transitions in poly-L-lysine: studies using Fourier transform infrared spectroscopy. *Biochim. Biophys. Acta* **998,** 75-79.

Kalichevsky, M.T., Blanshard, J.M.V., Tokarczuk, P.F. (1993) Effect of water content and sugars on the glass transition of casein and sodium caseinate. *Int. J. Food Sci. Technol.* **28,** 139-151.

Klausner, R.D., Kumar, J.N., Blumenthal, R., Flavin, M. (1981) Interaction of tubulin with phospholipid vesicles. I. Association with vesicles at the phase transition. J. Biol. Chem. **256,** 5879-5885.

Leopold, A.C., Sun, W.Q., Bernal-Lugo, I. (1994) The glassy state in seeds: analysis and function. *Seed Sci. Res.* **4,** 267-274.

Levine, H., Slade, L. (1992) *In:* Schwartzberg, H., Hatel, R.W. (eds.) Physical chemistry of Foods. pp. 83-221. Marcel Dekker, New York.

Prestrelski, S.J., Tedeschi, N., Arakawa, T., Carpenter, J.F. (1993) Dehydration-induced conformational transitions in protein and their inhibition by stabilizers. *Biophys. J.* **65,** 661-671.

Redgwell, R.J. (1980) Fractionation of plant extracts using ion-exchange Sephadex. *Anal. Biochem.* **107,** 44-50.

Roos, Y.H. (1995) Phase Transitions in Foods, Academic Press, London, pp. 1-360.

Sambrook, J., Fritsch, E.F., Maniatis, T. (1989) Molecular cloning: A laboratory manual. Cold Spring Harbor, NY: Cold Spring Harbor Laboratory Press.

Tetteroo, F.A.A., Bomal, C., Hoekstra, F.A., Karssen, C.M. (1994) Effect of abscisic acid and slow drying on soluble carbohydrate content in developing embryoids of carrot (*Daucus carota* L.) and alfalfa (*Medicago sativa* L.). *Seed Sci. Res.* **4,** 203-210.

Tetteroo, F.A.A., de Bruijn, A.Y., Henselmans, R.N.M., Wolkers, W.F., van Aelst, A.C., Hoekstra, F.A. (1996) Characterization of membrane properties in desiccation-tolerant and -intolerant carrot somatic embryos. *Plant Physiol.* **111,** 403-412.

Tetteroo, F.A.A., Hoekstra, F.A., Karssen, C.M. (1995) Induction of complete desiccation tolerance in carrot (*Daucus carota*) embryoids. *J. Plant Physiol.* **145,** 349-356.

Tetteroo, F.A.A., van Aelst, A.C., Von Recklinghausen, I.R., Golovina, E.A., Hoekstra, F.A. (1998) Membrane permeability, morphology and desiccation tolerance of *Daucus carota* somatic embryos as influenced by drying rate. *Protoplasma* **in press.**

Tiffany, M.L., Krimm, S. (1969) Circular dichroism of the "random" polypeptide chain. *Biopolymers* **8,** 347-359.

Van Bilsen, D.G.J.L., Hoekstra, F.A., Crowe, L.M., Crowe, J.H. (1994) Altered phase behavior in membranes of aging dry pollen may cause imbibitional leakage. *Plant Physiol.* **104,** 1193-1199.

Vertucci, C.W., Farrant, J.M. (1995) Acquisition and loss of desiccation tolerance. *In:* Kigel, J., Galili, G. (eds.) Seed development and germination, Marcel Dekker, New York, pp. 237-271.

Weges, R., Karssen, C.M. (1987) The influence of desiccation following pretreatment on germination of lettuce seeds. *Acta Hort.* **215,** 173-178.

Williams, R.J., Leopold, A.C. (1989) The glassy state in corn embryos. *Plant Physiol.* **89,** 977-981.

Wolkers, W.F., Bochicchio, A., Selvaggi, G., Hoekstra, F.A. (1998a) Fourier transform infrared microspectroscopy detects changes in protein secondary structure associated with desiccation tolerance in developing maize embryos. *Plant Physiol.* **116,** 1169-1177.

Wolkers, W.F., Hoekstra, F.A. (1995) Aging of dry desiccation-tolerant pollen does not affect protein secondary structure. *Plant Physiol.* **109,** 907-915.

Wolkers, W.F., Hoekstra, F.A. (1997) Heat stability of proteins in desiccation-tolerant cattail pollen (*Typha latifolia*): A Fourier transform infrared spectroscopic study. *Comp. Biochem. Physiol.* **117A**: 349-355.

Wolkers, W.F., Oldenhof, H., Alberda, M., Hoekstra, F.A. (1998b) A Fourier transform infrared microspectroscopy study of sugar glasses: Application to anhydrobiotic higher plant cells. *Biochim. Biophys. Acta* **1379,** 83-96.

Chapter 9

Dehydration-induced conformational changes of poly-L-lysine as influenced by drying rate and carbohydrates

Willem F. Wolkers, Maria G. van Kilsdonk and Folkert A. Hoekstra

Abstract

The conformation of hydrated and air-dried poly-L-lysine in thin films was studied using Fourier transorm IR spectroscopy in the amide-I region. Hydrated poly-L-lysine has a random coil conformation. Upon slow drying of small droplets of the polypeptide solution over a period of several hours, an extended β-sheet conformation is adopted. This conformational transition can be prevented by fast air-drying within 2-3 minutes. This leads, most likely, to timely immobilization of the polypeptide molecules in a viscous solid state before conformational changes can take place. Slow air-drying in the presence of sucrose also preserves the aqueous conformation and results in the formation of a glassy state. Sucrose interacts with poly-L-lysine, as deduced from the shift to lower wavenumber of the OH-band upon addition of the polypeptide. Comparison of shifts of this band with temperature indicates that sucrose/poly-L-lysine mixtures form a molecularly more densely packed glassy matrix, having a higher glass transition temperature (T_g), than sucrose alone. Whether direct interaction of sugar and polypeptide or glass formation is involved in the stabilization during slow air-drying was studied by drying in the presence of glucose or dextran, having differential glass forming properties. Compared with dextran (and sucrose to a lesser extent), glucose gives superior protection. Glucose has the lowest T_g and the best interacting properties. We conclude that either immobilization by fast air-drying or sufficient interaction with stabilizing sugars can prevent conformational changes in dehydration-sensitive proteins during dehydration.

Submitted for publication in Biochimica et Biophysica Acta

Introduction

The functional structure of a protein is determined by electrostatic forces, hydrogen bonding, van der Waals interactions, and hydrophobic interactions. All these interactions are influenced by water. Therefore, water is thought to be essential to the functional folding of most proteins (e.g., Kuntz and Kauzmann, 1974). Dehydration can completely and irreversibly inactivate some proteins with enzymic function (Hanafusa, 1969; Carpenter *et al.*, 1987a,b), presumably through loss of structure. Subsequent FTIR studies have shown that (freeze-)drying of proteins indeed often results in conformational changes (Carpenter and Crowe, 1989; Prestrelski *et al.*, 1993; Dong *et al.*, 1995). The extent of the changes depends on the type of protein. These changes can be irreversible, but full reversibility also has been observed (Griebenow and Klibanov, 1995).

It is of considerable importance to stabilize and preserve proteins of commercial interest in the dry state. There are two practical ways by which water can be removed from an aqueous protein solution: freeze-drying and evaporative drying. Because low temperature is generally envisaged to enhance stabilization, freeze-drying has become the established method of drying (Pikal, 1990a,b). However, evaporative drying at elevated temperature has been shown to effectively preserve functional activity, particularly in the presence of suitable carbohydrates, presumably due to a rapid embedding in a glassy matrix (Franks *et al.*, 1991).

The presence of sugars during freeze-drying preserves the native structure of proteins in the dry state (Prestrelski *et al.*, 1993). This protecting effect of sugars correlates directly with preservation of the enzymic activity. The mechanisms by which the sugars stabilize proteins during drying have been reviewed by Crowe *et al.* (1997). Both the ability of the sugars to form a glassy state (Franks *et al.*, 1991; Kalichevsky *et al.*, 1992, 1993; Roos, 1995; Chang *et al.*, 1996) and to interact directly with the protein through hydrogen bonding (Carpenter and Crowe, 1989; Carpenter *et al.*, 1992) have been suggested to account for this stabilization.

In studies on protein secondary structure in the dry state, FTIR is a powerful tool (Carpenter and Crowe, 1989; Prestrelski *et al.*, 1993; Wolkers and Hoekstra, 1995; Wolkers *et al.*, 1998a). The amide-I region between 1700-1600 cm^{-1} arising predominantly from the C=O stretching vibrations of the peptide groups is particularly informative (Susi *et al.*, 1967). Differences in the amide-I band profile can be used in the assignment of different types of protein secondary structure (Surewicz *et al.*, 1993). Recently, a FTIR method has been developed to characterize glassy sugar matrices (Wolkers *et al.*, 1998b). From the temperature dependence of the IR-band arising from the OH-stretching vibrations of the sugar (3500-3000 cm^{-1}) information can be derived on the average strength of the hydrogen bonding.

In this paper we characterize the effects of drying rate, and soluble carbohydrates having differential glass forming and interaction properties, on the conformation of air-dried poly-L-lysine, using FTIR. Poly-L-lysine was chosen because it makes only a minor contribution to the OH-stretching vibration band of the carbohydrates, rendering it very suitable to study carbohydrate-polypeptide interactions. We also tested whether fast air-drying of small poly-L-lysine droplets in the absence of carbohydrates could preserve the aqueous conformation of poly-L-lysine in the dry state. Previously, Prestrelski *et al.*, (1993) have found that poly-L-lysine transforms reversibly from a random coil conformation in solution into an extended β-sheet upon freeze-drying.

This work originates from our investigations on organisms and organs that are able to survive almost complete dehydration. The mechanisms by which these anhydrobiotic organisms protect their proteins and membranes against dehydration-induced stresses have formed a challenge to biologists over the past decades (Crowe *et al.*, 1997).

Materials and methods

Sample preparation

Poly-L-lysine (57.4 kDa) was purchased from Sigma Chemical Co. (St Louis, MO), glucose and sucrose from Pfahnstiel (Waukegan, IL, USA), and

dextran T500, MW 480 kDa, from Pharmacia (Uppsala, Sweden). The polypeptide was dialyzed for 24 h at 4°C against 2 mM Tris-HCl (pH = 7.5), or against 100 mM NaCl in 10 mM Tris-HCl (pH = 7.5), changing the buffer 3 times. Polypeptide samples in D_2O were obtained by mixing an aliquot of the lyophilized, dialyzed material with D_2O. Dry poly-L-lysine films were prepared by air-drying of a droplet of polypeptide solution (10 mg/ml buffer) on circular (2 x 13 mm) CaF_2 infrared windows. Droplets of 5 to 25 µl were placed on these windows and subjected to either slow or rapid air-drying.

Rapid drying was performed by placing the CaF_2 windows with the droplets in a cabin continuously purged with dry air (RH < 3% at 45°C). The diameter of the droplets (5 - 25 µl) was kept at 7 mm (the droplets only varied in height). Thus, the total drying time of the droplets varied as a function of the droplet volume and was measured by a thermocouple inserted in the droplet. The sudden increase in temperature that was measured when the sample fell dry was taken as the total drying time of the droplet.

Slow drying was performed by exposing the poly-L-lysine droplets at 25°C to different RHs generated by different saturated salt solutions [NaCl (75% RH); $Ca(NO_3)_2$ (51% RH); $CaCl_2$ (30% RH)] inside ventilated containers. The samples remained in each container for 4 h, in descending order of RH. Finally, the samples were dried in a box continuously purged with dry air (RH of approximately 3%) at 25°C.

Fourier transform infrared spectroscopy

IR spectra were recorded on a Perkin-Elmer 1725 Fourier transform IR-spectrometer (Perkin-Elmer, Beaconsfield, Buckinghamshire, UK) equipped with a liquid nitrogen-cooled mercury/cadmium/telluride detector and a Perkin-Elmer microscope interfaced to a personal computer as described previously (Wolkers and Hoekstra, 1995, 1997; Wolkers *et al.*, 1998a,b). Each sample was hermetically sealed between two IR-windows, using a rubber O-ring, and mounted into a temperature-controlled brass cell that was cooled by a liquid nitrogen source. The temperature was regulated by a computer-controlled device that activated a liquid nitrogen pump, in conjunction with a power supply

for heating of the cell. The temperature of the sample was recorded separately using a Pt-100 element that was located very close to the sample windows. The optical bench was purged with dry CO_2-free air (Balston; Maidstone, Kent, UK) at a flow rate of 25 l min^{-1}. The acquisition parameters were: 4 cm^{-1} resolution, 32 coadded interferograms, 3500-900 cm^{-1} wavenumber range.

Spectral analysis and display were carried out using the Infrared Data Manager Analytical Software, version 3.5 (Perkin-Elmer). For protein studies, the spectral region between 1720 and 1580 cm^{-1} was selected. This region contains the amide-I absorption band of the peptide backbone. The melting of glasses during heating of the sample at 1.5°C/min was monitored by observing the position of the band around 3300 cm^{-1} (OH-stretching vibration), and T_g and WTC were determined as outlined by Wolkers *et al.* (1998b).

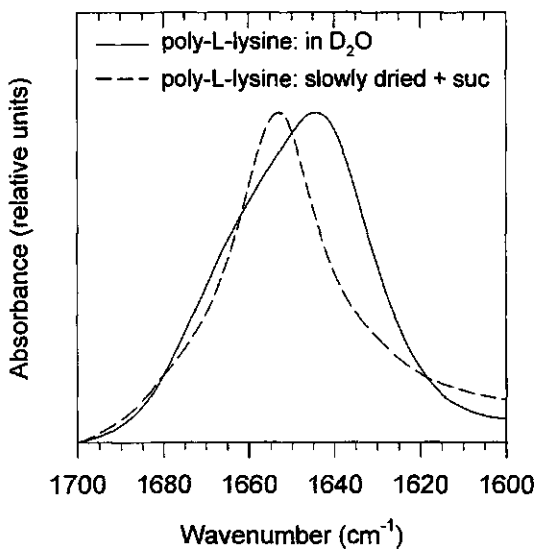

Figure 1. IR absorption spectra in the amide-I region of poly-L-lysine in D_2O and of poly-L-lysine that was slowly-dried in the presence of sucrose (mass ratio = 1:1).

Results and discussion

Air-drying of poly-L-lysine in the presence of sucrose

Figure 1 shows the IR spectrum of poly-L-lysine in solution at neutral pH. To avoid the interfering effect of H_2O in the amide-I band, this IR spectrum was recorded in D_2O. One broad band with an absorption maximum around 1644 cm^{-1} is apparent in the amide-I region of the IR spectrum. The band position together with the broadness of this band indicate that the polypeptide has a random conformation. This is in agreement with earlier FTIR observations on the aqueous structure of this molecule at neutral pH (Jackson *et al.*, 1989). Other conformations have been observed depending on pH, ionic strength and temperature, such as α-helical at pH = 11 and β-sheet at pH = 11.0 + heating (Jackson *et al.*, 1989). Figure 1 further shows that when poly-L-lysine is slowly air-dried (from H_2O) in the presence of sucrose, the band position of the

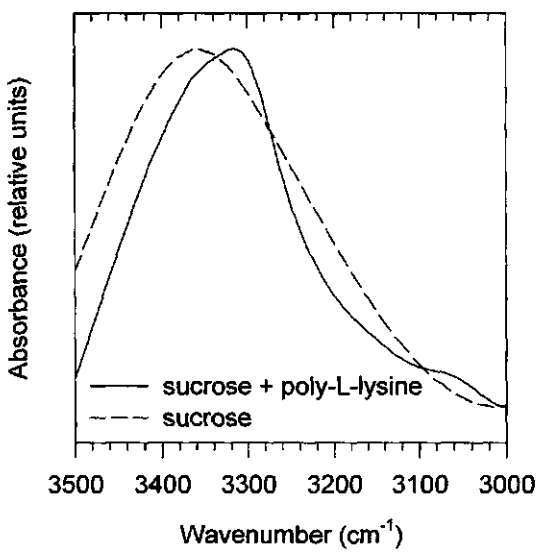

Figure 2. IR absorption spectra in the OH-stretching region (3500-3000 cm^{-1}) of rapidly dried sucrose (to prevent crystallization) and slowly dried sucrose/poly-L-lysine mixture (mass ratio = 1:1). Ten μl droplets were subjected to rapid air-drying.

absorption maximum is located at approximately 1653 cm^{-1}. This was also true for rapid drying in the presence of sucrose (spectrum not shown). This means that random coil is the main conformation that is present after air-drying of the polypeptide in the presence of sucrose (see Susi, 1969; Surewicz and Mantsch, 1988; Bandekar, 1992; Haris and Chapman, 1992; Surewicz *et al.*, 1993; for the general application of IR spectroscopy to study protein secondary structure). An absorption maximum around 1658 cm^{-1} would have been indicative of a large α-helix contribution to the spectrum. On freeze-drying of poly-L-lysine in the presence of sucrose a similar protection of the aqueous conformation has been observed (Prestrelski *et al.*, 1993).

From Figure 1 it can also be observed that the wavenumber position of the amide-I band in D_2O is lower than that in the dry sucrose matrix. This is due to a rapid hydrogen-deuterium exchange of the peptide N-H groups in D_2O. Especially for random coil structure, a large shift of the amide-I band to lower frequency can be observed [in D_2O between 1647 - 1640 cm^{-1} (Haris *et al.*, 1989)]. The linewidth of the dry sucrose/polypeptide film is less than that of the

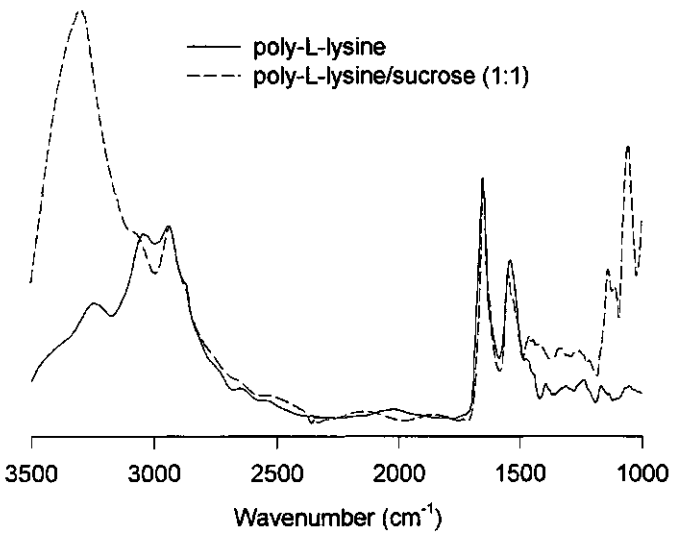

Figure 3. Comparison of IR spectra of rapidly dried poly-L-lysine and the mixture of poly-L-lysine and sucrose (1:1, mass ratio). Spectra were normalized according to the amide-I band.

polypeptide in D_2O (Fig. 1). This is indicative of a more homogeneous structure of the polypeptide in the dried state.

Figure 2 shows IR spectra in the OH-vibration region of dried sucrose and of poly-L-lysine that was slowly dried in the presence of sucrose (mass ratio 1:1). Sucrose alone gives a broad band with an absorption maximum around 3350 cm^{-1}, which shifts to lower wavenumber (around 3320 cm^{-1}) in the presence of poly-L-lysine and decreases in linewidth. The absorption in this region can be attributed, almost entirely, to OH-groups of the sucrose, because poly-L-lysine has only a minor contribution around 3240 cm^{-1} arising from N-H vibrations (Fig. 3). The lower band position of the sucrose/polypeptide mixture with respect to that of sucrose alone indicates that the hydrogen bonding network has changed. Furthermore, the absence of sharp bands in the spectra indicates that both the sucrose and the sucrose/poly-L-lysine mixture are in an

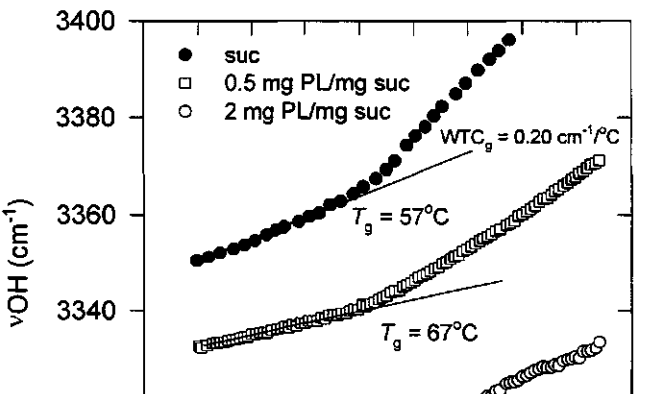

Figure 4. Wavenumber *vs* temperature plot (FTIR) of the OH-stretching vibration band of dry sucrose and sucrose/poly-L-lysine (PL) glasses. The glass transition temperatures (T_g) were determined from the intersection between the regression lines in the liquid and that in the glassy state.

amorphous state and that no crystallization of sucrose has occurred (Wolkers *et al.*, 1998b). Therefore, the change in the OH-stretch profile of the dried mixture as compared to the dried sucrose alone is the result of sugar-peptide interactions and does not reflect a change in sugar-sugar interaction as occurs when sucrose crystallizes [pure sucrose crystallizes when slowly dried above 75% RH (Wolkers *et al.*, 1998b)].

The glassy behavior of the dried sugar/polypeptide mixture was studied on account of the temperature-dependent shifts in the νOH of sucrose during heating (Fig. 4). As reported previously, T_g can be determined by FTIR from such a νOH *vs* temperature plot at the intersection point of linear regressions in the liquid and in the glassy state (Wolkers *et al.*, 1998b). The WTC values ($cm^{-1}/°C$) that can be derived from such plots give information on the molecular packing density of the glassy state. Because monitoring of the OH-stretch of poly-L-lysine alone is impossible due to the absence of OH-groups in this polypeptide, we studied sucrose/polypeptide mixtures with increasing amounts of the polypeptide.

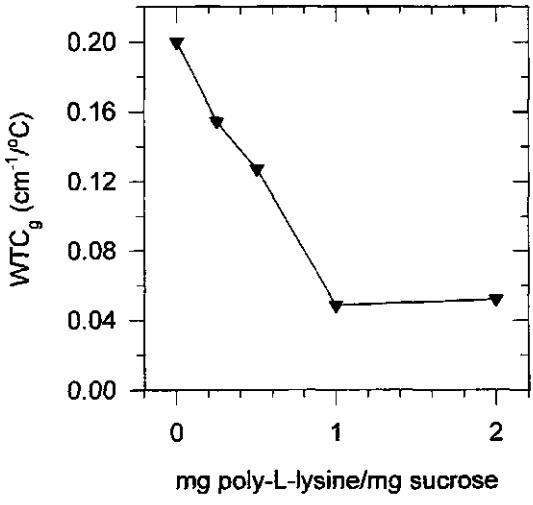

Figure 5. Plot of the WTC values in the glassy state (WTC_g; see Fig. 4) *vs* the amount of poly-L-lysine added to the sucrose matrix.

From the νOH *vs* temperature plot of the dry sucrose glass, the T_g was determined at 57°C (Fig. 4), and calculation of the WTC in the glassy state (WTC_g) gave 0.20 $cm^{-1}/°C$ (Fig. 5). In the presence of increasing amounts of poly-L-lysine, a progressive decrease in the absorbance in the region from 3500 to 3000 cm^{-1} can be observed (data not shown); T_g increases, whereas the WTC_g decreases linearly from 0.20 to 0.05 $cm^{-1}/°C$ in the range from 0 to 1 mg poly-L-lysine/mg sucrose, respectively (Fig. 5). This suggests that poly-L-lysine directly interacts with sucrose to form a tightly packed network. The WTC_g does not further decrease when the amount of polypeptide is further increased above 1 mg/mg sucrose. Apparently, the polypeptide has its hydrogen bonding requirements of polar groups satisfied with sucrose at a 1:1 mass ratio.

An important factor that influences the glassy behavior of dried samples is the plasticizing effect of residual water molecules (Franks *et al.*, 1991; Levine and Slade, 1988). This residual water can be removed by heating the sample above T_g. Therefore, to avoid the interfering effect of residual water on the amide-I and OH-stretching bands we routinely heated the sucrose and the sucrose/poly-L-lysine films to 100°C in dry air for 10 min prior to the measurements. It was observed that the broad band around 1650 cm^{-1} representing residual water had disappeared after the heating.

Rapid air-drying of poly-L-lysine alone

The question now arises whether hydrogen bonding of a sugar to the protein is pivotal to preserving the aqueous conformation of the peptide, or whether the formation of a highly viscous state alone is sufficient for protection. To investigate this we have studied the effects of rapid and slow air-drying on the dry poly-peptide conformation (Fig. 6). It can be expected that rapid air-drying prevents intermolecular peptide-peptide interactions, due to a lack of time for rearrangements. A similar lack of time for intermolecular rearrangements required for crystal formation occurs when a sucrose solution is dried rapidly (Franks, 1991; Wolkers *et al.*, 1998b).

Poly-L-lysine droplets were subjected to slow or rapid air-drying, and the conformation of the dry polypeptide films was measured using FTIR. In the amide-I band profile of slowly dried poly-L-lysine (Figure 6 A and B, dashed lines) a major band around 1625 cm^{-1} and a minor band around 1695 cm^{-1} can be observed. These bands can be assigned to the formation of intermolecular β-sheet structures (Susi, 1969; Surewicz and Mantsch, 1988; Bandekar, 1992; Haris and Chapman, 1992; Surewicz *et al.*, 1993). From the intensity of these bands it can be concluded that after slow drying, the poly-peptide is almost entirely in a β-sheet conformation. On freeze-drying in the absence of sugar, the conformation of poly-L-lysine also transforms from random coil into β-sheet (Prestrelski *et al.*, 1993).

Rapid air-drying of the polypeptide from the buffer containing 100 mM NaCl (Fig. 6A) shows that the shape of the amide-I band is dependent on the droplet size and thus on the total drying time of the droplet, varying from 2.2

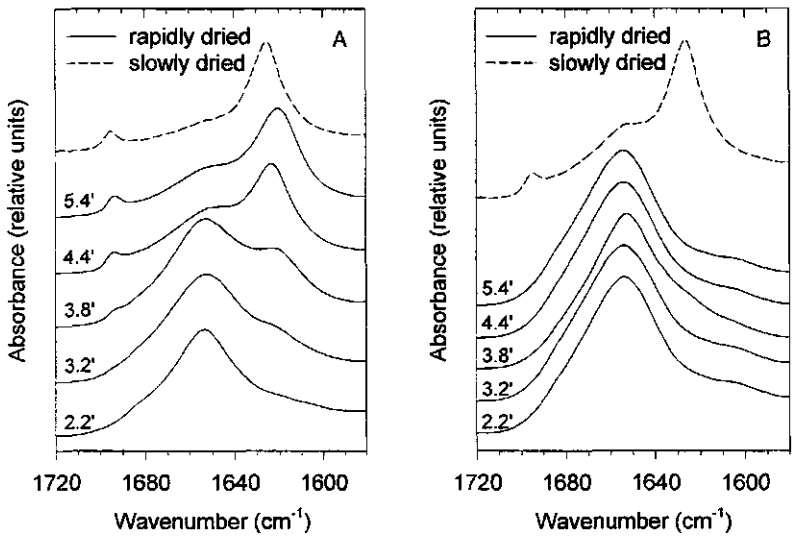

Figure 6. IR absorption spectra in the amide-I region of slowly and rapidly dried droplets of poly-L-lysine solution. The solution contained poly-L-lysine (10 mg/ml) in 100 mM NaCl, 10 mM Tris-Cl, pH = 7.5 (A) or 2 mM Tris-Cl, pH = 7.5 (B). Droplets of various volumes (5 to 25 µl), but with the same surface area, were rapidly dried in a box continuously purged with dry air (RH < 3%, 45°C). Total drying times of the droplets are indicated in the figures.

min (5 µl droplets) to 5.4 min (25 µl droplets). The amide-I band of the polypeptide film dried within 2.2 min is very broad, with an absorption maximum around 1654 cm^{-1}. This indicates that the polypeptide in this film is in a random coil conformation. When the drying time is increased, bands characteristic of the formation of β-sheet structures (between 1625 and 1620 cm^{-1} and, between 1695 and 1690 cm^{-1}) appear. In the dry film which is formed within 5.4 min of air-drying, the polypeptide is almost entirely in a β-sheet conformation. In the absence of 100 mM NaCl in the buffer, rapid air drying can entirely prevent the formation of β-sheet structures, for all the drying times used (Fig. 6B). The broad amide-I band in all these rapidly dried polypeptide films has an absorption maximum at approximately 1654 cm^{-1}, which is indicative of random coil structure.

Effect of carbohydrates with differential glass-forming properties

To gain more insight into the effect of the glass forming properties of carbohydrates in the stabilization of dehydrating poly-L-lysine, glucose, sucrose and a high MW dextran were tested under conditions that favor β-sheet formation, i.e. slow drying and 100 mM NaCl in the buffer. While glucose is a relatively bad glass former [T_g = 27°C (Wolkers *et al.*, 1998b and references

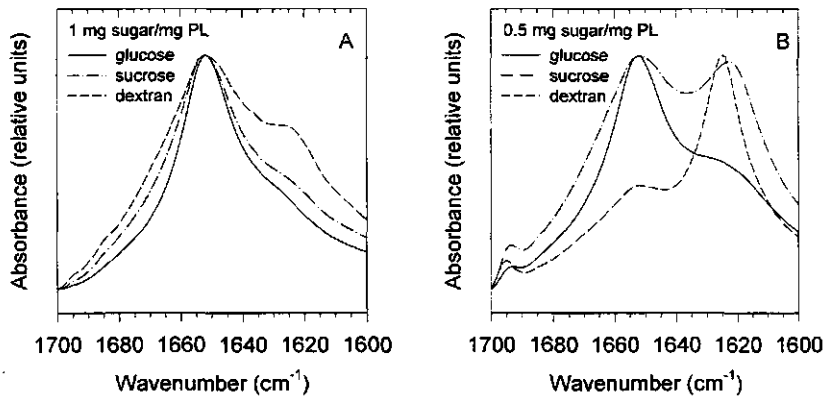

Figure 7. IR absorption spectra in the amide-I region of poly-L-lysine that was slowly dried in the presence of glucose, sucrose and dextran (at 22°C). (A) Mass ratio carbohydrate:poly-L-lysine = 1:1; (B) mass ratio carbohydrate:poly-L-lysine = 1:2.

therein)], high MW dextran is a good glass former [T_g > 110°C (Crowe *et al.*, 1996)], sucrose being intermediate (57°C, Fig. 4).

Figure 7A shows IR spectra in the amide-I region of poly-L-lysine that was dried in the presence of glucose, sucrose and dextran (mass ratio 1:1). In the presence of glucose no sign of β-sheet structures is observed. At lower mass ratio of glucose to poly-L-lysine (1:2) small signs of β-sheet structures can be observed (Fig. 7B). In the presence of sucrose (1:1 mass ratio), small signs of β-sheet formation are visible, which further increase at lower mass ratio of sucrose to poly-L-lysine (compare Fig. 7A and B). However, in the presence of dextran, β-sheet structures are already formed at a 1:1 mass ratio, and at a 1:2 mass ratio, the polypeptide is almost entirely in a β-sheet conformation. This indicates that in spite of its good glass forming properties, dextran can hardly prevent the formation of β-sheet structures.

The extent of interaction of the different carbohydrates with the dried poly-L-lysine is derived from IR-spectra in the OH-vibration region. Figure 8

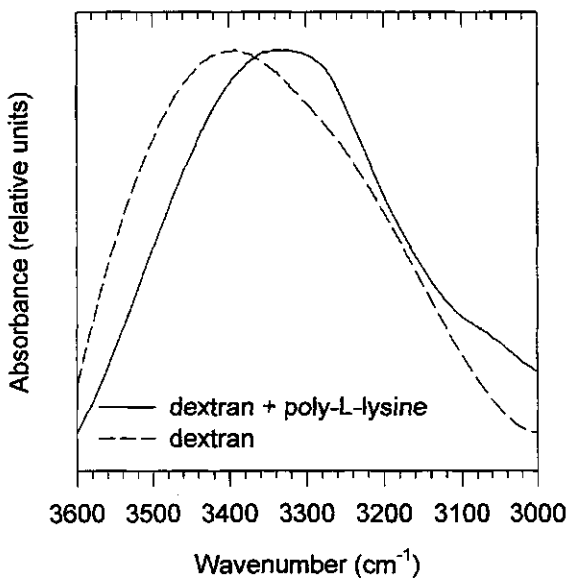

Figure 8. IR absorption spectra in the OH-stretching region (3600-3000 cm^{-1}) of slowly dried dextran and dextran/poly-L-lysine mixture (mass ratio = 1:1). Ten µl droplets were subjected to slow air-drying (at 22°C).

shows that on addition of the polypeptide, the OH-stretching band of dextran shifts to a lower wavenumber position, indicative of interaction of the two compounds. This also occurs in the case of the dried glucose - poly-L-lysine mixture (spectra not shown). However, when the spectra of the OH-bands of the mixture of poly-L-lysine with the carbohydrates (mass ratio 1:1) are compared, the OH-band of the dextran/poly-L-lysine mixture is broader and at higher wavenumber position than those of the mixtures of poly-L-lysine with glucose or sucrose (Fig. 9). Furthermore, the OH-band profile of the sucrose mixture is slightly broader than that of the glucose mixture. Taken together, this indicates that the average strength of hydrogen bonding is lowest in dextran and highest in glucose.

Mechanism

We attribute the transition of poly-L-lysine from an unordered conformation in solution to a β-sheet conformation in the dried state to the loss

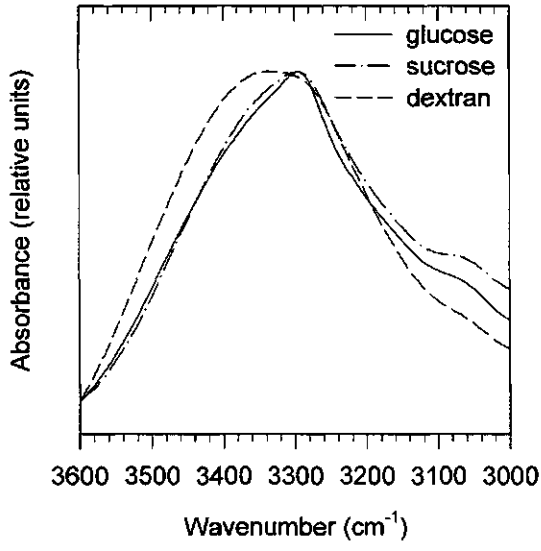

Figure 9. IR absorption spectra in the OH-stretching region (3600-3000 cm^{-1}) of slowly dried mixtures of poly-L-lysine with either glucose, sucrose or dextran (mass ratio = 1:1). Ten μl droplets were subjected to slow air-drying (at 22°C).

of hydrogen bonding of water to the peptide. In solution, the unordered polypeptide backbone has its hydrogen bonds satisfied with water. On drying, the hydrogen bonds with the water are replaced for intermolecular hydrogen bonds between peptide backbones, thus leading to the formation of β-sheet structures. The presence of salt in the buffer facilitates the formation of β-sheet structures, even when the droplets are subjected to rapid drying. The reason for this may be that the salt screens the positively charged lysine groups, thus facilitating peptide-peptide interactions.

We show here that when poly-L-lysine is air-dried (slow or rapid) in the presence of sucrose, the aqueous structure is conserved, at least when the salt concentration is low. Different mechanisms have been suggested by which sugars protect proteins during drying. Some authors (Carpenter and Crowe, 1989; Carpenter *et al.*, 1992) suppose that sugar molecules are serving as water substitutes through a direct interaction with the protein molecules in the dry state. Others (Levine and Slade, 1988; Franks *et al.*, 1991; Slade and Levine, 1991; Roos, 1995) attribute the stabilizing effect of sugars on dried proteins mainly to the glass forming properties of the sugars.

Our results indicate that a mixture of poly-L-lysine and sucrose forms a glassy state upon air drying (both slow and rapid), in which the sugar OH-groups are more tightly hydrogen-bonded than in a pure sucrose glass. This seems to support both the water substitution hypothesis and the immobilization hypothesis. However, the aqueous structure of poly-L-lysine also is conserved when small droplets of the polypeptide solution without sucrose are subjected to rapid air-drying. This shows that the addition of a stabilizer is not mandatory for preservation of the aqueous structure in the dry state, at least for this polypeptide. A likely mechanism for the retention of the aqueous conformation upon rapid air-drying is that the polypeptide molecules are immobilized due to the rapid formation of a viscous solid state. That proteins are able to form a glassy state upon dehydration has been described earlier (Kalichevski *et al.*, 1992, 1993; Roos, 1995).

When glass forming properties of added carbohydrates would be the decisive factor in the conformational protection of proteins during slow drying,

dextran would have been the best protectant. The shapes of the state diagrams of the carbohydrates used would predict that during drying, dextran enters into a glassy state at higher water content than sucrose or glucose. However, we found just the opposite: glucose, with the worst glass-forming properties, is a considerably better protectant than dextran, sucrose being intermediate. Glucose, probably due to its small size, interacts more strongly than an equal amount of the much larger sized dextran. This finding provides evidence that during slow drying the interaction properties are more important in protein stabilization than the glass forming properties. The rapid drying experiments nevertheless show that retention of the aqueous structure of the polypeptide is possible in the absence of sugar. We suggest that a time factor is at stake here. If the polypeptide can be immobilized fast enough, there will be no time for polypeptide conformational changes. During slow drying without sufficient interaction with the added carbohydrate, conformational changes apparently occur before glasses are formed. A sufficient level of interaction through hydrogen bonding may prevent precocious protein conformational changes.

It is expected that protection of the aqueous structure in the dried state also protects protein function. Extensive works on the protective effect of soluble carbohydrates on various (freeze-)dried enzymic proteins have shown that disaccharides are particularly good stabilizers and monosaccharides are less suitable in that respect (Carpenter *et al.*, 1987a,b). The discrepancy between our finding of a superior protective effect of glucose on maintaining structure and the inferior preservation of enzymic function as described in the literature (Carpenter *et al.*, 1987a,b), may stem from other properties of the monosaccharides used, such as involvement in Maillard and Amadori reactions in the dry state (Wettlaufer and Leopold, 1991; Sun and Leopold, 1995).

Franks *et al.*, (1991) have found that various dehydration-labile enzymes have a higher residual activity after evaporative-drying than after freeze-drying. Our results on drying rate in relation to the preservation of the conformation of air-dried poly-L-lysine support, on a molecular level, the beneficial effects of evaporative drying. Retention of the native conformation by rapid air-drying in

the absence of sugary stabilizers also was found in other dehydration-labile proteins (Wolkers, unpublished data).

We suggest that depending on drying rate, either immobilization of dehydration labile proteins (fast drying) or interaction with a protectant through hydrogen bonding (slow drying) plays the leading role in the preservation of the aqueous structure.

Acknowledgements

This project was financially supported by the Life Sciences Foundation, which is subsidized by the Netherlands Organization for Scientific Research.

References

Bandekar, J. (1992) Amide modes and protein conformation. *Biochim. Biophys. Acta* **1120,** 123-143.

Carpenter, J.F., Arakawa, T., Crowe, J.H. (1992) Interactions of stabilizing additives with proteins during freeze-thawing and freeze-drying. *Dev. Biol. Stand.* **74,** 225-238.

Carpenter, J.F., Crowe, J.H. (1989) An infrared spectroscopic study of the interactions of carbohydrates with dried proteins. *Biochemistry* **28,** 3916-3922.

Carpenter, J.F., Crowe, L.M., Crowe, J.H. (1987a) Stabilization of phosphofructokinase with sugars during freeze-drying: characterization of enhanced protection in the presence of divalent cations. *Biochim. Biophys. Acta* **923,** 109-115.

Carpenter, J.F., Martin, B., Crowe, L.M., Crowe, J.H. (1987b) Stabilization of phosphofructokinase during air drying with sugars and sugar/transition metal mixtures. *Cryobiology* **24,** 455-464.

Chang, B.S., Beauvais, R.M., Dong, A., Carpenter, J.F. (1996) Physical factors affecting the storage stability of freeze-dried interleukin-1 receptor antagonist: glass transition and protein conformation. *Arch. Biochem. Biophys.* **331,** 249-258.

Crowe, J.H., Crowe, L.M., Carpenter, J.F., Prestrelski, S.J., Hoekstra, F.A. (1997) Anhydrobiosis: cellular adaptations to extreme dehydration. *In:* Dantzler, W.H. (ed.) Handbook of Physiology section 13, Comparative Physiology, Vol II, Oxford University Press, Oxford. pp. 1445-1477.

Crowe, J.H., Hoekstra, F.A., Nguyen, K.H.N., Crowe, L.M. (1996) Is vitrification involved in depression of the phase transition temperature in dry phospholipids? *Biochim. Biophys. Acta* **1280,** 187-196.

Dong, A., Prestrelski, S.J., Allison, S.D., Carpenter, J.F. (1995) Infrared spectroscopic studies of lyophilization- and temperature-induced protein aggregation. *J. Pharm. Sci.* **84.** 415-424.

Franks, F., Hatley, R.H.M., Mathias, S.F. (1991) Materials science and production of shelf stable biologicals. *BioPharm.* **4 (9),** 38-42.

Griebenow, K., Klibanov, A.M. (1995) Lyophilization-induced reversible changes in the secondary structure of proteins. *Proc. Natl. Acad. Sci. USA* **92,** 10969-10976.

Hanafusa, N. (1969) Denaturation of enzyme protein by freeze-thawing and freeze-drying. *In:* Tokio N (ed.) Freezing and freeze-drying of microorganisms. University Park Press, Baltimore, pp. 117-129.

Haris, P.I., Chapman, D. (1992) Does Fourier-transform infrared spectroscopy provide useful information on protein secondary structures. *Trends Biochem. Sci.* **17,** 328-333.

Haris PI, Coke M, Chapman D (1989) Fourier transform infrared spectroscopic investigation of rhodopsin structure and its comparison with bacteriorhodopsin. Biochim Biophys Acta **995:** 160-167.

Jackson, M., Haris, P.I., Chapman, D. (1989) Conformational transitions in poly-L-lysine: studies using Fourier transform infrared spectroscopy. *Biochim. Biophys. Acta* **998,** 75-79.

Kalichevsky, M.T., Blanshard, J.M.V., Tokarczuk, P.F. (1993) Effect of water content and sugars on the glass transition of casein and sodium caseinate. *Int. J. Food Sci. Technol.* **28,** 139-151.

Kalichevsky, M.T., Jaroszkiewicz, E.M., Blanshard, J.M.V. (1992) Glass transition of gluten. 1: Gluten and gluten-sugar mixtures. *Int. J. Biol. Macromol.* **14,** 257-266.

Kuntz, I.D., Kauzmann, W. (1974) Hydration of proteins and polypeptides. *Adv. Protein Chem.* **28,** 239-345.

Levine, H., Slade, L. (1988) Water as a plasticizer: physico-chemical aspects of low-moisture polymeric systems. In F Franks, ed, Water Science Reviews Vol 3, Cambridge University Press, Cambridge, pp. 79-185.

Pikal, M.J. (1990a) Freeze-drying of proteins Part I: process design. *BioPharm.* **3 (8),** 18-27.

Pikal, M.J. (1990b) Freeze-drying of proteins Part II: formulation selection. *BioPharm.* **3 (9),** 26-30.

Prestrelski, S.J., Tedeschi, N., Arakawa, T., Carpenter, J.F. (1993) Dehydration-induced conformational transitions in proteins and their inhibition by stabilizers. *Biophys. J.* **65,** 661-671.

Roos, Y.H. (1995) Phase Transitions in Foods, Academic Press, London, pp. 1-360.

Slade, L., Levine, H. (1991) A food polymer science approach to structure property relationships in aqueous food systems: non-equilibrium behavior of carbohydrate-water systems. *In:* Levine, H., Slade, L. (eds.) Water Relationships in Food, Plenum Press, New York, pp. 29-101.

Sun, W.Q., Leopold, A.C. (1995) The Maillard reaction and oxidative stress during aging of soybean seeds. *Physiol. Plant.* **94,** 94-104.

Susi, H. (1969) Structure and stability of biological macromolecules. *In:* Biological Macromolecules, Vol 2, Marcel Dekker, New York, pp. 525-663.

Susi, H., Timasheff, S.N., Stevens, L. (1967) Infrared spectra and protein conformations in aqueous solutions. I. The amide-I band in H_2O and D_2O solutions. *J. Biol. Chem.* **242:** 5460-5466.

Surewicz, W.K., Mantsch, H.H. (1988) New insight into protein secondary structure from resolution-enhanced infrared spectra. *Biochim. Biophys. Acta* **952,** 115-130.

Surewicz, W.K., Mantsch, H.H., Chapman, D. (1993) Determination of protein secondary structure by Fourier transform infrared spectroscopy: a critical assessment. *Biochemistry* **32,** 389-394.

Wettlaufer, S.H., Leopold, A.C. (1991) Relevance of Amadori and Maillard products to seed deterioration. *Plant Physiol.* **97,** 165-169.

Wolkers, W.F., Bochicchio, A., Selvaggi, G., Hoekstra, F.A. (1998a) Fourier transform infrared microspectroscopy detects changes in protein secondary structure associated with desiccation tolerance in developing maize embryos. *Plant Physiol.* **116,** 1169-1177.

Wolkers, W.F., Hoekstra, F.A. (1995) Aging of dry desiccation-tolerant pollen does not affect protein secondary structure. Plant Physiol. **109,** 907-915.

Wolkers, W.F., Hoekstra, F.A. (1997) Heat stability of proteins in desiccation-tolerant cattail pollen (*Typha latifolia*): A Fourier transform infrared spectroscopic study. *Comp. Biochem. Physiol.* **117A,** 349-355.

Wolkers, W.F., Oldenhof, H., Alberda, M., Hoekstra, F.A. (1998b) A Fourier transform infrared microspectroscopy study of sugar glasses: application to anhydrobiotic higher plant cells. *Biochim. Biophys. Acta* **1379,** 83-96.

Chapter 10

Isolation and characterization of a D-7 LEA-like protein from pollen

Willem F. Wolkers, Sue McCready, Wolf Brandt, Folkert A. Hoekstra, and George G. Lindsey

Abstract

A heat stable protein isolated from *Typha latifolia* pollen was characterized with respect to its amino acid sequence, protein secondary structure, and its effect on the molecular structure of sucrose glasses. The protein was purified from an aqueous extract heated for 30 min at 80°C. It has a molecular mass of 9 kDa, is very rich in hydrophilic and small hydrophobic amino acids, but lacks tryptophan and cysteine residues. One of the major peptide fragments that was produced after cleavage of the protein with cyanogen bromide, AQGASDAVKNA, showed excellent homology with LEA proteins: a D-7 LEA protein (LE7_GOSHI) from cotton (first best alignment) and LE76_brana (third best alignment). Another fragment, RKKAEETAQQAQVK, only showed homology with LE76_brana from rape (fifth best alignment). The secondary structure of the purified protein in solution and in the dry state was resolved using Fourier transform IR spectroscopy. In solution, the protein adopts a random coil conformation. Fast air-drying (5 minutes) leads to the formation of α-helical structure, whereas slow drying (few hours) leads to both α-helical and intermolecular extended β-sheet structures. When dried in the presence of sucrose, the protein adopts predominantly α-helical conformation, irrespective of drying rate. Drying of a mixture of LEA protein and sucrose increased the glass transition temperature and the average strength of hydrogen bonding when compared with the same parameters of a pure sucrose glass. We suggest that LEA proteins might be involved in the formation of a

Submitted for publication in Plant Journal

tight molecular network in the dehydrating cytoplasm of anhydrobiotic organisms, which may contribute to desiccation tolerance.

Introduction

LEA proteins are small hydrophilic proteins, the mRNAs for which accumulate in seeds during maturation and in vegetative tissues in response to water stress and the stress response hormone, ABA (Close, 1996). Numerous studies have reported the nucleotide sequence of LEA genes and the transcriptional response of these genes to stress. From the amino acid sequences, six different LEA gene families have been defined (Dure *et al.*, 1989). Only three LEA proteins, however, have thus far been purified. These are the LEA group II dehydrin protein (Ceccardi *et al.*, 1994), and the LEA group I proteins Em and p11 from wheat germ and pea seeds, respectively (Espelund *et al.*, 1992; Russouw *et al.*, 1997).

Like seeds, pollen generally can withstand severe desiccation (see Hoekstra 1986, for a review). During the independent life of pollen, after release from the mother plant, water may be lost almost completely. It is therefore not surprising that desiccation- and ABA-responsive genes are expressed in pollen (Michel *et al.*, 1994; Del Mar Parra *et al.*, 1996; Rouse *et al.*, 1996). In fact, ABA accumulates in microspores during their development (Yang *et al.*, 1985; Chibi *et al.*, 1995). Several floral organ-specific proteins accumulate just before anthesis (Bedinger and Edgerton, 1990; Detchepare *et al.*, 1989), and two such proteins from *Lilium longiflorum* pollen were found to be soluble at 90°C and rich in glutamic acid/glutamine and glycine (Wang *et al.*, 1996), a property typical of LEA proteins.

Since LEA proteins are highly hydrophilic and are synthesized in response to water stress, their involvement in the protection of cells against dehydration stress has been postulated (Galau *et al.*, 1986). This particularly concerns roles in the sequestration of ions to reduce the effective ionic strength and in the replacement of the hydrogen bonding function of water (Dure *et al.*, 1989; Dure, 1993). A similar role has been proposed for soluble carbohydrates (Crowe *et al.*, 1997a), possibly in conjunction with the formation of a glassy

state at low water content (Williams and Leopold, 1989; Buitink *et al.*, 1996). Mature seeds and pollen contain significant quantities of soluble non-reducing sugars. Typically, sucrose together with raffinose or stachyose occur in seeds (Amuti and Pollard, 1977; Koster and Leopold, 1988; Horbowicz and Obendorf, 1994), whereas sucrose is the major soluble carbohydrate in pollen (Hoekstra *et al.*, 1992).

For the LEA proteins to accomplish such a general role, it would be necessary to be present in substantial quantities. Northern blotting to determine the presence of specific mRNA transcripts and western blotting to determine the presence of specific proteins give little information on the relative abundance of the proteins involved. We have therefore adopted the approach of purifying and characterizing the most prevalent protein in the 80°C heat-soluble fraction of a tissue. Utilising this approach we have identified the protein in this fraction from pea seed axes to be a LEA group I protein (Russouw *et al.*, 1995) and in that from yeast to be the LEA-like protein HSP 12 (Mtwisha *et al.*, 1998). From their amino acid sequences, it has been suggested that some classes of LEA proteins exist as random coil structures and others as amphipathic α-helical structures (Dure *et al.*, 1989). Although NMR spectroscopy has shown that isolated LEA proteins exist as random coil structures in solution (Lisse *et al.*, 1996), circular dichroism spectroscopy has indicated that the structure of these proteins is dependent on the ionic strength of the solution (Russouw *et al.*, 1997). No information is available on the structure of these proteins in the dry state.

FTIR permits assessment of protein secondary structure in the dry state. The amide-I band profile, the C=O stretching vibration located between 1600 and 1700 cm^{-1}, can reveal information on the relative contributions of α-helix, β-sheet and turn structures (Susi *et al.*, 1967, Byler and Susi, 1986; Surewicz and Mantsch, 1988).

In the present paper, we report on the isolation, purification, characterization and databank homology of the major heat-soluble protein in *T. latifolia* pollen. The secondary structure of the protein both in the hydrated state and after drying, also in the presence of sucrose was investigated, using FTIR.

In the light of the effect of the protein on the molecular structure of the sucrose glass, the possible role of the protein in desiccation tolerance is discussed.

Materials and methods

Plant material

Mature male inflorescences of *Typha latifolia* L. were collected in 1997 from field populations in The Netherlands and allowed to shed their pollen in the laboratory. Pollen was cleaned by sieving through a fine copper mesh, allowed to dry in dry air until the water content reached 5 to 7 % on a fresh weight basis, bottled, and stored at -20°C until use (Hoekstra *et al.*, 1991).

Protein extraction and purification

Five g pollen was ball-milled for 2.5 minutes in 50 mM NaCl, 10 mM Tris-HCl pH 7.4. The ball-mill was cooled with CO_2 gas and operated for 15 s bursts at 45 s intervals (total cycle time of 60 s) to ensure that the temperature remained below 5°C. The homogenate was centrifuged at 15 000 g for 10 min after which the supernatant was incubated for 30 min at 80°C. Heat-coagulated protein was removed by centrifugation as above. The supernatant was adjusted to pH 2 with HCl and loaded onto a Sephadex G50 column equilibrated with 20 mM HCl. Protein, eluted using this same buffer, was pooled and lyophilized before further fractionation by HPLC. Initial HPLC purification was carried out using a C18 Vydac column in 0.1 % heptafluorobutyric acid (HFBA); a 0-70 % gradient of acetonitrile in 0.1 % HFBA was used as the eluent. Protein fractions of interest were further purified on a C18 Jupiter column in 0.1 % trifluoroacetic acid (TFA) using a 28 - 42 % gradient of acetonitrile in 0.1 % TFA as the eluent.

Protein characterization

Cyanogen bromide (CNBr) cleavage was carried at room temperature in 0.1 M TFA under nitrogen. The resultant peptides were separated by HPLC using a C18 Jupiter column in 0.1 % TFA; a 14 - 49 % gradient of acetonitrile in 0.1 % TFA was used as the eluent. Peptide sequencing by Edman degradation

was carried out using a gas phase sequencer constructed as outlined by Hewick *et al.* (1981) and modified as described by Brandt *et al.* (1984). The converted phenylthiohydantion amino acids were identified by an isocratic on-line HPLC system using a C18 column as described by Lottspeich (1985). Amino acid analysis was carried out as described by Lottspeich (1985).

SDS-PAGE on 20 % gels containing 0.125 % N,N'-methylene bisacrylamide was carried out as described by Laemmli (1970) or as described by Schagger and von Jago (1987). 2-mercaptoethanol was routinely added to the sample application buffer.

FTIR

Dry protein films were prepared by slow or rapid air-drying of a droplet (10 µl) of protein solution (10 mg/ml water) on circular (2 x 13 mm) CaF_2 infrared windows. Protein samples in D_2O were obtained by dissolving an aliquot of lyophilized material in D_2O. Dry sucrose or protein/sucrose films were prepared by air-drying of a droplet as described above. Sucrose was obtained from Pfahnstiel (Waukegan, IL, USA). Rapid drying was carried out at 25°C at 3 % relative humidity generated by dried compressed air. The protein films lost most of their water within 5 min, but the samples were left under these conditions for 3 h. Slow drying was carried out for 4 h at 25°C at 51 % relative humidity generated by a saturated $Ca(NO_3)_2$ solution, after which the samples were air-dried for another 3 h at 25°C and 3 % relative humidity.

IR spectra were recorded on a Perkin-Elmer 1725 Fourier transform IR-spectrometer (Perkin-Elmer, Beaconsfield, Buckinghamshire, UK) equipped with a liquid nitrogen-cooled mercury/cadmium/telluride detector and a Perkin-Elmer microscope interfaced to a personal computer as described previously (Wolkers and Hoekstra, 1995). Each sample was hermetically sealed between two IR-windows using a rubber O-ring, and mounted into a temperature-controlled brass cell that was cooled by a liquid nitrogen source. The temperature was regulated by a computer-controlled device that activated a liquid nitrogen pump, in conjunction with a power supply for heating the cell. The temperature of the sample was recorded separately using two Pt-100

elements that were located very close to the sample windows. Spectra were recorded every minute at temperature increments of 1.5°C/min. The optical bench was purged with dry CO_2-free air (Balston; Maidstone, Kent, UK) at a flow rate of 25 l/min. The acquisition parameters were: 4 cm^{-1} resolution, 32 coadded interferograms, 3500-900 cm^{-1} wavenumber range. Spectral analysis and display were carried out using the Infrared Data Manager Analytical Software, version 3.5 (Perkin-Elmer). For protein studies, the spectral region between 1800 and 1500 cm^{-1} was selected. This region contains the amide-I and amide-II absorption bands of the peptide backbone. Curve fitting of the original absorbance spectra was performed with Peakfit (Jandel software) of the original absorbance spectra between 1800 and 1500 cm^{-1} assuming Pearson band shapes.

The melting of glasses during heating of the sample at 1.5°C/min was monitored by observing the position of the band around 3300 cm^{-1} (OH-stretching vibration). The spectral region between 3500 and 3000 cm^{-1} was selected and normalised to unity. The band position was calculated as the average of the spectral positions at 80 % of the total peak height. The glass transition temperatures were determined by linear regression of the νOH *vs*

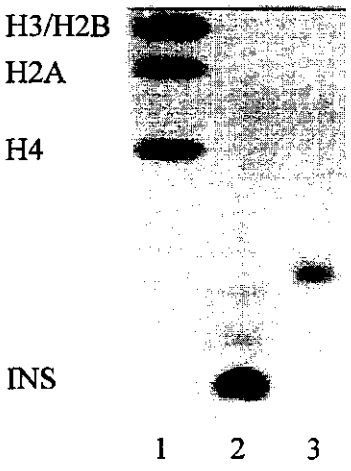

Figure 1. Tricine-SDS-PAGE of the purified pollen protein (lane 3). The standards used were chicken erythrocyte core histones (lane 1) and insulin (lane 2). Approximate molecular sizes in kDa are: histone H3: 15; histones H2A and H2B: 12.5; histone H4: 10; insulin:6.

temperature plot in both the liquid and the solid-like regions of the plot. The point of intersection of these two regression lines is defined as T_g (Wolkers *et al.*, 1998b). The linear regressions of νOH as a function of the temperature is defined as the wavenumber-temperature-coefficient, WTC.

Results

Protein purification and characterization.

Total soluble proteins were extracted from *T. latifolia* pollen using Tris-buffer. A number of proteins of molecular size between 300 and 5 kDa were extracted by this procedure. Most of these proteins were insoluble at high temperature and were not present after incubation of this extract for 30 mins at 80°C. However, a low molecular weight protein was relatively abundant after such treatment.

In order to further characterize this protein, it was purified to homogeneity from the heat soluble fraction by Sephadex G 50 chromatography and reversed phase HPLC. The material eluted from the C18 reversed phase Jupiter column was electrophoresed on SDS-PAGE where it migrated as a

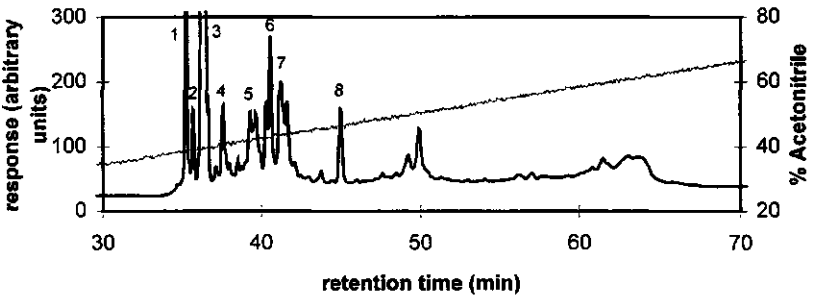

Figure 2. HPLC profile of the CNBr cleaved LEA-like protein. The cleaved products (excess amounts of cyanogen bromide, 1 mM TFA for 24 hour at 20°C) were dissolved in 4 M urea plus 0.1 % TFA, centrifuged and applied to a C18 Jupiter column in 0.1 % trifluoroacetic acid. A 0-70 % gradient of acetonitrile in 0.1 % trifluoroactetic acid was used as the eluent. Peptides 1, 4, 5, 6 and 7 were lyophilized and gas-phase sequenced.

single band (Fig. 1). The molecular size of this protein, that migrated between chicken erythrocyte histone H4 and insulin was estimated to be approximately 9 kDa.

This protein was hydrolysed and the amino acid composition determined (Table 1). The protein was very rich in hydrophilic amino acids, notably glutamic acid/glutamine which represented almost 20 % of the composition of this protein. The small amino acids, alanine and glycine were also relatively abundant, each representing approximately 10 % of the composition. No tryptophan or cysteine residues were detected. Although the individual amino acid composition of this protein was very different from the pea seed p11 LEA group I protein (Russouw *et al.*, 1995) and the yeast LEA-like HSP 12 protein (Mtwisha *et al.*, 1998), the overall compositions of these three proteins were remarkably alike if the compositions were compared after adding together the moles % of similar amino acids (Table 2). The high hydrophilic amino acid content of 62.3 % was most likely responsible for the solubility of the pollen protein at 80°C.

The pure protein was subjected to gas phase sequencing. No sequence was obtained indicating that the protein, in common with the pea seed p11

Table 1. Amino acid content (moles %) of the purified heat soluble pollen protein.

Residue	Moles%
Glx(Z)	19.8
Ala(A)	11.8
Gly(G)	11.6
Asx(B)	10.4
Lys(K)	9.8
His(H)	9.3
Thr(T)	6.4
Met(M)	6.3
Ser(S)	6.2
Val(V)	4.8
Phe(F)	1.3
Leu(L)	0.8
Ile(I)	0.7
Arg(R)	0.4
Tyr(Y)	0.3

Table 2. Comparison of the amino acid content (moles %) of the purified heat soluble pollen protein (A) with that from the pea seed p11 protein (B) and the yeast HSP 12 protein (C) after adding together similar residues.

Residue type	Residues grouped	A	B	C
small	A+G	23.4	24	23.8
Hydroxyl	S+T	12.6	9.9	10.7
Acidic + Amide	Z+B	30.2	29.4	33.4
Basic	H+K+R	19.5	15.1	18.9
Hydrophilic	S+T+Z+B+H+K+R	62.3	54.4	63.0
Non-Polar	I+L+M+V	12.6	11.5	12.5
Aromatic	F+W+Y	1.6	3.6	4.6

protein and the yeast HSP 12 protein, was blocked at the N-terminus. The protein was therefore subjected to CNBr hydrolysis to cleave the protein after methionine residues. HPLC of the CNBr digest resulted in a number of peptide fractions eluting from the C18 column (Fig. 2). Edman degradation was carried out on the major peptide fragments in order to determine their primary sequences. Peptides with sequences AQGASDAVKNA and RKKAEETAQQAQVK were found to be present in peaks 6 and 7, respectively. Other peaks eluted from the HPLC column either gave similar sequences probably resulting from incomplete protein cleavage or could not be sequenced, suggesting that these were derived from the N-terminus of the pollen protein. A search was carried out for homology between these determined sequences and protein sequences present in the Databank. The peptide AQGASDAVKNA had considerable homology with LEA proteins; the best alignment of this peptide was with a D-7 LEA protein (LE7_GOSHI) from cotton and the third best alignment was with LE76_brana from rape. The other peptide RKKAEETAQQAQVK only showed homology with LE76_brana, which was the fifth best alignment found. These results therefore suggest that the pollen protein isolated was a member of the LEA group III family of proteins.

Protein secondary structure in the hydrated and dry states.

To investigate if the purified LEA protein contains specific structures that can be related to their function, the protein secondary structure was studied in the hydrated and in the dry state.

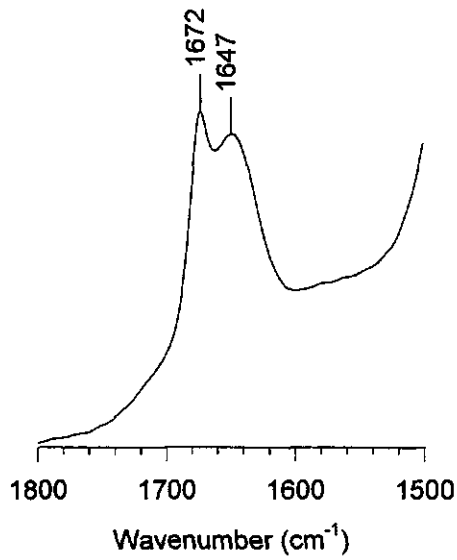

Figure 3. IR absorption spectrum in the amide-I region of the LEA-like protein in D_2O.

The IR spectrum of the purified protein was recorded in D_2O to avoid interference of the H-O-H scissoring vibration with the amide-I region between 1700 and 1600 cm^{-1}. Two bands at 1672 and 1647 cm^{-1} were visible in the amide-I region of the spectrum (Fig. 3). The broad band with an absorption maximum at 1647 cm^{-1} was assigned to random coil structures and the sharper band with an absorption maximum at 1672 cm^{-1} to turn structures (for the application of IR spectroscopy to protein secondary structure see Surewicz and Mantsch, 1988; Surewicz *et al.*, 1993). Curve fitting of the absorbance spectra to determine the relative contributions of random coil and turn structures to the overall spectrum revealed that turn structures represented approximately 25 % of the structure, with the remaining 75 % being in a random coil conformation. The absence of an amide-II band around 1550 cm^{-1} indicated that almost all the amide protons (N-H) were exchanged for deuterium, a characteristic of unordered structures (Haris *et al.*, 1989).

In order to determine whether the rate of drying affected the conformation of the dry protein, droplets of protein solution in H_2O were subjected to either slow or rapid air-drying before FTIR analysis of the dry protein film. Two major bands at 1657 cm^{-1} and 1625 cm^{-1} and a shoulder at

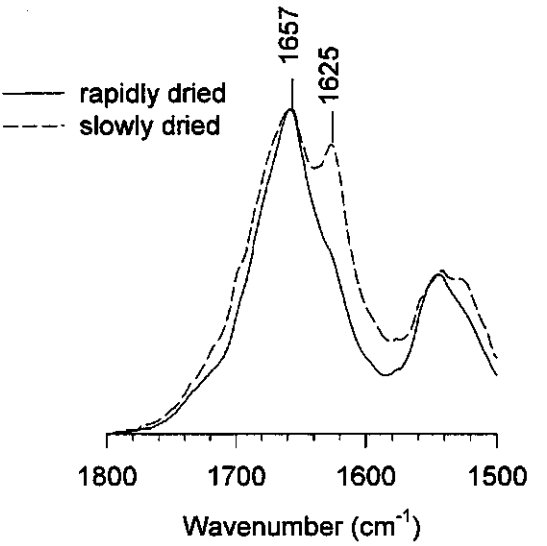

Figure 4. IR absorption spectra of rapidly and slowly dried LEA-like protein. Spectra were normalized according to the amide I band.

1695 cm^{-1} were observed (Fig. 4) in the amide-I band portion of the spectrum of slowly dried protein. The band around 1625 cm^{-1} was assigned to intermolecular β-sheet structures and the band around 1657 cm^{-1} to α-helical structures. (Susi, 1969; Surewicz and Mantsch, 1988; Bandekar, 1992; Haris and Chapman, 1992; Surewicz *et al.*, 1993;). The shoulder at 1695 cm^{-1} is indicative of β-sheet structures. The spectrum of the rapidly dried protein film was substantially different from that of the slowly dried film. The amide-I band region was now dominated by the band at 1657 cm^{-1} suggesting that the conformation of the rapidly dried protein was predominantly α-helical. The characteristic bands for intermolecular β-sheet at 1625 cm^{-1} and 1695 cm^{-1} were far less pronounced.

To determine whether slow or rapid drying resulted in an irreversible conformational change in the protein, the protein film after slow drying was rehydrated, rapidly air-dried and the spectrum determined. It was found (not shown) that the spectrum was essentially identical to that previously found after rapid drying. The characteristic β-sheet bands present in the spectrum of the slowly dried sample disappeared after rehydration and subsequent rapid drying. Similarly, if the protein film after rapid drying was rehydrated and slowly air-

dried, the spectrum was essentially identical to that previously found after slow drying. These results showed that the structure of the protein in the dry state is dependent on the rate of drying and that the conformations adopted are not fixed.

Structure of the protein embedded in a sucrose glass.

Sucrose is present in significant quantities in *T. latifolia* pollen where it represents 23 % of the dry weight (Hoekstra *et al.*, 1992). To investigate the effect of sucrose on the conformation of the dried pollen protein, the structure of the protein embedded in a dry sucrose matrix was also studied. Both slow and rapid drying conformations were investigated after air-drying a droplet of a protein-sucrose solution.

After slow drying in the presence of sucrose, the α-helical band around 1659 cm^{-1} was the dominant band in the amide-I region. The absorbance around 1625 cm^{-1} was even lower than after rapid drying of the protein in the absence of sucrose (compare Figs. 4 and 5), indicating that sucrose prevented the formation of intermolecular β-sheet structures. Rapid drying of the protein in the presence of sucrose gave a similar amide-I band profile as slow drying

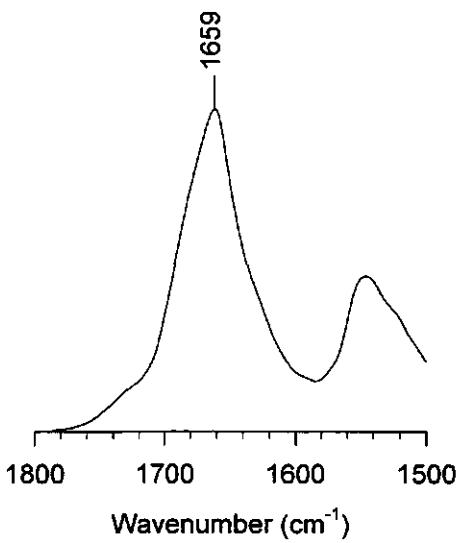

Figure 5. IR absorption spectrum of air-dried LEA-like protein in the presence of sucrose (1:1 mass ratio).

(data not shown).

Effect of the protein on the molecular structure of a sucrose glass

Since the presence of sucrose during drying effected the conformation of the pollen protein, it is possible that the presence of the protein effected the properties of the glassy state assumed by sucrose at low water content. The glassy behavior of dried sugar/protein mixtures was studied by determination of the temperature-dependent shifts in the maximum wavenumber of the OH-stretching vibration in the 3500 - 3000 cm^{-1} region of the IR spectrum.

The OH-band arises predominantly from the sucrose rather than from the protein component of such a mixture. As reported previously (Wolkers *et al.*, 1998b), T_g, the temperature of the glass to liquid transition, can be determined from such a plot by determining the intersection point of linear regressions in the liquid and glassy states. The WTC values (cm^{-1}/°C) that can be derived from

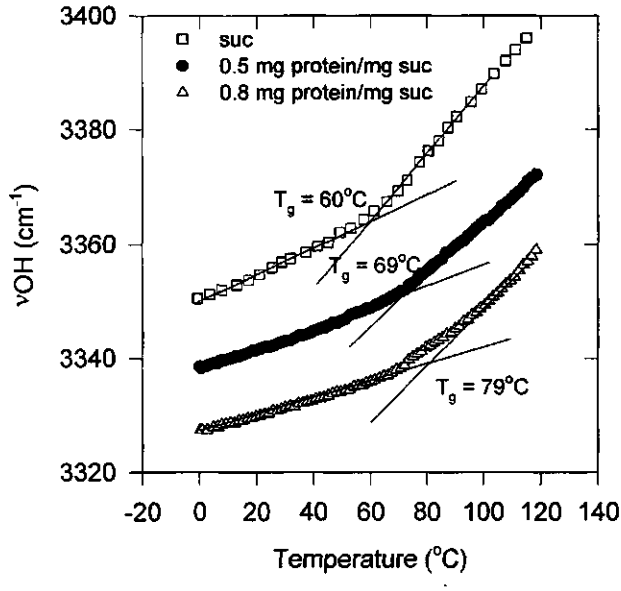

Figure 6. Wavenumber *vs* temperature plot (FTIR) of the OH-stretching vibration band of dry sucrose and sucrose/LEA-like protein glasses. The glass transition temperatures (T_g) were determined from the intersections between the regression line in the liquid and that in the glassy state.

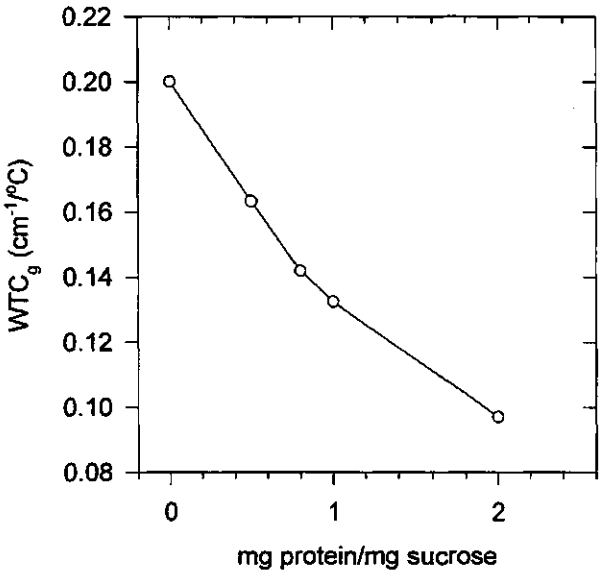

Figure 7. Plot of the WTC values in the glassy state (WTC_g see Fig. 6) as a function of the amount of added LEA-like protein in the sucrose matrix.

such plots give information on the molecular packing density of the glassy state.

Such a plot of the maximum wavenumber of the OH-stretching vibration *vs* temperature is shown in Figure 6 for sucrose alone and together with the pollen protein at concentrations of 0.5 mg and 0.8 mg/mg sucrose. Analysis of the data for sucrose alone gave a value of T_g of 60°C; the WTC in the glassy state (WTC_g) was calculated to be 0.20 cm^{-1}/°C. A clear glass transition was still observed when the pollen protein was added to the sucrose solution at concentrations up to 2 mgs protein per mg sucrose, indicating that the protein was embedded together with the sucrose in a glassy matrix. The T_g was found to increase to 69°C in the presence of 0.5 mg protein per mg sucrose and to 79°C when the protein concentration was further increased to 0.8 mg protein per mg sucrose (Fig. 6). The WTC_gs were calculated to be 0.16 and 0.14 cm^{-1}/°C respectively.

Plotting the WTC_g versus the amount of protein added per mg sucrose (Fig. 7) showed an approximately linear negative relationship up to 1 mg

protein per mg sucrose. Increasing the protein concentration above this value resulted in lesser decreases in the value of the WTC_g up to 2 mg protein per mg sucrose. No further decrease in the WTC_g was observed at protein concentrations higher than the 2 mg/mg.

Discussion

In the present study, we purified a heat stable 9 kDa protein from *T. latifolia* pollen and characterized it with respect to composition and sequence of its amino acids and to protein secondary structure. The protein was highly hydrophilic (62% of its amino acids). In particular, glutamic acid/glutamine and aspartic acid/asparagine comprised most of the residues present, together with glycine and alanine. The high content of hydrophilic amino acids is probably linked with the excellent solubility of the protein at 80°C. Both its high temperature solubility and its amino acid composition already suggest that the protein is a LEA protein (Ceccardi *et al.*, 1994; Russouw *et al.*, 1995,1997; Wang *et al.*, 1996). Sequence alignment of peptide fragments of the protein with sequences of proteins from the Databank revealed homology with two D-7 LEA proteins. The typical LEA characteristics and the alignment results suggest that the protein from the pollen can be classified as a D-7 LEA-like protein. The D-7 family of LEA proteins is characterized by a tandemly-repeating 11-mer (Dure *et al.*, 1989; Dure, 1993). There is a large variation in size among members of this protein family, which can be attributed to the number of repeats of the 11-mer.

We show here that in solution the protein adopts an entirely unordered conformation. In the dry state, the structure turned out to be dependent on the drying rate and the presence of stabilisers (sucrose). Upon slow drying in the absence of sucrose, the protein transformed into both α-helical and intermolecular extended β-sheet structures, whereas upon rapid drying, the protein predominantly adopted an α-helical conformation. The transition of the protein from the unordered conformation in solution to highly ordered (α-helical and β-sheet) in the dry state can be attributed to the loss of hydrogen bonding of water to the protein (Prestrelski *et al.*, 1993). On drying, hydrogen bonds with

water are substituted for inter- and intra-molecular hydrogen bonds in and between proteins, which may lead to the observed drastic dehydration-induced conformational transitions. However, such protein clustering is fully reversible.

The structure of LEA proteins purified from pea axes was found also to be predominantly unordered in solution, but to depend on salt concentration. The α-helical content increased from 6% in 0.1 M NaCl to 15% in 2 M NaCl (Russouw *et al.*, 1995). NMR spectroscopy indicated that a dehydrin-related protein from the resurrection plant, *Craterostigma plantagineum*, was entirely unordered in solution (Lisse *et al.*, 1996). Here, we present for the first time experimental data on the structure of a LEA protein in the dry state. The drastic dehydration-induced conformational transition of this protein suggests that the structure is very much dependent on the environment.

When the protein was dried in the presence of sucrose, the formation of extended β-sheet structures could be prevented, and the protein almost entirely adopted an α-helical conformation. The effect of sugars in preventing protein aggregation has been described previously, also using FTIR (Prestrelski *et al.*, 1993; Dong *et al.*, 1995). Both the ability of sugars to interact with proteins through hydrogen bonding and the glass forming properties of sugars may play a role in the adopted structure in the dry state (Carpenter and Crowe, 1989; Chapter 9 and references therein). In a previous study we have analysed the overall protein secondary structures in dry *T. latifolia* pollen, and found that α-helical structures comprise ca. 40% of the total and that intermolecular β-sheet structures were absent (Wolkers and Hoekstra, 1995). We suggest that it is very likely that the LEA protein *in situ* in the dry pollen grain exists as an α-helix, similarly as in the sucrose glass of Figure 5, the more so as sucrose is abundantly present (23% on a DW basis in *T. latifolia* pollen; Hoekstra *et al.*, 1992) and the cytoplasm exists in a glassy state (Buitink *et al.*, 1996).

Also in maize embryos (Wolkers *et al.*, 1998a) and *Daucus* somatic embryos (Chapter 8) we have found major contributions of α-helical structures to the overall protein secondary structure. The proportion of these α-helical structures in the above mentioned anhydrobiotic organisms increases during the acquisition of desiccation tolerance. Generally, the synthesis of the LEA

proteins during embryo maturation coincides with the acquisition of desiccation tolerance (Blackman *et al.*, 1995; compare Mao *et al.*, 1995 and Wolkers *et al.*, 1998a). In the light of our data on the structure of the purified LEA protein in a sucrose glass, we suggest that the observed increase in proportion of α-helical structures during the acquisition of desiccation tolerance in maize embryos and *Daucus* somatic embryos can be attributed, at least partly, to newly synthesized LEA proteins.

An intriguing question is whether the structure of LEA proteins can somehow be related to their function. Based on computer predictions, it has been suggested that several LEAs exist as α-helical structures (Dure *et al.*, 1989; Dure, 1993). For LEA proteins belonging to the D-7 group the 11-mer repeat unit has been predicted to exist as an amphiphilic α-helix, having a hydrophobic and a hydrophilic side. On the basis of this property, Dure (1993) suggested that these proteins can play a role in binding phosphate- and iron-ions in the cytoplasm. However, our results put such suggested structure-function relationship, solely based on computer predictions, in a different perspective, because of the considerable influence of the environment on the structure of these proteins.

Taking into consideration that many anhydrobiotic organisms have accumulation of sugars and LEA-like proteins in common (Close, 1996; Crowe *et al.*, 1997a), we also studied the effect of the LEA protein on the molecular structure of a sucrose glass. On the one hand, sucrose plays a crucial role in the adopted structure of the dry protein, but on the other hand, proteins may also have an effect on the physical properties of the glass, which could shed new light on the role of LEA proteins in desiccation tolerance. While most other studies have focused on the protective effect of either sugars or LEA proteins, we considered the interactive capability of these compounds to form stable glasses.

We applied a novel IR spectroscopy method, previously developed to study carbohydrate and cytoplasmic glasses in anhydrobiotic organisms (Wolkers *et al.*, 1998b), to study the effect of LEA proteins on sucrose glasses. By comparison with a pure sucrose glass, the presence of the pollen protein

increased both the T_g and the average strength of hydrogen bonding. The clear breaks in Figure 6 illustrated that, even when equal masses of sucrose and protein were present, the characteristic glassy behavior of the latter was still observed. This suggests that the protein acted synergistically with the sucrose in the formation of the glassy matrix.

We may now address the question as to how far the 9 kDa D7 LEA-like protein is unique in its ability to contribute to desiccation tolerance. LEA proteins are also produced under stress conditions that do not lead to full dehydration (Michel *et al.*, 1994). A possible role for this protein in ion sequestering has been proposed, in which the α-helical structure is pivotal (Dure, 1993). Earlier studies have shown that high ion concentrations lead to such α-helical structures (Russouw *et al.*, 1995). However, under the still hydrated conditions, the cytoplasm cannot assume a glassy state. We show here that during drying the protein adopts almost entirely an α-helical structure, most likely before the cytoplasm turns into a glass. In addition, we demonstrate that the protein interacts with sucrose to form a stable glass. While the conformational change from unordered structure into α-helical structure during dehydration may be fairly unique, the interaction with sugars may be more general. We derive this from studies on protein conformational transitions with drying on the one hand (Prestrelski *et al.*, 1993; Allison *et al.*, 1996), and from studies on the dehydration-induced interactions of proteins and polypeptides with soluble carbohydrates, on the other hand (Bell and Hageman, 1996; Chapter 9). The array of properties which are expressed at different stages of dehydration may render the LEA protein unique.

We conclude that LEA proteins might play a role together with carbohydrates in the formation of a tight hydrogen bonded network in dehydrated pollen and, possibly, in other anhydrobiotic organisms. The role of LEA proteins would thus be a structural one in that they might serve as anchors in a tight molecular network to provide stability to macromolecular and cellular structures in the cytoplasm of anhydrobiotes in the dry state. In the highly viscous or vitreous cytoplasmic matrix, this network would inhibit fusion of cellular membranes (Sun *et al.*, 1996; Crowe *et al.*, 1997b), denaturation of

cytoplasmic proteins (Crowe *et al.*, 1997a), and the effects of deteriorative free radical reactions (Leopold *et al.*, 1994).

Acknowledgements

This project was financially supported by the Life Sciences Foundation, which is subsidized by the Netherlands Organization for Scientific Research, the South African Foundation for Research Development, the University of Cape Town research fund as well as South African Breweries.

References

Allison, S.D., Dong, A., Carpenter, J.F. (1996) Counteracting effects of thiocyanate and sucrose on chymotrypsinogen secondary structure and aggregation during freezing, drying, and rehydration. *Biophys. J.* **71,** 2022-2032.

Amuti, K.S., Pollard, C.J. (1977) Soluble carbohydrates of dry and developing seeds. *Phytochemistry* **16,** 529-532.

Bandekar, J. (1992) Amide modes and protein conformation. *Biochim. Biophys. Acta* **1120,** 123-143.

Bedinger, P.A., Edgerton, M.D. (1990) Developmental staging of maize microspores reveals a transition in developing microspore proteins. *Plant Physiol.* **92,** 474-479.

Bell, L.N., Hageman, M.J. (1996) Glass transition explanation for the effect of polyhydroxy compounds on protein denaturation in dehydrated solids. *J. Food Sci.* **61,** 372-378.

Blackman, S.A., Obendorf, R.L., Leopold, A.C. (1995) Desiccation tolerance in developing soybean seeds: the role of stress proteins. *Physiol. Plant.* **93,** 630-638.

Brandt, W.F., Alk, H., Chauhan, M., von Holt, C. (1984) A simple modification converts the spinning cup sequencer into a vapour phase sequencer. *FEBS Lett.* **174,** 228-232.

Buitink, J., Walters-Vertucci, C., Hoekstra, F.A., Leprince, O. (1996) Calorimetric properties of dehydrating pollen. Analysis of a desiccation-tolerant and an intolerant species. *Plant Physiol.* **111,** 235-242.

Byler, D.M., Susi, H. (1986) Examination of the secondary structure of proteins by deconvolved FTIR spectra. *Biopolymers* **25,** 469-487.

Carpenter, J.F., Crowe, J.H. (1989) An infrared spectroscopic study of the interactions of carbohydrates with dried proteins. *Biochemistry* **28,** 3916-3922.

Ceccardi, T.L., Meyer, N.C., Close, T.J. (1994) Purification of a maize dehydrin. *Protein Expression and Purification* **5,** 266-269.

Chibi, F., Angosto, T., Matilla, A. (1995) Variations of the patterns of abscisic acid and proline during maturation of *Nicotiana tabacum* pollen grains. *J. Plant Physiol.* **147,** 355-358.

Close, T.J. (1996) Dehydrins: Emergence of a biochemical role of a family of plant dehydration proteins. *Physiol. Plant.* **97,** 795-803.

Crowe, J.H., Crowe, L.M., Carpenter, J.F., Prestrelski, S.J., Hoekstra, F.A. (1997a) Anhydrobiosis: cellular adaptations to extreme dehydration. *In:* Dantzler, W.H. (ed.) Handbook of

Physiology section 13, Comparative Physiology, Vol II, Oxford University Press, Oxford, UK, pp. 1445-1477.

Crowe, J.H., Oliver, A.E., Hoekstra, F.A., Crowe, L.M. (1997b) Stabilization of dry membranes by mixtures of hydroxyethyl starch and glucose: The role of vitrification. *Cryobiology* **35,** 20-30.

Del Mar Parra, M., del Pozo, O., Luna, R., Godoy, J.A., Pintor-Toro, J.A. (1996) Structure of the dehydrin tas14 gene of tomato and its developmental and environmental regulation in transgenic tobacco. *Plant Mol. Biol.* **32,** 453-460.

Detchepare, S., Heizmann, P., Dumas, C. (1989) Changes in protein patterns and protein synthesis during anther development in *Brassica oleracea*. *J. Plant Physiol.* **135,** 129-139.

Dong, A., Prestrelski, S.J., Allison, S.D., Carpenter, J.F. (1995) Infrared spectroscopic studies of lyophilization- and temperature induced protein aggregation. *J. Pharm. Sci.* **84**: 415-424.

Dure, III L. (1993) A repeating 11-mer amino acid motif and plant desiccation. *Plant J.* **3,** 363-369.

Dure, III L., Crouch, M., Harada, J., Ho, T.H.D., Mundy, J., Quatrano, R., Thomas, T., Sung, Z.R. (1989) Common amino acid sequence domains among the LEA proteins of higher plants. *Plant Mol. Biol.* **12,** 475-486.

Espelund, M., Saeboe-Larssen, S., Hughes, D.W., Galau, G.A., Larsen, F., Jakobsen, K.S. (1992) Late embryogenesis-abundant genes encoding proteins with different numbers of hydrophilic repeats are regulated differentially by abscisic acid and osmotic stress. *Plant J.* **2,** 241-252.

Galau, G.A., Hughes, D.W., Dure, III L. (1986) Abscisic acid induction of cloned cotton late embryogenesis-abundant (Lea) mRNAs. *Plant Mol. Biol.* **7,** 155-170.

Haris, P.I., Chapman, D. (1992) Does Fourier-transform infrared spectroscopy provide useful information on protein secondary structures. *Trends Biochem. Sci.* **17,** 328-333.

Haris, P.I., Coke, M., Chapman, D. (1989) Fourier transform infrared spectroscopic investigation of rhodopsin structure and its comparison with bacteriorhodopsin. *Biochim. Biophys. Acta* **995,** 160-167.

Hewick, R.M., Hunkapiller, M.W., Hood, L.E., Dreyer, W.J. (1981) A gas-liquid solid phase peptide and proteinsequencer. *J. Biol. Chem.* **256,** 7990-7997.

Hoekstra, F.A. (1986) Water content in relation to stress in pollen. In Leopold, A.C. (ed.) Membranes, Metabolism and dry Organisms, Cornell University Press, Ithaca, NY, pp. 102-122.

Hoekstra, F.A., Crowe, J.H., Crowe, L.M. (1991) Effect of sucrose on phase behaviour of membranes in intact pollen of *Typha latifolia L.*, as measured with Fourier transform infrared spectroscopy. Plant Physiol. **97,** 1073-1079.

Hoekstra, F.A., Crowe, J.H., Crowe, L.M., Van Roekel, T., Vermeer, E. (1992) Do phospholipids and sucrose determine membrane phase transitions in dehydrating pollen species? *Plant Cell Environ.* **15,** 601-606.

Horbowicz, M., Obendorf, R.L. (1994) Seed desiccation tolerance and storability: dependence on flatulence-producing oligosaccharides and cyclitols - review and survey. *Seed Sci. Res.* **4,** 385-405.

Koster, K.L., Leopold, A.C. (1988) Sugars and desiccation tolerance in seeds. *Plant Physiol.* **88,** 829-832.

Laemmli, U.K. (1970) Cleavage of structural proteins during the assembly of the head of Bacteriophage T4. *Nature* **227,** 680-685.

Leopold, A.C., Sun, W.Q., Bernal-Lugo, I. (1994) The glassy state in seeds: analysis and function. *Seed Sci. Res.* **4,** 267-274.

Lisse, T., Bartels, D., Kalbitzer, H.R., Jaenicke, R. (1996) The recombinant dehydrin-like desiccation stress protein from the resurrection plant *Craterostigma plantagineum* displays no defined three-dimensional structure in its native state. *Biol. Chem.* **377,** 555-561.

Lottspeich, F. (1985) Micro-scale isocratic separation of the phenylthiohydantion amino acid derivatives. *J. of Chromatogr.* **326,** 321-327.

Mao, Z.Y., Paiva, R., Kriz, A.L., Juvik, J.A. (1995) Dehydrin gene expression in normal and viviparous embryos of Zea mays during seed development and germination. *Plant Physiol. Biochem.* **33,** 649-653.

Michel, D., Furini, A., Salamini, F., Bartels, D. (1994) Structure and regulation of an ABA- and desiccation-responsive gene from the resurrection plant *Craterostigma plantagineum. Plant Mol. Biol.* **24,** 549-560.

Mtwisha, L., Brandt, W.F., McCready, S. & Lindsey, G.G. (1998). HSP 12 is a LEA-like protein in yeast (*Saccharomyces cerevisiae*). *Plant Mol. Biol.* In press.

Prestrelski, S.J., Tedeschi, N., Arakawa, T., Carpenter, J.F. (1993) Dehydration-induced conformational transitions in protein and their inhibition by stabilizers. *Biophys. J.* **65,** 661-671.

Rouse, D.T., Marotta, R., Parish, R.W. (1996) Promoter and expression studies on an *Arabidopsis thaliana* dehydrin gene. *FEBS Lett.* **381,** 252-256.

Russouw, P.S., Farrant, J., Brandt, W., Lindsey, G.G. (1997) The most prevalent protein in a heat-treated extract of pea (*Pisum sativum*) embryos is an LEA group I protein; its conformation is not affected by exposure to high temperature. *Seed Sci. Res.* **7,** 117-123.

Russouw, P.S., Farrant, J., Brandt, W., Maeder, D., Lindsey, G.G. (1995) Isolation and characterization of a heat-soluble protein from pea (*Pisum sativum*) embryos. *Seed Sci. Res.* **5,** 137-144.

Schagger, H., von Jago, G. (1987) Tricine-sodium dodecylsulphate-polyacrylamide gel electrophoresis for the separation of proteins in the range 1 to 100 kDa. *Anal. Biochem.* **166,** 368-397.

Sun, W.Q., Leopold, A.C., Crowe, L.M., Crowe, J.H. (1996) Stability of dry liposomes in sugar glasses. *Biophys. J.* **70,** 1769-1776.

Surewicz, W.K., Mantsch, H.H. (1988) New insight into protein secondary structure from resolution-enhanced infrared spectra. *Biochim. Biophys. Acta* **952,** 115-130.

Surewicz, W.K., Mantsch, H.H., Chapman, D. (1993) Determination of protein secondary structure by Fourier transform infrared spectroscopy: a critical assessment. *Biochemistry* **32,** 389-394.

Susi, H. (1969) Structure and stability of biological macromolecules. *In:* Biological Macromolecules, Vol 2, Marcel Dekker, New York, pp. 525-663.

Susi, H., Timasheff, S.N., Stevens, L. (1967) Infrared spectra and protein conformations in aqueous solutions. I. The amide I band in H_2O and D_2O solutions. *J. Biol. Chem.* **242,** 5460-5466.

Wang, C.S., Wu, T.D., Chung, C.K.W., Lord, E.M. (1996) Two classes of pollen-specific, heat-stable proteins in *Lilium longiflorum. Physiol. Plant.* **97,** 643-650.

Williams, R.J., Leopold, A.C. (1989) The glassy state in corn embryos. *Plant Physiol.* **89,** 977-981.

Wolkers, W.F., Bochicchio, A., Selvaggi, G., Hoekstra, F.A. (1998a) Fourier transform infrared microspectroscopy detects changes in protein secondary structure associated with desiccation tolerance in developing maize embryos. *Plant Physiol.* **116,** 1169-1177.

Wolkers, W.F., Hoekstra, F.A. (1995) Aging of dry desiccation-tolerant pollen does not affect protein secondary structure. *Plant Physiol.* **109,** 907-915.

Wolkers, W.F., Oldenhof, H., Alberda, M., Hoekstra, F.A. (1998b) A Fourier transform infrared microspectroscopy study of sugar glasses: Application to anhydrobiotic higher plant cells. *Biochim. Biophys. Acta* **1379,** 83-96.

Yang, Z.H., Barendse, G.W.M., Linskens, H.F. (1985) Abscisic acid in the reproductive organs of *Petunia hybrida* and *Lilium longiflorum*. *Acta Bot. Neerl.* **34,** 73-82.

Chapter 11

General discussion

Dehydration and molecular interactions

Desiccation tolerance can be defined as the capacity of a tissue to resume vital metabolism after severe dehydration and subsequent rehydration. In this work the mechanisms that provide this tolerance of desiccation were studied only in higher plants. However, the underlying principles may also apply to other organisms such as mosses and ferns, bacterial spores, yeasts, nematodes, Tardigrades, and some Crustacea cysts (Crowe *et al.*, 1997).

The main goal of this work was to study the consequences, on the molecular level, of removal of the bulk cellular water from plant cells. This removal causes changes in inter- and intra-molecular interactions, eventually leading to a viscous cytoplasmic matrix and a higher degree of molecular ordering. Upon drying of biomolecules such as proteins and lipids, the loss of hydrogen bonding with water is being compensated by hydrogen bonding with other molecules. This may result in forced intermolecular interactions between molecules that normally would not interact with each other in the presence of bulk water, but will do so upon dehydration. For example, sugars and phospholipids do not interact at high water contents, but in the dry state, sugar-OH groups interact with the polar headgroups of the phospholipids through hydrogen bonding (Crowe *et al.*, 1992; 1997). Molecules of the same type may also interact with one another. For example, in proteins, the loss of hydrogen bonding with water can be compensated by protein-protein interactions. In some cases, these dehydration-induced protein-protein interactions can lead to irreversible conformational changes and to loss of enzyme activity if the proteins have enzymic function. In phospholipids, water loss may lead to the formation of gel phase, being the result of a higher degree of ordering in the acyl chains.

We hypothesize here that in desiccation-tolerant plant cells molecular interactions during drying are controlled in such a way that the loss of hydrogen bonding is compensated by reversible interactions and that a sufficient level of molecular disorder is retained. In contrast, lack of control of such interactions may lead to a high degree of ordering and is characteristic of desiccation-sensitivity. In desiccation-tolerant cells biomolecules and cellular structures are apparently well protected from breakdown.

Assessment of macromolecules in dry anhydrobiotes

A main objective of this work was to study the structure of biomolecules in dried desiccation-tolerant cells. FTIR microspectroscopy is one of the few techniques that can be used to investigate biomolecules in their native environment, irrespective of the hydration state (Crowe *et al.*, 1984). The disadvantage of FTIR in the analysis of a biological tissue is that it is an averaging technique: an IR absorption band reflects the superposition of all molecular vibrations contributing to a specific molecular group vibration. This makes it difficult to unambiguously assign a molecular vibration to specific molecules. However, the advantage of measuring *in situ* outweighs this disadvantage, because it is impossible to inspect with other methods biomolecules such as proteins in a dehydrating cellular environment. Nevertheless, model experiments are necessary to unravel the molecular origin of *in situ* IR bands.

Role of sugars and proteins in desiccation tolerance

Part of the work presented in this thesis concerns an investigation of the physical properties of sugar glasses with the aim to elucidate the molecular interactions that are pivotal to stabilization of the dry cytoplasmic matrix of anhydrobiotes. In the course of this project it was hypothesized that, apart from a sufficient level of disorder, a high molecular packing density of the cytoplasm benefits stability and longevity of desiccation-tolerant cells. Special emphasis was placed on the cooperative effect of proteins and sugars to form stable

glasses, because an important role in desiccation tolerance has been attributed to both sugars and proteins (Crowe *et al.*, 1987).

The two main working hypotheses for the role of sugars in desiccation tolerance are the "water replacement hypothesis" and the "glass formation hypothesis". The water replacement hypothesis suggests that sugars play a role in the protection of cellular and macromolecular structure in anhydrobiotes by replacing the water with respect to hydrogen bonding (Crowe *et al.*, 1992; 1997). The glass formation hypothesis suggests that sugars are involved in the formation of a glassy matrix in the cytoplasm. This glassy matrix results in molecular immobilization, which gives protection to the dry organism. This immobilization may also include toxic components such as free radicals, preventing their migration to sensitive targets and preserving cellular structures of vital importance.

Sugars in pollens and seeds

In pollens of higher plants, sucrose often comprises up to 20% of the dry weight (Hoekstra *et al.*, 1992). In seeds, in addition to sucrose, oligosaccharides occur in substantial quantities. These oligosaccharides accumulate during the later stages of seed development, and monosaccharides disappear (Fischer *et al.*, 1988; Leprince *et al.*, 1990). Oligosaccharides are thought to play a role in cellular stabilization of desiccating and dry cells, because they accumulate in association with the acquisition of desiccation tolerance. However, a quantitative correlation between oligosaccharides and desiccation tolerance has not been clearly established, thus far (Steadman *et al.*, 1996). We also found no clear correlation between oligosaccharide contents and desiccation tolerance in both maize zygotic embryos and carrot somatic embryos (Chapter 5 and 8, respectively). In carrot somatic embryos, the trisaccharide, umbelliferose accumulates in response to slow drying, at the expense of sucrose. However, this trisaccharide appears to be fully exchangeable for sucrose, which depreciates its possible specific role in desiccation tolerance. In maize embryos, raffinose is synthesized during the later stages of seed development, but immature maize embryos lacking

raffinose also are able to survive desiccation (Bochicchio *et al.*, 1994). As an alternative, it was suggested that oligosaccharides are beneficial to survival during long-term storage rather than to desiccation tolerance *per se* (Leopold *et al.*, 1994). The generally better glass forming properties of oligosaccharides in comparison with di- and mono-saccharides, are thought to account for this extended longevity. However, in order to play such a role, substantial quantities should be present in the cytoplasm. The low amounts of oligosaccharides (less than 1 % of the dry weight) being reported here for maize embryos (Chapter 5) and for *Arabidopsis* seeds (Chapter 7) question such a role.

Also the direct relation between total sugar content and desiccation tolerance is unclear, because high sugar contents do not seem to correspond with a better tolerance (Chapter 7 and 8). Nevertheless, the widely observed presence of sugars in anhydrobiotes (Crowe *et al.*, 1984, 1992, 1997) would suggest that a minimum amount of sugars is required for desiccation tolerance.

Molecular interactions in sugar glasses

As already mentioned, sugars are known to be good glass forming compounds. In Chapter 6 a novel FTIR method is described to study the molecular structure of sugar glasses, which also can be applied to dry cells. The method is based on a temperature study of characteristic molecular group vibrations arising from sugars. We found that intermolecular hydrogen bonding interactions play an important role in the stabilization of sugar glasses, and that melting of glasses coincides with drastic changes in hydrogen bonding interactions. The rate of change of the wavenumber of the OH-stretch with temperature, the wavenumber temperature coefficient, WTC, was used to study the molecular interactions that occur in the glassy state. This parameter can be considered as a measure of the molecular expansion of hydrogen bonds with heating. High WTC values may be indicative of a relatively more loose molecular packing of the glassy matrix. Interestingly, oligosaccharide glasses, having high T_gs, were found to have a more loose molecular structure than monosaccharide glasses. In the light of our hypothesis that desiccation-tolerant cells preferably have a densely packed molecular structure, the generally

observed accumulation of oligosaccharides during acquisition of desiccation tolerance in seeds is surprising. Pure oligosaccharide glasses tend to have a lower molecular packing density than di- or mono-saccharide glasses. However, the generally low T_g of monosaccharide glasses (below room temperature) probably makes them unsuitable as biological stabilizer.

Protein-sugar interactions

Apart from sugars, also proteins are synthesized in association with desiccation tolerance. The impact of proteins on the molecular properties of sugar glasses may be considerable (Kalichevski *et al.*, 1993). To obtain a better understanding of the effect of proteins on sugar glasses, the interaction between them in the dry state was studied using poly-L-lysine and sucrose (Chapter 9). If pure sucrose is dried, crystallization may occur. In sugar crystals the molecular ordering is high and sugar molecules have defined molecular interactions (Lutz and Van der Maas, 1994). Similarly, if poly-L-lysine is dried in the absence of sucrose, highly ordered intermolecular peptide aggregates may be formed. However, when a mixture of poly-L-lysine and sucrose is dried, a considerable molecular disorder is retained in the dry state. Apparently, specific sugar protein interactions prevent this drying-induced molecular ordering (sugar crystals or protein aggregates). We show that sugars and polypeptides indeed directly interact through hydrogen bonding (Chapter 9). The average strength of hydrogen bonding is higher in a sugar/polypeptide glass than in a pure sugar glass and, moreover, the T_g of the dried polypeptide/sugar mixture is higher than that of the dried sugar alone.

In Chapter 10 similar studies were performed concerning the effect of a LEA-like protein isolated from pollen on the molecular properties of sugar glasses. LEA proteins are synthesized during seed (Mao *et al.*, 1995) and pollen (Wang *et al.*, 1996) development and in response to dehydration (Michel *et al.*, 1994) and application of ABA (Blackman *et al.*, 1995), and are suggested to be involved in cellular protection. Similarly as for the poly-L-lysine/sugar mixtures, when the LEA/sugar mixtures are dried, molecular ordering of either

compound is prevented. Moreover, T_g and the average strength of hydrogen bonding of the mixtures are higher than those of pure sugar glasses.

It is likely to assume that also in the cytoplasm of anhydrobiotes, proteins and sugars interact through hydrogen bonding in the dry state. Thus, sugars and proteins may play a role in the molecular organization of the dry cytoplasm when they occur in the same cellular compartment. This may lead to the formation of a stable (high T_g) and molecularly dense (low molecular expansion = low WTC) glassy cytoplasmic matrix in which a considerable molecular disorder is retained.

The observed impact of proteins on sugar glasses might give a clue as to why anhydrobiotes generally accumulate both sugars and LEA proteins prior to the onset of drying. In anhydrobiosis, the role of sugars could be that of a glass former and/or as a substitute for water; the LEA proteins could add to both of these properties. LEA proteins are able to form a tight molecular glassy network together with carbohydrates in the dry state and, due to their high content of hydrophilic amino acids, they may substitute for hydrogen bonds with water. Thus, a possible role of LEA proteins might be to serve as anchors in a tight hydrogen bonding network of sugars and proteins, which provides molecular stability to anhydrobiotes in the dry state.

Adaptations in protein composition in association with desiccation tolerance

The involvement of LEA proteins in the protection of cells against dehydration stress has been postulated by Galau *et al.*, (1986). On account of the primary amino acid sequences, Dure (1993) suggested that the LEA group III proteins occur as specific amphipathic α-helical structures. From the polarity distribution in these structures, a role in sequestering of ion combinations was proposed. Thus, these proteins may reduce the effective ionic strength in dehydrating cells and play a role in hydrogen bonding (Dure *et al.*, 1989, 1993).

In Chapter 5 we showed that maturation induced by slow drying of immature maize embryos leads to a syndrome of adaptations in the cytoplasmic protein profile (FTIR), sugar composition and membrane stability.

All these changes may be required for desiccation tolerance and longevity in the dry state. We argue in the discussion of Chapter 5, that a plausible explanation for the observed increased proportion of α-helical structures to the total protein profile could be associated with newly synthesized proteins, possibly LEAs. Relatively more α-helical protein structures were also observed in slowly dried, desiccation-tolerant carrot somatic embryos (Chapter 8).

Further support for the suggestion that LEA proteins adopt α-helical structures *in situ* came from conformational studies on isolated LEA proteins (Chapter 10). It was shown that these proteins indeed adopt α-helical structures in the dry state, whereas in solution they are fully unordered. The considerable effect of the environment on the structure of these proteins in solution suggests that the structure is only for a minor part determined by the primary amino acid sequence. For the LEA proteins to accomplish the proposed general role in desiccation tolerance, it would be necessary to be present in substantial quantities. This corresponds with the considerable increase in α-helical structures which we observed *in situ* and with a possible role in ion sequestering as suggested earlier.

Macromolecular heat stability and desiccation tolerance

One of the aims of the work presented in this thesis was to characterize the properties of the glassy matrix in the dry cytoplasm of desiccation-tolerant cells and to link these properties to (heat) stability of endogenous macromolecules (proteins). The (heat) stability of proteins is assumed to depend on the extent of cytoplasmic immobilization.

Desiccation-tolerant cells are not only programmed to survive drying but also to retain viability for prolonged periods of time. The plant hormone ABA is thought to play an important role in the considerable biochemical changes associated with these adaptive programs (Koornneef *et al.*, 1989; Ooms *et al.*, 1993). Therefore, mutations affecting ABA responsiveness are particularly suitable to study these biochemical adaptations in more detail.

In Chapter 7, several ABA-insensitive mutant seeds of *Arabidopsis thaliana*, with mutations in the *ABI3* locus, were studied with respect to protein

stability and molecular packing. It was found that the severity of mutation in the *ABI3* locus was manifested in protein stability and in molecular packing density of the seeds. The molecular packing density was less in ABA-insensitive mutant seeds than in wild-type seeds. This also coincided with a reduced heat stability of proteins in the mutant seeds. However, the observed changes in physical stability of the mutant seeds were manifested in reduced survival of dry storage rather than reduced desiccation tolerance *per se*. Apparently, the ABA-induced changes in molecular composition and organization of the cytoplasm are involved in long-term stability, in particular. The most important of these changes are found in carbohydrate and protein composition. Raffinose and stachyose are synthesized, monosaccharides disappear completely, and maturation-specific proteins such as LEA proteins are synthesized. ABA-insensitive mutant seeds have reduced contents of these typical compounds of late seed development.

A comparison between the average strengths of hydrogen bonding interaction *in situ* and in pure sugar glasses suggests that the dry matrix in seeds is much more tightly packed than that of carbohydrates (see Chapter 6, 7 and 8). Apparently, in seeds, compounds other than sugars are involved in the molecular packing, resulting in increased physical stability. Since oligosaccharides tend to decrease, and proteins tend to increase molecular packing density, we postulate that *de novo* synthesized (LEA) proteins rather than oligosaccharides are involved in superior macromolecular stability of seeds.

Macromolecular heat stability in seed vs pollen

While longevity of seed may be of crucial importance for bridging unfavorable growing seasons and, thus, for survival of the entire species, pollen may only require short-term desiccation tolerance during dehydration in the anther and transport to the receptive stigma. It is therefore not to be expected that pollen is specialized in long-term survival. Indeed, average survival times of dry pollen in gene banks is at least ten times less than those of dry seed at similar storage conditions (Hoekstra, 1995). Substantial differences in

macromolecular stability between seed (Chapter 7) and pollen (Chapter 3) were observed. Seeds have extremely high protein denaturation temperatures in the dry state, whereas the denaturation temperature of the pollen is considerably less, even at extremely low water contents. This indicates that the intrinsic (heat) stability of proteins is less in pollen than in seed. We also showed that protein denaturation in dry anhydrobiotes is preceded by a considerable molecular rearrangement in the cytoplasmic matrix.

The question arises whether specific compounds are responsible for the superior macromolecular stability of seeds as compared to pollen. Based on the previous discussion on the stabilizing effect of proteins on sugar glasses, one could argue that the lower molecular stability in pollen is due to the limited amount of LEA proteins. In Chapter 10 it is shown that LEA proteins are present in pollen, which suggests that LEA proteins play a role in the stabilization. The higher macromolecular stability in seeds could simply be due to a higher content of LEA proteins.

Macromolecular stability upon aging

Another aim of the work presented in this thesis was to study protein stability and membrane integrity in desiccation-tolerant cells in the course of natural (Chapter 4) and accelerated (Chapter 2) aging. Even in aged seeds that had lost viability completely during 20-30 years of dry storage at 15°C, the overall protein secondary structure highly resembled that of freshly harvested, viable seeds. We assume that preservation of protein secondary structure applies to every type of cytoplasmic and membrane protein, including enzymic proteins. In that respect, it is interesting to note that activity of some seed enzymes was retained for more than 100 years of storage, long after the loss of viability (Priestley, 1986). In contrast to the considerable stability of the protein secondary structure, the structural integrity of membranes in the naturally aged seeds is completely lost (Golovina *et al.*, 1997). The loss of viability of these seeds is likely to be linked with disrupted membranes rather than with protein structural injury.

Accelerated aging of pollen, i.e. under conditions of high RH, also did not lead to loss of protein structural integrity. This is surprising, considering the fact that the cytoplasmic matrix does not exist in the glassy state under these conditions. The possible interaction of proteins with sugars (see Chapter 9) and/or LEA proteins in the still viscous cytoplasm, may give protection to the proteins. However, extensive loss of membrane integrity was observed during the accelerated aging, coincident with the loss of germinability. This indicates that, similarly as observed for natural aging of dry seeds, cellular membranes are a primary site of injury, and proteins are not.

Concluding remarks

The most important aim of the work presented in this thesis was to investigate to what extent the molecular organization in dry desiccation-tolerant cells differs from that in dry desiccation-sensitive cells. Particularly the effect of the molecular environment on conformation and stability of macromolecules, such as proteins in dry cells was investigated. Because it is difficult to mimic the dry cytoplasmic environment in a model system, macromolecules were studied *in situ*. For this purpose, FTIR analysis methods were developed.

The *in situ* approach has led to new insights in the conformation of (LEA) proteins synthesized in response to desiccation stress. On account of the conformational behavior of a LEA protein purified from pollen, we could make it plausible that these newly synthesized proteins occur as an α-helical structure in the dry cytoplasm of desiccation-tolerant cells. Inspection of the overall protein secondary structure in desiccation-tolerant cells during dry storage has shown that proteins are generally extremely stable in the dry cytoplasmic environment.

FTIR heating studies gave new information on the molecular interactions involved in stabilizing macromolecular structures in desiccation-tolerant cells. Substantial differences in macromolecular (protein) heat stability were found between desiccation-tolerant and -intolerant tissues, and also between tissues differing in longevity. These differences could be linked with the molecular packing density of the glassy cytoplasmic matrix in the dehydrated organisms.

The physical stability as can be deduced from the extent of heat-induced protein denaturation may be used as a tool to predict recalcitrant and intermediate seed storage behavior.

Taken together, *in situ* FTIR studies can give additional information on molecular adaptations associated with the development of desiccation tolerance and longevity, when compared with other biochemical and physiological studies. The added value of this approach is that molecular behavior can be studied in the intact biological system.

References

Blackman, S.A., Obendorf, R.L., Leopold, A.C. (1995) Desiccation tolerance in developing soybean seeds: the role of stress proteins. *Physiol. Plant.* **93,** 630-638.

Bochicchio, A., Rizzi, E., Balconi, C., Vernieri, P., Vazzana, C. (1994) Sucrose and raffinose contents and acquisition of desiccation tolerance in immature maize embryos. *Seed Sci. Res.* **4,** 123-126.

Crowe, J.H., Crowe, L.M., Carpenter, J.F., Aurell Wistrom, C. (1987) Stabilization of dry phospholipid bilayers and proteins by sugars. *Biochem. J.* **242,** 1-10.

Crowe, J.H., Crowe, L.M., Carpenter, J.F., Prestrelski, S.J., Hoekstra, F.A. (1997) Anhydrobiosis: cellular adaptations to extreme dehydration. *In:* Dantzler, W.H. (ed.) Handbook of Physiology section 13, Comparative Physiology, Vol II, Oxford University Press, Oxford, pp. 1445-1477.

Crowe, J.H., Crowe, L.M., Chapman, D. (1984) Preservation of membranes in anhydrobiotic organisms: the role of trehalose. *Science* **223,** 701-703.

Dure, III L. (1993) A repeating 11-mer amino acid motif and plant desiccation. *Plant J.* **3,** 363-369.

Dure, III L., Crouch, M., Harada, J., Ho, T.H.D., Mundy, J., Quatrano, R., Thomas, T., Sung, Z.R. (1989) Common amino acid sequence domains among the LEA proteins of higher plants. *Plant Mol. Biol.* **12,** 475-486.

Fischer, W., Bergfeld, R., Plachy, C., Schafer, R., Schopfer, P. (1988) Accumulation of storage materials, precocious germination and development of desiccation tolerance during seed maturation in mustard (*Sinapis alba* L.). *Bot. Acta* **101,** 344-354.

Galau, G.A., Hughes, D.W., Dure, III L. (1986) Abscisic acid induction of cloned cotton late embryogenesis-abundant (Lea) mRNAs. *Plant Mol. Biol.* **7,** 155-170.

Golovina, E.A., Wolkers, W.F., Hoekstra, F.A. (1997) Behaviour of membranes and proteins during natural seed ageing. *In:* Ellis, R.H., Black, M., Murdoch, A.J., Hong, T.D. (eds.) Basic and Applied Aspects of Seed Biology. Proceedings of the fifth International workshop on seeds, Reading, 1995, Kluwer Academic Publishers, Dordrecht, pp. 787-796.

Hoekstra, F.A. (1995) Collecting pollen for genetic resources conservation. *In:* Collecting Plant Genetic Diversity. Guarino, L., Ramanatha, Rao, V., Reid, R. (eds.) CAB International, Oxon, UK, pp. 527-550.

Hoekstra, F.A., Crowe, J.H., Crowe, L.M., Van Roekel, T., Vermeer, E. (1992) Do phospholipids and sucrose determine membrane phase transitions in dehydrating pollen species? *Plant Cell. Environ.* **15,** 601-606.

Kalichevsky, M.T., Blanshard, J.M.V., Tokarczuk, P.F. (1993) Effect of water content and sugars on the glass transition of casein and sodium caseinate. *Int. J. Food Sci. Technol* **28,** 139-151.

Koornneef, M., Hanhart, C.J., Hilhorst, H.W.M., Karssen, C.M. (1989) In vivo inhibition of seed development and reserve protein accumulation in recombinants of abscisic acid biosynthesis and responsiveness mutants in *Arabidopsis thaliana*. *Plant Physiol.* **90,** 463-469.

Leopold AC, Sun WQ, Bernal-Lugo I (1994) The glassy state in seeds: analysis and function. *Seed Sci. Res.* **4,** 267-274.

Leprince, O., Bronchart, R., Deltour, R. (1990) Changes in starch and soluble sugars in relation to the acquisition of desiccation tolerance during maturation of *Brassica campestris* seed. *Plant Cell. Environ.* **13,** 539-546.

Lutz, E.T.G., Van der Maas, J.H. (1994) Hydrogen bonds in crystalline carbohydrates. A variable-temperature FT-IR study. *J. Mol. Struct.* **324,** 123-132.

Mao, Z.Y., Paiva, R., Kriz, A.L., Juvik, J.A. (1995) Dehydrin gene expression in normal and viviparous embryos of *Zea mays* during seed development and germination. *Plant Physiol. Biochem.* **33,** 649-653.

Michel, D., Furini, A., Salamini, F., Bartels, D. (1994) Structure and regulation of an ABA- and desiccation-responsive gene from the resurrection plant *Craterostigma plantagineum*. *Plant Mol. Biol.* **24,** 549-560.

Ooms, J.J.J., Léon-Kloosterziel, K.M., Bartels, D., Koornneef, M., Karssen, C.M. (1993) Acquisition of desiccation tolerance and longevity in seeds of *Arabidopsis thaliana*. A comparative study using abscisic acid-insensitive *abi3* mutants. *Plant Physiol.* **102,** 1185-1191.

Priestley, D.A. (1986) *Seed Aging: Implications for Seed Storage and Persistence in Soil*, pp. 1-304. Ithaca, Comstock Publ. Assoc.

Steadman, K.J., Pritchard, H.W., Dey, P.M. (1996) Tissue-specific soluble sugars in seeds as indicators of storage category. *Ann. Bot.* **77,** 667-674.

Wang, C.S., Wu, T.D., Chung, C.K.W., Lord, E.M. (1996) Two classes of pollen-specific, heat-stable proteins in *Lilium longiflorum*. *Physiol. Plant.* **97,** 643-650.

Summary

The work presented in this thesis concerns a study on the molecular interactions that play a role in the macromolecular stability of desiccation-tolerant higher plant organs. Fourier transform infrared microspectroscopy was used as the main experimental technique to assess macromolecular structures within their native environment.

Protein secondary structure and membrane phase behavior of *Typha latifolia* pollen were studied in the course of accelerated aging. The overall protein secondary structure of fresh pollen highly resembled that of aged pollen, which indicates that endogenous proteins in these pollen are very stable, at least with respect to their conformation. In contrast, large changes in membrane phase behavior were detected between fresh and aged pollen. Membranes isolated from fresh pollen occurred mainly in the liquid crystalline phase at room temperature, whereas the membranes of aged pollen were at least partly in the gel phase (Chapter 2).

The *in situ* heat stability of the proteins in this pollen was studied as a function of the water content of the pollen. Temperature-induced denaturation of proteins was accompanied by the formation of intermolecular extended β-sheet structures. Below 0.16 g H_2O g^{-1} dry weight (DW), the temperature at which the proteins began to denature increased rapidly and the extent of protein structural rearrangements due to heating decreased (Chapter 3).

Inspection of the overall protein secondary structure of thin slices of embryo axes of onion, white cabbage and radish seeds did not show signs of protein aggregation and denaturation after long-term dry storage. It was concluded that, despite the loss of viability and the long postmortem storage period, secondary structure of proteins in desiccation-tolerant dry seed is very stable and conserved during at least several decades of open storage (Chapter 4).

Adaptations in overall protein secondary structure in association with the acquisition of desiccation tolerance were studied using isolated immature maize embryos. Isolated immature maize (*Zea mays*) embryos acquire tolerance to

rapid drying between 22 and 25 days after pollination (DAP) and to slow drying from 18-DAP onwards. In fresh, viable 20- and 25-DAP embryo axes, the overall protein secondary structure was identical, and this was maintained after flash drying. On rapid drying, 20-DAP axes showed signs of protein breakdown and lost viability. Rapidly dried 25-DAP embryos germinated and had a protein profile similar to the fresh control. On slow drying, the α-helical contribution in both the 20- and 25-DAP embryo axes increased when compared with that in the fresh controls, and survival of desiccation was high. The protein profile in dry mature axes resembled that after slow drying of the immature axes. Rapid drying resulted in an almost complete loss of membrane integrity in 20-DAP embryo axes and much less so in 25-DAP axes. After slow drying, membrane integrity was retained in both the 20- and 25-DAP axes. It was concluded that slow drying of excised immature embryos leads to an increased proportion of α-helical protein structures in their axes, which coincides with additional tolerance of desiccation stress (Chapter 5).

A novel FTIR method was used to study glasses of pure carbohydrates and glasses in the cytoplasm of desiccation-tolerant plant organs. The method is based on a temperature study of the position of the OH-stretching vibration band (νOH). The glass transition temperatures (T_gs) of several dry carbohydrate glasses determined by this FTIR method resembled those of produced by other methods. FTIR analysis gives additional information on the molecular properties of glassy structures. The shift of νOH with temperature - the wavenumber-temperature coefficient (WTC) - is indicative of the average strength of hydrogen bonding in glasses. The WTC was found to be higher in sugar glasses having higher T_g. This suggests that carbohydrate glasses are more loosely packed when they have higher T_g. For *Typha latifolia* pollen and dried *Craterostigma plantagineum* leaves similar νOH *vs* temperature plots were obtained as for pure carbohydrate glasses, indicating that a glass transition was observed. The data suggested that the carbohydrates that are present in the cytoplasm of these plant organs are the primary components contributing to the glassy state (Chapter 6).

In order to find a relation between desiccation tolerance and physical stability, the heat stability of proteins and the properties of the glassy matrix in several dry maturation-defective mutant seeds of *Arabidopsis thaliana* were studied. Proteins in dried wild-type seeds did not denature up to 150°C. In dried desiccation-sensitive *lec1-1*, *lec1-3* and *abi3-5* seeds, protein denaturation occurs at temperatures below 100°C. In desiccation-tolerant *abi3-7* and *abi3-1* seeds, protein denaturation commenced above 120 and 135°C, respectively. The maximal rate of change of νOH with temperature was much higher in *abi3-5*, *lec1-1* and *lec1-3* mutant seeds than in wild-type, *abi3-1*, and *abi3-7* seeds. This was interpreted as a higher molecular packing density in dried desiccation-tolerant than in dried desiccation-sensitive seeds, which is associated with a higher, respectively lower protein denaturation temperature. The generally lower physical stability of the desiccation-sensitive mutant seeds coincides with a lack of biochemical adaptations that normally occur in the later stages of seed development (Chapter 7).

The relation between physical stability and desiccation tolerance was also studied in slowly dried (desiccation-tolerant) and rapidly dried (desiccation-sensitive) carrot somatic embryos. Although protein denaturation temperatures were similar in the embryos after slow or rapid drying, the extent of protein denaturation was higher in the rapidly dried embryos. Slowly dried embryos are in a glassy state at room temperature, whereas no clearly defined glass transition temperature was observed in the rapidly dried embryos. Moreover, the molecular packing density of the cytoplasmic glassy matrix was higher in the slowly dried embryos. While sucrose is the major soluble carbohydrate after rapid drying, on slow drying, the trisaccharide umbelliferose accumulates at the expense of sucrose. Dry umbelliferose and sucrose glasses have almost similar T_gs. Both umbelliferose and sucrose depressed the transition temperature of dry liposomal membranes equally well; prevented leakage from dry liposomes after rehydration, and preserved the secondary structure of dried proteins. The similar protecting properties in model systems and the apparent interchangeability of both sugars in viable dry somatic embryos suggest no special role for umbelliferose in the improved physical stability of the slowly

dried somatic embryos. It was suggested that LEA proteins, which are synthesized during slow drying together with the sugars, are responsible for the increased stability of the slowly dried embryos (Chapter 8).

The dehydration-sensitive polypeptide, poly-L-lysine was used as a model to study dehydration-induced conformational transitions of this polypeptide as influenced by drying rate and carbohydrates. In solution poly-L-lysine adopts a random coil conformation. Upon slow drying of small droplets of the polypeptide solution over a period of several hours, the polypeptide adopts an extended β-sheet conformation. Upon fast air-drying within 2-3 minutes, the aqueous polypeptide structure is preserved. Slow air-drying in the presence of sugars also preserves the aqueous conformation and results in the formation of a glassy state having a higher T_g than that of sugar alone. The importance of direct sugar - polypeptide interaction in stabilization during slow air-drying was studied by drying the polypeptide in the presence of glucose, sucrose or dextran. Compared to dextran (and sucrose to a lesser extent), glucose gives superior protection, while having the lowest T_g and the best interacting properties. It was suggested that during slow drying, a protectant with sufficient interaction is required for preservation of the aqueous protein structure (Chapter 9).

The structure of a D-7 LEA (late embryogenesis abundant)-like protein protein isolated from *Typha latifolia* pollen was studied using FTIR. In solution, the protein adopts a random coil conformation. Fast air-drying (5 minutes) leads to the formation of α-helical structure, whereas slow drying (few hours) leads to both α-helical and intermolecular extended β-sheet structures. When dried in the presence of sucrose, the protein adopts predominantly α-helical conformation, irrespective of drying rate. Drying of a mixture of LEA protein and sucrose results in the formation of a glassy state having higher T_g and a higher average strength of hydrogen bonding than a pure sucrose glass. It was suggested that LEA proteins might be involved in the formation of a tight molecular network in the dehydrating cytoplasm of anhydrobiotic organisms, which may contribute to desiccation tolerance (Chapter 10).

Taken together, *in situ* FTIR studies can give additional information on the molecular organization in desiccation-tolerant cells. The added value of this approach is that molecular structures and inter-molecular interactions can be studied in intact biological systems (Chapter 11).

Samenvatting

In dit proefschrift wordt het onderzoek beschreven naar de moleculaire interacties die een rol spelen bij de macromoleculaire stabiliteit van uitdroogtolerante organen van hogere planten. Fourier transform infrarood microspectroscopie werd veelvuldig gebruikt als experimentele techniek om macromoleculaire structuren te onderzoeken in hun natuurlijke omgeving.

De effecten van versnelde veroudering op de secundaire eiwitstructuur en het fase gedrag van membranen zijn onderzocht aan stuifmeel van lisdodde (*Typha latifolia* L.). De secundaire eiwitstructuur van vers stuifmeel vertoonde veel overeenkomsten met die van verouderd stuifmeel, wat wijst op grote stabiliteit van de eiwitten, tenminste wat betreft de conformatie. In tegenstelling hiermee zijn wel grote verschillen in fasegedrag gevonden tussen geisoleerde membranen uit vers en verouderd stuifmeel. Membranen die geisoleerd zijn uit vers stuifmeel bevonden zich in de vloeibaar-kristallijne fase bij kamertemperatuur, terwijl membranen uit verouderd stuifmeel zich gedeeltelijk in de gel-fase bevonden (Hoofdstuk 2).

De hittestabiliteit van eiwitten in dit stuifmeel is onderzocht als functie van het watergehalte. Door de inductie van eiwitdenaturatie bij hogere temperatuur worden er intermoleculaire β-sheetstructuren gevormd. Beneden 0.16 g H_2O g^{-1} drooggewicht, neemt de temperatuur waarbij de eiwitten beginnen te denatureren sterk toe, en neemt de mate van door verhitting geinduceerde structurele eiwitveranderingen sterk af (Hoofdstuk 3).

Na lange bewaring van droge zaden van ui, radijs en witte kool trad geen eiwit-aggregatie en -denaturatie op. Dit werd geanalyseerd aan de hand van FTIR analyse van dunne coupes van delen van de embryo-as. Hieruit werd geconcludeerd dat ondanks verlies van vitaliteit en de lange *post mortem* bewaarperiode, de secundaire eiwitstructuur in droge uitdroogtolerante zaden erg stabiel is en dat deze tientallen jaren geconserveerd blijft tijdens open bewaring (Hoofdstuk 4).

Aanpassingen in secundaire eiwitstructuur die gepaard gaan met het verkrijgen van uitdroogtolerantie zijn onderzocht met behulp van onrijpe mais

embryo's. Geisoleerde onrijpe mais (*Zea mays* L.) embryo's verkrijgen tolerantie tegen snel uitdrogen tussen de 22 en 25 dagen na bestuiving (DAP) en tegen langzaam uitdrogen vanaf 18 DAP. In verse embryo-assen van 20 en 25 DAP is de secundaire eiwitstructuur identiek. Na snel uitdrogen van de 20 DAP assen werden er tekenen van eiwitafbraak waargenomen en ging de vitaliteit verloren. Snel gedroogde 25 DAP embryo's waren kiemkrachtig en hadden een zelfde eiwitprofiel als de verse controle. Tijdens langzaam drogen, nam de bijdrage van α-helixstructuren toe in zowel de 20 als de 25 DAP embryo's, in vergelijking met de verse controles. Verder was de overleving na uitdrogen hoog. Het eiwitprofiel in droge rijpe assen was vergelijkbaar met die van de onrijpe langzaam gedroogde assen. Snel drogen resulteerde in een bijna totaal verlies van membraanintegriteit bij de 20 DAP embryo's en veel minder bij de 25 DAP embryo's. Na langzaam drogen bleef de membraanintegriteit behouden. Uit de verkregen resulaten werd geconcludeerd dat langzaam drogen van onrijpe embryo's leidt tot een stijging van het relatieve aandeel aan α-helixstructuren, die gepaard gaat met toegenomen tolerantie tegen uitdroogstress (Hoofdstuk 5).

Een nieuwe FTIR methode werd gebruikt om suikerglassen en cytoplasmatische glassen van uitdroogtolerante plantenorganen te bestuderen. De methode is gebaseerd op een temperatuurstudie van de positie van de OH-rekvibratieband (νOH). De aldus bepaalde glastransitietemperaturen (T_g's) van verschillende suikerglassen kwamen overeen met die zoals bepaald met andere methoden. Behalve T_g's geeft de FTIR methode additionele informatie over moleculaire eigenschappen van glasstructuren. De verschuiving van νOH met de temperatuur - de golfgetal-temperatuur coefficient (WTC) - is een maat voor de gemiddelde sterkte van de waterstofbruggen in glassen. De WTC bleek hoger te zijn in suikerglassen die een hogere T_g hebben. Dit suggereert dat suikerglassen losser gepakt zijn als ze een hogere T_g hebben. FTIR analyse van droog *Typha latifolia* stuifmeel en gedroogde bladeren van *Craterostigma plantagineum* gaven vergelijkbare νOH *vs* temperatuur plots als die van de suikerglassen, hetgeen een indicatie is dat er een glasovergang wordt waargenomen. Er werd gesuggereerd dat de suikers in het cytoplasma van

deze plantenorganen de belangrijkste structurele component vormen van het cytoplasmatische glas (Hoofdstuk 6).

De relatie tussen uitdroogtolerantie en fysische stabiliteit van cytoplasmatische componenten is onderzocht door de eigenschappen van de glasstructuur te bestuderen in zaden van *Arabidopsis thaliana* planten die gemuteerd zijn in de afrijping van het zaad. Eiwitten in gedroogde wild-type zaden konden tot 150°C worden verhit zonder te denatureren, in tegenstelling tot eiwitten in abscisinezuur-ongevoelige (*abi3*) en 'leafy cotyledon' (*lec*) mutant zaden. In droge, uitdrooggevoelige *lec1-1*, *lec1-3* en *abi3-5* zaden vond eiwitdenaturatie plaats beneden 100°C. In uitdroogtolerante *abi3-7* en *abi3-1* zaden, begon eiwitdenaturatie boven respectievelijk 120 en 135°C. De maximale snelheid van verandering van νOH met temperatuur (WTC_{max}) was veel hoger in *abi3-5*, *lec1-1* en *lec1-3* mutantzaden dan in *abi3-1*, *abi3-7*, en wild-type zaden. We hebben dit als volgt geinterpreteerd: droge uitdroogtolerante zaden met een hogere moleculaire pakkingsdichtheid hebben een hogere eiwitdenaturatietemperatuur dan droge uitdrooggevoelige zaden die een lagere moleculaire pakkingsdichtheid en een lagere eiwitdenaturatietemperatuur hebben. De lagere fysische stabiliteit van uitdrooggevoelige mutant zaden gaat kennelijk samen met het ontbreken van specifieke biochemische aanpassingen, zoals die normaliter in de latere stadia van de zaadontwikkeling plaatsvinden (Hoofdstuk 7).

De relatie tussen fysische stabiliteit en uitdroogtolerantie is ook onderzocht in langzaam (uitdroogtolerant) en snel (uitdrooggevoelig) gedroogde somatische embryo's van *Daucus carota* L.. Alhoewel de eiwitdenaturatietemperaturen van snel en langzaam gedroogde embryo's overeen kwamen, was de mate van eiwitdenaturatie in de snel gedroogde embryo's groter. Langzaam gedroogde embryo's zijn in een glastoestand bij kamertemperatuur, terwijl er geen duidelijk gedefinieerde glasovergang kon worden waargenomen in de snel gedroogde embryo's. Bovendien is de moleculaire pakkingsdichtheid van het cytoplasma hoger in de langzaam gedroogde embryo's. Terwijl sucrose de belangrijkste suiker is na snel drogen, accumuleerde de trisaccharide umbelliferose ten koste van sucrose tijdens

langzaam drogen. Droge umbelliferose- en sucrose-glassen hebben vergelijkbare T_g's. Zowel umbelliferose als sucrose konden de transitietemperatuur van droge liposomale membranen verlagen, lekkage van droge liposomen na rehydratatie voorkomen, en de secundaire structuur van gedroogde eiwitten preserveren. De vrijwel identieke beschermende eigenschappen in modelsystemen en de uitwisselbaarheid van beide suikers in levende droge embryo's suggereren dat umbelliferose geen speciale rol speelt in de verbeterde fysische stabiliteit van langzaam gedroogde embryo's. Er werd gesuggereerd dat LEA eiwitten, welke gesynthetiseerd worden gedurende langzaam drogen, samen met de suikers verantwoordelijk gesteld kunnen worden voor de toegenomen cytoplasmatische stabiliteit van de langzaam gedroogde embryo's (Hoofdstuk 8).

Het uitdrooggevoelige polypeptide, poly-L-lysine is gebruikt als model om conformatie overgangen van eiwitten te bestuderen als functie van de droogsnelheid en aanwezigheid suikers. In oplossing neemt poly-L-lysine een ongeordende kluwenconformatie aan. Langzaam drogen van kleine druppeltjes over een periode van enkele uren leidde tot vorming van β-sheetconformatie. Door snel te drogen binnen enkele minuten bleef de kluwenconformatie behouden. Door langzaam te drogen in aanwezigheid van suikers bleef de kluwenstructuur ook behouden en werd er een amorfe toestand gevormd met een hogere T_g dan die van de suiker alleen. Het belang van een directe suiker-eiwitinteractie voor het verkrijgen van stabilisatie tijdens langzaam drogen is bestudeerd door het polypeptide te drogen in aanwezigheid van glucose, sucrose of dextraan. Vergeleken met dextraan (en in mindere mate met sucrose) gaf glucose de beste bescherming, terwijl glucose de slechtste glasvormer was en de beste interacterende eigenschappen heeft. Er werd geconcludeerd dat er gedurende langzaam drogen een beschermende stof nodig is die in voldoende mate kan interacteren en zodoende de waterige eiwitstructuur kan preserveren (Hoofdstuk 9).

De structuur van een D-7 LEA-achtig eiwit geisoleerd uit *Typha latifolia* pollen is bestudeerd met FTIR. In oplossing neemt het eiwit een kluwenconformatie aan. Snel drogen (5 minuten) leidt tot de vorming van α-

helixstructuren, terwijl langzaam drogen leidt tot de vorming van zowel α-helix- als β-sheet-structuren. Wanneer het eiwit gedroogd werd in de aanwezigheid van sucrose, nam het eiwit voornamelijk een α-helixconformatie aan, onafhankelijk van de droogsnelheid. Wanneer een mengsel van LEA-eiwitten en suikers gedroogd werd dan resulteerde dit in de vorming van een amorfe toestand met een hogere T_g en gemiddeld sterkere waterstofbruggen dan die van een puur sucroseglas. Hieruit werd geconcludeerd dat LEA-eiwitten mogelijk betrokken zijn bij de vorming van een sterk moleculair netwerk in het uitdrogende cytoplasma, hetgeen bijdraagt aan uitdroogtolerantie (Hoofdstuk 10).

Samengevat kunnen *in situ* FTIR studies extra informatie geven over de moleculaire organisatie van uitdroogtolerante cellen. De toegevoegde waarde van deze aanpak ligt in het feit dat moleculaire structuren en intermoleculaire interacties bestudeerd kunnen worden in intacte biologische systemen (Hoofdstuk 11).

Dankwoord

Op de eerste plaats wil ik mijn directe begeleider en co-promotor Folkert Hoekstra bedanken voor de vele stimulerende discussies die wij gevoerd hebben en de urenlange sessies die wij, onder het genot van de nodige sigaren en glazen wijn, hebben gespendeerd om de tekst van dit proefschrift te verbeteren. Linus van der Plas wil ik bedanken voor zijn rol als promotor en het vlotte nakijken van de hoofdstukken. Mark Alberda wil ik bedanken voor zijn bijdrage aan de ontwikkeling van de FTIR opstelling. Futhermore I would like to thank George Lindsey and Wolf Brandt for giving me the opportunity to work in their Lab. The pleasant cooperation with Adriana Bochicchio and Giuseppe Selvaggi resulted in chapter 5 of this thesis. Verder wil ik Jet Oldenhof, Maaike van Kilsdonk en Hendrik van den Bergh bedanken, die als doctoraal student elk hun eigen bijdrage aan dit proefschrift hebben geleverd.

Op deze plaats wil ik ook mijn ouders bedanken voor steun en toeverlaat.

Wim

Curriculum Vitae

De schrijver van dit proefschrift, Willem Frederik Wolkers werd op 26 augustus 1966 te Amsterdam geboren. Na het behalen van het Atheneum-b diploma aan het christelijk Lyceum te Apeldoorn in mei 1986, werd een aanvang gemaakt met de studie moleculaire wetenschappen aan de Landbouwuniversteit in Wageningen. Het doctoraalexamen werd in augustus 1992 behaald met als hoofdvakken, biochemie en moleculaire fysica, en een onderzoeksstage biochemie aan de 'University of Knoxville' (TN, USA). Van september 1992 tot januari 1994 was de auteur werkzaam bij de vakgroep moleculaire fysica (Landbouwuniversiteit Wageningen). In januari 1994 is hij begonnen als onderzoeker in opleiding (OIO) voor de stichting levenswetenschappen gefinancierd door de Nederlandse Organisatie voor Wetenschappelijk Onderzoek in Nederland (NWO) bij de vakgroep plantenfysiologie van de Landbouwuniversiteit te Wageningen. Het onderzoek aan deze vakgroep heeft geleid tot dit proefschrift. Sinds 1 mei 1998 is de auteur als postdoc werkzaam bij 'Labaratoire de Chimie-Physique des Macromolecules aux Interfaces' van de 'Universite Libre de Bruxelles'.

List of publications

Publications in the field of desiccation tolerance

Wolkers, W.F., Hoekstra, F.A. (1995) Aging of dry desiccation-tolerant pollen does not affect protein secondary structure. *Plant Physiology* **109,** 907-915.

Tetteroo, F.A.A., de Bruijn, A.Y., Henselmans, R.N.M., Wolkers, W.F., van Aelst, A.C., Hoekstra, F.A. (1996) Characterization of membrane properties in desiccation-tolerant and -intolerant carrot somatic embryos. *Plant Physiology* **111,** 403-412.

Hoekstra, F.A., Wolkers, W.F., Buitink, J., Golovina, E.A., Crowe, J.H., Crowe, L.M. (1997) Membrane stabilization in the dry state. *Comparative Biochemistry and Physiology* **117A,** 335-341.

Golovina, E.A., Wolkers, W.F., Hoekstra, F.A. (1997) Long term stability of protein secondary structure in dry seeds. *Comparative Biochemistry and Physiology* **117A,** 343-348.

Linders, L.J.M., Wolkers, W.F., Hoekstra, F.A., van't Riet, K. (1997) Effect of added carbohydrates on membrane phase behavior and survival of dried Lactobacillus plantarum *Cryobiology* **35,** 34-40.

Wolkers, W.F., Hoekstra, F.A. (1997) Heat stability of proteins in desiccation tolerant cattail pollen (Typha latifolia): A Fourier transform infrared spectroscopic study. *Comparative Biochemistry and Physiology* **117A,** 349-355.

Hoekstra, F.A., Wolkers, W.F., Buitink, J. Golovina, E.A. (1997) Desiccation tolerance and long-term structural stability, In R.H. Ellis (ed.), Basic and applied aspects of seed biology. pp. 1-12.

Golovina, E.A., Wolkers, W.F., Hoekstra, F.A. (1997) Behaviour of membranes and proteins during natural seed ageing. In R.H. Ellis (ed.), Basic and applied aspects of seed biology. pp. 787-796.

Wolkers, W.F., Oldenhof, H., Alberda, M., Hoekstra, F.A. (1998) A Fourier transform infrared microspectroscopy study of sugar glasses: Application to anhydrobiotic higher plant cells. *Biochimica et Biophysica Acta* **1379,** 83-96.

Wolkers, W.F., Bochicchio, A., Selvaggi, G., Hoekstra, F.A. (1998) Fourier transform infrared microspectroscopy detects changes in protein secondary structure associated with desiccation tolerance in developing maize embryos. *Plant Physiol.* **116,** 1169-1177.

Wolkers, W.F., van kilsdonk, M.G., Hoekstra, F.A. (1998) Dehydration-induced conformational changes in poly-L-lysine can be prevented by rapid air-drying. submitted for publication in *Biochimica et Biophysica Acta. submitted.*

Wolkers, W.F., Tetteroo, F.A.A., Alberda, M., Hoekstra, F.A. Protective role of umbelliferose and sucrose in desiccation tolerant carrot (Daucus carota L.) somatic embryos. *Plant Physiology. submitted.*

Wolkers, W.F., Alberda, M., Koornneef, M., Hoekstra, F.A. Heat stability of proteins in maturation defective mutants of Arabidopsis thalania: a FT-IR microspectroscopy study. I *Plant Journal. submitted.*

Wolkers, W.F., Brandt, W., Lindsey, G. Isolation of a D-7 LEA like protein from Typha latifolia pollen. *Plant Journal. submitted.*

Other publications

Wolkers, W.F., Gregory, J.D., Churchich, J.E., Serpersu, E.H. (1991) Arrangement of the substrates at the active site of pyridoxal kinase. *The journal of Biological Chemistry* **266,** 20761-20766.

Bastiaans, P.I.H., van Hoek, A., Wolkers, W.F., Brochon, J.C., Visser, A.J.W.G. (1992) Comparison of the dynamical structures of lipoamide dehydrogenase and glutathion reductase by time resolved polarized flavin fluorescence. *Biochemistry* **31,** 7050-7070.

Wolkers, W.F., Haris, P.I., Pistorius, A.M.A., Chapman, D., Hemminga, M.A. (1995) FT-IR spectroscopy of the major coat protein of M13 and Pf1 in the phage and reconstituted into phospholipid systems. *Biochemistry* **34,** 7825-7833.

Wolkers, W.F., Spruijt, R.B., Kaan, A., Konings, R.N.H., Hemminga, M.A. (1997) Conventional and saturation-transfer EPR of spin-labeled mutant bacteriophage M13 coat protein in phospholipid bilayers. *Biochimica et Biophysica Acta* **1327,** 5-16.